UNIVERSITÀ DELLA CALABRIA

Università della Calabria

Dipartimento di Ingegneria per l'Ambiente e il Territorio e Ingegneria Chimica

Dottorato di Ricerca in Ingegneria Chimica e dei Materiali

SCUOLA DI DOTTORATO " PITAGORA " IN SCIENZE INGEGNERISTICHE

Con il contributo dell'Istituto per la Tecnologia delle Membrane del Consiglio Nazionale della Ricerca ITM-CNR

CICLO XXVI

BIODEGRADABLE POLYMERIC MEMBRANE SYSTEMS FOR TISSUE ENGINEERING APPLICATIONS

Settore Scientifico Disciplinare CHIM07 – Fondamenti chimici delle tecnologie

Coordinatore: Chiar.mo Raffaele Molinari

Supervisori: Dott.ssa Loredana De Bartolo
Ing. Efrem Curcio

Dottoranda: Dott.ssa Antonietta Messina

UNIVERSITÀ DELLA CALABRIA

UNIVERSITA' DELLA CALABRIA

Dipartimento di Ingegneria per l'Ambiente e il Territorio e Ingegneria Chimica

Dottorato di Ricerca in

Ingegneria Chimica e dei Materiali

Scuola di Dottorato "Pitagora" in Scienze ingegneristiche

Con il contributo dell'Istituto per la Tecnologia delle Membrane del Consiglio Nazionale della Ricerca ITM-CNR

CICLO

XXVI

BIODEGRADABLE POLYMERIC MEMBRANE SYSTEMS FOR TISSUE ENGINEERING APPLICATIONS

Settore Scientifico Disciplinare CHIM07 – Fondamenti chimici delle tecnologie

Coordinatore: Ch.mo Prof. Raffaele Molinari

Supervisori: Dott.ssa Loredana De Bartolo

Dott. Ing. Efrem Curcio

Dottorando: Dott.ssa Antonietta Messina

Table of contents

General introduction and Aim of work

Watching the cells grow and building up a new tissue outside the body has been the new insights appeared with the TE development. The deepening study on the interaction of cells and tissues with biomaterials in a specific arrangement contributed new cognitions about the influence of several technical and biological factors involved in the tissue regeneration process and consequently on the scaffolds design and its outcome. Such factors are for example mechanical loading, biomaterial degradation behavior, cell number or the cell type in contact with the material. The main future challenge is the complete investigation not onlu of the tissue properties that needs to be replaced and their transfer to the biomaterial used for the tissue regeneration, but above all the understanting of how the biomaterial properties influence the tissue formation and functionalization, that means definig the perfect biomaterial characteristics for each possible application in TE field and regenerative medicine. Otherwise an alternative approach to the classical scaffold-based TE, named scaffold-free TE has been developed, in order to reproduce the native embryonic condition during the tissue in vitro production, relying on the self assembly potential of cells and their secretion of a specific extracellular matrix network. Tissue spheroids have been used for this purpose, as building blocks for the biofabrication of three-dimensional functional living macrotissues and organ constructs, with no scaffolds or supports request. On the other side, not all the cells are able to self-assemble themselves without external stimuli, and the time requested for the spheroids to be compact enough for the handling, sometime is so long to ensure the perfect vitality of the engineered tissue, and eventually cells go through necrosis. Despite the amazing results reached and published all around the world, both the approaches appear to be still rich in disadvantages: scaffold degradation is rarely synchronized to neotissue formation, making the tissue remodeling and its integration difficult, thus compromising functional properties. Furthermore, toxicity and immunogenicity due to scaffold creation, seeding, or degradation are of concern [Liu et al., 2004], and the presence of a scaffold may also alter the phenotype of cells that come into contact with it [Levy-Mishali et al., 2009]. One can infer that in the near future new pathways able to overcome the limitations for both the TE approaches will be not easy available. This is the reason way, despite the considerable progress in the field of biomaterials and life science a continuous development of new insights is required for the recreation of a tissue engineered system.

Thus, this study aimed to the development and the design of new bio-artificial systems able to reproduce *in vitro* an engineered tissue/organ mimic usable for TE applications and furthermore investigations in the field of the regenerative medicine.

The first section of this report, will think back to the state of the art and the literature references about the two TE approaches (chapter 1-2-3), and then, the following chapters will present the experimental work done in the last three years.

1) (chapter 4) The development of polymeric membranes with biodegradable properties is shown. It is well known how the morphological, physicochemical, mechanical and dissolution properties of a polymeric substrates are dependent on the materials choosen and on the processing methods used for their preparation. Starting from the uncountable literature references available, Chitosan, Polycaprolactone and Polyurethane have been purposely choosen and molded through the phase inversion technique as flat biodegradable membranes and investigated in their properties, in order to understand if they could be eventually used as substrates for tissue engineering applications.
2) (chapter 5) The already set biodegradable polymeric membranes were tested to investigate the efficacy to promote the adhesion and differentiation of neuronal cells. The human neuroblastoma cell line SHSY5Y, a wellestablished system for studying neuronal differentiation, has been used as biological component on the bio-hybrid system. The investigation of viability and specific neuronal marker expression allowed assessment that the correct neuronal differentiation and the formation of neuronal network had taken place in vitro in the cells seeded on different biodegradable membranes.
3) (chapter 6) The biodegradable polymeric membranes were used to highlight if they can act as substrates for sustaining the fusion process of tissue spheroids, nowadays considered as the new building-blocks for the engineered tissue and organ mimics. Conbining the use of substrates with spheroids in a unique system is a completely new approach, in the TE field. Generally in fact a polymeric membrane or a scaffold are used for the development of bio-hybrid system that reproduce only partially the in-vivo regeneration process, being a 2D system; whereas the spheroids are investigated in an environment completely inert only focusing on the cell-cell interaction. On the contrary, in this case spheroids obtained from three defferent cell lines, SH SH 5Y, Fibroblast and Myoblast, and their fusion process, the biological activity and the level of necrosis hypoxia-induced have been investigated on the polymeric membranes

developed in order to highlights how the properties of the obtained substrates can influence the tissue maturation in time with respect to the scaffold-free TE approach, for this study represented by an agarose support.

4) (chapter 7) Polycaprolactone (PCL) and hydroxyapatite (HA) were used in order to develop novel controlled nanostructured biomaterials for bone tissue engineering applications. After preparation, membrane scaffolds were characterized in order to evaluate its morphological, physico-chemical and mechanical properties and then used for the osteoclast cell culture.

Chapter 1

Biodegradable polymeric membranes for Tissue engineering and medical applications

Introduction

Repairing and replacing damaged or malfunctioning parts of the human body is an objective with ancient roots in history. Etruscans and Egyptians learned more than 2500 years ago how to operate to substitute teeth, build a bridge with animal bones to sustain limb fractures and create amalgams in order to prevent infections and let wounds heal and regenerate. Since then in every time more sophisticated inventions were done all around the world in order to improve the existing medical discoveries and devices and create a few new ones. But it's only some decades ago that all the knowledge in medicine and sciences converged in what we all know as Tissue Engineering.

1.1 Tissue Engineering: history and definition

"…an interdisciplinary field that applies the principles of engineering and of life science towards the development of biological substitutes that restore, maintain and/or improve tissue or organ function […], thus the whole principles and methods suitable for establishing the foundations of structure-function relationships between healthy or pathologic mammalian tissues". That is the first official definition reported by Fox and Skalak to summarize the outlines of the Ist congress NSF held in 1988 in California, and in which the expression "Tissue Engineering" (TE) was coined [Fox et al., 1988]. For the first time then, TE emerged as the first real significant chance to transfer the fruit of the last decades to clinical practice: a new field able to create a potential alternative or complementary solution to transplantation, surgical repair, artificial prosthesis, mechanical device and drug therapy [Chapekar et al 2000]. Few difficulties arise when surgical transplantation is used. Taking a graft from a donor and implanted it in a patient is not easy, and eventually the collateral effects could be unpredictable. Moreover the insufficient donor organs number, pathogen transmission risk, lifetime immunosuppression therapy and rejection of the replaced tissue/organ with consequent fear of a replacement within days to years after the surgery, are just some of these difficulties. Besides artificial mechanical devices or sustenance machines when used as

prosthesis for treating injuries or damages on human body are not less dangerous.That's the reason why the chance to implant natural, synthetic or semi-synthetic tissue and organ mimics, that are fully functional form the start or that can be "planned" to grow into the required functionality, with the opportunity to use patient's own cells for the creation of an autogenic tissue construct or substitute *in vitro* is considered an excellent alternative to direct transplantation of donor organs [Langer et al., 1993; Fucks et al. 2001; Lanza et al., 2000; Saltzman et al., 2004]. In that case not dependency on donors is required and some of the limitations of direct transplantation particularly concerning rejection and pathogen transmission could be avoided or overcome.

Eventually the TE approach appeared and it is still today really promising. First sign of this new developing field appear in the 1960s when synthetic fibers were used as skin grafts for burn treatment; first step in the clinical evolution that lead in just a decade to the development of a collagen-based artificial skin used to treat severe burns [Burke J.F. et al. 1981] and to a collagen sponge skin substitute, cross-linked with chondroitin and covered with silicone for oral mucosa injuries treatments [Levin M.P. et al. 1979]. In the last 20 years more areas of tissue engineering have been explored and applied afterwords: skin, heart, vessels, bone and cartilage replacements used in clinical trials and applications are uncountable [Blitterswijk et al., 2008; Fong et al., 2006; Jawad et al., 2007; Nesic et al., 2006]. Ten years ago cardiovascular autografts obtained with patients own cells have been implanted on children with various complex heart diseases. Cells were isolated, cultured and subsequently seeded on a biodegradable polymer scaffold of poly(glycolic acid) combined with poly(lactic acid-ε-caprolactone) before the insert operation, and no post-operative complications were detected [Matsumura et al., 2003]. An allogenic engineered trachea has been designed and implanted *in vivo* in order to prevent an immune reaction. Macchiarini and colleagues removed from trachea all donor's cell and antigens and subsequently autogenic cells were re-cultured on the matrix, let multiply and transplanted into the patient's main bronchus. The tissue engineered trachea became functionalize and transplanted into the patient's main bronchus [Macchiarini et al., 2008]. The tissue engineered trachea behave perfectly already after only 4 months from the surgery showing a normal appearance and good functional properties. In truth, replacing failing or malfunctioning organs or promoting their partial or complete regeneration after an injuries or a pathology requires more than just a collection of acknowledgements and intuitions, and framing a new trend of medical research in order to coordinate the few advances already achieved in distant areas of science is not an easy task.

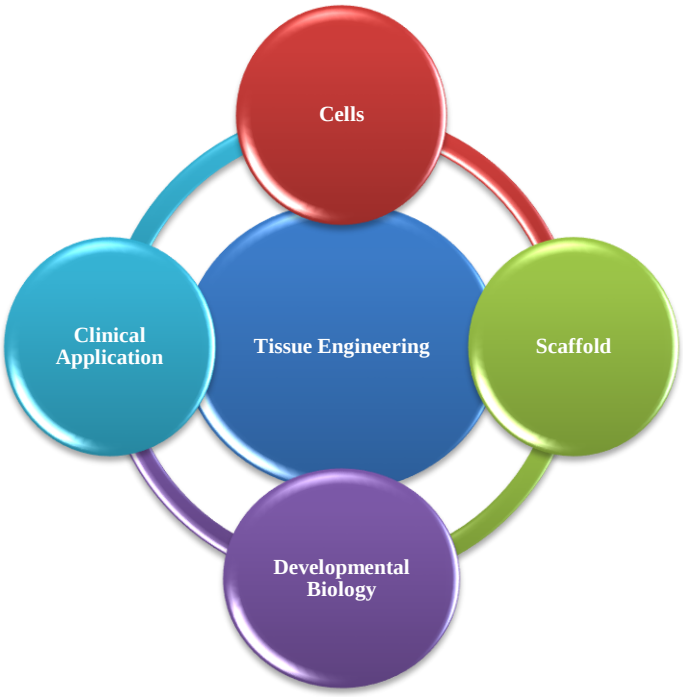

Fig. 1.1 Rational design of a functional tissue/organ mimic through Tissue Engineering approach

Engineering, chemistry, physics, biology, biotechnology and medicine must be confronted and engaged in a multi-disciplinary approach to tissue, in order to develop bioactive tissue substitutes as an alternative to inert systems. Therefore, the complexity of all biological tissues in terms of macromolecular composition, ultra-structural organization and interactions between cells and environment, made it hard to switch engineered constructs in the clinical trial. For many native tissues, the *in vvo* stresses and strains to which they are subjected are not well defined, and furthermore, tissue properties and answers in body vary with age, site and other host factors, making it difficult to match parameters, as mechanical and physicochemical properties, to design and develop a general list of criteria for engineered tissues [Badylak et al., 2002]. Moreover highly specialized structures as articular cartilage and cardiac tissue for example, show unique biomechanical properties required to move the limbs and circulate the blood. The loss of function of these tissue due to injury, disease, or aging origin a significant number of clinical disorders as consequence. Although different in many respects, these tissues share two features quite relevant for the tissue engineering approach: (1) they lack of intrinsic capacity for self-repair and (2) they do not perform biomechanically in vitro as in *in vivo* conditions (Praemer et al., 1999; Thom et al., 2006).

1.2 Biological aspects involved in TE approach

Biological and functional tissues basically consist of three key components: cells, signaling systems and extracellular matrix (ECM) [Lanza et al., 2000]. Therefore, combining together the three components and finding the best combination of stimuli and supports could generate an engineered tissue replacement *in vitro* appreciable as an excellent alternative to direct transplantation of donor organs [Langer et al., 1993; Fucks et al. 2001; Saltzman et al., 2004]. The cells, core of the tissue, are the main character of the tissue regeneration and repair, working and living in presence of a few stimuli and regulating factors In order to be used for TE applications, the cells' source must be accessible and the derived lines easily expandable with physiological and phenotypical properties and functions able to endure during the experimental operations. Due to a lack of human-organ availability, the current main source of hepatocytes for bioartificial systems is exogeneic material (rat, porcine, mouse, hamster), but although they demonstrate the same qualities of human cells, these type of cell sources carry the risk of xenogenic infections and lack of metabolic compatibility. Stem cells have been suggested as interesting alternative to animal source. Stem cells, are derived from a few human tissue, as bone marrow or umbelical cord, and they are the most flexible cells known in nature, being undifferentiated in morphology and biological pathways and expressing a remarkable ability to differentiate into a desired cell type under specific stimuli.

The signaling system consists of genes that secrete transcriptional products when differentially activated, and urgesspecific cues for each process involved in the tissue formation and differentiation [Lanza et al., 2000].

The ECM defined as network-like substance within the extracellular space, is able to supports cell attachment, cell-cell interactions and promotes cell proliferation [Badylak et al., 2007; Blitterswijk et al., 2008]. The native ECM is composed basically of water, proteins and polysaccharides, but in truth, each tissue has an ECM with a unique composition and topology, generated during tissue development through a dynamic biochemical and biophysical dialogue between the various cellular components and the cellular microenvironment. Indeed, the physical, topological, and biochemical composition of the ECM made it not only tissue-specific, but also highly heterogeneous. Moreover, the ECM is a highly dynamic structure that is constantly remodeled, through a few post-translational modifications. Thanks to these physical and biochemical characteristics the ECM generates the biochemical and mechanical properties requested of each organ, i.e. tensile and compressive strength and elasticity, mediating the extracellular homeostasis and the water

retention. Furthermore, the ECMs guides morphological organization and physiological function of a tissue by binding the growth factors (GFs) and interacting with cell-surface receptors to elicit transduction signals and regulating gene transcriptions [Frantz et al., 2010]. Collagen, is a fibrous protein and a major natural extracellular matrix component. It is the most abundant protein in mammals and is the main structural element

In skin, bone, tendon, cartilage and blood vessels and heart valve [Creighton, 1993; Kose et al., 2005; Lee et al., 2000; Taylor et al., 2006]. There are 25 types of collagen differing in their chemical composition and molecular structure have been identified. Te bulk of interstitial collagen is transcribed and secreted by fibroblasts, but a few cells can recruit it from neighboring tissues and collect it in their stroma [De Wever et al., 2008]. Due to the importance of the ECM in so many fundamental cellular processes, a lot of tissue-culture models have been developed to study its biochemical and biophysical properties in order to understand the mlolecular origins and the regulation mediated by ECM. Tissue engineers and biomaterial specialists have generated ECM scaffolds from various tissues [Macchiarini et al., 2008], and once combined with colonies of seeded cells, they showed the ability to reconstitute normal tissues with reasonable fidelity to the native one (Lutolf et al., 2009). ECMs have also been isolated and extracted from various tissues, such as small intestine, skin (from cadavers), pancreas and breast [Rosso et al., 2005], and they have been used to engineer skin grafts, for enhancing wound healing and to study tumor progression through the ECM changes in time [Badylak et al., 2007]. The role played by ECM proteins in tissue development was further demonstrated in relation with the surface chemistry and the topographic properties. The presence of a fibronectin layer adsorbed on a Ca-P thin film improved osteoblast response in terms of adhesion, proliferation and differentiation; moreover on underlying regular Ca-P surface topography cells showed negative statistically significant differences in focal adhesion assembly, protein expression and features [Cairns et al., 2010]. Appeared clear that the chance to reproduce through new biomaterials an ECM-like system would represent the best way to improve the biological answer and the tissue regeneration *in vitro*. The considerable progress in the field of biomaterials science led researchers nowadays to reproduce and then benefit artificial ECMs in different conformation (scaffolds or membanes) and use them as support for engineering a new tissue from isolated cells. Properly designed, these artificial ECMs provide an appropriate environment and the mechanical support for the tissue formation and regeneration [Langer et al., 1993; Abatangelo et al., 2001; Putnam et al., 1996].

1.3 Key concepts

TE in vitro approach, showed in figure 1.2, foresees three steps basically: 1) Cells isolation by biopsy from a patient or a donor and their consequent amplification in number with conventional methods in vitro. Cells are cultured under specific conditions and regulated parameters, as humidity, CO_2 level, pH, temperature and medium composition (growth factors and nutrients). 2) Cell seeding or impregnation on a biomaterial in form of scaffold, membrane, hydrogel or carrier where growth, proliferation and differentiation are stimulated and sustained. 3) Maturation of the new engineered construct until functional tissue/organ-like units are obtained. The new tissue answers are eventually monitored, investigated and recorded in order to collect informations about its biochemistry and physiology, main research step in order to use it for further *in vitro* studies, i.e. pharmacological treatment for the drug response, or the final implantation into the patient for in vivo experimentations, avoiding clinical problems as stress shieding, allergic reactions, wear particles and chronic inplammatory reactions.

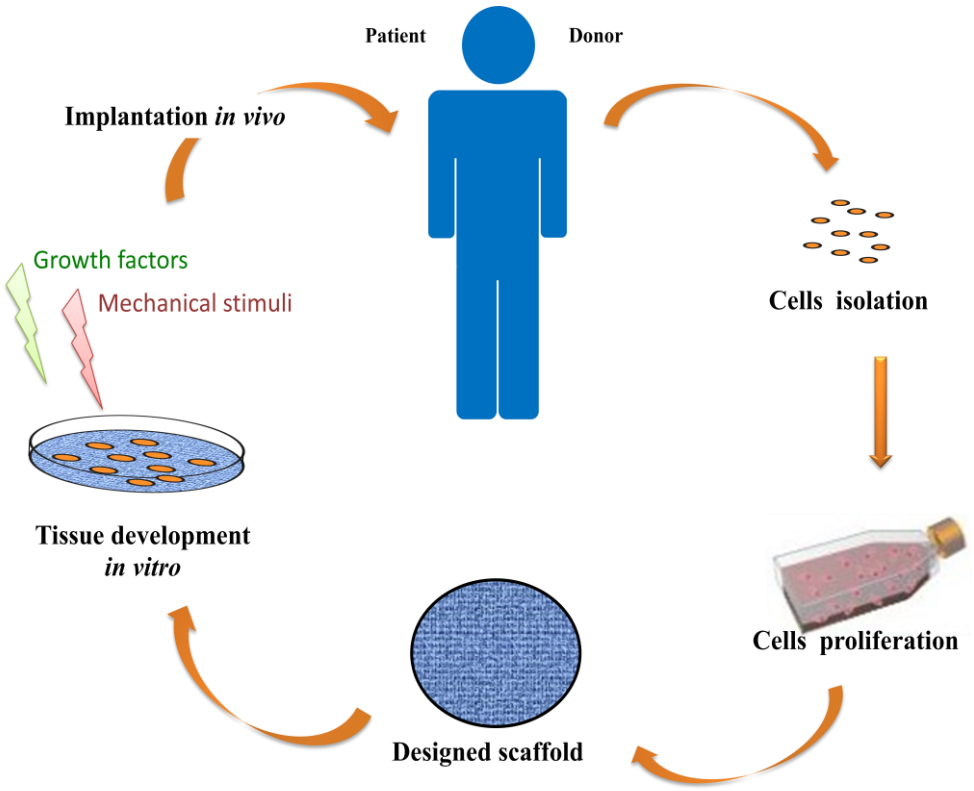

Fig. 1.2 Schematic illustration of Tissue Engineering approach

The ECM-like scaffolds, with specific physical, mechanical and biological properties, act as substrates for cellular growth, proliferation and support for new tissue formation. Then independently on the application it will be used for, the final bio-hybrid device need to imitate in their composition and structure the naïve and physiological condition for specific cells to perform complex biochemical funcions, including adaptive control and the replacement of normal living tissues, once the new mimic is obtained.

1.4 Scaffolds for TE

The design of a scaffold ultimately determines the functionality of the grown tissue. Scaffold design comprehends the material and the processing method used, and additionally the appearance of the construct (shape, size and surface topography). As already explained, since each type of tissue requires particular conditions, the understanding of all the specific natural biological environment requested *in vivo* must be known to allow optimization of culturing *in vitro*. Mass transport and biophysical signaling, showed to improve and control the structure, composition, and functional properties of engineered tissues. A scaffold is defined as a solid biomaterials properly designed in order to perform specific functions and can be considered as a surrogate of the ECM, that biologically contributes to mechanical integrity and has important signaling and regularity functions in development, maintenance and regeneration of tissues [Langer et al., 2004; Muschler et al., 2005; Lutolf et al., 2005]. Although the final requirements depend on the specific purpose of the scaffold and its final application, several characteristics (fig. 1.3) are specifically requested for all designs [Hutmacher et al., 2000; Moroni et al., 2008]. The scaffold should be/have: 1) biocompatible; it should induce an appropriate biological response in a specific application and prevent any adverse response of the surrounding tissue [Babensee et al., 1998; Williams et al., 2008]. 2) biodegradable; the scaffold materials should degrade in tandem with tissue regeneration and remodeling its matrix into smaller non-toxic substances without interfering with the function of the surrounding tissue [Hutmacher et al., 2001]. The decomposition rate of a scaffold directly depends on the chemical-physical characteristics of the biomaterial it is made of, and it can be adjusted by modification of the crystal phase and structure of the starting material and the ratios of all the elements in the system. The degradation rate has to be adapted to the tissue reconstruction going along with the progressive healing and tissue synthesis process, thus the cutback of the scaffold can be varied within the time scale between several weeks to months,

with products of degradation that must not disturb the cell and the regeneration process. 3) promote cell attachment, spreading and proliferation; required for the regulation of cell growth and differentiation [Ito et al., 2007]. The adhesion process is for most cell types a prerequisite for a functional differentiation, matrix production and survival. Its quality (e.g. adhesion kinetics and bonding strength between biomaterial and cell) depends on the charge distribution, the wettability and the surface structure in the nanometer scale. The proliferation rate and migration too are higher on smooth materials than on rougher surfaces, then regulating the scaffold surface topography the tissue formation can be sustained and improved in terms of organization and increasing of functions [Wang et al., 2010; De Bartolo et al., 2007, 2008; Papenburg et al., 2007]. 4) suitable mechanical strength; scaffold endurance and stiffness should be comparable to *in vivo* tissue in the site of implantation; that means, a scaffold requires flexibility or rigidity depending on its final application, i.e. cardiovascular versus bone prostheses [Mitragotri et al., 2009]; 5) good transport properties; if it has to be used as container for cell culture it must ensure sufficient nutrient transport towards the cells and removal of waste products, then good porosity and pore connectivity are essential [Agrawal et al., 2001; Karande et al., 2004]. A sufficient nutrient supply and exchange of metabolic products of cells within a scaffold is the main request *in vitro* and *in vivo* conditions, then the basis of a successful tissue engineering product lies in a scaffold able to combine them in its substructure. Large pore sizes with an interconnective pore structure can create the perfect conditions for the mass transport and the diffusion of nutrients and growth factors necessary to keep the cells inside vivid, and lower ones ensure the requested integrity and sustainability when mechanical load is applied [Chirila 2001]. The needed pore properties of a scaffold that enable the ingrowth of functional tissue in a scaffold material depend on the desired tissue type; for the synthesis of vital tissue it has been proved the necessity of a mean pore diameter of about 50 µm for the soft systems, about 100 µm diameter for the ingrowth of rigid material (as the extracellular phase of osteoblasts), and at least 450 µm diameter for a vivily vascularized tissue. 6) easy to connect to the vascular system of the host as soon as implanted; to ensure good nutrient supply throughout the scaffold post-implantation, the scaffold should be connected to the natural nutrient supplying system [Hutmacher et al., 2000; Agrawal et al., 2001, Kannan et al., 2005].

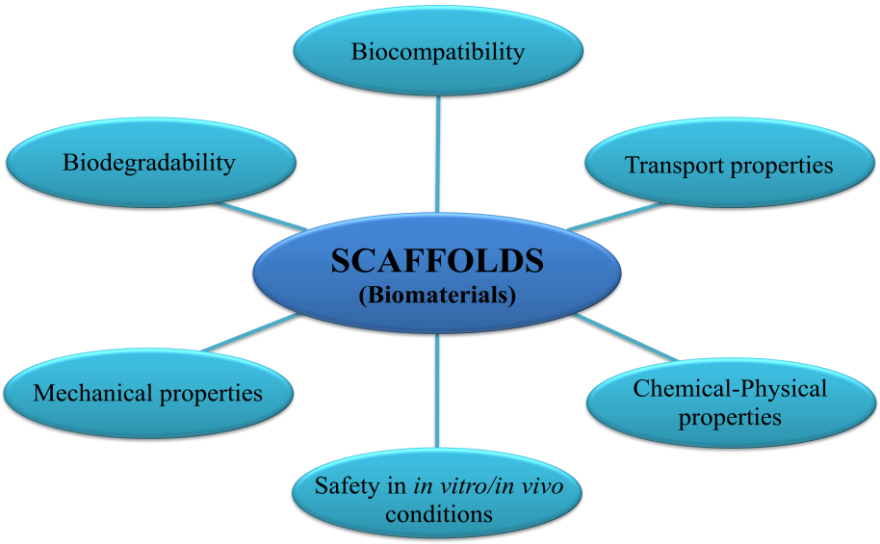

Fig. 1.3 Characteristics requested for a scaffolds (biomaterials) suitable for Tissue Engineering applications

These requirements are fulfilled by choosing the proper biomaterial and a specific production process as described in the following paragraphs.

1.5 Scaffolds production and processing methods

Many methods have been used for the production of scaffolds, membranes or hydrogels to be used as framework materials for the creation of microenvironments that reproduce the metastable tissues surrounding. The TE community has begun to capitalize all the methods available for the material processing since 1980s, in order to highlight the best techniques through which rproduce scaffolds able to mimic the native ECM. This section reports only some of the more representatives between the processing methods for the scaffold preparation, whereas a summary presentation of other techniques is reported in table 1.1.

i. *Solid freeform fabrication (SFF)* uses a computer-generated models to layer-manufacturing supports for tissue culture with improved parameters such as pore size, porosity and pore distribution. Layer by layer every section of the scaffold is generated and linked one to another until the final shape and dimension is reached. As results of oxygen and nutrients mass transport into the inner mesh of the scaffold are increased supporting cellular growth in all the regions [Sachlos et al., 2003].

ii. *Electrospinning* [Pham et al., 2006] allows the production of polymer fibers with variable diameters [Subbiah et al., 2005]. The process consists of applying to a solution an electric field through a high voltage source inducing in a charge repulsion

within the solution. When the generated system is stable a jet stream is initiated and the solvent is induced to evaporate from the solution and the resulting fiber is collected. Controlling and varying the process parameters, as viscosity of the solution, the dielectricconstant of the solvent, its conductivity, the surface tension of the polymer, its molecular weight, the distance between tip and collector, the flow rate, the strength of the electric field, it is possible to obtain a final product with all the specific characteristics required.

iii. The *Solvent Casting methods* foresees the dissolution of a polymer, in an specific solvent. The homogeneous solution obtained is treated with pore-forming substances before being filled into a mold, and the precipitation of the polymer occur. Salts, saccharose, ice, gelatine or paraffin are just some of the porogens usable [Yannas et al.1989]. The pore builders determine the later pore size, distribution and porosity. After the casting process, the solvent evaporates and a termic treatment or a bath are used to leach or evaporate the pore builders, revealing a porous scaffold. Natural materials like peptides can be use too in order to produce substrates and/or scaffolds for supporting cell culture in TE applications by this method.

iv. Due to their *self assembling* properties the mostly amphiphilic molecules with a strong *b*-sheet configuration in water (or sucrose), a hydrophobic face (e.g. the $–CH_3$ groups of the Alanin residues) and a hydrophilic face (the –COOH groups of the aspartic acids and the –NH2 groups of the arginine groups) react in a specific way rearranging their natural structures and originating a scaffold. Peptides spontaneously self-assemble in anti-parallel arrangement, forming a network of interweaving fibers of several mm in length (with an average thickness of 10 nm) and pores of 5 to 200 nm in diameter [Garreta et al., 2006] when anion stremgth is increased or pH values are raised to neutrality (e.g. physiological salt concentrations, culture media, buffers).The RAD16-I peptide is such a self assembling protein available in the form of the BD PuraMatrix Peptide Hydrogel®, it is used to form suitable scaffold for osteoblasts and liver cells [Zhang et al., 2003].

v. The *Photopolymerization,* mainly used for the production of hydrogels, is a processing method carried out using resins as mixtures of simple low-molecular-weight monomers capable of chain reacting to form solid long-chain polymers when activated by radiant energy within specific wavelength range [Yang et al., 2002]

vi. *Freeze Drying* is a commonly used technique to process heat sensitive bioproducts. The method is based on the formation of ice crystals that induce porosity after their

sublimation and desorption. Even if the structural stability of the final sacaffold and its mechanical properties are not easy to ensured (consequence of the hydratation during the final step), through this technique it is possible to control and determine the porosity level by varying the freezing time and the annealing stage [Liapiz et al., 1996; Hottot et al., 2004].

Method	Material	Application	References
Biodegradable porous scaffold fabrication			
Solvent casting/salt leaching method	PLLA, PLGA, collagen	Bone and cartilage tissue engineering	Mikos et al., 1993, 1994 Ochi et al., 2003
Ice particle leaching method	PLLA & PLGA	Porous 3D scaffolds for bone tissue engineering	Holy et al., 2000 Karp et al., 2003 Kang et al., 2006
Gas foaming/salt leaching method	PLLA, PLGA & PDLLA	Drug delivery and tissue engineering	Mooney et al., 1996 Yoon et al., 2001 Murphy et al., 2002
Microsphere fabrication			
Solvent evaporation technique	PLGA, PLAGA	Bone repair	Laurencin et al., 1996 Devin et al., 1996 Woo et al., 2001
Particle aggregated scaffold	Chitosan, HAP	Bone, cartilage, or osteochondral tissue engineering	Borden et al., 2003 Malafaya et al., 2005, 2008
Freeze drying method	PLLA, PGA, PLGA, PPF, Collagen, and Chitosan	Scaffolds for TE	Zhang et al., 1999 Ohya et al., 2003, 2004
Hydrogel scaffold fabrication			
Micromolding	Alginate, PMMA, HA, PEG	Insulin delivery, gene therapy, bioreactor, and immunoisolation	Yeh et al., 2006 Fukuda et al., 2006 Khademhosseini et al., 2006
Photolithography	Chitosan, fibronectin, HA, PEG, PNIAAm, PAA, PMMA, PAam, and PDMAEM	Microdevices, biosensors, growth factors, matrix components, forces, and cell-cell interactions	Beebe et al., 2000 Liu et al., 2002 Dendukuri et al., 2006
Microfluidics	PGS, PEG, calcium alginate, silicon and PDMS	Sensing, cell separation, cell-based microreactors, and controlled microreactors,	Nisisako et al., 2002 Burdick et al., 2004 Nie et al 2005
Emulsification	Gelatin, HA, and collagen	Sustainable and controllable drug delivery therapies	Peppas et al., 1993 Alexakis et al., 1995 Reis et al., 2003
Fibrous scaffold fabrication			
Nanofiber electrospinning process	PGA, PLA, PLGA, PCL copolymers, collagen, elastin, and so forth	Drug delivery, wound healing, soft tissue synthetic skin, and scaffolds for tissue engineering	Doshi et al., 1995 Li et al., 2003 Zheng et al., 2005
Microfiber wet-spinning process	PLGA, PLA, chitosan, and PCL	Solar sails, reinforcement, vascular grafts, nonwetting textile surfaces, and scaffolds for tissue	Hirano et al., 2000 Ponfret et al., 2000 Okuzaki et al., 2009
Nonwoven fibre by melt-blown process	Polyesters, PGA, and PDO	Filtration, membrane separation, protective military clothing, biosensors, wound	Lyons et al., 2004 Ellison et al., 2007 Kin et al., 2009

		dressings, and scaffolds for tissue engineering	
Ceramic scaffold fabrication			
Sponge replication method	PUsponge, PVA, TCP, BCP or calcium sulfate	Bone tissue engineering	Sepulveda et al., 1999 Chen et al., 2006 Shin et al., 2009
Simple calcium phosphate coating method	Coating on: metals, glasses, inorganic ceramics and organic polymers (PLGA, PS, PP, silicone, and PTFE), collagens, fibres of silk, and hairs	Orthopedic application	Li et al., 2002 Chen et al., 2006 Yang et al., 2008
Keratin scaffold fabrication			
Self-assembled process	Keratin	Drug delivery, wound healing, soft tissue augmentation, synthetic skin, coatings for implants, and scaffolds for tissue engineering	Tachibana et al., 2002, 2005 Katoh et al., 2004

Table 1.1 Scaffolds' fabrication techniques in tissue engineering applications

1.6 Biomaterials for scaffold fabrication

Due to the variation in mechanical properties required in 'soft' versus 'hard' TE applications [Mitragotri et al., 2009], different classes of biomaterials could be used for the design of a scaffold and the production of a tissue engineered constructs. For soft TE applications, e.g. skeletal muscle or cardiovascular substitutes, generally a wide variety of polymers are applied. On the other hand, hard tissue replacements, e.g. bone substitutes, are generally based on more rigid polymers, ceramics and metals. Choosing, modifying and developing a biomaterial able to interface with biological systems is not a simple task. An appropriate substructure, charge conditions, permeability, pore size, degradation rate, mechanical properties (e.g. youngs modulus, aggregate modulus, poisson ratio) and viscoelasticity are the requirements that allow a biomaterial to be processed into a defined shape and to act as a suitable support for the tissue regeneration, driving the spreading of the cells and their rearrangement towards a definite tissue. To serve in the process of tissue reconstruction and regeneration the properties of the biomaterial must ideally have defined characteristics [Eisenbarth et al., 2007], that reflect on the final scaffold properties, already described in section 1.4: **a.** The biomaterial must support cell processes with a suitable surface chemistry for cell attachment, proliferation and differentiation. **b.** The crystalline substructure has to maximize the space for cellular adhesion, growth, extracellular matrix secretion, revascularization, adequate nutrition and oxygen supply without compromising mechanical strength, in order to assist the cellular ingrowth and the transport of nutrients and oxygen. **c.** The biomaterial must degrade along with the reconstruction of the newly build tissue. The degradation products must not be toxic and not affect the tissue regeneration and remodeling process. **d.** The biomaterial must be sterilizable to avoid toxic contamination through hot or chemical treatment. Biomaterials used for this purpose are polymers, ceramics, bioglass, and metals either of natural or synthetic origin. They can undergo a large variety of processing methods in order to reach a final form with the appropriate properties for a special application. Collagen, Chitosan, Alginate derivates, have been useful to hold up the regeneration of the cartilage tissue [Cho et al., 2010; Lu et al., 2001; Gutowska et al., 2001; Nettles et al., 2002, Shu et al., 2003], whereas Polyglycolic acid (PGA), Poly(L)-lactat (PLA) and other, are currently applied in skin tissue regeneration and generally for suture applications [Lebourg et al., 2008; Donlan et al., 2002]. The first biomaterials chosen for tissue engineering boast to have natural origin as collagen, fibrin or silk. Later degradable synthetic polymers and hydrogels were used to better meet the special requirements thanks to

a better adjustability of their properties. In fact operating on the biomaterial characteristics, as substructure, charge conditions, hydrofilicity, pore size, degradation rate, mechanical properties (e.g. youngs modulus, aggregate modulus, poisson ratio) and viscoelasticity, all the engineeristic requirements can be perfectly fulfilled. The differentiation status of the cells is based on a biochemical support (e.g. growth factors) and the properties of the biomaterial the cells interact with, as already said, in terms of charge conditions, mainly the surface energy, the substructure, the mechanical properties of the material and the degradation kinetics. The adhesion process (e.g. adhesion kinetics and bonding strength between biomaterial and cell) for example is, for the most cell types, a prerequisite for a functional differentiation, matrix production and survival. Table 1.2 summarizes biomaterials, forms, production methods used for tissue engineering.

Biomaterials	**Form of Applications**	**Processing method**	**Engineered tissue**
Natural origin: Collagen networks, Alginate, Chitosan, Gelatin Fibrin and Hyaluronic acids	Polymers Hydrogel o Scaffold 3D Membranes	Solvent casting Cryo Etching Electrospinning e Mineralization	Cartilage, Heart muscle Nerve cells, spinal cord optical neurites epidermal cells
Synthetic origin: Polyglycolic acid (PGA), Poly Lactic acid (PLA), Poly(L-lactide-co-glycolide) (PLGA), Poly-hydroxymethyl methacrylate, (PHEMA), Chitosan, Poly-l-lactic acid (PLLA), Polycaprolactone (PCL)	Hydrogel Scaffold Polymeric films Membranes	Solid free form fabrication Solvent casting Electrospinning	Tendons Intervertebral disk spinal cord smooth muscle epidermal cells
Ceramics Calcium phosphates Bioglass	Scaffold, Carrier, Coating	Sintering from natural bone Sol-Gel-Process	Scaffold or coating for bone Carriers for cartilage
Metals Tantalum Magnesium	Metals Scaffolds	Powder metallurgy Casting	Bone or cartilage contact

Table 1.2 Biomaterials: forms, production methods used for tissue engineering

Collagen, one of the main structural element of the ECM, and the most abundant protein in the body, it has been proved supply tensile strength, regulate cel adhesion, support chemotaxis and migration, and direct tissue development [Rozario and De Simone, 2010]. Among the 25 distinct forms identified, type I collagen has been the most investigated for biomedical applications and usd for TE, especially for soft tissue repair such us skin [Kose et al., 2005], but it offers also a suitable environment for the induction of osteoblastic differentiation *in vitro* and osteogenesis *in vivo*. Having high mechanical strength, good biocompatibility and low antigenicity, it favors cellular attachment as well as being chemotactic to cells. Furthermore, collagen is widely used on its own, or as a component of a composite, for tissue engineering applications [Kikuchi et al., 2004; Ma et al., 2004 a, b; Rodrigues et al., 2003; Rothamel et al., 2005], and even its denatured form (gelatin) has been processed into porous materials for tissue repair [Choi et al., 1999]. Despite these results there are concerns with the use of collagens regarding their immunogenicity where applied to the biomedical devices production [Lynn et al., 2004], in terms of potential pathogen transmission and immune reactions [Ma et al., 2004]. Various efforts such as cross-linking of collagen and hybridization with other biomaterials are being made to overcome these potential drawbacks. Ma et al. [2004a, b] have reported using a water soluble cross-linking agent, that in vitro biodegradation degree of the collagen can be greatly decreased resulting in a more biological stable scaffold. Moreover collagen based composites (either with bioceramics or biopolymers) exhibited the advantages of both the hybrid biomaterial and collagen [Chang and Tanaka 2002a, b; Chen et al., 2001; Kikuchi et al., 2004; Rodrigues et al., 2003; Sukhodub et al., 2004]. These include increased mechanical strength with enhanced cell seeding and promoted cell interactions. Moreover growth factors and other bioactive molecules have been combined with collagen-based systems to prolong their release rate and increase the final therapeutic effects [Greiger et al., 2003; Wallace and Rosenblatt, 2003]. Other ECM components usable as materials for TE are available. The fibronectin, for example, is able to induce cell attachment and spreading through different binding and synergy sites on its structure. Deposited and oriented layer of fibronectin showed to enhance the viability of HUVECs with respect of classical culture systems [Calonder et al., 2005]. On the other side, the fibrin, even not being a regular component of the ECM, it has been found as a temporary matrix during the haemostatic and tissue repair processes; it has been fully ised for skin TE and as cell delivery matrix for cartilage TE, particularly in combination with alginate [Perka et al., 2000] and hyaluronic acid [Park et al., 2005]. Hyaluronic acid, is an important element of the connective tissue, the synovial fluid and the vitreus eyes humor. Being a polysaccharide, it

exhibits vicoelastic properties that make it a good lubrificant and a biological absorber easily produced in large scale through microbial fermentation, allowing its use as sponge for the treatment of osteochondral defects [Solchaga et al 2005], flat sheet scaffolds for vascular grafts [Arrigoni et al., 2006] and hydrogels [Leach et al 2003]. Chitosan is another important natural biopolymer obtained by deacetylation of chitin [Chung et al., 2002; Shen et al., 2000; Zhao et al., 2002]. It has been reported to be safe, haemostatic and osteoconductive and to promote wound healing. HA/chitosan-gelatin scaffolds have been fabricated and in vitro examination demonstrated that extracellular matrices could be synthesized and bone like tissue could be formed [Zhao et al., 2002]. Chitosan fibers, sponges, injectable cell delivery vehicles and tubes have been used for bone, cartilage and nerve regeneration [Tuzlakoglu et al., 2004; Nettles et al., 2002; Frieier et al., 2005; Hoemann et al., 2005]. An extensive presentation of all the characteristics and the applications of the CHT is reported in chapter 4.

PLA, PGA and their co-polymer, poly(DL-lactic acid-co-glycolic acid) (PLGA) are widely used in scaffold fabrication. Scaffolds made of electrospun PLGA nanofibres placed on a knitted PLGA demonstrated a good mechanical strength and internal hierarchical structure, and facilitated cell attachment and new ECM deposition, whereas non-woven, nano-fibred scaffold, fabricated from PLGA and PLA-PEG block copolymer was used for therapeutic application in gene delivery [Luu et al., 2003]. Poly(ε-caprolactone) (PCL) is a semicrystalline, bioresorbable polymer belonging to the aliphatic polyester family. It is regarded as a soft and hard tissue-compatible bioresorbable material and has been used as scaffold for tissue engineering applications [Burkersroda et al., 2002]. Its degradation makes it attractive for general tissue engineering, making it an appropriate candidate as a long-term drug delivery carrier. It is often combined with other materials, such as bioceramics, to manipulate its Young's modulus and adjust its biodegradation rate. Important synthetic biodegradable polymers are poly(ortho esters) and polyanhydrides (from nonphysiological monomers), with biocompatibility and well-defined degradation characteristics [Muggli et al., 1999]. Originally designed for controlling drug delivery devices [Burkoth et al., 2000; Hanes et al., 1998; Ibim et al., 1998], they have also been explored for the tissue engineering. Ibim et al. (1998) reported that the biocompatibility of poly(anhydride-co-imide) is equal to PLGA, and that it is able to support cortical bone regeneration. An implantable scaffold made from poly(anhydride-co-imide) has been used in orthopaedic surgery and other weight-bearing applications since 2000s [Burkoth et al., 2000]. Tyrosine-derived polycarbonates based on natural metabolites (the amino acid tyrosine) are another synthetic biopolymer currently used as tissue engineering scaffolds. An in vivo experiment carried out in a canine bone chamber

model revealed that tyrosine-derived polycarbonates, are comparable, if not superior, to PLA in terms of biocompatibility [Choueka et al., 1996]. Poly(propylene fumarate) (PPF) is a linear polyester degradable through hydrolysis of the ester bonds [Peter et al., 1998]. Its major advantage over many other biodegradable synthetic polymers is represented injectability, that means the PPF systems are usable for direct application into a patient's defect site and cross-linking in situ. It is often used also in cooperation with another osteoinductive component, such as b-tricalciumphosphate (b-TCP) [Peter et al., 2000], osteogenic peptides or proteins through the use of PLGA based microparticles [Hed berg et al., 2005 a, b; Kempen et al., 2006; Schek et al., 2006]. Peter et al. (1998) reported that the mechanical properties of PPF/TCP composite scaffold exhibit mechanical properties similar to human trabecular bone and maintained these properties over several weeks of degradation.

Then, the biomaterials usable originate from a wide range of natural as well as synthetic source and many progresses are reported in literature in TE field.

A single material alone might often not have sufficient mechanical strength or chemicalphysical characteristics to ensure all the main requested properties, then in order to generate everytime a better environment for tissue regeneration, the combination of two or more classes of materials is the bestb way for improving results and reinforcing the final products. A combination of two material types thus reduces their drawbacks while benefiting from their respective advantages [Zhao et al., 2008]. Synthetic inorganic materials in these cases are used in combination with polymers in order to increase the final properties of the scaffold. When bioactive ceramics, i.e. hydroxyapatite, are hybridized with biodegradable polymers, the final composite systems created posses a level of flexibility, appropriate mechanical properties, as well as improved biological activity and osteoconductivity [Shor et al., 2007; Lebourg et al., 2010; Kim et al., 2004]. There is a wide variety of biocompatible materials which includes bioceramics, synthetic and natural biopolymers available for tissue engineering. Each material has its own characteristics, and within each family of materials there is a range of properties and characteristics. There seems to be less emphasis on new materials, but rather on the combination, processing or other treatment of established systems in novel ways. The selection of materials therefore depends on the specific requirement dictated by the application and suitable fabrication technique. TCP and HA ($Ca_{10}(PO_4)_6(OH)_2$), and their combinations are the most frequently used bioceramics in scaffold manufacturing [Daculsi, 1996; Meenen et al., 1992]. These two bioceramics have excellent biocompatibility with hard tissues, and high osteoconductivity and bioactivity. They have neither antigenicity nor cytotoxicity and can be processed into porous form for use as

bone substitutes or scaffolds [Kikuchi et al., 2004; Liu, 1997; Miko and Temenoff, 2000; Sukhodub et al., 2004; Vail et al., 1999]. However, their use is limited because of their brittle nature and the difficulty in processing into highly porous structures with controlled porosity [Liu, 1997; Meenan et al., 2000]. To overcome these disadvantages and to enhance their biocompatibility and cell attachment, these bioceramics (HA and TCP) are usually combined with collagen to make HA/collagen composite scaffolds [Clarke et al., 1993; Rodrigues et al., 2003]. This can be fabricated by dissolving and thoroughly mixing fine HA powder and collagen in an acidic solution. The composite is harvested by centrifugation and then freeze dried. Kikuchi and co-workers [Kikuchi et al., 2004; Zhang and Ma, 1999b] have fabricated a bone-like HA/collagen composite by using a biomimetic co-precipitation method. The bone tissue reactions demonstrated excellent osteoclastic resorption and bone formation which is very similar to the reaction of a transplanted autogenous bone. The in vitro study using human osteoblasts revealed that the cells adhered and spread on both the HA particle surface and the collagen fibres, and was proposed as an ideal scaffold for osteoconduction. In truth, the bioceramics are not the only elements available for the production of composites: metals and carbon are nowadays fully employ too. Nanoparticles of noble metals have been investigated with high interest for biomedical applications since 1971 [Faulk et al., 1971], and from then they where used as probes for electron microscopy, drug delivery and detection, diagnosis and therapy; gold and silver are for sure the most used and well known. The silver in particular has the ability to release its ions in a controlled manner which in turn lead to an amazing antibacterial activity against a large range of bacteria [Falletta et al., 2008; Evanoff et al., 2005] allowing it to arise as a really interesting tool for design of new devices in the TE field and medical applications. Processed in form of nanotubes, the carbon, has the potential in providing the needed structural reinforcement for biomedical scaffolds. By dispersing a small fraction of carbon nanotubes into a polymer, significant improvements in the composite mechanical and electrical properties have been observed.

1.7 Polymeric membranes as biomaterials in TE and medical applications

Owing to their similarity with the extracellular matrix (ECM), polymers over all other biomaterials available, can satisfy the requirements of biomedical applications, also avoiding chronic inflammation or immunological reaction and toxicity. Whether it's natural or synthetic, a polymer is an organic compounds formed by monomeric units recurring as building blocks and linked together in a specific manner through covalence bonds. These

small units, matched with a specific industrial processing method, allow the control of the final polymeric structure in terms of chemistry (linear, branched, reticulate chain) and morphology (amorphous or crystalline phase). All these aspects eventually affect the mechanical-physical properties of the materials and their final applications. Molecular weight, polymerization degree, organization of the multiple chains, and then the response of the polymer to physical-chemical energy in form of temperature, mechanical strength and pH, are the parameters which determine the choice of a particular technique or a processing methods, suitable for obtaining the final form of the biomaterial for a specific biomedical application. Though scaffolds, hydrogel, carrier, are the most famous and used final form obtained from polymers, an amazing increasing in the last twenty years has been recorded in the use of polymers processed in form of membranes (table 1.3). Processes of purification and removal of toxic substances from soils, row or sea water treatment, and also the production of synthetic materials for the textile industry and the packaging for the food, are in truth well-known industrial applications where polymeric membranes have been used, but being easily reproducible and workable made them more interesting day by day in the field of the tissue engineering and regenerative medicine both for *in vivo* and *in vitro* study system. Polymeric membranes can be classified according to various parameters, such as the nature of the polymer used for their production (natural or synthetic), their structure (symmetric, asymmetric, porous, dense, etc..), configuration (flat or cylindrical) or physical-chemical properties of the final membrane (hydrophobic or hydrophilic). Despite being produced industrially, the main characteristic that a polymeric membrane has is certainly the ability to resemble the cellular membranes in terms of separation properties of substances and molecules of different kinds and sizes, then its permeability. This is the reason why even in the medical field a wide variety of polymeric membranes are of high importance. The mass transport process through a membrane is the one of the real attractive characteristics, fundamental for the breathing of cells and tissue. Being the driving force for the nutrient supply and the removal of the metabolites from a biological system across the membrane, the mass transport is a non-equilibrium process and is conventionally described by the phenomenological equations [Porter, 1990]. Today, the membranes are used for blood oxygenation and purification in replacement or substitution of pulmonary and renal function, and in hybrid artificial organs (bioartificial liver, bioartificial pancreas) for the therapeutic treatment of patients with deficiencies of type staff who are waiting for organ transplantation or regeneration partially damaged [Langer et al., 1993].

Polymer	Thermal and mechanical properties		TE applications	References
	Melting point [°C]	Glass transition temperature [°C]		
Polylactic acid PLA	173-178	60-65	Fracture fixation, Interference screws, suture anchors, meniscus repair	Shin et al 2003; Koegler et al 2004; Lu et al 2000; Bendix et al 2008
Polyglycolic acid - PGA	35-40	35-40	Suture anchors, meniscus repair, medical devices, drug delivery	Shin et al 2003; Koegler et al 2004;
Poly(3-caprolactone) PCL	58-63	-60	Suture coating, dental , orthopaedic implants	Lepoittevin et al 2002; Griffith et al 2000
Poly- latic-co-glycolic PLGA	Amorfo	50-55	Interference screws, suture anchors, ACL reconstruction; suture; drug delivery; artificial skin; wound healing	Shin et al 2003; Koegler et al 2004; Lu et al 2000
Poly(Propylene Fumarate) - PPF	30-50	-60	Orthopaedic implants, detal,foam coatings, drug delivery	Shi et al 2005; Sitharaman et al 2007
Chitosan - CHT	270	61	Tissue replacements; Wound dressings skin substitutes; wound dressings skin substitutes; drug/growth factor delivery	Liu et al., 2011; Madihally et al., 1999; Riva et al., 2011; Leedy et al., 2011
Polyurethane - PU	240		Transdermal drug delivery patches; Transient cardiovascular devices; Ventricular assist devices; Intra-aortic balloon pumps; Wound dressings and barrier scaffolds	Yoda et al., 1998;

In bioartificial organs, membranes act as immunoselettive barriers, which serve to prevent the contact between the cells and the immunocompetent species present in the blood of the patient, and at the same time permit the transport of nutrients and metabolites to and from the cells [Catapano et al., 1996]. In such devices, the membranes also function as a means for the oxygenation of the cells and as support for the anchorage-dependent cells like the hepatocytes [Bader et al. 1999; De Bartolo et al. 2000; Bader et al., 2000] mimicking *in vitro* the *in vivo* conditions and the cellular environment. For this reason membrane characteristics, as selective permeability, biostability, and induction of cell growth, can play a decisive role in the interaction cell-membrane. Therefore the choice of a particular polymeric membrane for a medical device depends on its permeability characteristics as well as its chemicalphysical properties and separation processes [De Bartolo et al., 1999; De Bartolo et al., 2004]. The importance of the morphological and physicochemical properties of the polymer surface in cell interactions has been demonstrated. Surface free energy, electric charge and morphology might all affect the cell attachment and behavior, and when correctly developed, they could support cell processes that build up a new functioning tissue [De Bartolo et al., 2008]. It has been proved also that cells morphology changes depending on the surface properties they adhere to [De Bartolo et al., 2006; Drioli et al., 2006]. Several degradable polymers, including Collagen, Chitosan, Hyaluronic acids, Polyglycolic acid (PGA), Poly(L)-lactat (PLA), Poly(DL)glycolactate (PLGA), Poly-l-lactic acid (PLLA), Polycaprolactone (PCL), Polyurethane (PU), have been used for many engineeristic purposes, due to their characteristics of biodegradability and biocompatibility. Nowadays in particular, synthetic polymeric membranes in various conformations (flat, capillary, hallow fiber, etc.), are widely used in innovative biomedical devices, thanks their stability and permeability characteristics. The ability to engineer specific surface features that will actively promote surface interactions can present an opportunity to control the cell response. Cells are constantly sensing, responding and modifying their behavior in response to their immediate environment, in a relationship "cell-biomaterials" that can be described as dynamic. The PEEK-WC-PU membranes, for example, combine both the starting polymers advantages (biocompatibility, mechanical strength, elasticity) optimizing properties as permeability, selectivity and geometry. Hepatocytes showed a high-profile adhesion when cultured on PEEK-WC-PU membranes, with results comparable to collagen and other natural substrates [Salerno et al., 2009]. In the engineering of liver tissue constructs for diagnostic and therapeutic applications, it is a challenge to support hepatocytes functionality for a long time, indeed they are known to rapidly lose their liver specific functions and to show strong spontaneous alterations in gene

expression patterns when maintained under standard *in vitro* culture conditions. Biodegradable and non-biodegradable polymeric matrices have been studied and used both in *in vivo* and *in vitro* systems, showing that polymers represent an optimal solution to be a support for hepatocytes, until they are replaced by living tissue. Polyglycolic acid (PGA), polylactic acid (PLA) and other natural and synthetic polymers have been also studied for the liver regeneration and engineering. The tissue engineering of the nervous system is the science of design and plan systems in which nerve cells are organized in a controlled manner to simulate the nervous system. The cellular organization must include the control of the cell-cell interactions and of the surrounding environment, since the functionality and repair of neuronal cells depends on their intrinsic genetic program and from the extracellular environment. In different regeneration context the surface micro-geometry [Aebischer et al., 1990], the molecular weight of polymer and the membranes' molecular weight cut-off (MWCO) [Aebischer et al., 1989], the electrical properties, and the rate of degradation of materials [Maquet et al., 2001] appear to have a marked influence on the tissue response, and also mechanical and chemical regulation have been proved to be important for the growth and differentiation of cells in biohybrid systems: when neuronal cells interact with polymeric substrates induction of specific cellular responses is revealed, allowing neurons to assume a definite orientation in space with the creation of a network of synaptic connections in an *in vitro* system. [De Bartolo et al., 2009]. Moreover recent investigation of viability and specific neuronal marker expression allowed assessment that neural cell responses depend on the nature of the biodegradable polymer used to develop a membrane, as well as on the dissolution, hydrophilic and above all, mechanical membrane properties. PCL and PU membranes showed to be useful for nerve TE to the point the neuritis outgrowth and synapse development resulted well characterized if neuronal cells were cultured on them or on the PCL-PU membranes, a polymeric blend membrane, exhibiting mechanical properties able to improve the expression of specific neuronal markers [Morelli et al., 2012]. Recent research strongly suggests that the choice of scaffold material and its internal porous architecture significantly affect regenerate tissue type, structure, and function [Hutmacher et al., 2010]. The effects of mean pore size have been extensively studied [Karageorgiou et al., 2005; Zeltinger et al., 2004], and Chang et al. showed that the direction of bone ingrowth was along the long axis of the porous channels [Chang et al., 2000]. In addition to possessing the appropriate material composition and internal pore architecture for regenerating a specific target tissue, scaffolds must also have mechanical properties appropriate to support the newly formed tissue [Hutmacher et al., 2001]. Bone tissue engineering in fact typically involves the

use of porous, bioresorbable scffolds to serve as temporary, three-dimensional scaffolds to guide cell attachment, differentiation, proliferation and subsequent tissue regeneration. Conventional single-component polymer materials cannot satisfy these requirements. Although various polymeric materials are available and have been investigated for tissue engineering, sometimes as already explained, a single biodegradable polymer cannot meet all the requirements for bone engineering applications. Therefore, the design and preparation of multi-component polymer systems represent a viable strategy in order to develop innovative multifunctional biomaterials. In particular, polymer–ceramic composites have been developed to combine the intrinsic properties of each component and to optimize the physicochemical and biological properties that the hard tissues required [Wang et al., 2003]. Traditional biodegradable polyesters used in biomedical field, as polylactide (PLA) polyglycolic acid (PGA) or Polycaprolactone (PCL), are easily reabsorbed, show ductile properties, and can be processed to different devices. Bioceramics such as hydroxyapatite (HA) and tricalcium phosphate (TCP) have shown to induce a good response from bony cells and have often been combined with biodegradable polymers to produce bone substitutes because of their structural similarity to the mineral phase of bone and their osteoconductive and bonebinding properties. Indeed Hydroxyapatite $(Ca_5(PO4)_3(OH))_n$ is the main mineral component of bone and because of its high bioactivity and biocompatibility is commonly used as filler in polymer-based bone substitutes [Azevedo et al., 2003]. This approach also offsets the problems of brittleness and the difficulty of shaping hard ceramic materials to fit bone defects [Zhao et al., 2007]. In fact they are currently in use in orthopedics, despite their fragility, scarce remodeling, low flexibility and moldability. A combination of both material types thus reduces their drawbacks while benefiting from their respective advantages [Zhao et al., 2007]. When bioactive ceramics are hybridized with biodegradable polymers, the composite systems possess a level of flexibility, appropriate mechanical properties, as well as improved biological activity and osteoconductivity [Shor et al., 2007; Lebourg et al., 2010; Kim et al., 2004]. Hydroxyapatite (HA) produced from corals has been reportedly used for orthopedic bone defect reconstruction. These porous coral HA scaffolds are reported to exhibit a hydrothermal exchange reaction thereby converting porous coralline skeletal materials into HA that have similar microstructure as the starting carbonate skeletal material. A bioactive and bioresorbable scaffold fabricated from medical grade PCL (mPCL) and incorporating 20% beta-tricalcium phosphate (mPCL–TCP) has been well characterized and studied by Hutmacher et al. [Lam et al. 2008, 2007; Sawyer et al. 2009; Hutmacher et al. 2008, 2000] and all the results reveal that composite scaffolds made with polymer/ceramics matrix could

provide a suitable environment for bone regeneration acting as bone graft substitutes [Abbah et al. 2009].

Hollow fiber membranes in TE applications.

An efficient exchange of nutrients and metabolites to maintain the viability and cellular functions in vitro is really a big challenge for each *in vitro* regenerative process. Hence, the greatest innovation in the engineering and biomedical field, is represented by the hollow fiber membranes. Their particular three-dimensional structure, porosity and inner cavity allow the compartamentalization of the system and the passing through of molecular species by sieving mechanisms with their eventual separation across the membrane walls and the generation of two solutions: one constituted by the smaller in size able to permeate through the membrane, called "permeate", and the other one, constituted by molecules of larger size, hence not able to pass through, called instead, "retentate". That is the reason why the hollow fiber membranes are classified according to the molecular weight cut-off (MWCO), which is defined as the molecular weight of the species for the 90% retained by the membrane. Membranes with molecular weight cut-off in the range of 50000-100000, have been extensively used as barriers to prevent the passage of immunoselettive immunocompetent species, present in the blood of patients undergoing transplantation. However, starting from 1999, when Lamers showed that cytokines can be produced by T lymphocytes using two parallel cellulose acetate (CA) hollow fiber membrane bioreactors, numerous have been being the progresses in the development of this new kind of bioreactor devices where the HF membranes are the engineered components. Jasmund et al., some years later proposed a modified QUADROX oxygenator for the oxygenation of blood and the removal of the dioxide of carbon. Fibers of polyethylene (PE) suitable to the exchange of heat and O_2. Thereafter a complete purification of blood samples was obtained by modifying a hollow fiber membrane of cellulose acetate (CA) with copolymers of MPC (2-meta-criloilossietilfosforilcolina): PMB 30 and the PMA 30 (MPC-co-n-butyl methacrylate, and MPC-co-metacrilicacid) [Sang et al., 2006]. Other important goals were achieved in designing membrane bioreactor and one of the forefront devices seems to be system that allow the long term culture system. De Bartolo et al in 2007, developed and tested two more sophisticated bioreactors made by a bundle of PEEK-WC fibers, arranged in a parallel manner within a cylindrical glass chamber (arrangement that leads to the formation of two communicating compartments: an intraluminal, inside the fibers, and an extraluminal, outside of them), and a multi- compartmentalized membrane bioreactor, in which three membranes PESM (polyethersulfone modified), each containing 7 compartments for the T-limphocytes and the hepatocytes cells culture respectively. During the

experimentation, lasting for 14 days, adhesion, spreading growth and the production of specific factors have emerged to be higher than classic culture systems, providing a more in-vivo like systems for the cell viability [De Bartolo et al., 2007]. HFs membranes used in bioreactors then provide *in vitro* a closed reproduction to *in vivo* conditions for cell growth, but also because they allow systematic studies of the analyzed tissue responses to vatious physical and mechanical stimuli it is subjected. They also can provide technical data to understand the specific biological responses and effects to chemical and physical agents. Thus, the process of a cell line culture in a bioreactor can be well defined and standardized. In a summary it could be infer that the HF membranes: 1) offer the cells a three-dimensional structure on which to build a fabric. 2) compartmentalize the cells in a well controlled microenvironment. 3) minimize the surface / volume ratio, that is, for equal volume, a larger surface area is available for cell adhesion and exchange of metabolites, compared to a flat membrane 4) allow culture at high densities. The *in vitro* cultivation of three-dimensional constructs that support an efficient nutrition of the cells, combined with the application of a direct mechanical stimulation affect the cellular activity, differentiation and the specific functionality. Today, a wide variety of bioreactors have been developed for the engineering of tissues such as retina, skin, muscles, ligaments, tendons, bones, cartilage and liver. Ideally, a bioreactor should enable to control considerable environmental factors (pH, O2, temperature, nutrient transfer, waste removal, etc…) at well-defined levels, and allow operations as sampling and feeding and to avoid the contamination that normally could verify in a traditional culture. The levels of oxygenation, in particular, have proved to be critical for the matrix components production in the cultivation of cartilage cells, despite the controversy about the benefits of a high or low oxygen concentration. It's now known that the mechanical forces improve or accelerate tissue regeneration and cell growth. The fluid dynamic stress, or shear stress induced by the fluid flow through the surface of the construct and the open pore space, is believed to be the most important mechanical stimulus for the activation of mechanic transductional signal [Vance et al., 2005]. In 2000, De Bartolo et al., designed and characterized a flat membrane bioreactor for a high density hepatocytes culture, and simultaneously, in a microenvironment that would guarantee adequate delivery of oxygen. The hepatocytes were cultured within two layers of collagen between polymeric membranes permeable to oxygen, carbon dioxide and water vapor and monitored for 18 days in terms of synthesis of urea and albumin, elimination of ammonia and metabolism of diazepam by the cells. These membranes allow an unlimited supply of O_2 and the correct geometry for cell adhesion and the rearrangement of an architecture that is specific for all cellular functions [De

Bartolo et al., 2000]. Furthermore confermations of the amazing increasing in the liver TE in bioreactors with respect to the classical culture systems arrived in the last four years. A crossed hollow fiber membrane bioreactor was developed with the aim to reproduce the human vascular system, for supporting the long-term maintenance and differentiation of human hepatocytes. The bioreactor consisted of two types of HF membranes with different MWCO and physicalchemical properties crossassembled in alternating manner: modified polyetheretherketone (PEEK-WC) and polyethersulfone (PES), used for the medium inflow and outflow, respectively. The combination of these two fibers set prodiced and extracapillary network for the adhesion of cells and a high mass exchange through the cross-flow of culture medium. The optimized perfusion conditions of the bioreactor allowed the maintenance of liver functions in terms of urea synthesis, albumin secretion and diazepam biotransformation up to 18 days of culture. In particular the good performance of the bioreactor was confirmed by the high levels of the cytochrome P450 isoenzymes expressed. These devices then may be considered as a new potential tool in the liver tissue engineering for drug metabolism/toxicity testing and study of disease pathogenesis alternatively to animal experimentation [De Bartolo et al., 2009].

References

- Abatangelo G., Brun P., Radice M., et al. (2001). *Integrated biomaterial science.* Barbucci R., editor.New York: Kluwer Academic; P.885-945
- Abbah SA, Lam CXL, Hutmacher DW, et al. (2009). *Biomaterials*;30:5086–93.
- Aebisher P., Guenard V., Brace S., (1989). *Neurosci*.; 9:3590-3595
- Aebisher P., Guenard V., Valentini R.S., (1990). *Brain Res.*, 531: 211-218
- Agrawal CM, Ray RB. (2001). *Journal of Biomedical Materials Research*; 55(2): 141- 50.
- Azevedo MC; Reis RL; Claase MB; et al. (2003). *J. Mater. Science: Materials in medicine* 14: 103-107
- Babensee JE, Anderson JM, McIntire LV, Mikos AG. (1998). *Advanced Drug Delivery* 33 (1-2):111-139.
- Bader, L. De Bartolo and A. Haverich, (2000). *J. Biotechnology*, 81, 95.
- Bader, N. Fruhauf, M. Tiedge et al., (1999). *Exp. Cell Res*, 246, 221.
- Badylak SF. (2007). *Biomaterials*;28 (25): 3587- 3593.
- Blitterswijk CA, Thomsen P. (2008). *Tissue engineering*. 1st ed. Amsterdam; Boston: Elsevier/Academic Press.
- Burke J.F. et al (1981). *Ann. Surg.* 194, 413-428,
- Burkersroda Fv., Schedl L., Gopferich A., (2002). *Biomaterials* 23(21): 4221–4231.
- Burkoth A.K., Burdick J. and Anseth K.S., (2000). *Journal of Biomedical Materials Research*, 51: 352–359.
- Cairns ML., Meenan BJ., Burke GA., Boyd AR., (2010). *Colloids and surfaces B: Biointerfaces* 78: 283-290
- Catapano G, De Bartolo L, Lombardi C.P. and E. Drioli, (1996). *Int. J. Artif. Organs*, 19, 61.
- Chang B-S et al. (2000). *Biomaterials* 21(12):1291–8.
- Chang M.C. and Tanaka J., (2002a). *Biomaterials*, 23(24): 4811–4818.
- Chang M.C. and Tanaka J., (2002b). Biomaterials, 23: 3879–3885.
- Chapekar M.S., (2000). *Tissue engineering: challenger and opportunities*, Chemistry and life science.
- Chen G.P., Ushida T. and Tateishi T., (2001). *Materials Science and Engineering* C 17: 63–69.
- Chirila T. V., *Biomater.* 2001, *22*, 3311.
- Cho Youngnam, Riyi Shi and Richard B. Borgens,(2010). *The Journal of Experimental Biology* 213, 1513-1520
- Choi, Y.S., Hong, S.R., Lee, Y.M. et al. (1999). *Journal of Biomedical Materials Research*, 48: 631–639.
- Choueka, J., Charvet, J.L., Koval, K.J., et al. (1996). *Journal of Biomedical Materials Research*, 31(1): 35–41.
- Chung T.W., Yang J., Akaike T., et al. (2002). *Biomaterials*, 23: 2827–2834.
- Clarke K.I., Graves S.E., Wong A.T.C. et al. (1993). *Journal of Materials Science: Materials in Medicine*, 4: 107–110.
- Creighton T.E., (1993). *Proteins*. (W. H. Freeman, New York, USA).
- Daculsi, G., (1996). *Proceeding of the 5th World Biomaterials Congress*, 664.
- De Bartolo L., Catapano G., Della Volpe C., Drioli E., *J. Biomat. Sci. -Polymer Edn.*, 1999, 10, 641.
- De Bartolo L., Jarosch-Von Schweder G., Haverich, A. Bader A., *Biotech. Progress*, 2000, 16, 102.
- De Bartolo L., Morelli S., Rende M., et al. (2004). *Biomaterials* 25: 3621–3629
- De Bartolo L., Morelli S., Rende M., et al. (2007). *Biosci.* 7, 671–680
- De Bartolo L., Rende M., Morelli S., (2008). *J. of Membrane science* 325: 139-149
- De Bartolo L., S. Morelli, L. Giorno, et al. (2006). Journal of Membrane Science 278: 133–143
- De Bartolo L., Salerno S., Curcio E., et al. (2009). *Biomaterials* 30 (13): 2531-43.
- De Wever, O., Demetter, P., Mareel, M. and Bracke, M. (2008). *Int. J. Cancer* 123, 2229-2238.
- Donlan RM, Costerton JW. (2002). *Clin Microbiol Rev* 167: e93.
- Drioli E., De Bartolo L., (2006). *Artificial organs* 30: 793-802

- Eisenbarth E. (2007). *Advanced Engineering Materials* 9, 12
- Fong P, Shin'oka T, Lopez- Soler RI, Breuer C. (2006). *Progress in Pediatric Cardiology* 21 (2): 193199.
- Fox CF, Skalak R, (1988). *Tissue Engineering.* New York: Alan R. Liss, Inc. Proceeding books.
- Frantz C., Stewart K.M. and Weaver V.M. (2010). *Journal of Cell Science* 123, 4195-4200
- Fucks JR, Nasseri BA, Vacanti JP. (2001). *Annual Thorac Surgery* 72: 577591.
- Garreta E., E. Genove, S. Borros,C. E. Semino (2006). *Tissue Eng., 12*, 2215.
- Gutowska A., Jeong B, Jasionowski M., (2001). *Anat. Rec., 263*, 342.
- Porter M.C. (1990). *Handbook of industrial membrane technology* Noyes publication.
- Hanes, J., Chiba, M. and Langer, R., (1998). *Biomaterials*, 19: 163–172.
- Hedberg, E.L., Kroese-Deutman, H.C., Shih, et al. (2005). *Biomaterials*, 26(22): 4616.
- Hutmacher D.W., Singh H., (2010). *Trends in Biotechnology vol.26, N°4*
- Hutmacher DW, Woodruff MA. Fabrication and characterisation of scaffolds via solid free form fabrication techniques. In: Chu PK, Liu X, editors. Handbook of fabrication and processing of biomaterials. Boca Raton: CRC Press/Taylor and Francis Group; 2008. p. 45–68.
- Hutmacher DW. J Biomater Sci Polym Ed 2001;12:107–24
- Hutmacher DW. (2000). *Biomaterials* 21(24): 2529-2543.
- Ibim S.M., Uhrich K.E., Bronson R., et al. (1998). *Biomaterials*, 19: 941–951.
- Ito Y, Zheng J, Imanishi Y. (1997). *Biomaterials* 18(3):197- 202.
- Jawad H, Ali NN, Lyon AR, et al. (2007). *Journal of Tissue Engineering and Regenerative Medicine* 1(5):327- 342.
- Kannan RY, Salacinski HJ, Sales K, et al. (2005). *Biomaterials*;26(14):1857- 1875.
- Karageorgiou V, Kaplan D. (2005). *Biomaterials*; 26(27):5474–91.
- Karande TS, Ong JL, Agrawal CM. (2004). *Annals of Biomedical Engineering* 32(12):17281743.
- Kempen, D.H.R., Lu, L., Kim, C., et al. (2006). *Journal of Biomedical Materials Research* 77A: 103–111.
- Kikuchi, M., Ikoma, T., Itoh, S., et al. (2004). *Composites Science and Technology* 64: 819–825.
- Kim HW, Knowles JC, Kim HE. (2004). *J Biomed Mater Res* B 70B:240–9.
- Kose, G.T., Korkusuz, F., Ozkul, A., et al. (2005). *Biomaterials*, 26(25): 5187–5197.
- Lam CXF, Hutmacher DW, Schantz J-T, et al. (2007). *J Biomed Mater Res* Part A; 90: 906–19.
- Lam CXF, Savalani MM, Teoh SH, et al. (2008). *Biomed Mater*;3:1–15.
- Langer R, Vacanti JP. (1993). *Science* 260:920- 926.
- Langer, R., and Tirrell, D. A. (2004). *Nature* 428, 487–492.
- Lanza RP, Langer RS, Vacanti J. (2000). *Principles of tissue engineering*. 2nd ed. San Diego, CA; Academic Press.
- Lebourg M., J. Suay Antón, J.L. Gomez Ribelles (2010). Composites Science and Technology 70: 1796–1804
- Lebourg M., J. Suay Antón, J.L. Gómez Ribelles (2008). European Polymer Journal 44: 2207–2218
- Lee, C.R., Breinan, H.A., Nehrer, S. and Spector, M. (2000). *Tissue Engineering*, 6(5): 555–565.
- Levin M.P. et al. (1979). *J. Periodontol.* 50, 250-253,
- Liu, D.M. (1997). *Journal of Materials Science*: Materials in Medicine, 8: 227–232.
- Lu L., M. J. Yaszemski, A. G. Mikos (2001). *J. Bone Joint Surg. Am.*, 83-A Suppl 1, 282.
- Lutolf, M. P., and Hubbell, J. A. (2005). *Nat. Biotechnol.* 23, 47–55.
- Lutolf, M. P., Gilbert, P. M. and Blau, H. M. (2009). *Nature* 462, 433-441.
- Luu, Y.K., Kim, K., Hsiao, et al. (2003). *Journal of Controlled Release*, 89(2): 341–353.
- Lynn, A.K., Yannas, I.V. and Bonfield, W. (2004). *Journal of Biomedical Materials Research* Part B: Applied Biomaterials, 71B: 343–354.

- Ma, L., Gao, C., Mao, Z., et al. (2004a). *Biomaterials* 25: 2997–3004.
- Ma, L., Gao, C.Y., Mao, Z.W., et al. (2004b). *Journal of Biomedical Materials Research* 71A: 334–342.
- Macchiarini P, Jungebluth P, Go T, et al (2008). *The Lancet* 372 (9655): 2023-2030.
- Maquet V., Martin D., Scholtes S., et al. (2001). *Biomaterials* 22 (10): 1137-1146
- Matsumura G, Hibino N, Ikada Y, et al. (2003). *Biomaterials* 24(13):2303- 2308.
- Meenen, N.M., Osborn, J.F., Dallek, M. et al. (1992). *Journal of Materials Science: Materials in Medicine* 3: 345–351.
- Miko, A.G. and Temenoff, J.S. (2000). *Electronic Journal of Biotechnology*, 13(2): 114–119.
- Mitragotri S, Lahann J. (2009). *Nat Mater* 8(1):15-23.
- Moroni L, De Wijn JR, Van Blitterswijk CA. (2008). *Journal of Biomaterials Science-Polymer* Ed. 19(5):543-572.
- Muggli, D.S., Burkoth, A.K. and Anseth, K.S. (1999). *Journal of Biomedical Materials Research* 46(2): 271–278.
- Muschler, G. F., Nakamoto, C., and Griffi th, L. G. (2004). *J. Bone Joint Surg. Am.* 86-A, 1541–1558.
- Nesic D, Whiteside R, Brittberg M, et al. (2006). *Advanced Drug Delivery Reviews* 58(2):300- 322.
- Nettles D. L., S. H. Elder, J. A. Gilbert (2002). *Tissue Eng.*, *8*, 1009.
- Papenburg BJ, Vogelaar L, Bolhuis- Versteeg LAM, et al. (2007). *Biomaterials* 28(11):1998- 2009.
- Peter, S.J., Lu, L., Kim, D.J. and Mikos, A.G. (2000). *Biomaterials*, 21: 1207–1213.
- Peter, S.J., Miller, M.J., Yasko, A.W., et al. (1998). *Journal of Biomedical Materials Research* 43: 422–427.
- Pham Q. P., U. Sharma, A. G. Mikos (2006). *Tissue Eng.*, *12*, 1197.
- Praemer A., Furner S., and Rise D.P. (1999). *American Academy of Orthopedic Surgeon*, Rosemont, IL.
- Putnam AJ., Mooney DJ. (1996). *Nat Med* 2:824-6
- Rodrigues C.V.M., Serricella P., Linhares A.B.R., et al. (2003). *Biomaterials*, 24: 4987– 4997
- Rosso, F., Marino, G., Giordano, et al. (2005). *J. Cell Physiol.* 203, 465-470.
- Rothamel D., Schwarz F., Sager M. et al. (2005). *Clinical Oral Implants Research*, 16(3): 369–378.
- Rozario T. and DeSimone D. W. (2010). *Dev. Biol.* 341, 126-140.
- Sachlos E., J. T. Czernuszka (2003). *Eur. Cell Mater. 30*, 29.
- Salerno S., Piscioneri A., Laera S., (2009). *Biomaterials* 30 (26): 4348–56.
- Saltzman WM. (2004). *Tissue Engineering: principles for the design of replacement organs and tissues*. 1st ed. Oxford: Oxford University Press.
- Sang Ho Ye, Watanabe J., Takai M., Iwasaki Y., Ishihara K. (2006). *Biomaterials* 27: 1955-1962
- Sawyer AA, Song SJ, Susanto E, et al. (2009). *Biomaterials* 30:2479–88.
- Schek, R.M., Wilke, E.N., Hollister, S.J. and Krebsbach, P.H. (2006). *Biomaterials* 27(7): 1160.
- Shen, F., Cui, Y.L., Yang, L.F., Yao, K.D. and Dong, X.H. (2000). *Polymer International*, 49: 1596–1599.
- Shor L, Güçeri S, Wen X, Gandhi M, Sun W. (2007). *Biomaterials* 28:5291–7.
- Shu R., M. J. Baumann, L. R. McCabe (2003). *J. Biomed. Mater. Res. A*, *67*, 1196
- Subbiah T., G. S. Bhat, R. W. Tock, S. Pararneswaran, S. S. Ramkumar (2005). *J. Appl. Polym. Sci. 96*, 557.
- Sukhodub, L.F., Moseke, C., Sukhodub, L.B., et al. (2004). *Journal of Molecular Structure* 704(1–3): 53–58.
- Taylor, P.M., Cass, A.E.G. and Yacoub, M.H. (2006). *Progress in Pediatric Cardiology*, 21: 219–225.
- Thom T., Haase N., Rosamond W. ee al. (2006). *Circulation* 113, e85.
- Vance J, Galley S, Liu DF, Donahue SW. *(2005) Tissue Eng 11: 832–1839*
- Wang Gan, Qiang A, Kai Gong, et al. (2010). *Acta Biomaterialia* 6: 3630–3639
- Wang M. (2003). Biomaterials 24: 2133–51
- Williams DF. (2008). *Biomaterials*;29 (20): 2941-2953.

- Yang S., K. F. Leong, Z. Du, C. K. Chua (2002). *Tissue Eng. 8*, 1.
- Yannas I. V., E. Lee, D. P. Orgill, et al. (1989). *Proc. Natl. Acad. Sci.* USA, 86, 933.
- Zeltinger J et al. (2004). *Tissue Eng* 7 (5): 557–72.
- Zhang S. (2003). *Nat. Biotechnol., 21*, 1171.
- Zhang, R.Y. and Ma, P., (1999a). *Journal of Biomedical Materials Research*, 44: 446–455.
- Zhang, R.Y. and Ma, P., 1999b, Porous poly(L-lactic acid)/apatite composites created by biomimetic process, Journal of Biomedical Materials Research, 45: 285–293.
- Zhao J., L.Y. Guo, X.B. Yang, J. Weng (2008). *Applied Surface Science* 255 2942–2946
- Zhao, F., Yin, Y.J., Lu, W.W., et al. (2002). *Biomaterials*, 23: 3227–3234.

Chapter 2

Preparation and characterization of Polymeric membranes

Introduction

Natural or synthetic, organic or inorganic, electrical charged or neutral polymers may be used for the preparation of membranes [Baker et al., 2004]. Depending on the application a membrane is designed for, a suitable preparation technique must be selected in order to fasten a proper structure and conformation (flat, tubular, hollow fiber, etc), chemical-physical characteristics, function and transport properties, chemical stability and specific mechanical properties. A few techniques can be used for processing a starting material and obtaining a membrane. Changing or modifying the working parameters like temperature, humidity, solvent evaporation rate, pH and the supports used for the molding and choosing the materials concerning their distinctiveness (molecular weight, solubility, density, etc.) allow to produce a variety of different membranes classified as porous, dense, symmetric or asymmetric, integral or composite.

2.1 Polymeric membrane preparation

Since a monomer is the basal unite which build a macromolecule from, this little elements can be used as starting blocks for the preparation of membrane with different configurations and characteristics, due to the nature, the concentration and when more monomers are involved, the ratio used during the preparation steps. The *Polymerization* techniques allow to fuse together those building blocks obtaining the final polymer, with specific characteristics and properties. Two polymerization methods can be used in order to obtain the polymer needed for a membrane preparation: the *mass polymerization*, in which a very high processing temperature causes the linking between the molecules and then no solvent or liquid are used; and the *interfacial polymerization* where two reactive monomers are dissolved in immiscible solvents and a very slow poly-condensation reaction incurs at the interface created by the two liquids. Both methods are not fast and easy to handle but they allow to obtain not only the final polymer usable for the preparation of a membrane, but a membrane itself. Actually symmetric and asymmetric dense membrane are prepared through them as thin films and

deposited onto a porous support in order to obtain a composite final membrane [Baker et al., 2004]. The *extrusion* methods is the one that allow to use the polymer powder without dissolving it in a solvent. It is considered the simplest and fastest way to prepare a dense membrane. The polymeric powder is melted at a temperature just lower than its specific melting point until the complete fusion. Collected in an extruder the polymer is then pushed out at high pressure through a thin shaped opening that allow to produce membranes with specific shapes and conformations (fig. 2.1). The rate of the process is very high (V >> 1000 m/min) and the collection speed of the final product affects the final thickness: faster is the collection, thinner is the membrane produced; moreover, due to the elongational shear flow applied, selective membranes are producible: the induced orientation of the polymeric chains obliges them to assume a liner disposition instead of a chaotic one.

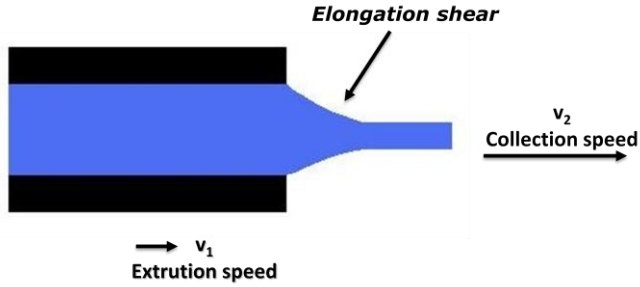

Fig. 2.1 Extrusion system for membrane preparation

The *Sintering* method (fig. 2.2) is the most widely used technique to obtain porous membranes from an organic or inorganic materials selected according to the application of the final membrane, as the gas separation or the filtration of colloidal solutions and suspensions. The protocol foresees that a powder, not easily dissolvable in solvent, with particle size included in the range of 0,2-20 µm, is pressed into a film or a plate and then sintered just below the melting point of the starting material. The result is a membrane with 10-40% of porosity and an irregular pore structure with wide pore size distribution depending on the material used (i.e. porosity: 10-20% when polymers are used and 80% for metals).

Fig. 2.2 Sintering method for membrane preparation

When a polymeric film of partial crystallinity is obtained extruding a hydrophobic polymer powder at a temperature close to the melting point, a rapid drawdown of the porous polymeric film takes place and in order to increase the porosity of the system changes in its structure are made through *Stretching* [Mulder et al., 1991]. The porous polymeric film is stretched perpendicularly to the direction of the drawing in order to obtain uniform pores shape and distribution with a final membrane highly permeable for gases and vapors but, up to specific hydrostatic pressure, impermeable for aqueous solutions. For this reason the membranes are usable for sterile filtration and membrane distillation processes. The T*rack-Etching* technique (fig. 2.3) allow to produce nearly perfect porous membranes, but with a low porosity degree (10%) and very small pores size (0,2-10 μm). A polymeric film or a foil previously prepared, is exposed in a nuclear reactor to collimated high energy charged particles applied perpendicular to the film. Passing through the film, the particles weaken the chemical bonds between the atoms damaging the polymer back-bone. The film is then placed in an etching bath (acid or alkaline) and all the hit sensitized areas leave tracks that originate uniform cylindrical pores. The pore density and diameters are determined by the resident time of the film in the irradiator and the time in the etching bath respectively [Strathman et al., 2006]. Membranes obtained this way find application in microbiology, and diagnostic procedures.

Fig. 2.3 Track-Etching method for membrane preparation

The *Micro-Lithography* and the T*emplate Leaching* are other two methods for obtaining porous membranes usable for microfiltration processes. The template-leaching in particular is

the technique suitable for preparing porous membranes from polymers which do not dissolve in common organic solvents. In this technique, a homogeneous film is prepared from a mixture of membrane matrix material and a leachable component. After the film has been prepared, the leachable component is removed by a suitable chemical treatment leaving a template or a network in the structure of the remaining undissolved material. At the right conditions, a porous structure is formed as a result. The minimum pore size reachable with this technique is 0,05 µm and the silica membranes are the main examples [Strathman et al., 2006]. Phase separation technique, also known as *Phase Inversion* or solution precipitation technique, is the most important technique by which almost half of all microporous membranes are developed. In this technique, a clear polymer solution is precipitated into two phases: a solid polymer-rich phase that forms the membrane matrix and a liquid polymer-poor phase that forms the membrane pores upon evaporation [Mulder et al., 1991]. A few different procedures are available and by changing the polymer, its concentration, the solvent and the precipitation conditions, different kind of membranes are obtained with symmetric or asymmetric structure and a pore size included in the range 0,1- 20 µm. Generally the precipitation of the polymer from the starting solution is due to the treatment with a non-solvent as soon as the membrane is molded: the non-solvent molecules substitute the solvent of the started system in the structure allowing the formation of pores with size and shape dependent from the time and the rate of the non-solvent treatment; the technique it's in that case called *non-solvent diffusion induced phase separation (DIPS or NIPS)* (fig.2.4). When the separation of the two phases and the precipitation of the film is due to a change in the temperature the methods is defined instead as *temperature induced phase separation (TIPS).*

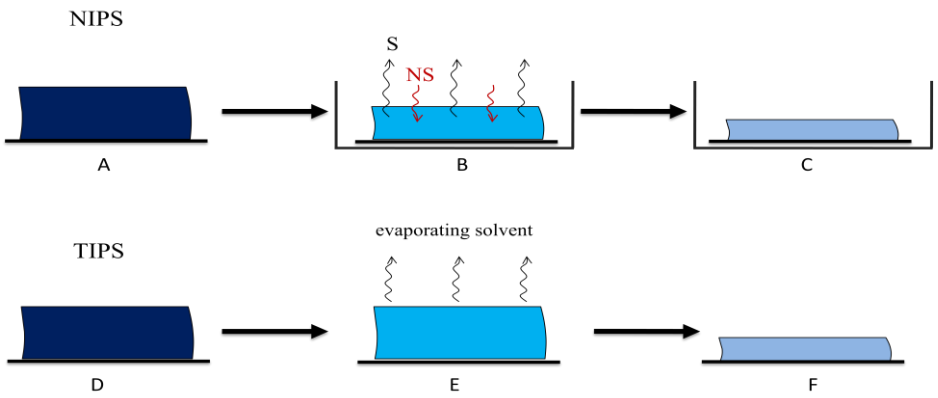

Fig. 2.4 Phase Inversion Processes NIPS (A,B,C) and TIPS (D,E,F)

The polymeric solution is obtained dissolving a polymer at high temperature in a proper solvent that evaporate as soon as the solution is spread as thin film due to the following cooling process. Homogeneous pores size and distribution are reached. Though the previous phase inversion techniques are wide used due to the high results, there are phase inversion techniques where the precipitation is simply a consequence of the solvent evaporation both for a two component (polymer/solvent) than a three component solution (polymer/precipitant/solvent). The method is called *precipitation for solvent evaporation process* and allow to produce membranes with a low degree of porosity and a dense structure where a pore size generally included in the nanometers range. Depending on the polymer characteristics and properties, a *gelation* phase can incur. The polymer freezes into a three-dimensional network as result of chemical or physical crosslinking, and further removal of solvent may result in a porous structure. Unfortunately, many polymers and membranes with good selectivities and permeabilities are not well suited for specific applications involving gas mixtures or liquid solutions since the diffusion process in an omogeneous polymer matrix is relatively slow. Therefore, membranes with an asymmetric structure are necessary. Two different kind of asymmetric membranes can be produced: the integral membranes where the selective barrier layer and the microporous support always consist of the same polymer; and the composite membrane, where different polymers may be or are used for the microporous support and the selective barrier layer. This means polymers which show the desired selectivity for a certain separation problem, but have poor mechanical strength or poor film forming properties, can be supported by a basal structure and be useful. An integral asymmetric membrane is obtained precipitating a polymeric solution in form of a continuous solid phase through a cooling process, a solvent evaporation or the adding of a non-solvent. Each one of these processes led the formation of the liquid phase that originate the membrane pores. When the film is deposited on a different porous support the results is the *composite asymmetric membrane*. The best advantage is the chance of combining the properties of different materials. The techniques used for the preparation of composite structures may be grouped into four general types: 1) Casting of the barrier layer separately, e.g., on the surface of a water bath followed by lamination to the microporous support film. 2) Dip-coating of the microporous support film in a polymer, a reactive monomer or a pre-polymer solution followed by drying or curing with heat or radiation. (3) Gas-phase deposition of the barrier layer of the microporous support film from a glow discharge plasma. (4) Interfacial polymerization of reactive monomers on the surface of the microporous support film. Generally the average pore diameter of the support structure is small enough to avoid the

penetration of the solution that has to be treated, and a high mechanical strength is requested to withstand high temperature and pressure. The selective layer is on the contrary more delicate and must be protected with a high permeable coating sheet. The flat conformation is not the only one available for a polymeric membrane. Tubular membranes, capillaries and hollow fibers have a wide application in a few of industrial, chemical and bio-medical processes and. They are generally classified for dimension: the tubular membranes have the largest diameter, d > 5 mm; the capillary membranes are included in a diameter range of 0.5-5 mm whereas the hollow fibers are the smallest with d < 0.5 mm. Since the structures of this kind of membranes are so different from the equivalent flat, even the preparation technique are diverse. Depending on the final results that it want to be achieved a specific methods and proper conditions are used. The so-called *melt spinning* is a specific extrusion method through which hollow fibers are obtained by the action of the temperature [Mulder et al., 1991]. The polymer is melted at a temperature just lower than the melting point until it fused in an extruder and pushed out at high pressure through an annular opening. Since the final product can collapse on itself, often through the inner ring of the extruder an inert gas or air is introduced in order to support the structure. Another method to produce hollow fibers consists in the *dry-wet spinning* and it can be considered a middle course form of both the NIPS and the extrusion process. It foresees that in place of the air or the inert gas in the annular opening of the spinneret a fluid consisting in a non-solvent is pumped in the system. A viscous polymeric solution and the bore fluid are pushed at determined pressure in the tube of the spinneret and left for a short period of time in the air in order to induce the polymer precipitation and the fiber formation. After this short period (the dry step) the fibers are immersed in a non-solvent coagulation bath and then collected. When the bath is not requested the technique is called *dry spinning*. The wet-dry method allow to produce fibers with specific dimension and diameter, both fixed after the coagulation bath, whereas in the extrusion or the melt spinning techniques the dimension can be manipulated by changing the process and the collection rate and by the magnitude of the power used to push the air in the annular opening. One of the main characteristics of a hollow fiber or a capillary is that they are self-supporting and with a high stability. The tubular membranes otherwise, are not self-supporting and their preparation foresees the casting of the polymeric solution on a tubular support. The device used consists of a reservoir in which the polymeric solution is contained, and a hollow tube, the central part of the system, containing at the end a “casting bob” with porous walls. Thanks to a proper pressure applied on the reservoir the solution is pumped in the tube and forced through the holes of the bob that is mechanically or by gravitation moved

vertically until it is completely out of the system. This movement produce the casting of the polymeric solution on the walls of the tube and after a coagulation bath the tubular fiber is obtained [Mulder et al., 1991].

The *electro-spinning* method is another preparation method of fibrous mats from a liquid or a polymeric solution. The advantages of the electro-spinning technique are the production of very thin fibers, on the order of few nanometers or micrometers, with a large specific surface areas and superior mechanical properties. The process does not require the use of coagulation chemistry or high temperatures to produce solid threads from solutions. This makes the process particularly suited to the production of fibers using large and complex molecules [Merritt et al., 2011; Kowalewski et al., 2005; Greiner et al., 2007]. A high electric field is applied to the droplet of a fluid which may be a melt or solution coming out from the tip of a die, which acts as one of the electrodes. This leads to the droplet deformation and finally to the ejection of a charged jet from the tip of the accelerating cone towards the counter electrode leading to the formation of continuous fibers. The standard laboratory setup for electrospinning consists of a spinneret (typically a hypodermic syringe needle) connected to a high-voltage (5 to 50 kV) direct current power supply, a syringe pump, and a grounded collector. A polymer solution, sol-gel, particulate suspension or melt is loaded into the syringe and this liquid is extruded from the needle tip at a constant rate by a syringe pump. Alternatively, the droplet at the tip of the spinneret can be replenished by feeding from a header tank providing a constant feed pressure [Greiner et al., 2007]. Specifically Electrospinning occurs when the electric forces at the surface of a polymer solution or melt overcome the surface tension and cause an electrically charged jet to be ejected. Modification of the spinneret and/or the type of solution can allow for the creation of fibers with unique structures and properties: a coaxial setup for example, uses a multiple solution feed system which allows for the injection of one solution into another at the tip of the spinneret; an emulsions can be used to create core shell or composite fibers without modification of the spinneret by simply adding surfactants. Electrospinning of polymer melts eliminates the need for volatile solvents in solution electrospinning, and even polymers generally immiscible with each can be processed with this technique by using a very similar setup to that employed in conventional electrospinning processes. When a membrane is developed or when it has to be chosen for a specific application, knowing the characteristics in terms of chemical-physical and mechanical properties is essential. Membranes can show different performances if prepared following diverse processing methods even if made with the same polymer [Merritt et al., 2011; Kowalewski et al., 2005].

2.2 Membrane characterization

Then different techniques are required for a characterization depending on the kind of membrane considered. Permeability and selectivity are parameters investigated for each kind of membrane, but specifically porous membranes are characterized in term of flux, pore size and distribution and molecular weight cut-off; a dense and homogeneous membrane is investigated in terms of diffusion process and rate through it, rejection coefficient and separation coefficient. Unrelated with the membrane considered, the starting point of a characterization is the structure analysis by means microscopic techniques as scanning electron microscopy (SEM), field emission electron microscopy (FEM), transmission electron microscopy (TEM) and atomic force microscopy (AFM). Each samples (surface or a cross section) before the analysis must be treated specifically then they have to be stored in the perfect condition not for damage them. Every technique give a specific analysis and even the determination of the pore size is possible: the scanning electron microscopy can visualize pores of 5 nm, whereas the field and the transmission electron have resolution of 0,6-0,7 nm and 0,4-0,5 nm respectively [Mulder et al., 1991]. The determination of the pore size and distribution on the membrane is specifically achieved by a few techniques as the mercury porosimetry, the gas-liquid displacement, the liquid-liquid displacement, the bubble-point test and the Perm-Porometry. The bubble-point test is a structure-related characterization methodology which make available the classification of the maximum pore size in a membrane. It is based on the capillary effect due to surface tension forces. The membrane is placed on a filter and immersed in a liquid (e.g. water) which fills all its pores. From the bottom side of the same filter air or nitrogen gas is introduced with an increasing pressure. At a specific pressure value, the air replace the liquid in the largest pores, permeate the membrane and a bubble rising from the surface can be detected. The relationship between the pressure and the pore size (radius) is done by Laplace equation:

$$r_p = \frac{2\gamma}{\Delta P} \cos\theta$$

where r_p is the radius of a capillary shape pore, γ is the surface tension at the liquid/air interface and θ is the contact angle of the bubble observed. Other techniques to determine the pore size distribution are also used based on the same principle of the bubble-point test, and they cover different pore size ranges when different pressure range are applied. The Perm-Porometry is one of these techniques. The Perm-Porometry is based on the principles of

capillary condensation as adsorption-desorption hysteresis. The adsorption and the desorption isotherm of an inert gas is determined as a function of the relative pressure [Mulder et al., 1991]. The adsorption isotherm starts at a low relative pressure. At a certain minimum pressure the smallest pores will be filled with the gas used, and as the pressure increases, also the largest pores are filled. Near the saturation pressure all the pores are blocked. In Perm-Porometry the blockage of pores by means of a condensable gas is linked with the simultaneous measurement of gas flux through the membrane, and the method proceeds recording not only the dried flow through described above, but also the wet flow, in which a starting membrane filled with a liquid, is subjected to a reduction of the pressure. In this case, the condensed vapor is removed from the largest pores, and the diffusive gas flow through these open pores is measured. On reducing the relative pressure still further, smaller pores become available for gas diffusion, and when it is reduces to zero, all the pores are open and gas permeate through all them (fig.2.5). Because a certain pore radius (Kelvin radius r_k) is related to a specific pressure, a measurement of the gas flow provides information about the number of these specific pores.

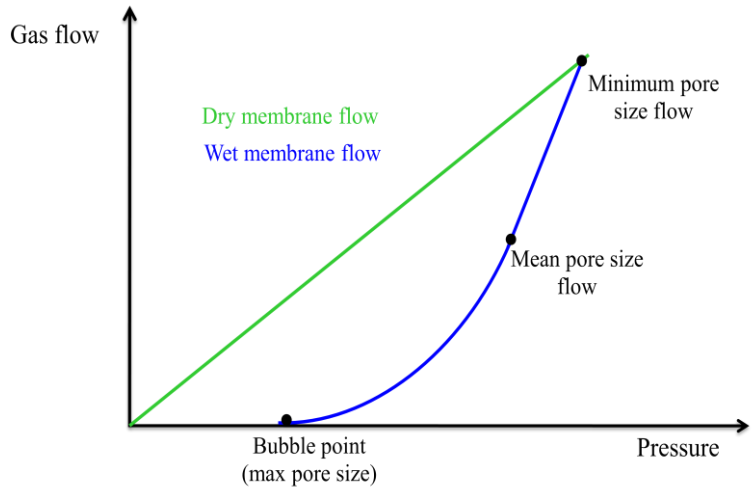

Fig. 2.5 Diagram of the MWCO determined measuring the retention of the membrane for components with different molecular weight by Perm-Porometry

Knowing the porosity of a membrane is possible to investigate the pure water flux or the "pure water permeability" of it. The flux J through the structure is dependent form the driving force involved, the hydrostatic pressure and the presence of pores and according with the Darcy's law is inversely proportional to the solvent viscosity. Prior the flux measurement the membrane must be washed in order to eliminate preservatives, residual and then pressurized

by filtration of pure water at higher pressure than the operating condition to stabilized the system before the analysis [Strathman et al., 2006].

The equation used is: $J = L_p \Delta P / \eta$

where L_p is the hydrodynamic solvent permeability, P is the pressure and η is the viscosity of the solution passing through the pores of the membrane investigated. Another important parameter of characterization is based on the sieving mechanism concept for which particles smaller than the pores size are allow to pass through the membrane the separation properties whereas the bigger ones are completely detained by the membrane structure. This analysis is done in order to reveal the molecular weight cut-off, fundamental for the mass transport properties definition. The relation between the particle size and the pore size for the retention properties of a membrane is described by the Ferry equation for the rejection:

$$R = \left[\left(1 - \frac{r_s}{r_p}\right)^2\right]^2$$

where r are the radius of the pores and the particles if considered as spheres. The sharpness of the cut-off of a membrane is determined by measuring the retention of the membrane for components with different molecular weights and shapes (dextrans and proteins) and a typical plot of the retention obtained in percentage,

$$R = \left(1 - \frac{C_p}{C_f}\right) x\ 100$$

where C are permeate and feed concentration, versus one of their molecular weight expressed in Da is showed in fig.2.6.

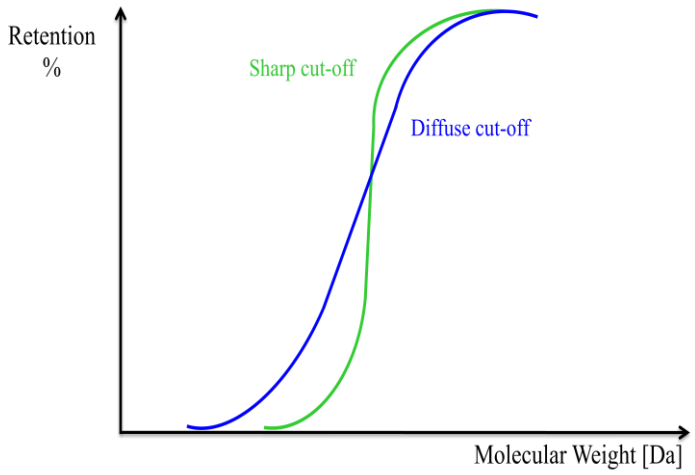

Fig. 2.6 Retention plot

The obtained profile is dependent from the pore distribution in the membrane and since the MWCO measurement is sensitive to the experimental condition it is very important to run the analysis at the standard parameters (trans-membrane pressure of 100 KPa, solution concentration of 0,1% and test temperature 25°C) [Mulder et al., 1991]. The chemical-physical characteristic of the polymer used to prepare a membrane affect not only the structure and the perm-selectivity of it but the mechanical stability and the swelling behavior too. They are both properties dependent on the crystallinity and the cross-linking of the polymer matrix and are related one to each other. The mechanical characterization concern the elastic or plastic properties and deformation of the membrane and it is obtained plotting the level of stress applied to the sample versus the strain. Generally the tensile strength test is run and defined in terms of Young modulus and elongation parameter. Young's modulus is a measure of the stiffness of a material. It is defined as the ratio of the uniaxial stress over the uniaxial strain in the range of stress in which Hooke's Law holds, predicting how much a material sample extends under tension or shortens under compression, and its values are normally indirectly proportional to elongation parameters values. Since the water content in a membrane affects highly the mechanical properties, for this analysis must be used always dried samples. A tipical stress/strain diagram is shown in fig. 2.7. Because natural ECM is a fully hydrated gel, as reported in chapter 1, the wettability and the water sorption of a membrane are a key consideration factor for defining and understanding its biocompatibility. The water sorption of a membrane is dependent on a few parameters: nature of the polymer, cross-linking density, ions and their concentration, and so on [Strathman et al., 2006]. The

total water uptake, in weight percentage, is defined measuring the differences between a membrane in its wet and dry state in weight, following the equation:

$$Swelling\ \% = \left(\frac{W_{wet}}{W_{dry}}/W_{wet}\right) x100$$

where W referred to the weigh in the dry and wet state of the sample.

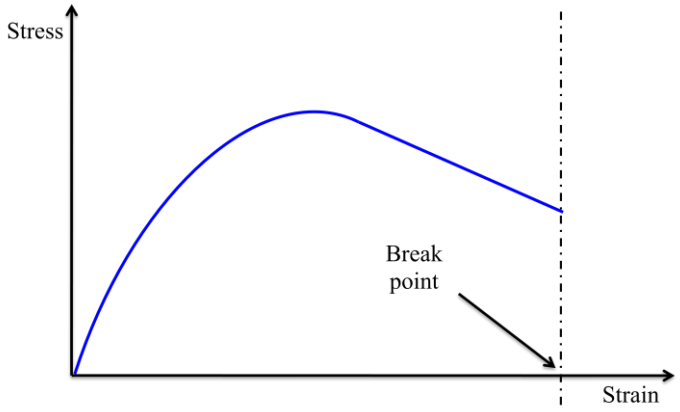

Fig. 2.7 Mechanical stress vs strain plot for a polymeric membrane

The wettability, parameter defining the hydrophilicity/hydrophobicity of a material, is otherwise obtained recording the advancing and receding water contact angles, which are representatives of the apolar and polar functional groups of the membrane surface. According to the Van Oss theory and Chaudhury's method [Van Oss et al., 1985], a biomaterials is considered hydrophilic when the water contact angle is lower than 90° (fig. 2.8). To better understand the nature of the interfaces used in TE applications, a thermodynamic quantization of the free energies involved between the polar and the apolar domains at the membrane surface can be done. Knowing the contact angle values revealed for a surface for different liquids, i.e. distilled water, diiodomethane and glycerol; the apolar γ^{LW}, the acid–base γ^{ab}, acid (electron acceptor) γ^{+}, and the base (electron donor) γ^{-} components of surface free energy can be derived. Last, but not for importance, the dissolution behavior, better defined as degradability is another very important parameter that allow to understand how long in time is the stability of a membrane under chemical stress conditions: the weight loss after treatment with salted solutions, acids or alkali or biochemicals and enzyme is defined by the equation:

$$Dissolution\ \% = \frac{W_0/W_t}{W_t}\ x\ 100$$

where W_0 referred to the sample weigh in the dry state at the beginning of the test and W_t is the weight recorded at the time point during the analysis [Strathman et al., 2006].

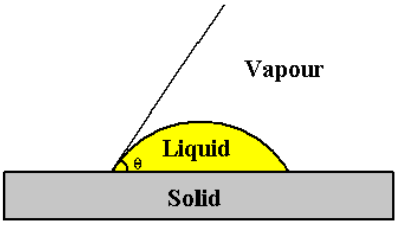

Fig. 2.8 Schematic rapresentation of a contact angle done by a drop on a solid

2.3 Thermodynamic principles

Dissolving one or more polymers in a unique solvent (polymer/solvent system) or a proper mix all the Phase Inversion Processes allow to produce membranes. In order to ensure a perfect combination of membrane structure and chemical-physical properties, the polymeric solution must be thermodynamically stable, which means, at the standard condition (constant temperature and pressure), in the system in account all the chemical components should be in a perfect equilibrium state in a sole phase and should not run in de-mixing process. In fact two or more reagents in solution can originate a liquid phase perfectly homogeneous or can re-arrange in phases immiscible with each other, in which all the components are differently shared. Knowing the characteristics of the elements and the proper condition that serves the complete control of the reaction provide the understanding of the thermodynamics information about how to blend together different elements. Though for a pure substance the thermodynamic properties of the system are directly functions of two parameters only, temperature and pressure, for a more complex one all variables in the composition, number of moles of the components, intermolecular forces (dispersion forces, polar forces, hydrogen bonding, etc), activity and the chemical potential of the polymer, are really important. A binary and/or a ternary polymeric system spontaneously turn in a state of minimum energy called Free Enthalpy of mixing $\mathbf{\Delta G_m}$ that described the equilibrium properties of the solution. Knowing the parameters and the independent variables which ΔG_m is dependent from, the thermodynamic properties of the system can be derived. At constant temperature and pressure ΔG_m is defined by the expression:

$$\mathbf{\Delta G_m} = G - \sum_i n_i \bar{G}_i^0 \qquad [1]$$

where n_i is the number of moles of the component *i* and $\bar{G}_i^0$ refers to the Gibbs molar function of the pure component, but it can be expresses as the results of the entropic (ΔS_m) and the enthalpic (ΔH_m) contribution in the system, then:

$$\mathbf{\Delta G_m} = \Delta H_m - T\,\Delta S_m \qquad [2]$$

where ΔH_m is the enthalpy of mixing and ΔS_m is the entropy of mixing. Two components will spontaneously blend together if the free enthalpy of mixing is negative ($\Delta G_m < 0$), as consequence of the complete dissolution of the solute in the solvent. For a polymer/solvent solution the effect of the entropy of mixing on the system is very small than the free enthalpy of mixing are determined by the ΔH_m only. The enthalpy of a system is defined as the sum of the internal/external motion liberty degree and the intermolecular forces contribution, and the last one above all may be considered the main important parameter for the determination of the enthalpy of mixing of an ideal system. In terms of energy, those forces are due to the movement of all the electrons in the molecules that originate the fluctuations of the dipoles in all the chemicals and consequentially the coordination of the charges in the system that causes an energy decrease. When the dispersion and repulsion forces between the positive and the negative charge of the dipoles are balanced the energy of the system reach a state of is minimal value defining the so-called energy of interaction **ε**, namely the level of energy requested to separate the molecules of a component in a milliliter of liquid that is expressed in terms of cohesive energy density $\boldsymbol{e}$ as function of the enthalpy of vaporization of the component involved:

$$\boldsymbol{e} = \frac{\Delta H_{vap} - RT}{V_i} \qquad [3]$$

where V_i is the molar volume of the liquid. Considering a binary system, then the $\boldsymbol{e}$ of two elements, the enthalpy of mixing is done by Hildebrand expression:

$$\Delta \boldsymbol{H_{mix}} = V_m[(e_1)^{0,5} - (e_2)^{0,5}]^2 v_1 v_2 \qquad [4]$$

Since the square root of the cohesive energy density is the solubility parameter **δ** of a molecule, the expression 4 can be simplified as:

$$\Delta \boldsymbol{H_{mix}} = V_m(\delta_1 - \delta_2)^2 v_1 v_2 \qquad [5]$$

where V_m is the molar volume of the solution, *v* are the volume fraction and δ are the solubility parameters of the solvent and the polymer referred with number 1 and 2 respectively. As clear, when $\delta_1 \sim \delta_2$, the value of ΔH_m approaches zero then the components are miscible (because ΔS_m is always positive). In reality except when involved particular

interactions, the polymers are usually soluble just in a few organic solvents because of their heavy chains and volume; in fact with respect to the low molecular weight molecules, they can not freely move in the system and just a few re-arrangements in space are possible when they are mixed with other components. This concept is well explained by the Flory-Huggins theory of the lattice model (fig.2.9)

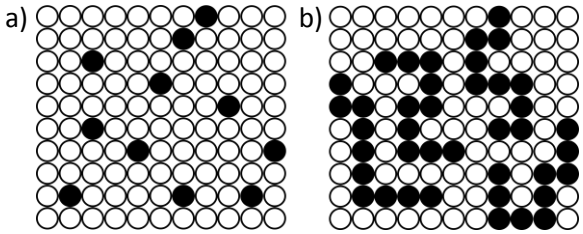

Fig.2.9 Flory-Huggins lattice model: molecular distribution in a binary system of *a)* atoms or monomers and *b)* polymers in a low-molar-mass solvent.

In a binary system where A (solvent) and B (solute) are the components with small molecular weight, each molecule of A can be imagined as surrounded by *z* particles of A or B, where *z* is the coordination number of the reticule, and the particle motion depends on the translation, rotation and vibration liberty in the system AB. Three different kind of interactions are possible: A-A, B-B and/or A-B. For each one of them a specific energy of interaction **ε** can be calculated and the enthalpy of the system is the results of their coordination:

$$\Delta \boldsymbol{H_{mix}} = H - H_A - H_B \qquad [6]$$

where H is the contact energy for the solution and the components respectively. Assuming that the molecules surface is homogeneous, every point in which them contact between each other is equivalent to another and that the lowest number of interactions is 2 (per molecule), knowing the total number of moles N, the equation for defining the H for A, B and the solution are:

$$\boldsymbol{H_A} = \frac{z\, N_A \varepsilon_{AA}}{2} ; \boldsymbol{H_B} = \frac{z\, N_B \varepsilon_{BB}}{2} \qquad [7,8]$$

The probability for a molecule of A to contact with B depends on the molar fraction of B, and can be calculated as:

$$\boldsymbol{N_{AB}} = z\, N_A\, p_B \qquad [9]$$

then the expression of H for the solution is:

$$\boldsymbol{H} = N_{AB}\, \varepsilon_{AB} + \frac{(z\, N_A - N_{AB})\, \varepsilon_{AA}}{2} + \frac{(z\, N_B - N_{AB})\, \varepsilon_{BB}}{2} \qquad [10]$$

Replacing the the equations 7,8 and 10 in the the ΔH_m expression 6, a new equation is obtained:

$$\Delta \boldsymbol{H_{mix}} = N_{AB} \left(\varepsilon_{AB} - \frac{(\varepsilon_{AA} - \varepsilon_{BB})}{2}\right) = N_{AB}\, \Delta\varepsilon_{AB} \qquad [11]$$

And more, in terms of molar fractions:

$$\Delta \boldsymbol{H_{mix}} = \frac{z\, \Delta\varepsilon_{AB} N_A N_B}{N_A + N_B} = n_A\, x_B\, N_{av}\, z\, \Delta\varepsilon_{AB} \qquad [12]$$

When a polymer is dissolved in a solvent the probability that a portion of space is occupied by a segment of the macromolecule is as higher as concentrated and heavy the polymer is (fig. 2.9), then the equation of the enthalpy of mixing doesn't have to be expressed by the molar fraction as for small molecules anymore but as function of the volume fraction, that is:

$$\Delta \boldsymbol{H_{mix}} = n_1\, \phi_2\, N_{av}\, z\, \Delta\varepsilon_{12} = RT\, n_1\, \phi_2\, X_{12} \qquad [13]$$

where numbers 1 ad 2 refer to the solvent and the polymer and X_{12} is the Flory-Huggins interaction parameter of the system. For ideal solutions, $\Delta H_m = 0$ and the ΔG_m is determined by the ΔS_m only. As said earlier, in a binary system AB, each molecule of A is surrounded by *z* particles, where *z* is the coordination number of the reticule, and the ability of A to move in the system is linked to the parameters that define an entropic degree of disorder: translation, rotation and vibration liberty. Assuming again an ideal system, the entropy of mixing is due to the molecular disposition of the component in space, then the only entropic contribution which being concerned of, is the entropy of configuration:

$$\mathbf{S_{conf}} = K \ln \mathrm{W} \qquad [14]$$

where *K* is the constant of Boltzmann and W, dependent on how the molecules of A (N_A) can arrange with respect to B, is the number of all the microscopic states possible, quantified as:

$$\boldsymbol{W} = \frac{N_A + N_B!}{N_{A\,!}\, N_B!} \qquad [15]$$

Expressing the number of molecules N as function of the molar fraction of the particles and the number of moles, for a component *i*, can be obtained:

$$\boldsymbol{x_i} = \frac{N_i}{N_{tot}} \qquad [16]$$

where: $\boldsymbol{N_{tot}} = \sum_i N_i$ and $\boldsymbol{n_i} = \frac{N_i}{N_{av}}$ [17,18]

The expression of the entropy of configuration 14, substituting properly the equation earlier described, becomes:

$$\boldsymbol{S_{conf}} = -R\,(n_A\,lnx_A + n_B\,lnx_B) \quad [19]$$

When the solute is a macromolecule, the degree of motion of the particles is strongly lower due to the dimension and the concentration of the molecule in the solution, then assuming that the polymer is linear and composed by σ segments, the entropy is expressed again in terms of volume fraction ϕ and refers directly to the mixing process. For a total number of sites equal to:

$$\boldsymbol{n_t} = n_1 + Pn_2 \quad [20]$$

the volume fraction for a system polymer/solvent are:

$$\boldsymbol{\phi_1} = \frac{n_1}{n_1 + \sigma n_2} \quad \text{and} \quad \boldsymbol{\phi_2} = \frac{\sigma n_2}{n_1 + \sigma n_2} \quad [21,22]$$

where 1 and 2 are the solvent and the polymer, then the equation of ΔG_m is:

$$\Delta\boldsymbol{S_{mix}} = -R\,(n_1\,ln\phi_1 + n_2\,ln\phi_2) \quad [23]$$

When two polymers are mixed together the equation is re-arranged considering:

$$\boldsymbol{n_1} = \left(\frac{\phi_1}{P_1}\right) n_t \quad \text{and} \quad \boldsymbol{n_2} = \left(\frac{\phi_2}{P_2}\right) n_t \quad [24,25]$$

Combining the expression of ΔH_m 13 and ΔS_m 23 for a polymer/solvent system the free enthalpy of mixing resultant is:

$$\Delta\boldsymbol{G_{mix}} = RT\,(n_1\,ln\phi_1 + n_2\,ln\phi_2 + n_1\phi_2 X_{12}) \quad [26]$$

For a pure component i , the molar partial Gibbs function is the expression of the chemical potential μ_i^o of the component, since

$$\boldsymbol{\mu_i^o} = \frac{\partial G_i}{\partial n_i} \quad [27]$$

subsequently for a molecule of small dimension it is possible to derive the value of μ_i for the component in a solution:

$$\boldsymbol{\mu_i} - \boldsymbol{\mu_i^o} = \left(\frac{\partial \Delta G_{mix}}{\partial n_i}\right)_{P,T,n_{j\ldots}} \quad [28]$$

Replacing the ΔG_m expression 26 with the equation 28 obtained for the low molecular components, for a solution AB, new formula are derived:

$$\frac{\boldsymbol{\mu_A - \mu_B^o}}{\boldsymbol{RT}} = lna_A = lnx_A + x_{AB}\,x_B^2 \quad [29]$$

$$\frac{\boldsymbol{\mu_B - \mu_A^o}}{\boldsymbol{RT}} = lna_B = lnx_B + x_{AB}\,x_A^2 \quad [30]$$

where **a** is the activity of the components. As subscribed earlier in ideal solutions the $\Delta H_m = 0$ then the x_{AB} value is null, this means that the activity coincide with the molar fraction of the chemicals in the system:

$$\boldsymbol{\mu_i} - \boldsymbol{\mu_i^o} = RT\ ln\ x_i \qquad [31]$$

Expressing the free enthalpy of mixing as function of equations 27, 29 and 30, we obtain:

$$\Delta \boldsymbol{G_{mix}} = RT\ (n_1\ lnx_1 + n_2\ lnx_2) \qquad [32]$$

where the molar fraction *x* will be substituted by the volume fraction ϕ when a binary polymer/solvent system is considered.

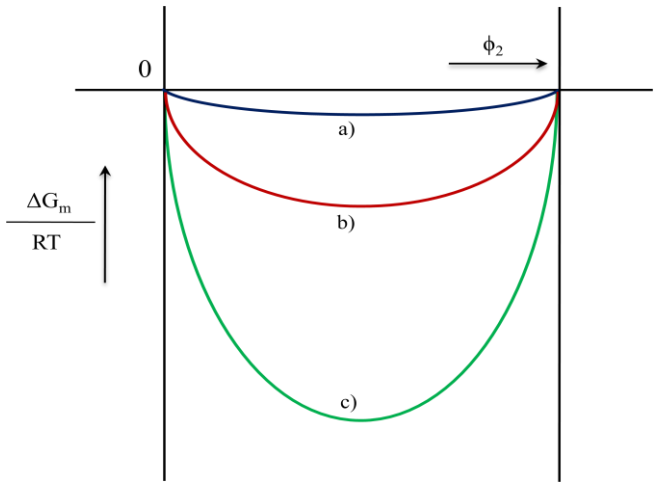

Fig. 2.10 Diagram of the Free enthalpy of mixing ΔG_m for: a) polymer/polymer system, b) polymer/solvent system and c) small molecules system.

In fig.2.10 is shown the enthalpy of mixing of the binary solutions described until now as function of the volume fraction (ϕ) of the solute: the small molecules system is drawn in green, the polymer/solvent system in red and the polymer/polymer systems in blue. It is clear that simpler the system is, in terms of nature and size of the components, lower are the values of the ΔG_m. The trend of the three curves is symmetric and this means that in ideal conditions, the miscibility of the elements is certain for all the compositions possible. As explained earlier, when polymers are involved in a solution the effect of the entropy of mixing on the system is very small then the free enthalpy of mixing is determined by the sole enthalpy (ΔH_m) and even the least change in the temperature of the system can determine the incur of the phases separation and the solution will eventually de-mix. Analyzing the same polymer/solvent system (eq. 32) at two different temperature T_1 and T_2 (fig.2.11), where $T_1 > T_2$, the thermodynamic behavior of the system follow a different trend with respect to what described for ideal solutions. When the components are blended at high temperature (T_1

near the melting point of the polymer), negative values of ΔG_m are obtained. Even if the curve is not symmetric, at all the points of the graph it is possible to drawn a tangent and all the points have the same derivate:

$\Delta\mu_i = \frac{\partial \Delta G_m}{\partial n_i}$. Since the intercept at the axes meet value of μ_i for the components always different, at any ratio and any composition the solute results miscible in the solvent. When a lower temperature is used (T_2) in the graph are recognizable: two points of minima and two points of inflections where the curve shifts its convexity/concavity. The points of minima lie on the same tangent, unique for the graph, and the intercept crosses the axes at specific values of chemical potentials for the components. At every temperature a new tangent can be drawn and eventually the points intercepted on the components axes will coincide defining the so called Critical point, which is the temperature up to which the system is stable at all the compositions.

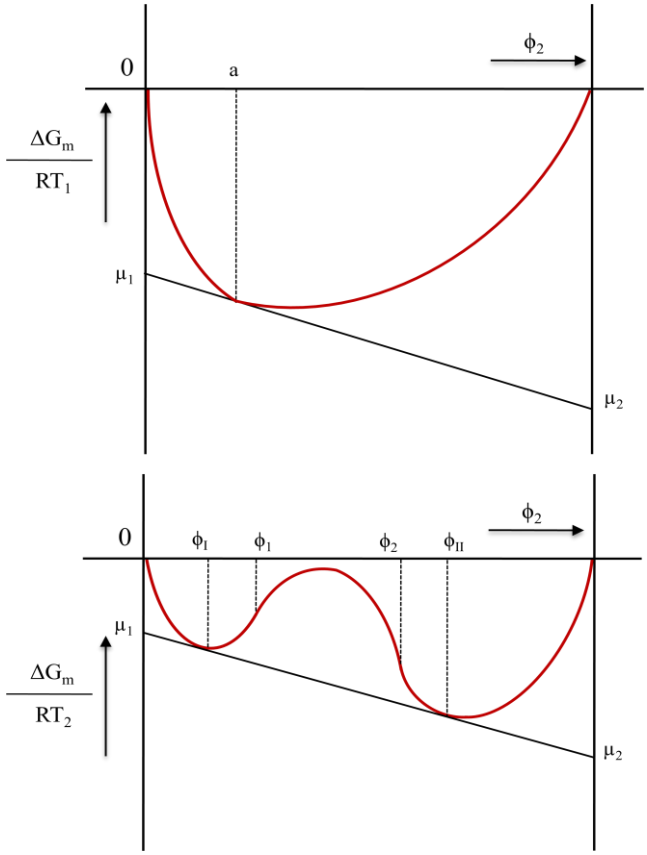

Fig. 2.11 Diagram of the Free enthalpy of mixing ΔG_m for a polymer/solvent system at two different temperature T_1 and T_2 as function of the volume fraction of the components.

The points of minima and inflections described earlier are important to understand the stability of the system when a membrane has to be obtained from a polymeric solution. They are derived when the first and the second derivate of the ΔG_m are both equal to zero (fig.2.12). Specific regions and ranges of concentrations are bounded and different trends of the curves are defined. For compositions where the solvent concentration is higher than the polymer, that is $0 > \phi < \phi_I$, the values of ΔG_m are descendent and the solution in this volume fractions range is thermodynamically stable due to the perfect miscibility of the components. With the increasing of the polymer concentration, the miscibility starts to decrease, as explained by the Flory-Huggins theory, and the free enthalpy of mixing raises, leaving a point of minimum (ϕ_I) and reaching the first point of inflection at a volume fraction equal to ϕ_1. From this point the highest values of ΔG_m are recorded and the solution for volume fractions included between ϕ_1 and ϕ_2 is thermodynamically instable and incurs in de-mixing. When the concentration of the polymer exceeds ϕ_2 a phase rich in solute is formed and the system results in stability again.

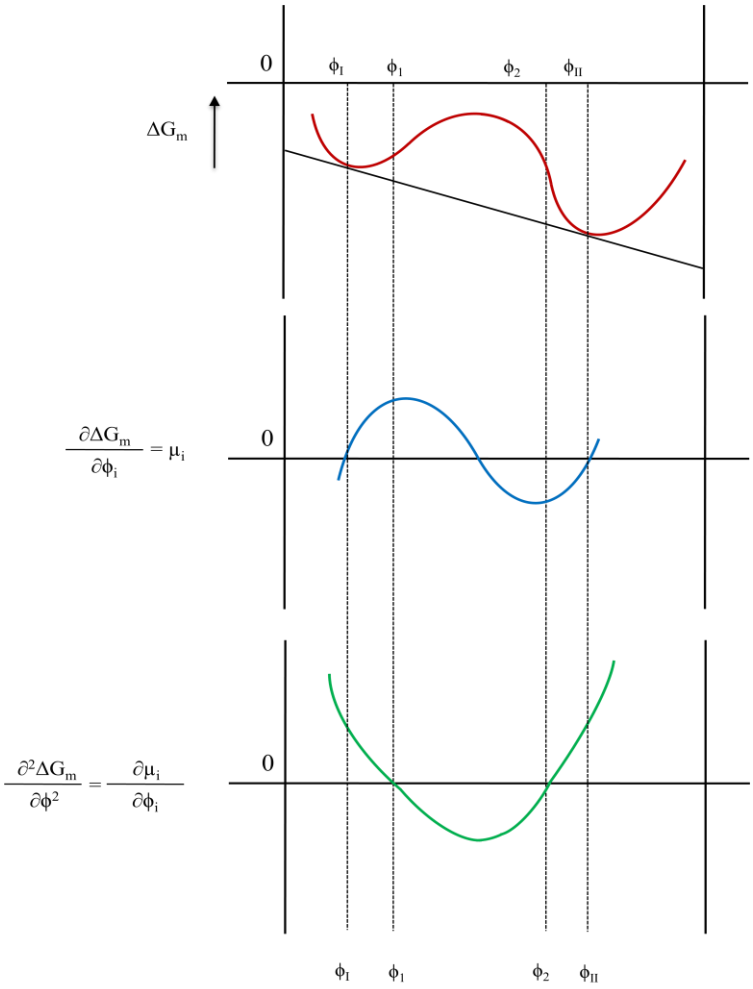

Fig. 2.12 Diagrams of the Free enthalpy of mixing ΔG_m , the first and the second derivates for a polymer/solvent system as function of the volume fraction of the components. The lowest graph represents

The plots of the first (in blue) and the second derivate (in green) underlined what said above. In particular for volume fraction ϕ included between ϕ1 and ϕ 2 the second derivate (lowest part of fig.2.12) is negative, implying that the solution is instable and de-mixing incur spontaneously. Plotting the points of minima and the points of inflection for a polymeric solution the binodal and the spinodal curves can be depicted as function of the volume fraction, and a temperature/composition diagram can be obtained (fig 2.13). Referring on the Flory-Huggins theory more complex is the system less wide and symmetric are the binodal and the spinodal curves and the critical point shifts towards the left of the graph near the solvent axis.

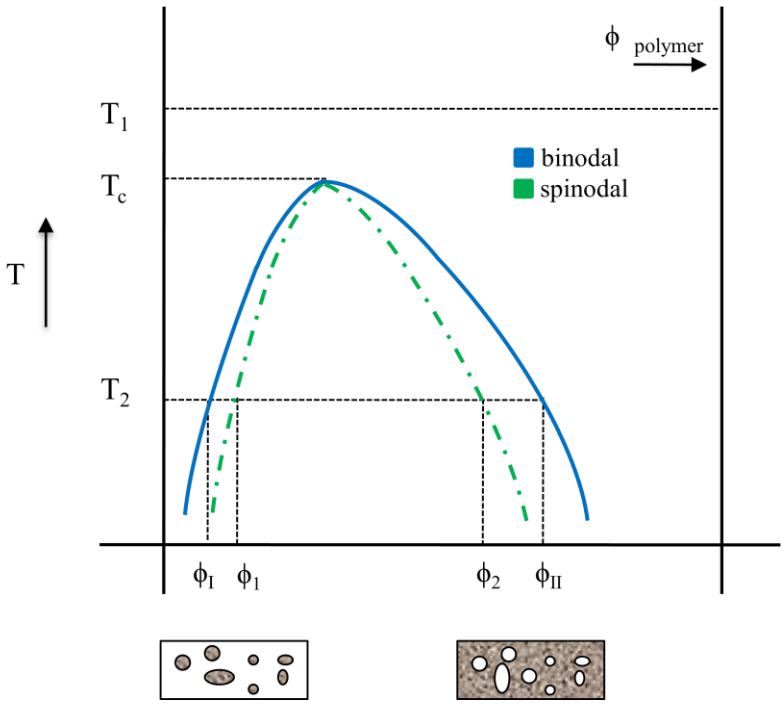

Fig. 2.13 Diagrams of the binodal and the spinodal curves for a polymeric solution as function of the volume fraction

The point where binodal and spinodal coincide is the critical point, as said the temperature up to which the system is stable at all the compositions. In fact for all the temperature higher than T_c, every single ratio between the polymer and the solvent in the system allow to obtain a homogeneous solution and as described in fig. 2.11, the free enthalpy of mixing is always negative. When a lower temperature is used (T_2) with the increasing of the polymer

concentration the binodal curve is reached (ϕ_I) and the stability of the system starts to be reduced. At that point, for all the composition included in the range ϕ_I- ϕ_1, the phenomenon called nucleation occur and the solution is characterized by the presence of little drops of polymer dispersed in the solvent. Those drops are in equilibrium, then the system is stable due to the absence of driving forces that can destabilize it. Same is valid for the ratio included in the ϕ_{II}- ϕ_2, where in the polymeric phase little drops of solvent are dispersed. Those two regions are called metastable, and they are particularly important for the membrane preparation with a Phase Inversion process: when a polymer/solvent solution with composition included in the subscribed ranges is used, if the droplets in the solution coalesce before the polymer solidifies following the precipitation process, an open porous system will result. But when the composition used are in the region bounded by ϕ_1- ϕ_2 under the spinodal curve, the de-mixing incur due to the growth of the drops dispersed: two different phases one rich in solvent and one in polymer are formed and the enthalpy of the system decreases in order to stabilize the system. Therefore, the de-mixing process is due to the destabilization of the system further to variation in the nature and complexity of the components, the temperature and the final composition. Adding a third element in the system is another important cause of de-mixing, the stability of a ternary system then, depends not only on the polymer/solvent ratio, but also on this third element, the non-solvent, used in a few phase inversion methods. From the Flory-Huggins theory discussed earlier (eq. 26), a free enthalpy of mixing expression for three elements can be derived:

$$\Delta \boldsymbol{G_{mix}} = RT\,(n_1\,ln\phi_1 + n_2\,ln\phi_2 + n_3\,ln\phi_3 + n_1\phi_2X_{12} + n_1\phi_3X_{13} + n_2\phi_3X_{23}) \quad [33]$$

and the chemical potential expressions for the three species in solution are:

$$\frac{\mu_1-\mu_1^o}{RT} = ln\phi_1 + (1-\phi_1) - \phi_2\frac{V_1}{V_2} - \phi_3\frac{V_1}{V_3} + V_1(X_{12}\phi_2 + X_{13}\phi_3)(\phi_2+\phi_3) - X_{23}V_1\phi_2\phi_3 \quad [34]$$

$$\frac{\mu_2-\mu_2^o}{RT} = ln\phi_2 + (1-\phi_2) - \phi_1\frac{V_2}{V_1} - \phi_3\frac{V_2}{V_3} + V_2(X_{12}\phi_1 + X_{23}\phi_3)(\phi_1+\phi_3) - X_{13}V_2\phi_1\phi_3 \quad [35]$$

$$\frac{\mu_3-\mu_3^o}{RT} = ln\phi_3 + (1-\phi_3) - \phi_1\frac{V_3}{V_1} - \phi_2\frac{V_3}{V_2} + V_3(X_{13}\phi_1 + X_{23}\phi_2)(\phi_1+\phi_2) - X_{12}V_3\phi_1\phi_2 \quad [36]$$

Then new diagrams and plots may be depicted, but in that case the system depends on three parameters and the temperature/composition graph assume a tridimensional conformation. As function of the temperature, three axes referring to the volume fraction of polymer, solvent and non-solvent build the diagram for a ternary system as represented in fig.2.14.

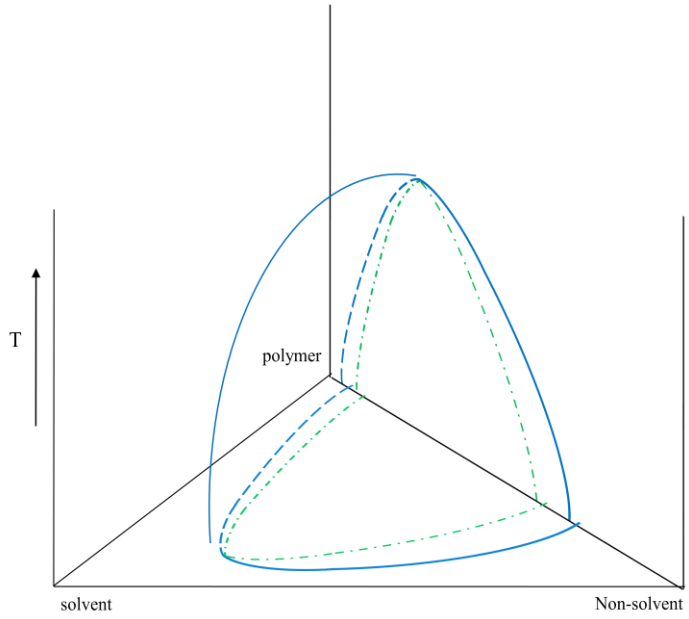

Fig. 2.14 3D Diagrams of the binodal and the spinodal curves for a ternary system polymer/solvent/non-solvent as function of the temperature

It is clear that even in that case where the two curves binodal (blue) and spinodal (green) coincide the critical point is determined, and at all the temperatures higher than Tc, each composition between the elements are possible, whereas when lower T are used the de-mixing area is reached and the phase separation incur. Crossing the diagram transversely, a bi-dimensional representation of the binodal and spinodal curves is obtained and the thermodynamic trend of the system can be analyzed at a determined temperature (isothermal system). The corners of the triangle depicted refer to the three components at the maximum of their concentration (100%) and consequently each point on the sides of the diagram represent a specific composition of the solution and a determined ratio (ϕ) between the two components placed on the ends of the same side, whereas all the points in the triangle area ascribe to a specific composition of the three elements together (fig. 2.15).

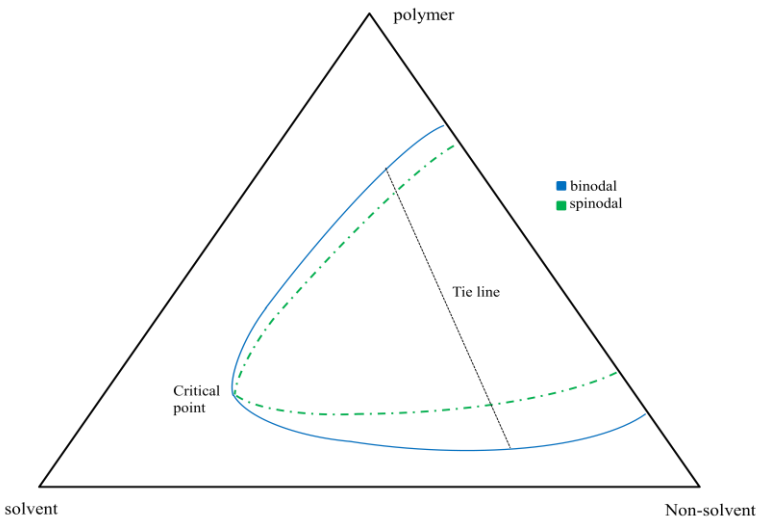

Fig. 2.15 Isothermal graph of a ternary system

As described for the binary system, the metastable regions bounded by the binodal and the spinodal curves contains the volume fractions values that refer to the solution in which the nucleation occur and two separated liquid phases are created. Droplets of solvent and non-solvent in the polymer rich phase and *vice-versa* are formed and start to growth and coalesce leaving a porous structure after the solidification of the continuous phase: then a porous membrane is obtained with a ternary metastable system as with a binary one. When the volume fractions are included under the spinodal curves the de-mixing will incur.

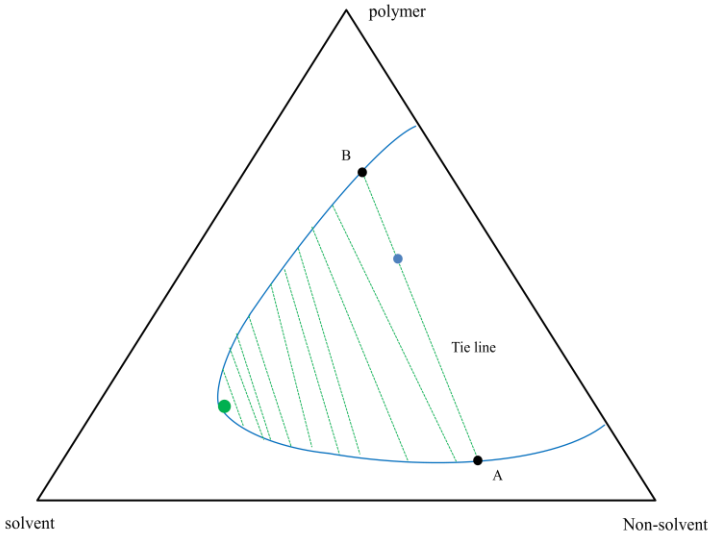

Fig. 2.16 Tie lines for an isothermal graph of a ternary system: two points (A and B) placed on the binodal curve depicted from a specific composition for the solution considerate (point in blue)

When a point is placed under the binodal, on the curve itself can be located two points referring to the phase composition in equilibrium, which generate a tie line if linked together. For each ternary phase diagram a set of tie lines is depicted and as soon as the top of the binodal is reached they narrow to a point called plait point, where le composition of the two phases coincide (fig.2.16). Characteristics and structure of a membrane are functions of the composition of the polymeric solution as much as the nature and the affinity between the elements of the system. Using the phase diagram the process for a membrane production from a ternary system foresees four steps (fig.2.17):

1. Preparation of a homogeneous polymeric solution (red point in the graph)
2. Adding of the non-solvent: the rate of the exchange between the solvent and the non-solvent depends on their affinity. Higher is the affinity faster is the exchange.
3. Crossing of the binodal region and beginning of the de-mixing process. This can be instantaneous when the solvent/non-solvent affinity is high and the diffusion process followed by the exchange is quick, or it can be retarded otherwise.
4. Final composition (A) of the ternary system with two phases in equilibrium: one rich in solvent (A') and one rich in polymer (A''). Their composition in terms of volume fraction lie on the tie line.

The choice of proper solvent and non-solvent depends on the nature of the polymer requested for the membrane preparation and they not only have to be similar but must be completely miscible with each other. In that way the exchange process will occur a membrane with a specific structure can be obtained. Generally quicker is the exchange rate higher is the final porosity of the membrane, but it is possible to control the process by adding little quantity of one of the liquid: more solvent in the system moves the equilibrium of the reaction decreasing the rate of exchange raising the density of the final membrane, whereas little amounts of non-solvent achieve the opposite effect, and a porous membranes is obtained.

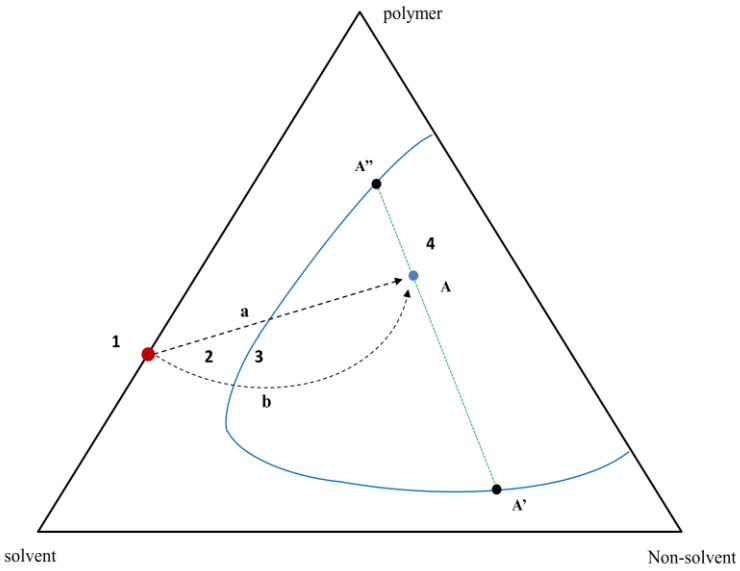

Fig. 2.17 Graphic representation of the four steps (1-4) involved in the miscibility of ternary system. The rate of exchange between solvent and non-solvent are named with the small letters a and b upon the arrows.

References:

- Baker R.W. (2004). *Membrane technology and applications*
- Greiner A, Wendorff JH. (2007). *Electrospinning: a fascinating method for the preparation of ultrathin fibers*
- Kowalewski T.A., Błoński S., and Barral S. (2005). *Experiments and modelling of electrospinning process*
- Merritt Sonia R., Exner Agata A., Lee Zhenghong, et al. (2011). *Electrospinning and Imaging; Advanced Engineering Materials*
- Mulder M. (1991). *Basic principles of membrane technology*
- Strathman H., Giorno L., Drioli E. (2006). *An introduction to membrane science and Technology*
- Van Oss C.J, Moore L.L., Good R.J. and Chaudhury M.K. (1985). *J. Protein Scie.* 4, 245

Chapter 3

Tissue Enginnering Scaffold-Free: a new approach

Introduction

Tissue engineering, developed by combining knowledge from molecular biology, materials science, biomechanics, and medicine, intends to produce tissue constructs to repair or replace native tissues compromised by trauma, pathology, or age. The components of the traditional tissue engineering are cells, signals, and scaffolds. Cells, which are necessary to form tissues, need to reside in significant numbers within scaffolds, meanwhile signals or stimuli (e.g., mechanical, electrical, or biochemical) drive these cells to produce the tissues of interest. Exogenous scaffolds are useful for providing structure to a developing tissue and allowing cells to adhere, proliferate, differentiate, and most importantly, secrete extracellular matrix (ECM) in a three-dimensional fashion. Scaffolds are attractive for additional reasons: in applications in which immediate load bearing is necessitated, the presence of an exogenous scaffold may provide the required mechanical integrity; also they facilitate the tailoring of mechanical anisotropy and afford the ability to precisely control the release of growth factors and other signals into the surrounding environment. However, issues with scaffold-based tissue engineering hinder its use in certain applications. Scaffold degradation is rarely synchronized to neotissue formation, making remodeling and integration difficult, thus compromising functional properties. Furthermore, toxicity and immunogenicity due to scaffold creation, seeding, or degradation are of concern [Liu et al., 2004]. The presence of a scaffold may also alter the phenotype of cells that come into contact with it [Levy-Mishali et al., 2009]. Although tissue engineering is still a young field, problems associated with the use of scaffolds, and strong desire for clinical and experimental application, have motivated research into alternate tissue engineering approaches. In particular, the scaffoldless technologies, taking advantage of cells' natural ability to synthesize tissue and respond to signals, have also appeared. Scaffoldless tissue engineering approaches include traditional techniques, such as pellet [Zhang et al., 2004] and aggregate culture [Furukawa et al., 2003]; but actually refers to any application that does not require cell seeding or adherence within an exogenous material. Scaffoldless approaches demonstrate certain advantages over traditional scaffold-based approaches by overcoming limitations associated with the use of scaffolds.

First, scaffoldless tissue engineering does not involve the exposure of cells spinner shear, elevated temperatures, toxic polymerizing chemicals, that are linked to the scaffold-based constructs production, a difference that leads to increased cell viability [Vunjak-Novakovic et al., 1999]. Additionally, without an intervening scaffold, tissue synthesis and remodeling may occur more readily and without the need for scaffold degradation that normally release by-products potentially immunogenics [Anderson et al., 2001]. Each of these advantages underscores an essential step in the process of tissue synthesis for clinical translation. Thus, scaffoldless technologies represent significant advances in tissue engineering, especially with regard to clinical applications.

3.1 Self-assembly and self-organization

The term self-assembly has been used to describe many distinct phenomena in science and engineering, including crystal growth, protein folding [Jacobs et al., 2002; Hartgerink et al., 2001], and in general refers to systems in which order results from disorder in a spontaneous manner, that is, without the use of external energy or force [Whitesides et al., 2002]. Often the expression self-assemble is erroneously used and mistaken with the self-organization process. In physics, chemistry, and biology, definitions of these terms are based on the field of thermodynamics, where the self-organization describes a process in which order appears when external energy or forces are input into the system [Halley et al., 2008; John et al., 2005], by contrast, for a self-assembling process, no external forces are required to promote order [Whitesides et al., 2002]. With the above definition in mind, bioprinting and cell-sheet engineering can be categorized as examples of self-organization. These techniques use external forces, such as physical manipulation or thermal input, to direct cell position, after which cell-driven remodeling (e.g. tissue fusion, described in Section 2.1) occurs [Jakab et al., 2010; Nishida et al., 2004]. Bioprinting first places cells into a templated pattern and then takes advantage of the ability of these cells to secrete ECM and fuse into a continuous tissue with the appropriate morphology [Jakab et al., 2010]. Similarly, in cell-sheet engineering, separate cell sheets are first seeded in monolayers and then detached with the use of heat. Afterward, these monolayers are stacked or rolled and undergo remodeling and fusion into patches or tubes of tissue with clinically relevant sizes [Nishida et al., 2004]. Underlying these examples are the biological mechanisms by which self-organization takes place, most notably the process of tissue fusion, which is also observed during tissue development in vivo. Furthermore, some self-organizing tissues possess appreciable functional properties, with

values at times comparable to those of their native counterparts. Thus, the relevance and significance of self-organization techniques in tissue engineering are that highly biomimetic constructs, which are more easily translated toward applications, are produced.

3.2 Energy Minimization during the Self-Assembling Process

By applying the characteristics of self-assembly in thermodynamics, the self-assembling process in tissue engineering can be defined as a scaffoldless technology that produces tissues that demonstrate spontaneous organization without external forces; this occurs via the minimization of free energy through cell-to-cell interactions. As in thermodynamics, the difference between the terms self-assembling process and self-organization in tissue engineering is whether external energy or forces are introduced into the system. Although both are subsets within scaffoldless tissue engineering, the self-assembling process is unique in that organization arises without the input of external forces. Self-assembling tissues possess the following specific characteristics: (*a*) the use of a nonadherent substrate to minimize tissue free energy, (*b*) a sequential set of phases that recapitulate native tissue formation, (*c*) tissue constructs with sufficient size and morphology to be clinically relevant, and (*d*) functional properties with values comparable to those of native tissue. Notably, self-assembling tissues follow the differential adhesion hypothesis, a fundamental mechanism of developmental biology. Thus, self-assembling tissues are highly biomimetic and comprise promising candidates for clinical application. In various instances and stages of tissue development, cells interact to minimize the overall free energy of the tissue they comprise, resulting in several phenomena including cell sorting. When biologists observed the sorting behavior of dissociated germ layer cells, models to describe this behavior began to be formulated. The most successful of these is the differential adhesion hypothesis, which states that a tissue will tend to minimize the adhesive free energy of its cell populations via cell-to-cell binding [Foty et al., 2005; Steinberg et al., 1970]. Accordingly, a mass of cells may be conceptualized as a liquid that works to minimize its surface tension (known as tissue surface tension). Tissue surface tension will determine whether these cells sort to the center or periphery when mixed with another cell population to form a heterogeneous tissue, with cells from the tissue of higher surface tension maximizing their intercellular adhesion and, thus, being enveloped [Steinberg et al., 2007]. The cell-to-cell adhesion molecules thought to be primarily responsible for differential adhesion are cadherins, which are calcium-dependent transmembrane proteins. Indeed, tissue surface tension has been shown to be linearly

correlated to the number of cadherin molecules present, although theoretically any cell-to-cell adhesion molecule may drive differential adhesion [Foty et al., 2005]. Although the differential adhesion hypothesis is the most widely accepted model of these phenomena, recently, another explanation, the differential interfacial tension hypothesis, has been gaining recognition [Youssef et al., 2011; Krieg e al., 2008; Brodland et al., 2002; Harris et al., 1976; Dean et al., 1989]. This explanation also conceptualizes tissue as a liquid that acts to reduce its surface tension, but it highlights the possibility that forces generated by cellular components such as the membrane and cytoskeleton may dictate cell sorting. The differential adhesion hypothesis and the differential interfacial tension hypothesis may be related. The underlying driving tendency of cells in a tissue to minimize their free energy does not change between these theories [Brodland et al., 2002]. Recent work has brought these two hypotheses together, showing that induced germ layer cells display differential binding affinities as well as different cell cortical tensions[Krieg e al., 2008]. Alongside of this, it has also been reported that intracellular cytoskeletal reorganization can occur as a result of cadherin-mediated adhesion [Berrier et al., 2007] and that tissue surface tensions measured from actomyosin contractility outweigh those generated by cadherin interactions[Evans et al., 1989; Amack et al., 2012]. Thus, it is reasonable to speculate that energy minimization in a developing tissue may be due to initial cadherin interactions leading to downstream signaling and cytoskeleton reorganization, resulting in cell aggregation and sorting [Amack et al., 2012]. The self-assembling process works by the principle of free energy minimization (fig. 3.1). During the self-assembling process, cells are seeded upon a nonadhesive surface [Hu et al., 2006; Hoben et al., 2007]. This prevents cell attachment and thus compels cells in a developing neotissue to spontaneously adhere to one another in order to minimize free energy. Consequently, immunohistochemical staining, at 1 day and 4 days after cell seeding, displays extensive N-cadherin-mediated cell-to-cell binding, which occurs without the influence of external forces [Ofek et al., 2008]. This mimics the process of mesenchymal condensation, in which N-cadherin levels increase dramatically prior to chondrogenesis [Oberlender et al., 1994].

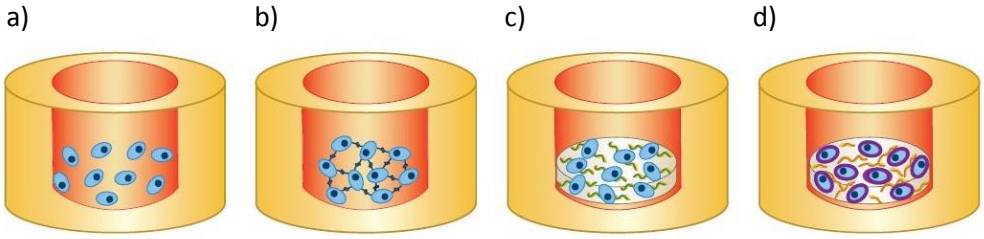

Fig.3.1 Phases in the development of self-assembling process: a) High-density cell seeding in nonadherent substrate; b) Minimization of free energy via binding of cell adhesion receptors; c) Cell migration and production of extracellular matrix; d) Distinct regional matrix formation and tissue maturation

Accordingly, the first characteristic of the self-assembling process is the use of a nonadherent mold to minimize construct free energy. Energy minimization will also lead to cell sorting, and indeed, groups utilizing the self-assembling process to investigate cell sorting have seen the segregation of endothelial cells and fibroblasts seeded in agarose wells [Youssef et al., 2011]. Furthermore, this sorting mechanism and the self-assembling process have also been seen to depend on the cytoskeleton [Kinoshita et al., 2008; Dean et al., 2008]. Therefore, differential interfacial tension may also be relevant to this culture system, as interfacial tensions are generated in part by the cytoskeleton [Brodland GW. 2002; Brodland et al., 2000; Harris AK. 1976]. In summary, the self-assembling process in tissue engineering follows the principle of free energy minimization without external forces, leading to the recapitulation of mechanisms relevant to native tissue development.

3.3 Tissue Fusion in Self-Organizing Tissues

Tissue fusion comprises a series of events in developmental biology that are involved, for example, in neural tube formation, skeletal patterning, and cardiovascular development. Tissue fusion has been defined as the process by which two or more isolated cell populations make contact and adhere [P´erez-Pomares et al., 2006]. This includes cell-to-cell contact and/or cell-to-matrix contact of two previously separated cell populations. In addition, tissue fusion includes matrix-to-matrix contact and ECM remodeling. Interestingly, a biological process similar to tissue fusion also occurs in self-organizing and self-assembling tissues. For example, self-organization approaches in engineering musculoskeletal, cardiovascular, neurosensory, and digestive tissues all display a fusion process in which previously isolated cells and/or ECM converge into a continuous whole [Eiraku et al., 2011; Vallier et al., 2010;

Riccalton-Banks et al., 2003; Halley et al., 2008; John et al., 2005; Calve et al., 2004; Syed-Picard et al., 2009; Paxton et al., 2010]. Self-organizing optic and liver tissues are engineered such that micromasses fuse into a continuous neotissue [Eiraku et al., 2011; Riccalton-Banks et al., 2003]. Self-organizing nerve, bone, tendon, and ligament tissues all rearrange into cylindrical tubes following seeding, concomitant with tissue fusion of opposite ends of an initial cell sheet [Vallier et al., 2010; John et al., 2005; Syed-Picard et al., 2009; Paxton et al., 2010]. Bioprinting and cell-sheet engineering, as self-organization technologies, also display tissue fusion. Bioprinted tissue solutions fuse together over time to form sheets, tubes, or other intended morphological features, after deposition onto a substrate [Norotte et al., 2009]. Similarly, cell sheet engineering of corneal, cardiac, and vascular tissues involves the fusion of distinct layers of ECM to form one continuous tissue [L'Heureux et al., 1998; Proulx et al., 2010; Shimizu et al., 2003]. These processes may occur once the cell sheets or bioprinted solutions are directed into contact with one another by the use of external forces. Finally, self-assembling cartilage and fibrocartilage also display tissue fusion, as separate cells eventually converge into a continuous tissue [Hu et al., 2006; Hoben et al., 2007].Therefore, self-organizing tissues and self-assembling tissues both exhibit a process reminiscent of the tissue fusion found in native tissue development.

3.4. Self-Assembling in Tissue Engineering

The self-assembling process for articular cartilage is a good example with which to describe the self-assembling process in tissue engineering because it has been reported to follow the characteristics of self-assembling tissues [Ofek et al., 2008]. The first two characteristics of these tissues are (*a*) the ability tominimize free energy without the use of external forces and (*b*) a distinct set of phases reminiscent of those in native tissue development. The first phase in developmentof self-assembling articular cartilage is high-density seeding of articular chondrocytes in a nonadherent agarose well. The nonadherent agarose well used here prevents substrate adhesion and promotes the minimization of free energy via cell-to-cell interactions in the second phase [Hut et al., 2004]. Instead of agarose, 2-hydroxyethyl methacrylate [Novotny et al., 2006] and semipermeable membranes [Brehm et al., 2006] have also been used as nonadherent substrates. The seeded articular chondrocytes express high levels of N-cadherin, which mediates cell-to-cell adhesion and tissue fusion, resulting in neotissue formation without the use of exogenous forces and collagen VI is produced throughout the self-assembling tissue, and high levels of the glycosaminoglycan (GAG) chondroitin-6-

sulphate are synthesized. ECM maturation is the final vital step in cartilage formation, and self-assembling articular cartilage mimics this aspect of native tissue development. Collagen VI localizes to the pericellular matrix as production of collagen II increases, and relative levels of chondroitin-6-sulphate and chondroitin-4-sulphate change to reproduce those seen during native cartilage development [Ofek et al., 2008]. Because collagens and GAGs confer tensile and compressive properties to native tissue, appropriate levels of these ECM components are tantamount to achieving adequate functional properties in engineered tissues. Fibrocartilages such as the knee meniscus and temporomandibular joint (TMJ) disc are tissues whose shape is specific to their mechanical functions. The self-assembling process allows tissues to be grown in anatomically correct shapes. For fibrocartilage, analogous to self-assembling articular cartilage, high-density cocultures of chondrocytes and fibrochondrocytes can be seeded in ringshaped nonadherent agarose molds to form anatomically shaped menisci that maintain the wedge profile of native menisci [Huey et al., 2011];. The generation of native tissue anisotropy is also possible with self-assembling tissue. For example, self-assembling fibrocartilage in an anatomically shaped mold displays mechanical properties on par with or approaching those of native tissue, with compressive instantaneous modulus values of up to 800 kPa and tensile stiffness of up to 3 MPa [Huey et al., 2011]. Similarly, in self-assembling articular cartilage [Responte et al., 2012; Elder et al., 2008; Elder et al., 2009]. Self-assembling tissue may also be grown to clinically relevant sizes. Articular cartilage up to 6 mm in diameter and 3 mm in thickness and fibrocartilage up to 13 mm in diameter and 1.5 mm in thickness have been reported with this process [Responte et al., 2012; Huey et al., 2011]. Self-organizing vascular constructs are one of the most promising scaffoldless engineered tissues currently in preclinical and clinical studies. Engineered grafts recapitulate native vascular morphology and biological responses to relaxation and contraction stimuli, such as cAMP and calcium ions [L'Heureux et al., 2001; L'Heureux et al., 2007]. These grafts can also undergo devitalization and freezing, followed by rehydration, for later implantation into patients [Wystrychowski et al., 2011]. This greatly increases their potential shelf life and thus clinical applicability. Because of these successes with early clinical application, self-organizing vasculature represents a model technology for clinical translation of tissue engineering. Aside from vascular constructs, self-organizing cornea using a detachable cell sheet grown on a thermally responsive hydrogel [Yang et al., 2006] has also shown promising results in human trials [Nishida et al., 2004]. Implantation of self-organizing corneas in patients suffering from Salzmann's nodular degeneration led to significant improvements in gross transparency and visual acuity, as reported by patients [Nishida et al.,

2004]. In corneal tissue engineering, epithelial-stromal interactions are important for the longterm survival of constructs *in vivo* [Nishida et al., 2003]. Accordingly, these self-organizing corneal constructs display an intrinsic ability to adhere to corneal stroma, representing an added clinical advantage, obviating the need for sutures during implantation. Furthermore, these constructs recapitulate native apical-basal cell and matrix organization [Nishida et al., 2004]. In addition to clinical applications, self-organizing and self-assembling tissues have also been used as in vitro models to screen drugs and to study injury and disease. Producing a tissue model that duplicates in vivo human conditions represents a major challenge. Self-organizing and self-assembling tissues have the advantage of recapitulating the morphological structure and organization of native tissues. Furthermore, some of these tissues also mimic fundamental biological processes seen in vivo. Therefore, self-organization and the self-assembling process are promising tools to study tissue formation, behavior, and trauma. Injury models, including wound healing in skin and cornea, as well as liver damage, represent one cogent application of self-organizing tissues. In vitro models of wound healing are limited by the absence of multiple epithelial cell layers and a lack of epithelial-mesenchymal interactions, characteristics that are both present in vivo [Zieske et al., 2001]. Accordingly, because of its multilayered structure, engineered cornea is a promising candidate for studying corneal wound healing [Carrier et al., 2008]. Similarly, liver spheroids have been used as in vitro models to screen drugs for liver injury [Kinoshita et al., 2008]. For example, cytochalasin D treatment affects spheroid formation and hepatocyte morphology in these tissues, resulting in fivefold lower albumin secretion. Therefore, self-organizing constructs can be used to study tissue injury. Disease models can also be investigated using self-organizing and self-assembling tissues. For example, cardiac hypertrophy, which is a consequence of increased biomechanical stress, often leads to pathological conditions [Hardt et al., 2004]. To study this complex disease in vitro requires the recapitulation of structural and functional features of native cardiac tissues. Recently, self-organizing cardiac tissues have been used as in vitro tools to study the hypertrophic phenotype [Chung et al., 2011]. Engineered cardiac tissue subjected to biomechanical stress in vitro successfully demonstrates structural remodeling, increased secretion of clinical hypertrophy markers such as atrial natriuretic peptide (ANP), and electrophysiological changes, as found in cardiac hypertrophy in vivo. Furthermore, clinically used pharmacological antihypertrophic treatments partially reversed this hypertrophic behavior, akin to what is observed in vivo [Chung et al., 2011]. Though a relatively new technology, self-organizing tissues represent a platform technology that can be employed to provide in vitro analogs of in vivo disease conditions. Thus, further

exploration of self-organizing and self-assembling tissues as research models may represent a promising area for future research.

3.5. Self-Organization in Tissue Engineering

Partly owing to the advantages conveyed by scaffoldless tissue engineering, substantial functional properties have been reported with many self-organizing tissues. Self-organization in tissue engineering has been used, through several different methods, to engineer a wide variety of tissues from various systems of the body (e.g., the musculoskeletal, cardiovascular, neurosensory, and digestive systems). Several tissues from the musculoskeletal system have been engineered using approaches that display self-organization. In general, self-organization in musculoskeletal tissues such as bone, tendon, ligament, and skeletal muscle starts with monolayer culture of cells in protein-coated (e.g. laminin) Sylgard plates with external anchors. These anchors are used to exert tensile forces on the seeded monolayer as it contracts and rolls up, leading to the formation of a cylindrically shaped tissue [Calve et al., 2004; Syed-Picard et al., 2009; Strohman et al., 1990; Huang et al., 2005]. Expression of cadherins and other adhesion molecules during self-organization of musculoskeletal tissues is uncharacterized and open to further research. Additionally, the role of the various coatings on self-organization is unclear; it is possible that coating degradation throughout culture exposes the initial monolayer to a nonadherent surface. Thus, it is conceivable that minimization of free energy will occur through the use of a nonadherent surface, but this needs to be examined. Self-organizing musculoskeletal tissues display morphological and structural features, as well as some mechanical functionality, reminiscent of those in corresponding native tissues. In self-organizing bone, localization of osteocytes in lacunae, formation of lumen-containing structures similar to blood vessels, and development of cellular areas similar to bone marrow all occur [Syed-Picard et al., 2009; Pirraco et al., 2011]. Self-organizing tendons and ligaments exhibit collagen fiber alignment reminiscent of that in native tissues [Calve et al., 2010]. Self-organizing skeletal muscle displays myoblast fusion into myotubes and the formation of muscle-specific structures (e.g. hexagonal architecture and Z lines) [Huang et al., 2005]. Additionally, both fast-twitch and slow-twitch muscle subtypes, with relative relaxation and contraction rates, have been engineered [Huang et al., 2007]. Engineered musculoskeletal tissues also maintain functional properties. For instance, selforganizing ligaments and tendons exhibit tangent modulus values of 15 to 17 MPa, concomitant with abundant collagen I and III staining [Calve et al., 2004; 63). Similarly, self-

organizing muscle has been reported to exert a specific force of up to 140 N/mm2, which is within the range displayed by native tissue, during culture and stimulation within an electrical bioreactor [Donnelly et al., 2010]. Self-organizing bone with tangent modulus of up to 29 MPa and compressive strength surpassing 1.5 MPa after 6 weeks of culture has also been reported [Syed-Picard et al., 2009; Ma et al., 2010]. By comparison, scaffoldless bone culture on an orbital shaker (i.e., aggregate culture) does not form large macroscopic tissue and thus is not mechanically testable [Hildebrandt et al., 2011]. However, mechanical properties of native bone can be much greater, with compressive stiffness reaching hundreds ofMPa and compressive strength in the range of tensof MPa [Fyhrie et al., 2000]. Therefore, self-organizing musculoskeletal tissues demonstrate promising results, especially with regard to tissue morphology and functional properties, and more research should be conducted to elucidate the potential of these technologies. Cardiovascular tissue engineering has benefitted from self-organization in tissue engineering, especially in the synthesis of vascular constructs, where a paradigm shift from polymeric scaffoldbased to cell-based scaffoldless techniques has occurred over the past decade [Peck et al., 2012]. Self-organizing vasculature has been demonstrated via the use of cell-sheet engineering, in which high confluence monolayers are harvested as a whole sheet, and external forces are then introduced by rolling the cell sheet on a mandrel [L'Heureux et al., 1998; Gauvin et al., 2010]. During culture, these initially separate layers spontaneously fuse to form a tube structure [L'Heureux et al., 1998]. Self-organizing vasculature mimics the layered organization of native blood vessels, with an inner endothelial lining, a medial smooth muscle cell layer, and an outer adventitia rich in ECM [Mironov et al., 2009]. These self-organizing constructs can reach tensile moduli of up to 2MPa and are capable of withstanding burst pressures of up to 465 kPa [Mironov et al., 2009]. Another reported technique uses high-density seeding of smooth muscle cells in annular agarose wells, similar to the ring-shaped mold used in self-assembling meniscus-shaped fibrocartilage [Aufderheide et al., 2007; Gwyther et al., 2011; Gwyther et al., 2011]. External forces are then introduced when these tissues are manually aligned, after which they fuse into vascular tubes, which display tensile strengths and moduli of up to 500 kPa and 2 MPa, respectively [Gwyther et al., 2011]. Because of their functional properties, these vascular constructs have great clinical potential, and currently some of them are in clinical trials [McAllister et al 2209]. In cardiac tissue engineering, one technique stacks multiple layers of cardiac muscle sheets together, before this construct self-organizes into a continuous tissue [Haraguchi et al., 2012]. Another example is bioprinting, which utilizes layer-by-layer deposition of cells onto a substrate to place cell aggregates in close proximity, eventually

leading to tissue fusion [Yang et al., 2012]. Self-organizing cardiac muscle displays native tissue structures, electrical conductivity, contraction rates similar to native tissues, and the ability to continuously contract without fatigue [Haraguchi et al., 2012; Baar et al., 2005; Kelm et al., 2004]. Although self-organizing cardiac muscle and vasculature display significant similarities to native tissue, developmental phases during construct formation, if any, are not characterized. Additionally, the use of external forces in engineering of self-organizing cardiovascular tissues makes them distinct from the self-assembling process in tissue engineering. Owing to its high potential for clinical translation and simple manufacturing procedures, self-organization may be a suitable platform to solve problems associated with cardiovascular tissues. Self-organizing neurosensory tissues, such as optic cup, cornea, and nerve, display structural features or functional properties similar to those of native tissues. Akin to tendon, self-organizing nerve starts with monolayer culture of tendon fibroblasts on laminin-coated Sylgard plates, with subsequent seeding of neural cells. This culture then contracts and fuses into a tube-shaped tissue around two anchors, with an inner nerve cell layer and an outer fibroblast layer. It has been shown that self-organizing nerve has conduction velocities (12.5 m/s) comparable to those of rat neonatal sciatic nerve [Vallier et al., 2010]. Furthermore, these self-organizing constructs have also been co-cultured in association with glial-like cells differentiated from adipose-derived stem cells, although conduction velocities were not measured [Adams et al., 2012]. Complex self-organizing optic tissues have also been engineered. In these, formation of a distinct optic cup is followed by segregation from stratified neurosensory tissue [Eiraku et al., 2011]. Self-organizing cornea is another example, in which corneal epithelial cells, limbal epithelial cells, and corneal fibroblasts have been used to recreate the layered structure of native cornea [Griffith et al., 2009]. Seeding of corneal endothelial and epithelial cells on each side of a self-organizing fibroblast layer leads to tissue fusion [Proulx et al., 2010]. The liver, as part of the digestive system, has been the topic of numerous tissue engineering approaches. Self-organization of liver tissues results in biochemical secretion of several functional enzymes, as well as native structural organization. This self-organization technique involves initial seeding of hepatocytes on a surface coated with adherent proteins (e.g., collagen or glycoproteins), which leads to the hepatocytes self-organizing into spheroid structures after several hours or days [Riccalton-Banks et al., 2003; Koide et al., 1990]. As this method uses an adherent coating for cell attachment, it is categorized as self-organization. Self-organizing liver tissues can reach up to 2.5 mm in diameter, and it has been shown that the size of these spheroids is linearly correlated with initial cell seeding concentration [Torisawa et al., 2007] Self-

organizing liver tissues also possess several features of developing tissues, such as bile canalicular formation, abundant cell-to-cell communication, cuboidal hepatocyte morphology, and cell sorting [Landry et al., 1985; Fukuda et al., 2006; Hansen et al., 1998]. Additionally, self-organizing liver tissues secrete several functional proteins. Albumin secretion rates are equivalent to those of freshly isolated hepatocytes, and prolonged secretion of cytochrome P450 oxidation enzymes has also been reported [Riccalton-Banks et al., 2003]. It has also been demonstrated that, on a per cell basis, self-organizing liver tissues can produce more α1-antitrypsin than individual hepatocytes can and that urea and bile excretion into canaliculi occurs [Ohashi et al., 1997; Meng et al., 2006; Abu-Absi et al., 2002]. Self-organizing liver tissues display a large variety of biochemical functions, and future research should investigate and enhance their translational potential. Self-organization in tissue engineering is not synonymous with the self-assembling process in tissue engineering. In contrast to the self-assembling process, self-organization often requires external forces, manipulation, or seeding on an adherent surface. Continued research on selforganizing tissues, especially focused on the basic mechanisms by which these tissues form, is needed.

Tissue/organ	Tissue engineering method	Properties attained	References
Vasculature	Self-organization by cell sheet engineering	Average burst pressure of 3,490 mm Hg (465 kPa)	L'Heureux et al. 1998, Gauvin et al. 2010, Mironov & Kasyanov 2009, Gwyther et al. 2011, McAllister et al. 2009, Haraguchi et al. 2012, L'Heureux et al. 2007
	Bioprinting	Engineered vascular tube of 900 μm diameter with 300 μm wall thickness	Norotte et al. 2009
Articular cartilage	Self-assembling process	~3-mm thick constructs with compressive aggregate modulus of 280 kPa; tensile stiffness at 2 MPa	Responte et al. 2012, Hu & Athanasiou 2006, Elder & Athanasiou 2009
	Pellet culture	~1-mm spherical construct	Zhang et al. 2004
	Aggregate culture	~500-μm spherical construct	Furukawa et al. 2003
Meniscus	Self-assembling process	Compressive instantaneous modulus of up to 800 kPa and tensile stiffness of up to 3 MPa (tensile modulus in circumferential and radial directions of up to 3 MPa and 1.5 MPa, respectively)	Hoben et al. 2007, Aufderheide & Athanasiou 2007, Huey & Athanasiou 2011, Huey & Athanasiou 2011
Eye	Self-organization	Transparent tissue of 55-μm thickness	Eiraku et al. 2011, Nishida et al. 2004, Proulx et al. 2010, Zhang et al. 2011, Nishida et al. 2004
Tendon and ligament	Self-organization	Tangent modulus of 15 to 17 MPa	Calve et al. 2004, Hairfield-Stein et al. 2007, Huang et al. 2005, Calve et al. 2010
Liver	Self-organization	Albumin production; prolonged secretion of the oxidation enzyme cytochrome P450; production of α1-antitrypsin	Tzanakakis et al. 2001, Koide et al. 1990, Landry et al. 1985, Hansen et al. 1998, Ohashi et al. 2007
Nerve	Self-organization	Conduction velocities of 12.5 m/s	Baltich et al. 2010, Adams et al. 2012

Table 3.1 Functional properties of tissue constructs engineered by self-organization and the self-assembling process

3.6 Conclusions and future directions of the scaffold-free TE

Self-organization in tissue engineering can be defined as a subset of techniques within scaffoldless tissue engineering that produce tissues that demonstrate spontaneous organization. The self-assembling process in tissue engineering is a separate subset within scaffoldless tissue engineering, defined as a technology that produces tissues that demonstrate spontaneous organization from the minimization of free energy through cell-to-cell interactions and without external forces. Self-organization and the self-assembling process are promising tissue engineering approaches that have already shown great potential for engineering complex tissues with functional property values approaching those of native tissue. Of particular significance is the fact that some self-organizing tissues have already been used in clinical applications. For example, self-organizing engineered vascular constructs have been used in hemodialysis patients [L'Heureux et al.,, 1998; McAllister et al., 2009; L'Heureux e tal., 2007] and self-organizing cornea constructs have achieved beneficial results in patients suffering from Salzmann's noduluar degeneration [Zhang et al., 2011; Nishida et al., 2004; Nishida e tal., 2004]. In addition to this, self-organized hepatocyte spheroids have been used in pharmacological screening of drugs [Tzanakakis et al., 2001]. Furthermore, self-assembling cartilage recapitulates sequential phases of development seen in native cartilage formation [Hu et al., 2006; Ofek et al., 2008]. These recent key findings pave the way for engineering more complex tissues with greater biochemical and mechanical properties, and they encourage future research to enhance self-organization and the self-assembling process for wider use. Future directions for research on self-organizing and self-assembling tissues should concentrate on achieving clinical application. The results thus far suggest that these processes can be employed in promising manners to fabricate some of the most complex tissues and structures of the body, including articular cartilage, fibrocartilage, bone, tendon, ligament, vasculature, cardiac muscle, liver, nerve, and cornea.

References

- Abu-Absi SF, Friend JR, Hansen LK, HuWS. (2002). *Exp. Cell Res.* 274:56–67
- Adams AM, Arruda EM, Larkin LM. (2012). *Neuroscience* 201:349–56
- Amack JD, Manning ML. (2012). *Science* 338:212–15
- Anderson JM. (2001). *Annu. Rev. Mater. Res.* 31:81–110
- Aufderheide AC, Athanasiou KA. (2007). *Tissue Eng.* 13:2195–205
- Baar K, Birla R, Boluyt MO, et al. (2005). *FASEB J.* 19:275–77
- Baltich J, Hatch-Vallier L, Adams AM, et al. (2010). *In Vitro Cell. Dev. Biol. Anim.* 46:438–44
- Berrier AL, Yamada KM.(2007). *J. Cell. Physiol.* 213:565–7353.
- Brehm W, Aklin B, Yamashita T, et al. (2006). *Osteoarthr. Cartil.* 14:1214–26
- Brodland GW. (2002). *J. Biomech. Eng.* 124:188–97
- Calve S, Dennis RG, Kosnik PE II, et al. (2004). *Tissue Eng.* 10:755–61
- Calve S, Lytle IF, Grosh K, et al. (2010). *J. Appl. Physiol.* 108:875–81
- Carrier P, Deschambeault A, Talbot M, et al. (2008). *Investig. Ophthalmol. Vis. Sci.* 49:1376–85
- Chung CY, Bien H, Sobie EA, et al. (2011). *FASEB J.* 25:851–62
- Dean DM, Morgan JR. (2008). *Tissue Eng. Part A* 14:1989–97
- Donnelly K, Khodabukus A, Philp A, et al. (2010). *Tissue Eng. Part C Methods* 16:711–18
- Eiraku M, Takata N, Ishibashi H, et al. (2011). *Nature* 472:51–56
- Elder BD, Athanasiou KA. (2008). *PLoS One* 3:e2341
- Elder BD, Athanasiou KA. (2009). *Tissue Eng. Part A* 15:1151–58
- Evans E, Yeung A. (1989). *Biophys. J.* 56:151–60
- Foty RA, Steinberg MS. (2005). *Dev. Biol.*278:255–63
- Fukuda J, Sakai Y, NakazawaK. (2006). *Biomaterials* 27:1061–70
- Furukawa KS, Suenaga H, Toita K, et al. (2003). *Cell Transplant.* 12:475–79
- Fyhrie DP, Vashishth D. (2000). *Bone* 26:169–73
- Gauvin R, Ahsan T, Larouche D, et al. (2010). *Tissue Eng. Part A* 16:1737–47
- Griffith M, JacksonWB, Lagali N, et al. (2009). *Eye* (*Lond.*) 23:1985–89
- Gwyther TA, Hu JZ, Billiar KL, Rolle MW. (2011). *J. Vis. Exp.* (57):e3366
- Gwyther TA, Hu JZ, Christakis AG, et al. (2011). *Cells Tissues Organs* 194:13–24
- Halley JD, Winkler DA. (2008). *Complexity* 14:10–17
- Hansen LK, Hsiao CG, Friend JR, et al. (1998). *Tissue Eng.* 4:65–74
- Haraguchi Y, Shimizu T, Sasagawa T, et al. (2012). *Nat. Protoc.* 7:850–5879.
- Hardt SE, Sadoshima J. (2004). *Cardiovasc. Res.* 63:500–9
- Harris AK. (1976). *J. Theor. Biol.* 61:267–85
- Hartgerink JD, Beniash E, Stupp SI. (2001). *Science* 294:1684–88
- Hildebrandt C, Buth H, Thielecke H. (2011). *Tissue Cell* 43:91–100
- Hoben GM, Hu JC, James RA, Athanasiou KA. (2007). *Tissue Eng.* 13:939–46
- Hu JC, Athanasiou KA. (2006). *TissueEng.* 12:969–79
- Huang YC, Dennis RG, Baar K. (2006). *Am. J. Physiol. Cell Physiol.* 291:C11–17
- Huang YC, Dennis RG, Larkin L, Baar K. (2005). *J. Appl. Physiol.* 98:706–13
- Huey DJ, Athanasiou KA. (2011). *Biomaterials* 32:2052–58
- Huey DJ, Athanasiou KA. (2011). *PLoS One* 6:e27857

- Jacobs HO, Tao AR, Schwartz A, et al. (2002). *Science* 296:323–25
- Jakab K, Norotte C, Marga F, et al. (2010). *Biofabrication* 2:02200129.
- John K, Bar M. (2005). *Phys. Rev. Lett.* 95:198101
- Kelm JM, Ehler E, Nielsen LK, et al. (2004). *Tissue Eng.* 10:201–14
- Kinoshita N, Sasai N, Misaki K, Yonemura S. (2008). *Mol. Biol. Cell* 19:2289–99
- Koide N, Sakaguchi K, KoideY, Asano K, et al. (1990). *Exp. Cell Res.* 186:227–35
- Krieg M, Arboleda-Estudillo Y, Puech PH, et al. 2008. *Nat. Cell Biol.* 10:429–36
- L'Heureux N, Dusserre N, Marini A, et al. (2007). *Nat. Clin. Pract. Cardiovasc. Med.* 4:389–95
- L'Heureux N, Paquet S, Labbe R, et al. (1998). *FASEB J.* 12:47–56
- L'Heureux N,McAllister TN, de la Fuente LM. (2007). *N. Engl. J. Med.* 357:1451–53
- L'HeureuxN, Stoclet JC, Auger FA, et al. (2001). *FASEB J.* 15:515–24
- Landry J, Bernier D, Ouellet C, et al. (1985). *J. Cell Biol.* 101:914–23
- Levy-Mishali M, Zoldan J, Levenberg S. (2009). *Tissue Eng. Part A* 15:935–44
- Liu X, Ma PX. (2004). *Ann. Biomed. Eng.* 32:477–86
- Ma D, Ren L, Liu Y, Chen F, et al. (2010). *J. Orthop. Res.* 28:697–702
- Maitre JL, Berthoumieux H, Krens SF, et al. (2012). *Science* 338:253–56
- McAllister TN, MaruszewskiM, Garrido SA, et al. (2009). *Lancet* 373:1440–46
- Meng Q, Wu D, Zhang G, Qiu H. (2006). *Biotechnol. Lett.* 28:279–84
- Mironov V, Kasyanov V. (2009). *Lancet* 373:1402–4
- Mironov V, Visconti RP, Kasyanov V, et al. (2009). *Biomaterials* 30:2164–74
- Nishida K, Yamato M, Hayashida Y, et al. (2004). *N. Engl. J. Med.* 351:1187–96
- Nishida K, Yamato M, Hayashida Y, et al. (2004). *Transplantation* 77:379–85
- Nishida K, Yamato M, Hayashida Y, Watanabe K, et al. (2004). *N. Engl. J. Med.*351:1187–96
- Nishida K. (2003). *Cornea* 22:S28–34
- Norotte C, Marga FS, Niklason LE, Forgacs G. (2009). *Biomaterials* 30:5910–17
- Novotny JE, Turka CM, Jeong C, et al. (2006). *Tissue Eng.* 12:2755–64
- Oberlender SA, Tuan RS. (1994). *Cell Commun. Adhes.* 2:521–37
- Ofek G, Revell CM, Hu JC, et al. (2008). *PLoS One* 3:e2795
- Ohashi K, Yokoyama T, Yamato M, et al. (2007). *Nat. Med.* 13:880–85
- P´erez-Pomares JM, Foty RA. (2006). *BioEssays* 28:809–21
- Paxton JZ, Grover LM, Baar K. (2010). *Tissue Eng. Part A* 16:3515–25
- Peck M, Gebhart D, Dusserre N, McAllister TN, L'Heureux N. (2012). *Cells Tissues Organs* 195:144–58
- Pirraco RP, Obokata H, Iwata T, Marques AP, Tsuneda S, et al. (2011). *Tissue Eng. Part A* 17:1507–15
- Proulx S, d'Arc Uwamaliya J, Carrier P, et al. (2010). *Mol.Vis.* 16:2192–201
- Responte DJ, Arzi B, Natoli RM, Hu JC, Athanasiou KA. (2012). *Biomaterials* 33:3187–94
- Riccalton-Banks L, Liew C, Bhandari R, Fry J, Shakesheff K. (2003). *Tissue Eng.* 9:401–10
- Shimizu T, Yamato M, Kikuchi A, Okano T. (2003). *Biomaterials* 24:2309–16
- Steinberg MS. (1970). *J. Exp. Zool.* 173:395–433
- Steinberg MS. (2007). *Curr. Opin. Genet. Dev.* 17:281–86
- Strohman RC, Bayne E, Spector D, et al. (1990). *In Vitro Cell. Dev. Biol.* 26:201–8
- Syed-Picard FN, Larkin LM, Shaw CM, Arruda EM. (2009). *Tissue Eng. Part A* 15:187–95
- Torisawa YS, Takagi A, Nashimoto Y, et al. (2007). *Biomaterials* 28:559–66
- Tzanakakis ES, Hansen LK, Hu WS. (2001). *Cell Motil. Cytoskelet.* 48:175–89

- Vunjak-Novakovic G, Martin I, Obradovic B, et al. (1999). *J. Orthop. Res.* 17:130–38
- Whitesides GM, Grzybowski B. (2002). *Science* 295:2418–21
- Wystrychowski W, Cierpka L, Zagalski K, et al. (2011). *J. Vasc. Access* 12:67–70
- Yang J, Yamato M, Nishida K, et al. (2006). *J. Control. Release* 116:193–203
- Yang X, Mironov V, WangQ. (2012). *J. Theor. Biol.* 303:110–18
- Youssef J, Nurse AK, Freund LB, Morgan JR. (2011). *Proc. Natl. Acad. Sci. USA* 108:6993–98
- Zhang W, Xiao J, Li C, Wan P, Liu Y, et al. (2011). *Tissue Eng. Part C Methods* 17:569–77
- Zhang Z, McCaffery JM, Spencer RG, Francomano CA. (2004). *J. Anat.* 205:229–37
- Zieske JD. 2001. Extracellular matrix and wound healing. *Curr. Opin. Ophthalmol.* 12:237–41

Chapter 4

Development of Biodegradable polymeric membranes for Tissue Engineering application

Introduction

The field of the Tissue Engineering aims at promoting the regeneration of failing or malfunctioning tissues combining a biomaterial that can act as a framework for single cells to build a vital and well functioning tissue, bioactive molecules and culture conditions in order to reproduce the native conditions requested for the development of tissues and organs mimics. Though in the last two decades numerous studies have been carried out for the development of bio-artificial systems and many types of natural and synthetic biodegradable materials have been proposed, polymeric membranes, in particular, seem to provide the required support to ensure the mechanical and chemical regulation of the growth and differentiation processes of different kind of cells. The importance of the morphological and physico-chemical properties of the polymer surface in cell interactions has been demonstrated. Surface free energy, electric charge and morphology might all affect the cell attachment and behavior and, when correctly developed, they could support cell processes that build up a new functioning tissue [De Bartolo et al., 2008]. Different processing methods could be used for a biodegradable polymeric membrane preparation. Between them, the Phase Inversion techniques have gained the larger attentions nowadays. Basically through these methods, polymers, at suitable concentrations, were dissolved in a proper solvents and the solutions, casted on an inert support, is molded in a determined shape inducing the solvent removal. Parameters as temperature and humidity, chemical-physical properties of polymer and solvent and the method used, influence the rate of the inversion/separation phenomena involved in the polymer precipitation and, as consequence operating on one or more of these parameters the final membrane structure could be controlled. Several degradable polymers, including Collagen, Chitosan, Hyaluronic acids, Polyglycolic acid (PGA), Poly(L)-lactat (PLA), Poly(DL)glycolactate (PLGA), Poly-l-lactic acid (PLLA), Polycaprolactone (PCL), Polyurethane (PU), have been used for many engineeristic purposes, due to their biodegradability and biocompatibility [Armentano et al. 2010]. In order to develop bio-hybrid membrane systems, three specific polymers were chosen and processed to obtain

biodegradable polymeric membranes for TE application: Chitosan, Polycaprolactone and Polyurethane. All of them posses a very interesting list of properties that made them appealing for the field of the regenerative medicine. Chitosan is a linear, semi-crystalline polysaccharide composed of (1-4)-2-acetamido-2-deoxy-b-D-glucan (N-acetyl D-glucosamine) and (1-4)-2-amino-2-deoxyb- D-glucan (D-glucosamine) units [Rinaudo et al., 2006]. It can be easily derived from two main sources, crustaceans and fungal mycelia, through the partial deacetylation of the natural polymer chitin, that is deacetylated in order to obtain a specific deacetylation degree, important for the determination of the principal chemical-physical characteristics of the final Chitosan, giving indication of the number of amino groups along the chains. To be named ‘‘chitosan’’, the deacetylated chitin should contain at least 60% of D-glucosamine residues [Acosta et al., 1993; Madihally et al., 1999]. Indeed, the amino groups of the D-glucosamine residues might be protonated providing solubility in diluted acidic aqueous solutions (pH < 6). Chitosan with protonated amino groups becomes a polycation that can subsequently form ionic complexes with a wide variety of natural or synthetic anionic species [Aranaz et al., 2009], such as lipids, proteins, DNA and some negatively charged synthetic polymers as poly(acrylic acid) [Madihally et al., 1999; Pavinatto et al., 2010; Takahashi et al., 1990; Kim et al., 2007]. As a matter of fact, chitosan is the only positively charged, naturally occurring polysaccharide [Pavinatto et al., 2010]. It can be biodegraded into non-toxic residues [Bagheri-Khoulenjani et al., 2009] that can be incorporated in metabolic pathways or be further excreted [Pangburn et al., 1982], with a rate of degradation highly related to the molecular mass of the polymer and its deacetylation degree. All these singular features make Chitosan an outstanding candidate for biomedical applications. Due to its positive charges, chitosan can also interact with the negative part of cells membrane, which can lead to reorganization and an opening of the tight junction proteins, explaining the permeation enhancing property of this polysaccharide. Being also a polysaccharide, which consequently contains breakable glycosidic bonds, Chitosan is actually degraded in vivo by several proteases, and mainly lysozyme [Aranaz et al., 2009; Dash et al., 2011; Kean et al., 2011]. Due to its aforementioned remarkable properties, Chitosan appears thus as a relevant candidate for the preparation of biomaterials, which could substitute for missing or damaged tissue and organ [Dutta et al., 2011], and allow cell attachment and proliferation [Jagur-Grodzinski et al., 2003]. Chitosan hydrogels have been extensively used in TE applications, presenting either reversible or irreversible gelation. Chitosan can indeed be either physically associated, coordinated with metal ions or irreversibly/chemically cross-linked into hydrogels [Dash et al., 2011]. Chitosan sponges also find many applications as

wound healing materials, in fact they can soak up the wound exudates, while helping the tissue regeneration. In bone tissue engineering, these sponges have been fully described as filling material [Costa-Pinto et al., 2011]: Chitosan [Seol et al., 2004], chitosan/tricalcium phosphate (TCP) [Costa-Pinto et al., 2011; Lee et al., 2000], and chitosan/collagen sponges [Arpornmaeklong et al., 2008] demonstrated to be highly useful for bone regeneration. Chitosan–ZnO composite sponges also prepared by freeze-drying [Jayakumar et al., 2011] showed good swelling, antibacterial and haemostatic activities, confirming their potential healing in wound dressing application. With dry and wet spinning from acetic acid solution chitosan fibers can be produced, and in order to decrease production cost and to improve fiber properties, blends of chitosan with other polymers were also considered: sodium alginate [Tamura et al., 2002], tropocollagen [Hirano et al., 2000], cellulose, sodium hyaluronate, sodium heparin, sodium chondroitin sulfate [Pillai et al., 2009], poly(acrylic acid) [Ohkawa et al., 2002] were thereby employed. The electrospinning of chitosan in presence of poly(ethylene oxide) (PEO) [Spasova et al., 2004; Duan et al., 2004; Matsumoto et al., 2007; Ojha et al., 2008; Bhattarai et al., 2005] and ultrahigh-molecular weight poly(ethylene oxide) (UHMWPEO) are commonly reported. Chitosan/PEO nanofibers prepared by ESP exhibit cellular biocompatibility [Jayakumar et al., 2010]. The structure of the fiber mats was found to promote the attachment of human cells, while preserving their morphology and viability. Chitosan membranes also have been extensively used for TE applications. Piscioneri et al., in 2011, investigated the proliferation of rat embryonic liver cells and the expression of differentiated functions on Chitosan membranes obtained by phase inversion techinique. They provided an optimal microenvironment for embryonic liver cells, giving them the means to acquire and maintain specific functions in a comparable way to those found in collagen, used as reference system. Cells proliferated, resulting in a significant increase in cell numbers, and formed a structure close to that of liver parenchyma, and underwent functional differentiation, showing urea synthesis, albumin production and diazepam biotransformation at significantly high levels, particularly on the chitosan membrane. Polyurethanes (PUs) are a large family of polymeric materials with an enormous diversity of chemical compositions, mechanical properties, tissue-specific biocompatibility and biodegradability, with mechanical flexibility and good biocompatibility. They are among the most extensively used synthetic polymers in biomedical applications, and remain the group of biomaterials mostly applied to medical devices and the healthcare system [Santerre et al., 2005]. These materials played a major role in the development of durable cardiovascular devices since the 1980s, such as blood bags, vascular catheters, bladders of the left ventricle assist device (LVAD), the total artificial heart

(TAH) and small caliber grafts for vascular access and bypass surgery [Zdrahala et al., 1999], and became extensively researched in particular for their susceptibility to biodegradation. The chemical synthesis of PUs is critical to understanding the mechanical properties and biodegradability of these polymers. Polyurethane is a family of copolymers in which the principle chain structure is composed of aliphatic or aromatic units R1 and R2 linked with polar urethane groups (−NHCOO−), where R1 is an aliphatic, aromatic or alicyclic moiety in the isocyanate monomers (R1 N C O), and R2 is a more complex group derived from the polyol component, either polyether (R O R_) or polyester (R COO R_) [Krol et al., 2007]. Hence, the synthesis of PUs requires two essential components: isocyanate (typically diisocyanate O C N R1 N C O) and a bi- or multi-functional polyol with two hydroxyl (OH) terminal groups. The principle of chemical reaction involved in the synthesis of PUs is the urethane-forming reaction between isocyanate and the hydroxyl group OH in the step growth copolymerization of diisocyanates and polyols. The use of diisocyanate and a bi-functional polyol results in thermoplastics without crosslinking, whereas the use of components with more than two functional groups (e.g., triisocyanate or a multi-hydroxyl polyol) will yield PUs with three-dimensional crosslinking. The properties of the final polyurethane produced are primarily dependent on the chemical nature (types of diol, diamine, or isocyanine) of these three building blocks, and the relative proportions used during synthesis [Castonguay et al., 2001]. The soft domains of PU are amorphous and elastomeric at room temperature due to the glass transition temperature of the polymer lower than 25°C. The hard domains act as physical crosslinks, able to fix each soft segment at its two ends, thus preventing the chains from flowing apart when they are stretched under applied stress. Without flow, the stretched polymer segments can then reshape elastically when stress is released [Guelcher et al., 2008]. Hence, PUs can exhibit rubber-like behavior. The biocompatibility of various polyurethanes has been intensively investigated both in vitro and in vivo for a wide range of applications, i.e. durable medical devices (such as vascular catheters, the total artificial heart and small diameter vascular grafts for artificial reconstruction or bypass surgery) [Zdrahala et al., 1996; Krol et al., 2007] and biodegradable implants used in tissue engineering [Guelcher et al., 2008]. The cell types used to assess the biocompatibility of PUs are frequently fibroblasts and endothelial cells, which are among the most commonly used for cytotoxicity tests of biomaterials. Other types of cells used include specific types of leukocytes, as well as specific epithelial cells representative of those that interface with the PU materials at sites of implantation in different tissues (e.g., skin, blood vessel, tympanum and cornea [Marois et al., 2001]). Novel membranes synthesised from a polymeric blend of modified

polyetheretherketone (PEEK-WC) and PU by phase inversion technique have been developed for the design of a biohybrid system and the in vitro maintenance of liver cell, that resulted differentiated and functional for more than 1 month [De Bartolo et al., 2007]. In general, a good biocompatibility is recognized, and sustained cell adhesion and proliferation rates in vitro [Zdrahala et al., 1996; Fromstein et al., 2006] are showed. As mentioned, PUs were traditionally developed as long-term implant materials [Lamba et al., 1998], and many attempts were made to create versions that resisted biodegradation processes. Converse to this, more recent attempts have been made to enhance the biodegradability of PUs. Since the late 1990s, scientists have been utilizing the flexible chemistry and diverse mechanical properties of PU materials to design degradable polymers for applications as varied as neural conduits [Borkenhagen et al., 1998], cardiac muscle engineering [Fujimoto et al., 2007; McDevit et al., 2003; Alperin et al., 2005], and bone replacements [Saad et al., 1997]. These materials have taken advantage of processes such as hydrolytic mechanisms, and have been made with varied molecular structure to allow controlled hydrolysis rates. The susceptibility of PUs to biodegradation lies in soft segment components of the polymer. These segments generally dominate the degradation characteristics of PUs, with higher proportions of soft segments tending to correlate with increased degradation rate [Pinchuk et al., 1994]. Along with hydrolysis of ester bonds, several decomposition mechanisms have been identified in PUs used as long-term implants, including oxidation, environmental stress cracking (ESC) and enzymatic degradation [Pinchuk etal., 1994; Jayabalan et al., 2000]. In contrast to traditional biomedical PU implants that are designed to have a long-term in vivo biostability, PUs used as tissue engineering scaffolds and drug delivery systems are designed to undergo faster hydrolytic degradation to non-cytotoxic decomposition products in vivo. The in vitro degradation rates of biodegradable PUs, typically in physiological solutions, can be controlled by altering the composition of the polyester polyol components of these polymers [Guelcher et al., 2007; Gorna et al., 2003; Guan et al., 2004; Storey et al., 2003; Skarja et al., 2000] Besides satisfactory biocompatibility, PUs can be tailored to have a broad range of mechanical properties. As with tuning the degradation rate, the mechanical properties can also be tuned by modifying the structure of the hard and soft segments. A wide range of Young's modulus (11–1690 MPa), ultimate tensile strength (UTS) (2–60 MPa) and elongation at break (50–570%) have been reported in literature. Unlike chemical crosslinking which renders materials insoluble and incapable of being further shaped by heat and pressure, physically crosslinked PU elastomers have a good processibility [Krol et al., 2007], such that they can be easily melted around 50°C. Hence, they can be fabricated into various complicated shapes,

such as fibers, sheets, and highly porous scaffolds by a number of techniques, such as extrusion [Richardson et al., 2011], wet spinning [Gisselfalt et al., 2002; Liljensten et al., 2002], electrospinning [Zhuo et al., 2011; Sambaer et al., 2011; Stankus et al., 2004; Stankus et al., 2007], thermally induced phase separation (TIPS) [Guan et al., 2005] and salt leaching/freeze-drying [Gogolewski et al., 2006; Gogolewski et al., 2007; Spaans et al., 1998]. By applying these fabrication techniques, different porosities, surface-to-volume ratios and three dimensional structures, PUs with concomitant changes in mechanical properties can be achieved to suit a wide range of soft tissue engineering applications including for repair of cardiovascular, muscular and neuronal tissue [Guelcher et al., 2008]: polyurethane elastomers have been studied since the early 1990s for soft tissue engineering, in particular the superelasticity of certain polyurethane elastomers has made them ideal for cardiac muscle repair [Fujimoto et al., 2007; McDevitt et al., 2003; Alperin et al., 2005]. Researchers from the University of Toronto [McDevitt et al 2003; Alperin et al., 2005] carried out a series of in vitro studies on the integrity of the cardiomyocytes grown on thin patterned polyurethane films. Adult or embryonic stem cell derived cardiomyocytes were seeded onto the films and cultured for up to 4 weeks. At the end of culture, multilayered cell populations (approximately 2–3 cell layers thick) had formed, with cardiomyocyte patterning aligning with that of the films. The cardiomyocytes were not only dense and linearly aligned, but were able to physically contract the underlying polyurethane films, as a kind of integrated and functional PU/muscle unit. These results are intriguing, and indicate that PU films could be promising heart-patch biomaterials. Heart patch too was developed with PU [Fujimoto et al., 2007; Hong et al., 2010; Soletti et al., 2011; Amoroso et al., 2011] in *in vivo* experimentations: sutured to an infracted region of rat cardiac muscle, it was able to promote contractile smooth muscle tissue formation, improved tissue remodelling and contractile function at the chronic stage. In addition to cardiovascular tissue engineering, PUs have proven highly versatile for the repair of other tissue types including nerves [Borkenhagen et al., 1998; Chiono et al., 2011; Soldani et al., 1998], blood vessels [Soletti et al., 2011] and load-bearing tissue including bone [Gogolewski et al., 2006; Gogolewski et al., 2007; Schlickewei et al., 2007; Hill et al., 2007], cartilage [Eglin et al., 2010], fibrocartilage [Klompmaker et al., 1991] and ligament [Gisselfalt et al., 2002; Liljensten et al., 2002]. PCL is a moderately wettable, semi-crystalline polymer with a number average molecular weight generally vary from 3000 to 80,000 g/mol. The good solubility of PCL, its low melting point (59–64 ◦C) and exceptional blend-compatibility has stimulated extensive research into its potential application in the biomedical field [Chandra et al., 1998; Okada et al., 2002; Nair et al., 2007]. PCL possesses superior

rheological and viscoelastic properties over many of other polymers, resulting easy to manufacture and manipulate into a large range of scaffolds [Luciani et al., 2008; Lee et al., 2003; Marrazzo et al., 2008; Huang et al., 2007; Zein et al., 2002], Furthermore, a quite important number of drug-delivery devices fabricated with PCL already have FDA approval. PCL is prepared by the ring-opening polymerization of the cyclic monomer ε-caprolactone, using stannous octoate as catalyst and low molecular weight alcohols to control the final molecular weight of the polymer [Storey et al., 1996]. There are various mechanisms which affect the polymerization of PCL and these are anionic, cationic, co-ordination and radical. Each method affects the resulting molecular weight, molecular weight distribution, end group composition and chemical structure of the copolymers [Okada et al 2002]. PCL is soluble in many solvents at room temperature, and generally a lower dissolution behavior is overcome by using higher operating temperature [Coulembier et al., 2006]. PCL can be blended with other polymers to improve stress crack resistance and adhesion and has used in combination with polymers such as cellulose propionate, cellulose acetate butyrate, polylactic acid and polylactic acid-co-glycolic acid for manipulating the rate of drug release from microcapsules [Chandra et al., 1998]. PCLs can be biodegraded by outdoor living organisms (bacteria and fungi), but they are not easy biodegradated in animal and human bodies because of the lack of suitable enzymes [Vert et al., 2009], then the process takes much longer. The dissolution of the PCLs can proceed via surface or bulk degradation pathways. Surface degradation or erosion involves the hydrolytic cleavage of the polymer backbone only at the surface [Vert et al., 1987]. This typically results in thinning of the polymer over time without affecting the molecular weight of the internal bulk of the polymer, which would generally remain unchanged over the degradation period. Bulk degradation occurs when water penetrates the entire polymer bulk, causing hydrolysis throughout the entire polymer matrix. If water molecules can diffuse into the polymer bulk, hydrolyse the chains enabling themonomers or oligomers to diffuse out, erosion will occur gradually and equilibrium for this diffusion–reaction phenomenon would be achieved. The homopolymer PCL has a total degradation of 2–4 years (depending of the starting molecular weight of the device or implant) [Holland et al., 1992; Middleton et al., 2000; Gunatillake et al., 2003]. Copolymerizations with other lactones or glycolides/ lactides can alter the rate of hydrolysis. Meek and colleagues studied the 2-year degradation and possible long-term foreign body reaction against PCLs nerve guides after implantation in the sciatic nerve of the rat. They demonstrated that nerve regeneration took place through the scaffold, and after 2-years of implantation no remains of the implant could be found macroscopically [Meek et al 2009]. These studies compound the

biocompatibility of the PCL and its composites. Drug delivery [Merkli et al., 1998; Freiberg et al., 2004; Sinha et al., 2004; Gaucher et al., 2005], Sutures [Middleton et al., 2000], Wound dressings[Ng et al., 2007; Jones et al., 2002], Contraceptive devices [Dhanaraju et al., 2006; Dhanaraju et al., 2003], Dentistry [Alani et al., 2009; Miner et al., 2006] are just some of the medical and health care application of the PCL nowadays reported. In tissue engineering application, the examples of devices, supports and scaffolds in different shapes are uncountable, and cover all fields possible in tissue regeneration. Electropun, aligned PCL nanofiber produced at different collector rotation speeds (0, 3000, 6000 rpm) have been investigated in terms of tensile strengths hardness and young's modulus in order to individuate and optimize parameters for a production process to gain mechanical properties for specific applications [Oh et al., 2007]. It has been demonstrated in fact that [Choi et al., 2008] electrospun PCL/collagen nanofibers of different orientations can induce the restore of large skeletal muscle tissue defects. Muscle cells achieved an alignment and myotubule formation. PCL cylindrical scaffolds with gradually increasing pore size along the longitudinal direction were examined for their in vitro cell interactions using different kinds of cells (chondrocytes, osteoblasts, and fibroblasts) and in vivo tissue interactions using a rabbit model (skull bone defects). It was observed that different kinds of cells and bone tissue respond to PCLs very well with effective cell growth and tissue regeneration. Human marrow stromal cells and trabecular osteoblasts rapidly proliferated on PCL/PLLA scaffold up to 3 weeks, promoting an oriented migration of bone cells along the fiber arrangement [Guarino et al., 2008]. A bioactive and bioresorbable scaffold fabricated from medical grade PCL (mPCL) and incorporating 20% beta-tricalcium phosphate (mPCL–TCP) has been well characterized and studied by Hutmacher et al. [Hutmacher et al.2000], and further developed for bone regeneration. Histological evidence of continuing bone remodelling and maturation was observed at 6 months from the implantation. PCL–TCP scaffolds too could act as bone graft substitutes by providing a suitable environment for bone regeneration in a dynamic load bearing setting such as in a porcine model of interbody spine fusion [Abbah et al., 2009]. Three-dimensional, nanofibrous PCL scaffolds were assessed by Li et al. [Li et al., 2003] for their ability to maintain chondrocytes in a mature functional state, showing to be a suitable candidate scaffold for cartilage tissue engineering [Wise et al., 2009, Shao et al., 2006]. A composite scaffold comprising a PCL stent and a type II collagen sponge for tissue-engineered trachea and hyaluronic acid/PCL scaffolds for meniscal tissue engineering, and so on for tendon and ligament engineering are other important examples of the PCL applications [Lin et al., 2008; Konet al., 2008; Klopp et al., 2008]. But references on cardiovascular

engineering, blood vessel, skin, and nerve engineering are uncountable [Hutmacher et al., 2010].

On the basis of the extensive literature available nowadays, the three class of polymers presented above have been chosen for this work. Chitosan, Polycaprolactone and Polyurethane membranes were produced by Phase Inversion technique using the Precipitation by Solvent Evaporation method and then characterized in terms of morphology, chemical-physical and mechanical properties. The results showed in this work suggest, with proper literature example that the biodegradable polymeric membranes obtained will be useful to act as support for cells answers and survival, with good level of biocompatibility in terms of cells adhesion, functionalization, spreading and differentiation achievable. Scanning Electron Microscopy (SEM), Permporometer, Contact Angle, mechanical strength and biodegradability were used for the characterization of membrane properties.

Materials and Methods

5.1 Thermodynamic analysis

Since different conditions and solvents are available for preparing a polymeric membrane, a qualitative/quantitative description of the possible ratios and combinations of the elements composing the starting polymeric solutions was done in order to evaluate the solubility characteristics and the demixing behavior of each system. Using the thermodynamics principles, important for all phase inversion process, as already described in chapter 2, the miscibility of two components is described by the free enthalpy of mixing profile (ΔG_{mix}) [Mulder et al., 1991]:

$$\mathbf{\Delta G_{mix}} = \Delta H_{mix} - T\,\Delta S_{mix}$$

where ΔH_{mix} is the enthalpy of mixing, T is the temperature of the system (°K) and ΔS_{mix} is the entropy of mixing. Two components will mix spontaneously if the free enthalpy of mixing has a negative value ($\Delta G_{mix} < 0$). For the simpler polymeric system (polymer/solvent) the enthalpy of mixing is done by Hildebrand expression, for which:

$$\mathbf{\Delta H_{mix}} = V_m\,(\delta_1-\delta_2)^2\,v_1\,v_2$$

where V_m is the molar volume of the solution, v is the volume fraction of the components and δ are the solubility parameters of the solvent and the polymer. Clearly, when $\delta_1 \sim \delta_2$, the value of ΔH_{mix} approaches zero and polymer and solvent are perfectly miscible (because ΔS_m is always positive). According to Flory-Huggins theory of the lattice model, the total number of

molecules involved in the polymer/solvent system is: $\mathbf{n_t} = n_t + Pn_2$, where P is the number of segments in the polymeric chain and n are the number of moles of the species involved, then expressing the entropy of mixing in volume fraction it is obtained:

$\mathbf{\Delta S_{mix}} = - R (n_1 \ln\phi_1 + n_2 \ln\phi_2)$

where the volume fractions are specifically expressed as $\boldsymbol{\phi_1} = n_1 / (n_1 + Pn_2)$ and $\boldsymbol{\phi_2} = Pn_2 / (n_1 + Pn_2)$ when the system consists in a polymer/solvent solution; whereas, $\boldsymbol{\phi_1} = n_1 / n_1 (P_2n_2 / P_1)$ and $\boldsymbol{\phi_2} = n_2 / n_2 (P_1n_1 / P_2)$, when a polymer/polymer solution is the analyzed system.

5.2 Membrane preparation

Biodegradable membranes were prepared and molded in flat configuration through the Solvent evaporation phase inversion technique. Chitosan membranes (CHT) were obtained by dissolving the polymer powder (75% deacetylated, Sigma, Milan, Italy) in a concentration of 4% (wt/v) in acetic acid solution 2% (v/v). Polyethylene glycol (PEG, Mw=6000 Da; Merck-Schuchardt, Hohenbrunn, Germany) was added to the solution at a 4:1 ratio and stirred until complete dissolution. The polymeric solution was cast on a glass plate and molded as thin film by a handle-casting knife (Elcometer, gap set at 250 μm), then dried at room temperature. A neutralization bath in a solution of 1% NaOH is needed in order to free all the chitosan domains from the acetylation caused by the action of the solvent, then repeated washings with distilled water are operated before the final drying process. Polycaprolactone (PCL) (Mn ~ 70,000-90,000 by GPC, Sigma, Milan, Italy) and Polyurethane membranes (PU) (Dow Chemical Noderland BV, Deefzijl, The Netherlands) were obtained by dissolving 10% and 15% (wt/v) of the corresponding polymeric pellets in pure 1,4-Dioxane and Formic acid respectively, at 50°C until complete dissolution. Then, the solutions were cast uniformly on a glass plate using the same method described for the Chitosan, and the obtained membranes were dried at room temperature until complete solvent evaporation before being washed with distilled water and dried again.

5.3 Morphological investigation

The dried biodegradable polymeric membranes were cut and mounted with double-faced conductive adhesive tape on metal stubs, and analyzed by scanning electron microscopy (SEM) (ESEM FEG QUANTA 200, FEI Company, Oregon, USA) in order to reveal the surface structures. Smoothness/roughness of the membranes, possible porosity and the thickness of the samples were exposed.

5.4 FT-IR analysis, Wettability, Surface properties and Porosity

The infrared spectroscopy was performed in order to identify the characterizing groups and the bonds of the atoms making up of the biodegradable polymeric membranes produced. The hydrophobic/hydrophilic character of the investigated membranes was estimated by the contact angle technique (CA) performed at room temperature with a CAM 200 contact angle meter (KSV Instruments, Ltd., Helsinki, Finland). CA measurements were performed under standard conditions, with three different liquids (water, glycerol, DIM), taking into account various parameters (e.g., temperature, cleanliness of sample, drop volume). Knowing the contact angle values in degrees of the pure liquid drops chosen once deposited on the membrane surfaces, the Surface Free Energy, the Lifshitz-Van Der Waals and the Short range surface tension parameters were derermined [Van Oss CJ, 1985]. The instrumentation supported by video camera and software allowed to obtain precise drop measurements. The mean pore size diameter of the pores were eventually detected through Perm-Porometric analysis, being the prepared polymeric membranes predicted to be with nano and micro porosity in their structure.

5.5 Mechanical properties determination

Tensile properties of the polymeric films were determined using a Zwick/Roell tensile testing machine. Samples from each group of membranes were cut in strips of 5 cm x 1 cm and mounted between two pneumatic grips. Grip separation was set at 3 cm and a testing speed of 5 mm/min was used. The thickness of the films was measured using a micrometer before every determination in order to reduce the mistakes during the data processing. Samples were subjected to uniaxial tension until failure. Ultimate tensile strength (UTS), Young's modulus (Emod) and Elongation parameter (ε) were recorded.

5.6 Dissolution profile: Biodegradability

The polymeric membranes, cut in square samples of 1,5 cm x 1,5 cm, were accurately dried and weighted, then completely immersed in a Lysozyme solution (1mgL/ml) for obtaining information on their decomposition rate profile. An incubator set at 37 °C was used in order to reproduce the biological condition of a culture system during all the experimental analysis. At the end of pre-determined incubation intervals, the samples were removed from the solutions, accurately washed with distilled water and dried with delicacy with a tissue paper

for the removal of the residual solution. Then the weights of all the samples were determined after a last dry process in a oven until a constant weight was reached. Dissolution percentages for the membranes were elaborated according to the following equation:
% Dissolution = [$(W_o - W_t) / W_o$] *100 ; where, W_o is the starting dry weight and W_t is the dry weight at time (t). Each test consisted of three replicate measurements.

Results

The diagrams of the free enthalpy of mixing (ΔG_{mix}) of all the polymeric solutions, elaborated as function of the polymer volume fraction (ϕ), for each system showed thermodynamic profiles quite closed to the typical one representative for a polymeric solution [Mulder et al., 1991]. As expected higher solubility is interrelated to small polymeric concentrations in solution, with the consequent increasing of the ΔG_{mix} values. In particular it was observed that for the polymer/solvent systems PCL-1,4 Dioxane and PU-Formic acid (fig. 4.1 and 4.2), both analyzed at the temperature of 50°C (323 K), condition used for the solutions preparation, the components are miscible for quite different polymeric concentrations: the percentage of Polycaprolactone miscible in the Dioxane is comprised in the range of 1-40%, with an equivalent polymer volume fraction equal to ϕ = 0,008-0,25; on the other side, the Polyurethane dissolution is ensured for a percentage range of 1-15% and then for a polymer volume fraction of ϕ = 0,005-0,08. Despite being both of them two synthetic elastomers, this different in terms of dissolution and thermodynamic profiles reflect perfectly the differences in structure, molecular weight and chemical reactivity between the two polymers. Higher soluble appears to be on the other side the Chitosan, as shown in figure 4.3, as results of its chemical structure, being this natural polymer highly rich in polar groups. A miscibility range of 1-70% was obtained and the Chitosan volume fractions are equal to ϕ = 0,004-0,48 in presence of acetic acid as solvent. These data analysis match perfectly with the experimental results. The differences observed through the thermodynamic analysis in terms of chemical reaction and dissolution properties of the polymer are also highlighted by the FT-IR analysis as reported in a row, where the functional and reactive groups of the biomaterials will be described. Then, although different kind of polymeric solutions were reproducible with different ratios and combinations of solutes and solvents, specific concentrations were chosen for each polymer in order to obtain a final solution perfect for being processed through the phase inversion technique selected, resulting in a homogeneous and easy handy biodegradable membrane. All the further investigations refer to the final membranes chosen for this work,

obtained as already described in section 5.2. The FT-IR spectra represent the fingerprints of the samples with all the absorption peaks corresponding to the frequencies of vibrations between the bonds of the atoms making up the materials used for the membrane preparation. The IR spectrum of the Chitosan membrane (fig. 4.4) exhibited a broad peak at 3454.36 cm^{-1}, easily assignable to the hydroxyl groups present in the structure, and displayed peaks around 901 and 1155 cm^{-1}, pertinent to the saccharine structure. The amino characteristic peak is recorded at 1591 cm^{-1} and the stretching values of the glycosidic linkage were observed at 1151.41 and 1035.43 cm^{-1}. In the end, but not for importance, the peaks at 2875.83, 1421.47 and 1325 cm^{-1} highlighted the symmetric/asymmetric CH_2 stretching vibration and the OH and CH vibrations of the ring. In the PCL membrane spectrum (fig. 4.5), two peaks are at once visible in the C–H stretch region, the higher one at 2949 cm^{-1} and the lower one at 2865 cm^{-1} assigned to the asymmetric and the symmetric modes of CH_2 respectively. The major absorption peak appeared at 1727 cm^{-1} according to the presence of the functional group C=O, while two bands are assigned to the ester respective alcohol of –C(O)–O– groups in the 1170-1240 cm^{-1} region. Typical infrared spectra of PU membranes (fig. 4.6) showed too the expected typical peaks: one at 3327,89 cm^{-1} in the NH stretching region, and another in the 3000–2850 cm^{-1} region, representatives of the $(CH_2)_5$– fragments; the carbonyl stretching peak is recognizable at 1728,71 cm^{-1}; whereas the ester/aldheyd group is given at 1698,49 cm^{-1}; the para di-substituted benzene absorbance at 1596,75 cm^{-1}, and two peaks at 1104.89 and 666.97 cm^{-1}, for the ether and –C(O)–O groups were also revealed. The SEM images showed as CHT (fig. 4.7a) and PU (fig. 4.7c) membrane surfaces are perfectly smooth, whereas the characteristic presence of a pentagonal microstructures distributed in a repetitive pattern, was clearly visible on the surfaces of the Polycaprolactone membranes (fig. 4.7b). It's important to underline how at the concentration of 10%, the PCL membranes used for this work, are lacking in macro-voids, sign of a perfect polymerization of the biomaterials, on the contrary noticed on the surfaces resultant of higher concentrations. Figure 4.8 showed the SEM images of the PCL membranes obtained with a concentration equal to 15 and 20%. The thickness, the mean pore size diameters and the contact angle values were recorded and reported in table 1. The perm-porometer investigation results in the awaited nanometric pores, typical for a membrane structure obtained by the solvent evaporation phase inversion technique [Mulder et al., 1991], with sizes equal to 26 - 22 and 82 nm were revealed respectively for the CHT, PCL and PU membranes. The dynamic water contact angle measurements (table 4.1) highlighted for all the biodegradable membranes showed a hydrophilic character, being the values recorded smaller than 90° [Van Oss et al., 1985]. The CHT membranes resulted in the most

hydrophilic substrates, with a water contact angle equal to 66° ± 0,25; whereas the synthetic biodegradable polymer membranes, PU and PCL, exhibited values closed to 70–77°, with a resultant lower hydrophilic properties. Taking in account the values of contact angles recorded with glycerol and DIM, the Lifshitz-Van Der Waals forces and the short range forces were also evaluated for each polymeric surfaces (table 4.1). Being the most important parameter by which the hydrophilicity is determined and quantify, a particular attention was paid to the γ^- values, that appeared as expected to be higher for the CHT membranes, with a value equal to ≈18 mJ/m^2, consequence of the deacetylation degree possessed by the polymer, followed by PCL membranes (≈14 mJ/m^2) and the PU membranes (≈12 mJ/m^2). Then, combining together these parameters according to the expression $\gamma^{tot} = \gamma^{LW} + \gamma^{SR}$ [Van Oss et al., 1985], the surface free energies, better known as surface tension parameters, were quantified: in order for PCL, CHT and PU samples decreasing values were obtained. The dissolution profiles of all the membranes in Lysozyme solution are showed in fig. 4.9. Up to 32 weeks, time for which the analysis was carried out, the three polymeric membranes showed quite different behaviors. The CHT, being a natural polymer, just after four weeks of treatment was completely degraded, on the contrary the synthetic polymers reached values in percentage equal to 40% and 64% for PU and PCL respectively. It is worth of notice that an appreciable mass loss for the Polycaprolactone membrane samples appeared only after 15 weeks of treatment, doubling its value just towards the end. The Polyurethane sample, on the contrary, starting from the 7th week, maintained constant its weight loss in time and decreasing the percentage of nearly the 10% in the final stage. In order to choose a biomaterial and to design a good bioartificial system for TE application, knowing the mechanical properties of the polymeric membrane produced is of high importance. The mechanical properties in terms of ultimate tensile strength (UTS), Young's modulus (Emod) and elongation parameter (ε) are reported in table 4.1. As expected for elastomers, the PCL and the PU values of Young's modulus were lower than the CHT that showed a superior stiffness and weakest mechanical strength. In particular the Polycaprolactone membranes revealed the higher elongation parameter, high appealing for TE application involving cells with high mechanical and contractile properties. A direct visualization of the mechanical properties of the biodegradable polymeric membranes developed are shown in Figures 4.10-11-12.

Discussion

The design and development of biodegradable polymeric membranes usable for TE applications, it is not an easy task, if it takes account of the real role played by a support for sustaining the cell answer in terms of adhesion, proliferation and differentiation. Chitosan, Polycaprolactone and Polyurethane were chosen as representatives of the natural and synthetic polymers due to their handy, chemical-physical properties and biocompatibility. To ensure a good design and the correct choice of the components involved in the processing methods selected, the phase inversion technique through the solvent evaporation process, a thermodynamic analysis was performed, and a specific polymer concentration and the proper solvents were chosen. The membranes obtained, all nanoporous as expected, showed homogeneous surfaces, important characteristic for cell attachment, spreading and proliferation [Ito et al., 2007] and a wettability degree, able to reproduce, partially at least, a support ECM-like, being the native ECM composed basically of water, proteins and polysaccharides [Frantz et al., 2010]. In particular the CHT, due to its chemical structure and deacetylation degree, resulted to be the higher hydrophilic membranes developed. Being the aim of this work the production of biodegradable bio-hybrid systems, a deep investigation on the dissolution properties of the polymeric membrane developed was performed. Even in that case the results reflect all the expectation, with the lower degradation profile recorded for the natural polymer used (CHT) and the higher one for the PCL, which reached a value equal to 64% after 32 weeks of enzymatic treatment. These are really important results because, as reported exhaustively in literature, the degradation rate has to be adapted to the tissue reconstruction going along with the progressive healing and tissue synthesis process [Hutmacher et al., 2010]. Tissue regeneration that requires longer time to occur will be better sustained by a stronger substrate, otherwise a faster maturation will prefer a weaker one in term of degradation. Moreover a suitable mechanical strength is requested to support the micromechanical control of the tissue formation and functionalization and it should be as possible comparable to *in vivo* tissue at the site of implantation. That means, a scaffold requires flexibility or rigidity depending on the application, e.g. cardiovascular versus bone prostheses [Mitragotri et al., 2009]. The biodegradable polymeric membranes developed showed different mechanical properties, and if on a side the CHT appeared to be the stiffer, on the other one the two elastomers showed good elasticity, with the higher values recorded for the PCL samples.

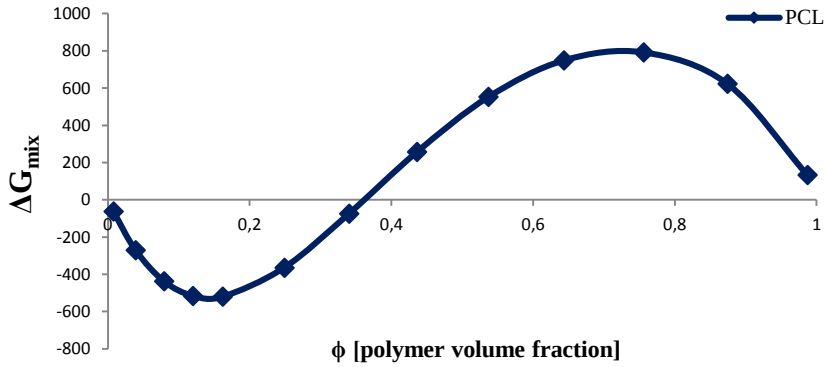

Fig. 4.1 Thermodynamic profile of the PCL - 1,4-Dioxane system

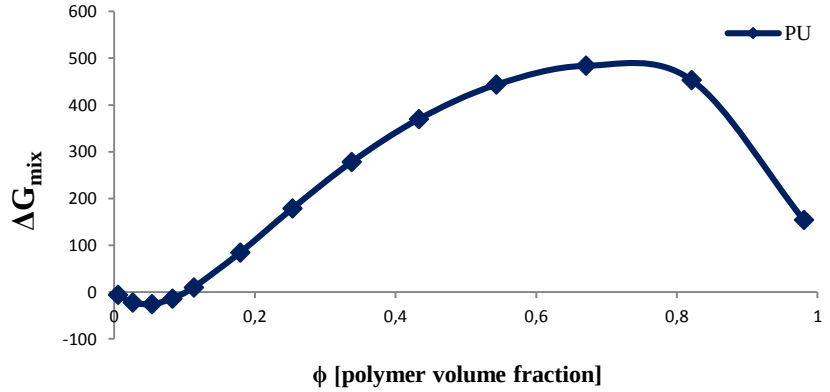

Fig. 4.2 Thermodynamic profile of the PU - Formic acid system

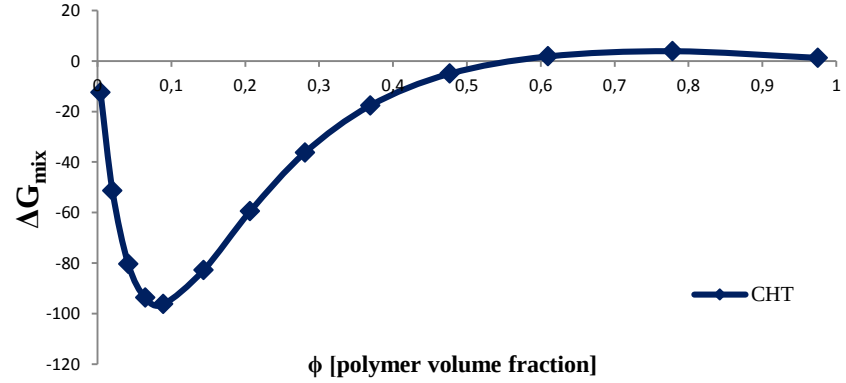

Fig. 4.3 Thermodynamic profile of the CHT - Acetic acid system

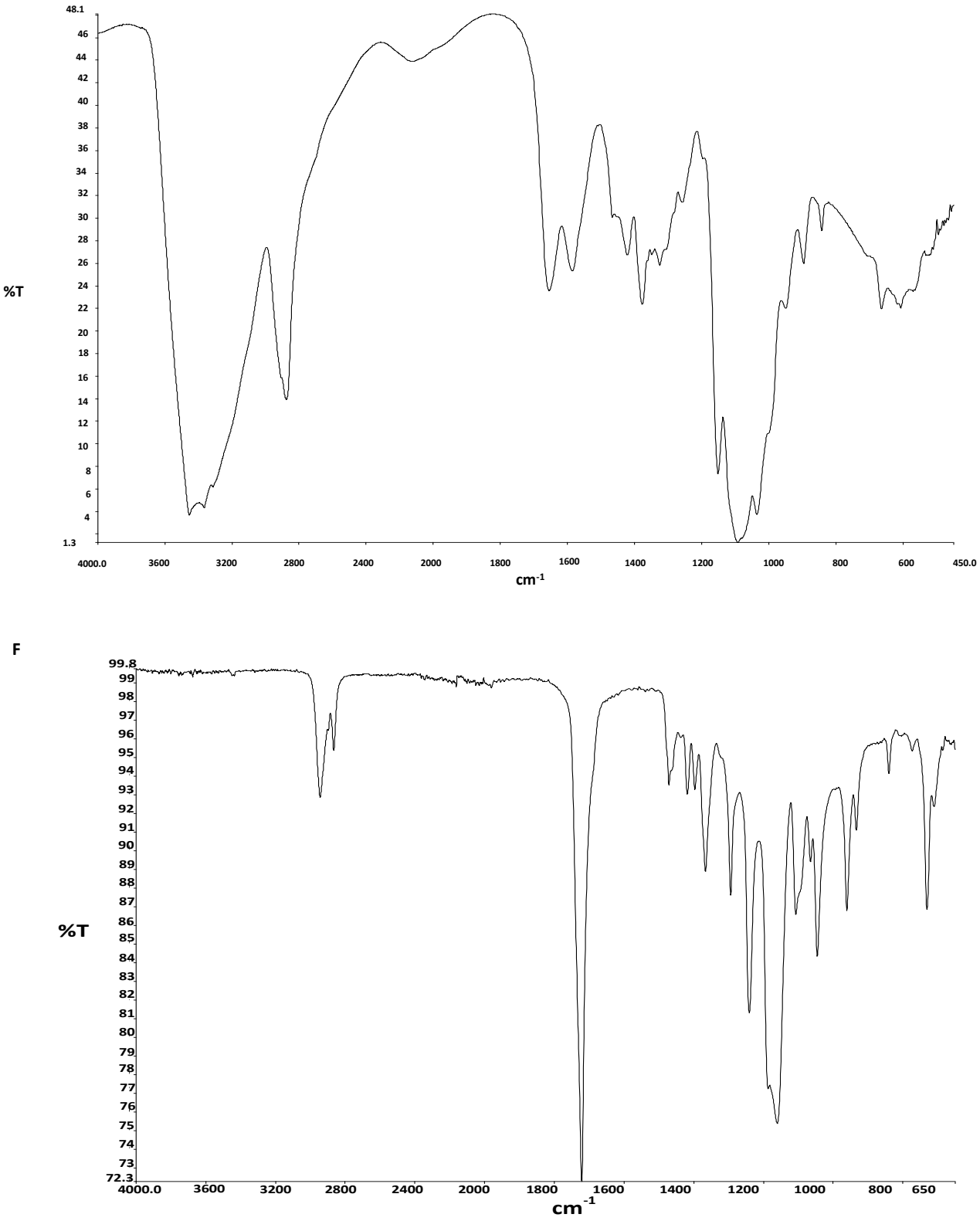

Fig. 4.5 FT-IR spectrum of the PCL membranes

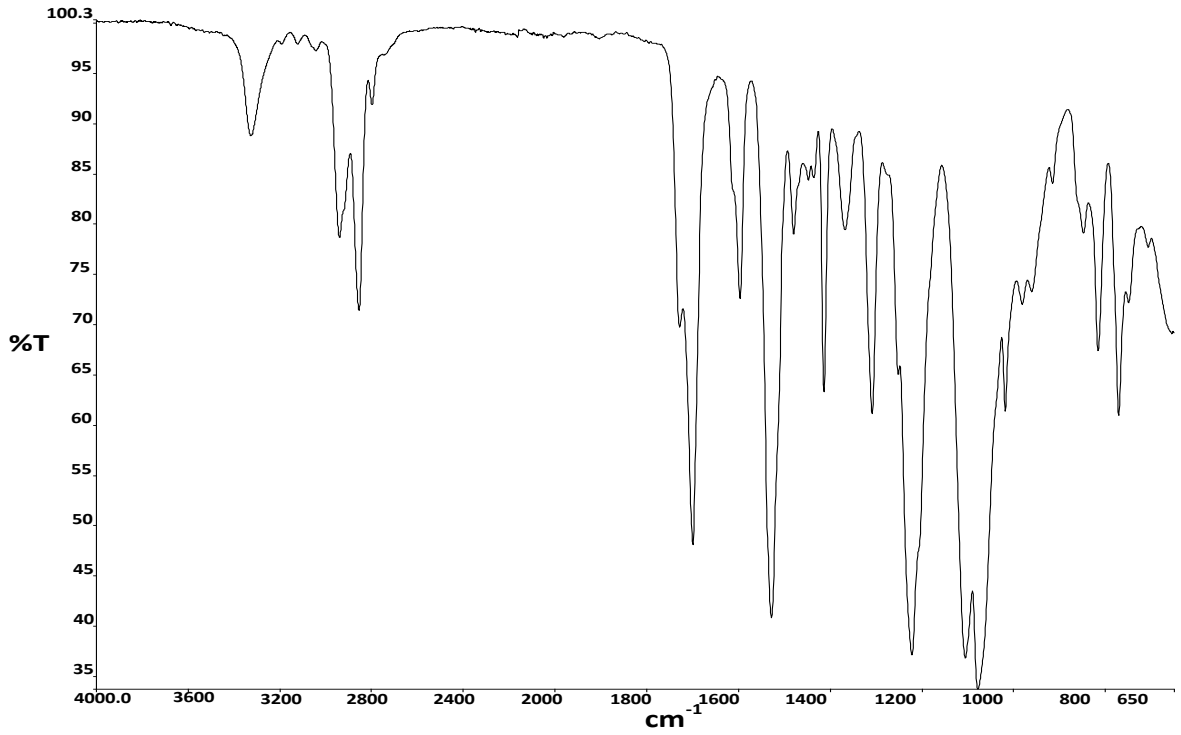

Fig. 4.6 FT-IR spectrum of the PU membranes

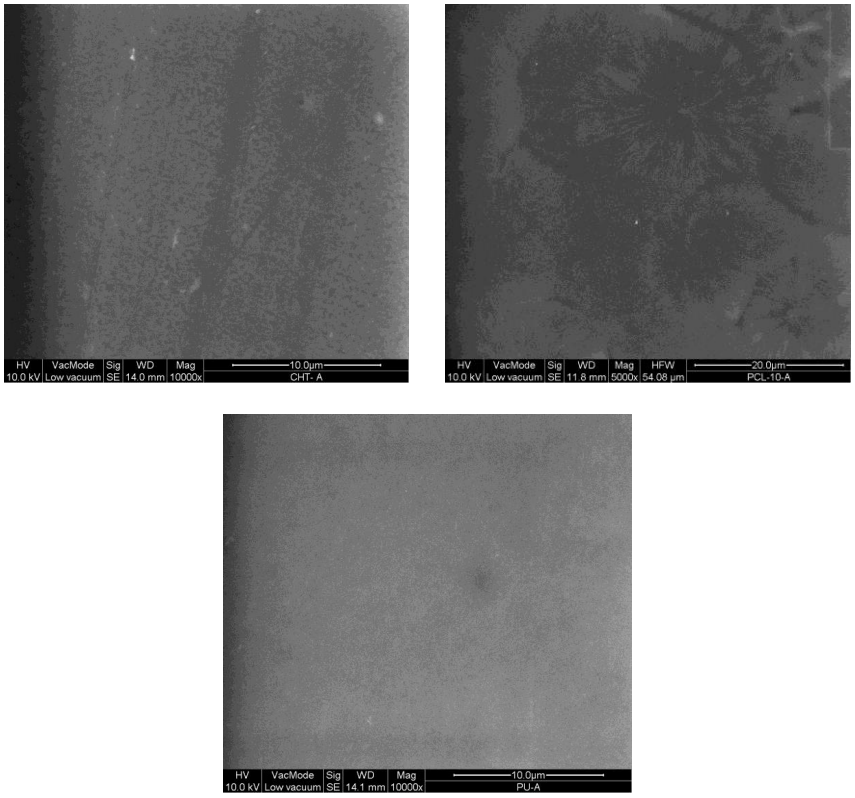

Fig. 4.7 SEM images of the biodegradable polymeric membrane surfaces a) CHT membrane, b) PCL membrane and c) PU membrane

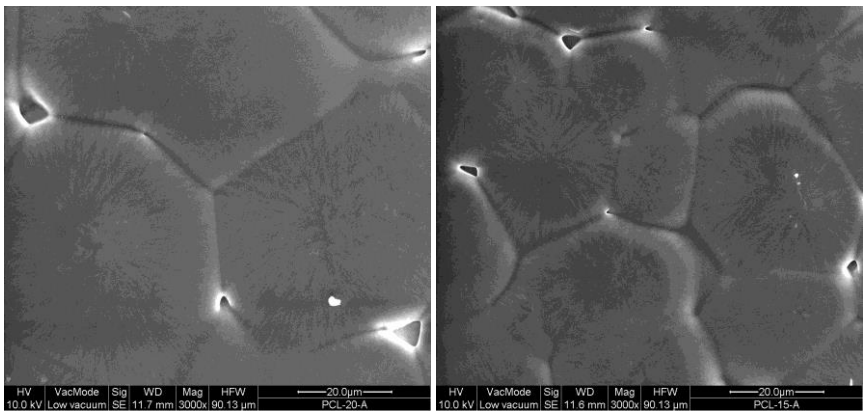

Fig. 4.8 SEM images of the Polycaprolactone membranes obtained with polymeric solution at 20 and 15 % in concentration

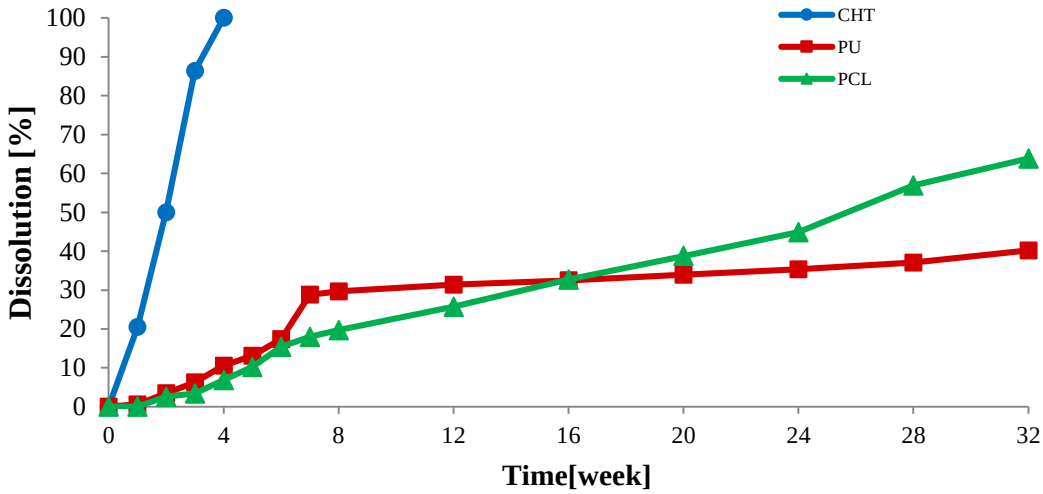

Fig. 4.9 Biodegradation profiles of the polymeric membranes developed CHT (blue), PCL (green) and PU (red)

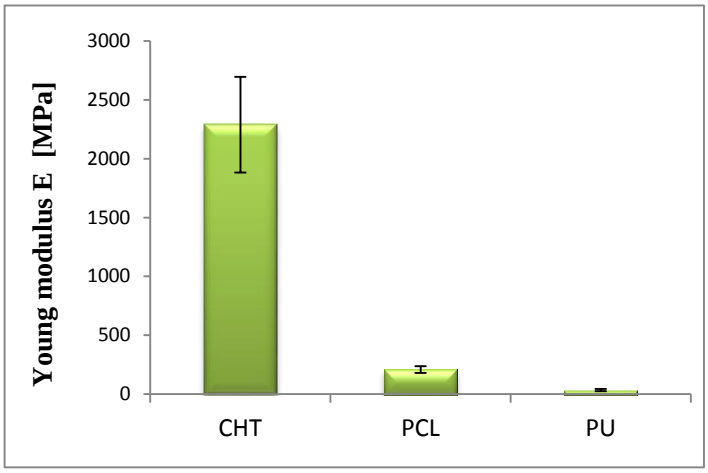

Fig. 4.9 Young's modulus diagram for the biodegradable polymeric membranes

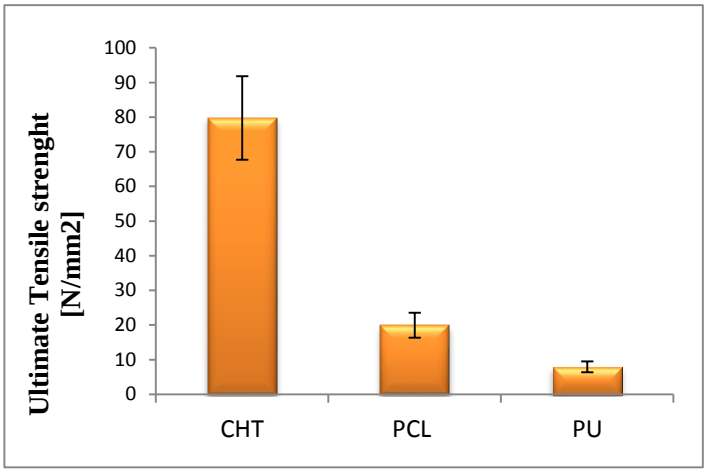

Fig. 4.10 Ultimate tensile strength diagram for the biodegradable polymeric membranes

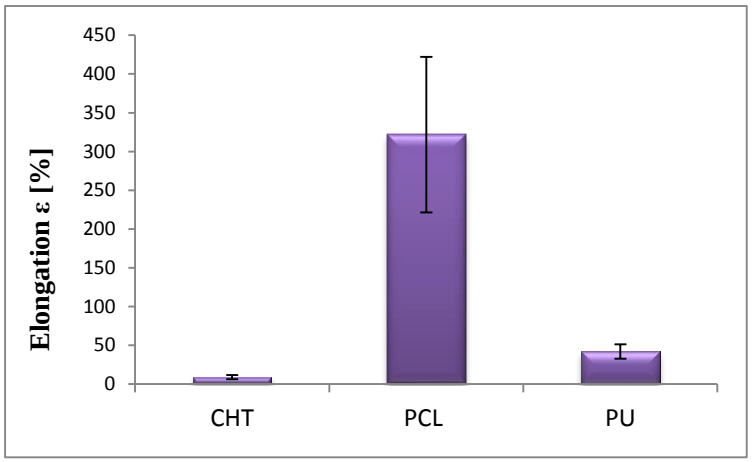

Fig. 4.11 Elongation parameter diagram for the biodegradable polymeric membranes

	Thickness [μm]	Mean Pore Size [μm]	E [MPa]	ε %	Dissolution [%]
CHT	8 ± 1	0,024	2288 ± 405	9 ±2,5	100*
PCL	5 ± 0,9	0,026	208 ±28	231 ±100	64 ±0,67
PU	19 ±1,9	0,082	35 ±9	42 ±9	40 ±3,63

	θ_{water} [°]	θ_{gly} [°]	θ_{DIM} [°]	γ^{LW} [mJ/m^2]	γ^+ [mJ/m^2]	γ^- [mJ/m^2]	γ^{AB} [mJ/m^2]	γ^{tot} [mJ/m^2]
CHT	66,56 ±0,25	65,71 ±1,33	43,07 ±2,33	38,03	0,0095	18,26	0,84	38,86
PCL	70,78 ±1,42	68,15 ±3,07	38,33 ±2,07	40,44	0,0079	14,35	0,68	41,12
PU	77,81 ±2,17	75,44 ±2,76	50,69 ±1,44	33,89	0,009	11,83	0,65	34,54

Table 4.1 Summary of the biodegradable polymeric membranes properties

References

- Abbah SA, Lam CXL, Hutmacher DW, et al. (2009). *Biomaterials*; 30:5086–93.
- Acosta N, Jimenez C, Borau V, Heras A. (1993). *Biomass Bioenergy* 5:145–53.
- Alani A, Knowles JC, Chrzanowski W, et al. (2009). *Dent Mater* 25:400–10.
- Alperin C, Zandstra PW, Woodhouse KA. (2005). *Biomaterials* 26:7377–86.
- Amoroso NJ, D'Amore A, Hong Y, (2011). *Advanced Materials* 23:106–11.
- Aranaz I, Mengibar M, Harris R, et al. (2009). *Curr Chem Biol* 3:203–30.
- Armentano I, Dottori M., Fortunati E. et al. (2010). *Polymer Degradation and Stability* 95: 2126-2146.
- Arpornmaeklong P, Pripatnanont P, Suwatwirote N. (2008). *Int J Oral Maxillofac Surg* ;37:357–66.
- Bagheri-Khoulenjani S, Taghizadeh SM, Mirzadeh H. (2009). *Carbohydr Polym* ;78:773–8.
- Bhattarai N, Edmondson D, Veiseh O, (2005). *Biomaterials* 26:6176–84.
- Borkenhagen M, Stoll RC, Neuenschwander P, (1998). *Biomaterials* 19:2155–65.
- Castonguay M, Koberstein JT, Zhang Z, (2001). *Landies Bioscience*; p. 1021
- Chandra R, Rustgi R. (1998). *Progr Polym Sci* 23:1273–335.
- Chiono V, Sartori S, Rechichi A, (2011). *Macromolecular Bioscience* 11:245–56.
- Choi JS, Lee SJ, Christ GJ, Atala A, Yoo JJ. (2008). *Biomaterials* 29:2899–906.
- Costa-Pinto AR, Reis RL, Neves NM. (2011). *Tissue Eng* Part B;17:331–47.
- Coulembier O, Degee P, Hedrick JL, Dubois P. (2006). *Progr Polym Sci* 31:723–47.
- Dash M, Chiellini F, Ottenbrite RM, (2011). *Prog Polym Sci* 36:981–1014.
- De Bartolo L., Morelli S., Rende M., et al. (2007). *Biosci.* 7, 671–680
- De Bartolo L., Rende M., Morelli S., et al. (2008). *Journal of Membrane Science* 325; 139–149
- Dhanaraju MD, Gopinath D, Ahmed MR, (2006). *J Biomed Mater Res* Part A;76: 63–72.
- Dhanaraju MD, Vema K, Jayakumar R, Vamsadhara C. (2003). *Int J Pharm* 268:23–9.
- Duan B, Dong C, Yuan X, Yao K. (2004). *J Biomater Sci Polym*; 15:797–811.
- Dutta P, Rinki K, Dutta J. (2011). *Advances in polymer science*. Heidelberg: Springer Berlin; 2011. p. 45–79.
- Eglin D, Grad S, Gogolewski S, Alini M. (2010). *Journal of Biomedical Materials Research* Part A; 92:393–408.
- Frantz C., Stewart K.M. and Weaver V.M. (2010). *Journal of Cell Science* 123, 4195-4200
- Freiberg S, Zhu X. (2004). *Int J Pharm*; 282:1–18.
- Fromstein JD, Woodhouse KA. (2006). Encyclopedia of biomaterials and biomedical engineering. New York: Marcel Dekker. p. 1–10.
- Fujimoto KL, Tobita K, Merryman WD, et al. (2007). *Journal of the American College of Cardiology* 49:2292–300.
- Gaucher G, Dufresne MH, Sant VP, et al. (2005). *J Control Release*;109: 169–88.
- Gisselfalt K, Edberg B, Flodin P. (2002). *Biomacromolecules*; 3:951–8.
- Gogolewski S, Gorna K, Turner AS. (2006). *Journal of Biomedical Materials Research* Part A;77:802–10.
- Gogolewski S, Gorna K. (2007). *Journal of Biomedical Materials Research* Part A;80:94–101.
- Guan J, Fujimoto KL, Sacks MS, (2005). *Biomaterials*; 26:3961–71.
- Guan JJ, Sacks MS, Beckman EJ, Wagner WR. (2004). *Biomaterials* 25:85–96.
- Guarino V, Causa F, Taddei P, et al. (2008). *Biomaterials* 29:3662–70.
- Guelcher S, Srinivasan A, Hafeman A, et al. (2007). *Tissue Engineering* 13:2321–33.
- Guelcher SA. (2008). *Tissue Engineering* Part B 14:3–17.
- Gunatillake PA, Adhikari R. (2003). *Eur Cells Mater* 5:1–16.
- Hill CM, An YH, Kang QK, et al. (2007). *Macromolecular Symposium* 253:94–7.

- Hirano S, Zhang M, Nakagawa M, Miyata T. (2000). *Biomaterials* 21:997–1003.
- Holland SJ, Tighe BJ. (1992). *Advances in pharmaceutical science*, vol. 6. London: Academic Press Inc. p. 101–64.
- Hong Y, Guan JJ, Fujimoto KL, Hashizume R, Pelinescu AL, Wagner WR. (2010). *Biomaterials* 31:4249–58.
- Huang H, Oizumi S, Kojima N, et al. (2007). *Biomaterials 2*8:3815–23.
- Hutmacher D.W., Singh H., (2010). *Trends in Biotechnology vol.26, N°4*
- Hutmacher DW. (2000). *Biomaterials* 21:2529–43.
- Ito Y, Zheng J, Imanishi Y. (1997). *Biomaterials* 18(3):197- 202.
- Jagur-Grodzinski (2001– 2002). *J. Biomedical applications of polymers*. e-Polym. 2003; Paper No. 12.
- Jayabalan M, Lizymol PP, Thomas V. (2000). *Polymer International* 49:88–92.
- Jayakumar R, Prabaharan M, Nair SV, Tamura H. (2010). *Biotechnol Adv* 28:142–50.
- Jones DS, Djokic J, McCoy CP, Gorman SP. (2002). *Biomaterials* 23:4449–58.
- Kean T, Thanou M. (2011). *Polysaccharides, proteins and polyesters*. 1st ed. London: Royal Society of, Chemistry; p. 292–318.
- Kim T-H, Jiang H-L, Jere D, Park I-K, et al. (2007). *Prog Polym Scie* 32:726–53
- Klompmaker J, Jansen HWB, Veth RPH, et al. (1991). *Biomaterials* 12:810–6.
- Klopp LS, Simon BJ, Bush JM, (2008). *Spine* 33:1518–26.
- Kon E, Chiari C, Marcacci M, et al. (2008). *Tissue Eng* Part A 14:1067–80.
- Krol P. (2007). *Progress in Materials Science* 52:915–1015
- Lamba NMK, Woodhouse KA, Cooper SL. (1998). *Boca Raton*: CRC Press p. 201–47.
- Lee KH, Kim HY, Khil MS, Ra YM, Lee DR. (2003). *Polymer* 44:1287–94.
- Lee Y-M, Park Y-J, Lee S-J, et al. (2000). *J Periodontol* 71:410–7.
- Li WJ, Danielson KG, Alexander PG, Tuan RS. (2003). *J Biomed Mater Res* Part A 67:1105–14.
- Liljensten E, Gisselfalt K, Edberg B, et al. (2002). *Journal of Materials Science Materials in Medicine* 13:351–9.
- Lin CH, Su JM, Hsu SH. (2008). *Tissue Eng* Part C 14:69–77.
- Luciani A, Coccoli V, Orsi S, (2008). *Biomaterials* 29:4800–7.
- Madihally SV, Matthew HWT. (1999). *Biomaterials* 20:1133–42.
- Marois Y, Guidoin R. (2001). *Biomed applications of polyurethanes.* Georgetown, TX: Landies Bioscience. p. 77–96.
- Marrazzo C, Di Maio E, Iannace S. (2008). Polym Eng Sci 48:336–44.
- Matsumoto H, Yako H, Minagawa M, Tanioka A. (2007). *J Colloid Interface Sci* 310:678–81.
- McDevitt TC, Woodhouse KA, Hauschka SD, et al. (2003). *Journal of Biomedical Materials Research* Part A 66:586–95.
- Meek MF, Jansen K. (2009). *J Biomed Mater Res* Part A 89:734–8.
- Merkli A, Tabatabay C, Gurny R, Heller (1998). *J. Progr Polym Sci* 23:563–80.
- Middleton JC, Tipton AJ. (2000). *Biomaterials* 21:2335–46.
- Miner MR, Berzins DW, Bahcall JK. (2006). *Endodontics* 31:723–47.
- Mitragotri S, Lahann J. (2009). *Nat Mater* 8(1):15-23.
- Mulder M. (1991). *Basic principles of membrane technology*
- Nair LS, Laurencin CT. (2007). *Progr Polym Sci* 32:762–98.
- Ng KW, Achuth HN, Moochhala S, Lim TC, Hutmacher DW. (2007). *J Biomater Appl Polym* 18:925–38.
- Oh SH, Park IK, Kim JM, Lee JH. (2007). *Biomaterials* 28:1664–71.
- Ohkawa K, Ando M, Shirakabe Y, et al. (2002). *Text Res J* 72:120–4.
- Ojha SS, Stevens DR, Hoffman TJ, et al. (2008). *Biomacromolecules* 9:2523–9.
- Okada M. (2002). *Progr Polym Sci* 27:87–133.

- Pavinatto FJ, Caseli L, Oliveira Jr ON. (2010). Biomacromolecules 11:1897–908.
- Pillai CKS, Paul W, Sharma CP. (2009). *Prog Polym Sci* 34:641–78.
- Pinchuk L. (1994). *Journal of Biomaterials Science Polymer* 6:225–67.
- Richardson TB, Mosiewicki MA, Uzunpinar C, et al. (2011). *Polymer Composites* 32:455–63.
- Rinaudo M. (2006). *Prog Polym Sci* 31:603–32.
- Saad B, Hirt TD, Welti M, et al. (1997). *Journal of Biomedical Materials Research* 36:65–74.
- Sambaer W, Zatloukal M, Kimmer D. (2011). *Chemical Engineering Science* 66:613–23.
- Santerre JP, Woodhouse K, Laroche G, (2005). *Biomaterials* 26:7457–70.
- Schlickewei C, Verrier S, Lippross S, (2007). *Macromolecular Symposium* 253:162–71.
- Seol Y-J, Lee J-Y, Park Y-J, Lee Y-M, et al. (2004). *Biotechnol Lett* 26:1037–41.
- Shao XX, Goh JCH, Hutmacher DW, Lee EH, Ge ZG. (2006). *Tissue Eng* 12:1539–51.
- Sinha VR, Bansal K, Kaushik R, Kumria R, Trehan A. (2004). *Int J Pharm* 278:1–23.
- Skarja GA, Woodhouse KA. (2000). *Journal of Applied Polymer Science* 75:1522–34.
- Soldani G, Varelli G, Minnocci A, Dario P. (1998). *Biomaterials* 19:1919–24.
- Soletti L, Nieponice A, Hong Y, Ye SH, et al. (2011). *Journal of Biomedical Materials Research* Part A 96:436–48.
- Spaans CJ, De Groot JH, Belgraver VW, et al. (1998). Journal of Materials Science Materials in Medicine 9:675–8.
- Spasova M, Manolova N, Paneva D, Rashkov I. (2004). e-Polym; [No pp.given].
- Stankus JJ, Guan J, Wagner WR. (2004). *Journal of Biomedical Materials Research* Part A 70:603–14.
- Stankus JJ, Soletti L, Fujimoto K, Hong Y, Vorp DA, Wagner WR. (2007). *Biomaterials* 28:2738–46.
- Storey RF, Taylor AE. (1996). *Abstr Pap Am Chem Soc* 211:114–20.
- Storey RF, Wiggins JS, Mauritz KA, Puckett AD. (1993). *Polymer Composites* 14:17–25.
- Takahashi T, Takayama K, Machida Y, Nagai T. (1990). *Int J Pharm* 61:35–41.
- Tamura H, Tsuruta Y, Tokura S. (2002). *Mater Sci Eng* C C20:143–7.
- Van Oss C.J, Moore L.L., Good R.J. and Chaudhury M.K. (1985). *J. Protein Scie.* 4, 245
- Vert M. (2009). *J Mater Sci Mater Med* 20:437–46.
- Vert R, Gupta R. (1987). *J Appl Polym Sci* 33:2411–29.
- Wise JK, Yarin AL, Megaridis CM, Cho M. (2009). *Tissue Eng* Part A 15:913–21.
- Zdrahala RJ, Zdrahala IJ. (1999). *Journal of Biomaterials Applications* 14:67–90.
- Zdrahala RJ. (1996). *Journal of Biomaterials Applications* 11:37–61.
- Zein I, Hutmacher DW, Tan KC, Teoh SH. (2002). *Biomaterials* 23:1169–85.
- Zhuo HT, Hu JL, Chen SJ. (2011). *exPress Polymer Letters* 5:182–7.

Chapter 5

Neuronal growth and differentiation on biodegradable membranes

Sabrina Morelli[1], Antonella Piscioneri[1], Antonietta Messina[1,3], Simona Salerno[1], Mohamed B. Al-Fageeh[2], Enrico Drioli[1,3,4] and Loredana De Bartolo[1]

1Institute of Membrane Technology, National Research Council of Italy, ITM-CNR, c/o University of Calabria, Rende, CS, Italy
2National Centre for Biotechnology, King Abdulaziz City for Science and Technology, Riyadh, Saudi Arabia
3Department of Chemical Engineering and Materials, University of Calabria, Rende, CS, Italy
4Hanyang University, WCU Energy Engineering Department, Seoul, South Korea

JOURNAL OF TISSUE ENGINEERING AND REGENERATIVE MEDICINE (2012)

Introduction

Many types of trauma are often complicated by peripheral nerve injury, which is a worldwide problem: several hundred thousand cases of this injury occur each year in Europe and in the USA [Belkas et al., 2004; Schnell et al., 2007]. In particular, nerve injury still represents a major problem in modern hand surgery and can result in significant disability, including loss of function of the innervated tissue and neuropathic pain. Therefore, despite its extreme complexity, the repair and reconstruction of damaged nerves with sufficient function remains a clinical challenge [Krarup et al., 2002; Nakamura et al., 2004; Evans, 2000]. Peripheral nerve fibres, unlike those of the central nervous system, are able to regenerate after injury. The resected fibres can thus regenerate along the graft and reach the distal nerve stump that will lead to their peripheral nerves. Segments of autologous sensory nerve may be an excellent material tomake nerve grafts, although this surgical technique has inevitable disadvantages, including, among many others, limited supply of available nerve autografts and certain donor site morbidity. Xenografts and allografts have been evaluated as alternatives to autografts but have a poor success rate and problems of immune rejection [Evans et al., 1998]. Thus, a wide range of biological materials (e.g. muscle, vessels) [Tos et al., 2007; Meek et al., 2004] and non-degradable materials (e.g. silicone tubes) have frequently been used for nerve regeneration [Wang-Bennett and Coker, 1990]. Artificial materials have the disadvantages of engendering a chronic foreign body reaction, due to scar tissue formation, inflexibility and lack of stability. To overcome the disadvantages associated with non-degradable polymeric conduits, recent research has been focused on the production of biodegradable artificial nerve guides, which degrade within a reasonable period of time and

manifest only mild foreign-body reactions. Biodegradable polymers are advantageous because of their flexibility and biocompatibility; degradation behaviour, porosity and mechanical strength can be altered by changing their chemical or engineering properties. In the last decade, with rapid advances in biomaterials technology, several types of natural and synthetic biodegradable polymer, including collagen [Stang et al., 2006], chitosan (CHT) [Lin et al., 2008], poly(glycolic acid) (PGA) [Weber et al., 2000; Nakamura et al., 2004], poly(L-lactic acid) (PLLA) [Evans et al., 2002], poly(L-lactide-co-glycolide) (PLGA) [Chang and Hsu 2006], poly(caprolactone) (PCL) [Chang, 2009; Schnell et al., 2007] and polyurethane (PU) [Hausner et al., 2007], have been reported as suitable for nerve regeneration, although the ideal physicochemical compositions, surface structure and functionalization of such materials have not yet been found. In this context, the fabrication of in vitro platforms for neuronal growth represents a valuable tool for the generation of microenvironments, controlled at molecular level, that mimic specific features of the in vivo environment. Our investigation was focused on the development of novel biodegradable membranes aimed at creating a permissive environment for the growth and differentiation of neuronal cells, to be used as a tool for studying neuronal regeneration mechanisms and the potential application in nerve injury. In particular, we developed CHT, PCL and PU flat membranes and a biosynthetic blend between PCL and PU by phase-inversion techniques. After the characterization of the morphological, physicochemical, mechanical and degradation membrane properties, we investigated the efficacy of these different biomaterials to promote the adhesion and differentiation of neuronal cells. We employed human neuroblastoma cell line SHSY5Y as a model cell system to study neuronal differentiation and neuritogenesis in vitro [Pahlman et al., 1995], as they may differentiate into neurites whose proliferation, alignment and direction/length depend on the substrate surface characteristics [Yang et al., 2005; Klein et al., 1999]. Moreover, the SHSY5Y cell line, after retinoic acid treatment, acquires morphological, neurochemical and electrophysiological properties of neurons [Kaplan et al., 1993]. In particular, the performance of the developed biomaterials was assessed in terms of their ability to improve cell adhesion, viability and differentiation, as well as for their ability to allow axonal growth from differentiated human SHSY5Y cells, with special attention to the formation of synapse connections between the neurons.

Materials and methods

5.1 Membrane preparation

Biodegradable membranes were prepared in flat configuration by the inverse phase technique. Chitosan membranes were obtained by dissolving 4% w/v chitosan from shrimp shell (≥ 75% deacetylated; Sigma, Milan, Italy) in acetic acid solution 2% v/v. Then polyethylene glycol (PEG, MW 6000 Da; Merck-Schuchardt, Hohenbrunn, Germany) was added to the solution at a 4:1 ratio and stirred for 2 h. The solution was cast on a glass plate by means of a handle-casting knife (Elcometer; gap set at 250 mm) and dried at room temperature. After drying, the membranes were immersed in a solution of 1% NaOH, and then washed with distilled water. PCL membranes were prepared by dissolving 10% w/w PCL (Mn~70 000–90 000; Sigma, Milan, Italy) in 1.4-dioxan (100%) at 50 °C until complete dissolution. Then, the solution was cast uniformly on a glass plate. The membranes were dried at room temperature until complete solvent evaporation, then washed with distilled water. PU membranes were obtained by dissolving 15% w/w Pellethane 2363-80A (PU; Dow Chemical Noderland BV, Deefzijl, The Netherlands) at 50 °C in formic acid (99%) for at least 2 days to guarantee complete dissolution of the polymer. The solution was cast on a glass plate, evaporated for 5 min, immersed in a solution of 1% NaOH and then washed with distilled water. For the preparation of the PCL–PU blend, the PU was dissolved at 15% w/w and the PCL (Mn ~ 10 000; Sigma) at 28% w/w, both in formic acid (99%), and stirred until they became clear. The two solutions of PCL and PU were mixed together at ratio 1:2 in order to reach the final concentration of solvent, around 80%. The solution was cast on glass and dried at room temperature. Then, the membrane was immersed in a solution of 1% NaOH and finally washed with distilled water.

5.2 Membrane characterization

The morphological properties of all membranes were characterized by scanning electronmicroscopy (SEM). Dried membrane samples in flat configurations were cut in cross section, mounted with double-faced conductive adhesive tape and analysed by SEM (ESEM FEG QUANTA 200, FEI Company, OR, USA) in order to establish the cross-sectional structure and thickness, the shape and sizes of the membrane pores as well as the distribution of pore size. The wettability of the biodegradable membranes was characterized by means of water dynamic contact angle (DCA) measurements at room temperature, using a CAM 200 contact angle meter (KSV Instruments Ltd, Helsinki, Finland). DCA measurements were

performed under standard conditions, taking into account various parameters (e.g. temperature, cleanliness of sample, drop volume). At least 30 measurements on different regions of each membrane sample were averaged for each DCA value. Degradation properties of developed membranes were investigated by treatment with an enzymatic solution. In particular, the samples (1.5x1.5 cm) were precisely weighed and immersed in lysozyme solution (1mg/ml in PBS 0.2M, pH 7.4), then incubated at 37 °C, refreshing the medium every 6 days. At the end of predetermined incubation intervals, three samples/group were removed for degradation analysis, washed with distilled water and dried at room temperature to constant weight, prior to the final determination. The dissolution index was calculated as: % Dissolution = [$(W_o – W_t) / W_o$] *100; where Wi is the sample weight before incubation in enzymatic solution and Wd is the dried sample weight after the dissolution test. Each test consisted of four replicate measurements. The mechanical properties of the biodegradable membranes were determined at room temperature, using a Zwick/Roell tensile testing machine. Samples from each kind of membrane, in the dry state, were cut into strips of 5x1 cm and their width was measured using a micrometer before every determination; then they were gripped within the pneumatic grips. Grip separation was set at 3 cm and a testing speed of 5mm/min was used. Ultimate tensile strength (UTS), Young's modulus (Emod) and elongation at break parameter (e) were evaluated. Five replicates of each sample type were tested per time point.

5.3 Cell culture

The human neuroblastoma cell line SH-SY5Y (ICLCIST, Genova, Italy) was routinely cultured in a 1:1 mixture of Ham's F12 (Invitrogen) and minimum essential Eagle's medium (EMEM) supplemented with 10% v/v heat-inactivated fetal calf serum (FCS), 2mM glutamine, 100 mg/ml penicillin–streptomycin. The cells were maintained in a 5% CO2 humidified incubator at 37 °C in 75cm2 flasks (PBI International, Milan, Italy). For cell culture experiments, SH-SY5Y cells were detached by means of trypsin–EDTA solution (Sigma), resuspended in Ham's F12-EMEM and seeded at a concentration of $1.5x10^3$ cells/cm2 on CHT, PU, PCL and PCL–PU membranes with surface area of 2.54 cm2. Polystyrene culture dishes (PSCDs) were used as reference substrates. Controls without cells were prepared for each type of substrate. After 24 h the culture medium was replaced with fresh Ham's F12-EMEM containing 10 mM retinoic acid (RA), in order to differentiate the cell line toward a neuronal phenotype. Then the cultures were fed every 3 days.

5.4 Measurement of 3-(3,4-dimethylthiazol-2-yl) -2,5 diphenyltetrazolium bromide (MTT) assay.

Cell viability was determined by MTT test, in which the yellow MTT is reduced to a purple formazan by mitochondrial dehydrogenase in the cells. Briefly, at 3 and 6 days in vitro (DIV3 and DIV6), SH-SY5Y cells were washed with PBS. The culture medium in each well of the plate was replaced with 400 ml MTT (5mg/ml). Metabolically active cells cleaved the yellow tetrazolium salt MTT to purple formazan crystals. After 2 h of incubation at 37 °C, the reaction was stopped by adding 400 ml lysis buffer (10% SDS, 0.6% acetic acid in DMSO, pH 4.7). The quantity of formazan product was directly proportional to number ofmetabolically active living cells. The optical density of each well was spectrophotometrically measured at 570 nm. The results were expressed as percentage of the PSCD control substrate.

5.5 Sample preparation for SEM

Samples of neurons grown on the different substrates were prepared for SEM by fixation in 2.5% glutaraldehyde, pH 7.4 phosphate buffer, followed by post-fixation in 1% osmium tetroxide and by progressive dehydration in ethanol. Samples were examined at SEM and representative images displaying both neuronal structural features and adhesive properties for the different membrane surfaces were obtained at DIV 3 and DIV6. NIH-Scion Image software was used in order to perform quantitative evaluations of the neurite length and the area filled by neurons, expressed as a percentage of the total membrane area for the two different developmental stages. The statistical significance of all experimental results was established using an ANOVA test followed by a Bonferroni t-test ($p<0.05$).

5.6 Immunostaining of neuronal cells and quantitative analysis

The morphological behaviour of the neurons at DIV6 on the different membranes was investigated and compared to PSCDs as controls by observing them with a laser confocal scanning microscope (LCSM; Fluoview FV300, Olympus, Milan, Italy) after immunostaining of the neuronal cytoskeleton marker protein, bIII-tubulin [De Bartolo et al., 2008] and the synaptic vesicles marker, synaptophysin. Six samples for each substrate were analysed. In particular, neuronal cells were rinsed with PBS, fixed for 15 min with paraformaldehyde (4%), permeabilized for 10 min with 0.25% Triton X-100 and subsequently blocked for

30min with 1% BSA at room temperature. To visualize βIII-tubulin, a rabbit polyclonal anti-bIII-tubulin (1:100; Sigma) and a goat anti-rabbit IgG FITC-conjugated (1:100; Invitrogen) were used. To visualize synaptophysin, a monoclonal mouse anti-synaptophysin (1:400; Chemicon, Millipore, Milan, Italy) and a goat anti-mouse IgG TRITC-conjugated (1:100; Invitrogen) were used. Primary antibodies were incubated overnight at 4 °C, secondary antibodies for 60min at room temperature. Nucleic acids were counterstained with DAPI (200 ng/ml; Sigma). Finally, the samples were rinsed, mounted and observed with an LCSM. Quantitative analysis was performed on confocal microscopy images of neurons at DIV6, using Fluoview 5.0 software (Olympus Corp.). The total fluorescence intensity for stained bIII-tubulin and synaptophysin was calculated in a series of squared areas (235x235 μm) of the x–y axis vs the z axis of acquired images. Each image was composed of 22 slices, having an optical thickness of 0.5 μm with a total depth of 11 μm.

5.7 Western blotting analysis

For western blotting analysis the proteins were extracted from cells before seeding (cell suspension) and from cells cultured on the different membranes at DIV6, according the procedure described previously [Piscioneri et al., 2011]. For the analysis, equal amounts of protein (50 mg) were boiled for 5 min, separated under denaturing conditions by SDS–PAGE on 8% polyacrylamide Tris–glycine gels and electroblotted to nitrocellulose membranes. Nonspecific sites were blocked with 5% non-fat dried milk in 0.1% Tween-20 in Tris-buffered saline (TBS-T) for 1 h at room temperature and incubated overnight with a rabbit polyclonal anti-bIII-tubulin antibody (1:100; Sigma). To visualize the neuronal axon marker protein, 43 kDa growthassociated protein (GAP-43), an incubation withmonoclonal mouse anti-GAP-43 (1:100; Sigma) was also carried out. The antigen–antibody complex was detected by incubation of the membranes for 1 h at room temperature with a peroxidase-coupled anti-IgG antibody (1:3000; Santa Cruz Biotechnology, Santa Cruz, CA, USA) and revealed using the ECL Pluswestern blotting detection system (Amersham, USA) according to the manufacturer's instructions. Each membrane was exposed to the film for 1 min.

Results

The design of this study aimed to evaluate the influence of different biodegradable membranes in promoting neuronal regeneration, therefore representing a valuable tool in neuronal tissue engineering. Taking into account the results obtained through a

thermodynamic investigation, different membranes were prepared, made up of different polymer solutions. All the membranes were fully characterized in terms of structural and mechanical properties and the data related to the membrane properties are listed in Table 5.1. Figure 5.1 shows SEM images of the biodegradable membranes prepared by the phase-inversion method, revealing the morphology of the membrane surfaces that had been in contact with glass during casting and on which the cells were seeded. Both CHT and PU membranes exhibit a homogeneous and very smooth surface (Figure 5.1a,c). The presence of repeated microstructures is clearly visible on the PCL surface (Figure 5.1b) and this patterned distribution was also revealed by SEM images on PCL–PU membrane. This quite singular morphology is typical of the PCL membranes and it is in fact conferred by the presence of this polymer in the casting solution. Because natural ECM is a fully hydrated gel, wettability is a key consideration factor; accordingly, different substrates were subjected to further physicochemical characterizations. All the prepared biodegradable membranes had a hydrophilic character, as demonstrated by dynamic contact angle measurements (Table 5.1). CHT membranes were the most hydrophilic substrates, with the contact angle measured at 59±4°, more or less similar to the control substrate, PSCD, at 62±5°. Synthetic biodegradable polymermade membranes, PU and PCL as well as PCL–PU blend, exhibited advancing contact angle values in the range 72–78°, as a result of their significantly lower hydrophilic properties ($p<0.05$) with respect to CHT membranes. The dissolution behaviour of the different biodegradable membranes was investigated for up to 24weeks and changed perceptibly during this period (Figure 5.2). As anticipated, CHT membranes being a natural polymer, CHT membranes were completely dissolved after 4weeks of enzymatic treatment. In contrast, the dissolution behavior of the synthetic biodegradable membranes was slower, but the index still increased with time, reaching values of 18%, 20% and 29% for PCL, PCL–PU and PU, respectively, after 7 weeks. Although after 7 weeks of treatment the PU membrane presents a dissolution behaviour that is slightly higher in comparison to the other substrates, this percentage is kept more or less constant at a value of 35% after 24weeks, which is, moreover, quite close to the value of 38% exhibited by the PCL–PU membrane (Figure 5.2). Mechanical properties of materials represent an important set of characteristics to consider in a biomaterial design or in choosing the right one. Since it is now widely demonstrated that mechanical properties are critical for determining cell behaviour, the matrix elasticity in terms of ultimate tensile strength (UTS), Young's modulus (Emod) and elongation parameter (ε) were evaluated. All the data regarding matrix stiffness are listed in Table 5.1. As expected, CHT membranes have a higher Young's modulus and UTS and a low percentage of

elongation at break compared to other biodegradable membranes. This would result in weak mechanical strength of the CHT membrane. After optimization of the membrane properties, the novel substrates were employed in the recreation of bio-artificial systems for the culture SHSY5Y neuroblastoma cells, in contrast to traditional PSCDs that were used as a control. In order to assess whether biodegradable membranes can effectively support neuronal cell growth, different in vitro assays were carried out. Initially, the determination of structural and functional cell features was carried out through the observation of possiblemorphological changes. In particular, the effects of various substrates on the behavior of neuronal cells were investigated by observing the cell morphology through SEM images at DIV3 and DIV6 of culture. Figure 5.3 shows that cells adhered and were grown on different biodegradable membranes, as well as on the PSCD. Already at DIV3 (Figure 5.3a,c, e, g, i), on each substrate, the cellswere able to differentiate, showing a neuronal-like phenotype with a spread cell body and with a wide extention of their neuritic processes; this kind of disposition became even more evident at DIV6 (Figure 5.3b, d, f, h, j). Cells on synthetic biodegradable polymeric membranes of PCL (Figure 5.3e), PU (Figure 5.3g) and PCL–PU blend (Figure 5.3i), showed morphological features very similar to those of the controls after 3 days (Figure 3a). After 6days of culture, cells grown on PCL–PU membranes were confluent (Figure 5.3j). In contrast, cells grown on CHTmembranes showed a different morphology, characterized bymuchmore spreading of the cell body, going deeper into the membrane surface structure (Figure 5.3c, d). In order to analyse howthe membrane properties can affect cell adhesion and proliferation, we performed quantitative measurements of the cell density and the area covered by cells on differentmembrane substrates (Figure 5.4a). The cell density increasedwith time as a result of cell proliferation on all membranes and also varied as a function of the membrane. On PCL–PU, PCL, PU and CHT membranes the cell density at DIV6 reached values of 5.7±0.25, 3.2±0.21, 3.2±0.9 and 1.5±0.29 cells/cm2, respectively. The cells displayed different morphological behaviours when seeded on different substrates. In particular, at DIV 3 the area covered by cells on PSCD (24%), PCL–PU (20%), PCL (19%) and PU (18%) membranes was significantly higher compared to CHT membranes, where neuron cell growth covered only 10% of the area. In agreement with SEM observations, the highest value at DIV6 was reached on PCL–PU membranes, therefore representing the most covered surface (50%). Further, cellmorphological featureswere also investigated by performing morphometric analysis in terms of neurite length of the cells (Figure 5.4b). After 3 days of culture, cells seeded on PCL, PU and PCL–PU membranes showed intense neurite sprouting, as evidenced by the average process length of 98 μm. Similar values were also

observed when cells were seeded on PSCD (102±8 μm) and were significantly higher compared to the neurite elongation measured on the CHT membrane (70±11 μm). Towards the end of the culture period (DIV6), the longest neuritic processes were obtained on PCL–PU membranes (105 μm). To determine whether biodegradable membranes were able to maintain viable neuronal cells, MTT tests were performed (Figure 5.5); all results were expressed as a percentage of the PSCD control substrate. Although an increase of cell viability over time was observed for all substrates, the percentage of cell viability was significantly higher when cells were cultured on PCL, PU and PCL–PU membranes than that detected on CHT membranes. The highest value of cell viability was reached when neuronal cells were cultured on PCL–PU membranes at DIV6. The capacity of SH-SY5Y cells to gain a neuronal-like phenotype once seeded on the different biodegradable membranes was further elucidated by immunocytochemical studies. Confocal microscopy imaging was used to study the distribution of some specific neuronal proteins, such as βIII-tubulin and synaptophysin, the first being a cytoskeletal protein present in the soma and in all neuronal processes, and the second the most frequent presynaptic marker of mature neurons and therefore an abundant integral membrane protein of synaptic vesicles. βIII-tubulin at DIV6 is widely distributed and, moreover, the cells on the biodegradable membranes of PCL, PU and PCL–PU appeared connected to each other through the extension of their neurites, giving arise to well-developed neural networks (Figure 5.6). These morphological features were also sustained by cells cultured on PSCD controls. In contrast, on CHT membranes the cells appeared much more spread, with short neurites, as evidenced by double-immunofluorescence. Anti-synaptophysin immune-cytochemistry revealed an intense and punctuate distribution of synaptophysin in neurons cultured on all substrates (Figure 5.6a–e), suggesting synaptic formation in vitro. In order to evaluate the changes in the expressions of neuronal markers, quantitative analysis in terms of the fluorescence intensity of bIII-tubulin and synaptophysin was then performed (Figure 5.7). The fluorescence intensity of bIII-tubulin was significantly higher in cells cultured on synthetic biodegradable membranes of PCL, PU and PCL– PU with respect to CHT membranes and PSCD controls. The highest average fluorescence intensity emission for synaptophysin was detected when the cells were cultured on PCL–PU membranes. To further substantiate successful differentiation of the cells towards a neuronal phenotype, we also investigated the effect of the different biodegradable substrates on the expression pattern profile of specific neuronal proteins: GAP 43, an axonal protein, and βIII-tubulin. GAP43, as shown in Figure 5.8, is strongly expressed by cells seeded on PU and PCL–PU membranes, as

well as on the reference system PSCDs, suggesting that these substrates supported axonal elongation well. In contrast, cell suspension and cells seeded on the other kinds of membrane exhibited lower GAP 43 expression. The expression of the structural cytoskeletal protein bIII-tubulin was strongly detected in all investigated substrates, as indicated by the thick bands obtained after immunoblotting (Figure 5.8). These results are in good agreementwith those obtained through morphometric analysis. In fact, cells were able to grow and extend their processes, therefore covering a wide substrate area, indicating that the cells can reorganize and polymerize their cytoskeletons correctly in the new artificial environment.

Discussion

This study describes the development of biodegradable membrane systems aimed at providing an environment with suitable properties for supporting regeneration in terms of cell adhesion and promotion of axonal outgrowth and differentiation. For this purpose, biodegradable membranes of CHT, PCL, PU and PCL–PU blend, designed as guidance structures, were produced by an inverse-phase technique and tested in cell culture assays. CHT was chosen because this natural polymer is an advantageous material for neural tissue engineering, as it is biocompatible, favours the migration of supporting cells and avoids the occurrence of toxic effects [Yuan et al., 2004]. Among synthetic biodegradable polymers, PCL is highly appealing, due to its physicochemical and mechanical characteristics, easy processing ability related to a relatively low melting temperature, non-toxic degradation products and Food and Drug Administration (FDA) approval for biomedical applications [Woodruff and Hutmacher, 2010]. In addition to possessing the requisite stiffness, another desirable mechanical characteristic of a biomaterial to serve as nerve guidance conduit is flexibility. Elastic polymers such as PU are widely used in several biomedical applications, including in the construction of nerve guidance conduits. On the other hand, PU is relatively soft with inherently poor mechanical strength and needs to be either co-polymerized or physically blended with another polymer to produce a neuronal guidance conduit [Jiang et al., 2010]. In order to outweigh this disadvantage, a blend of PCL and PU was therefore prepared to obtain a biomaterial with tailored characteristics in terms of degradation behaviour, mechanical performance and wettability, as a possible substrate for neuronal outgrowth and axonal elongation. This paper reports for the first time the use of PCL–PU membrane as a proposed material for neuronal regeneration. It is noteworthy that important parameters for a neuronal guidance include surface properties such as morphology, wettability and degradability.

Biodegradable membranes prepared in this study displayed different morphological properties in terms of thickness, shape and sizes of themembrane pores. In particular, PCL and PCL–PU membranes are characterized by the presence of repeated microstructures on the surface, which are typical for membranes made with PCL polymer [Wang et al., 2010; Lee et al., 2008]. The advancing and receding contact angle values, which are representatives of the apolar and polar domains, respectively, of the surface, evidenced the wettability properties of the different biodegradable membranes. CHT membranes are more hydrophilic compared to the other substrates, due to the presence of polar amino groups as a result of the removal of acetyl groups from the molecular chain of chitin, which occurs during the deacetylation process. The degree of deacetylation (75%) affects the percentage of amino groups and consequently the hydrophilic character [Li et al., 1992]. The important advantage of such biopolymers is the degradation process, because once degraded, the monomeric components of each polymer are removed from the body by natural pathways. The in vitro degradation behavior of different membranes was in agreement with our expectations. In fact, CHT membranes completely dissolved within approximately 4weeks, whereas PCL, PU and PCL–PU membranes have different degradation profiles characterized by a slower degradation rate. Materials for the fabrication of neural tissue constructs, including nerve guides, are required to have suitable mechanical properties, such as elasticity/stiffness and flexibility [Ciardelli and Chiono, 2006]. The biodegradable membranes reported in this study have different grades of tensile elasticity, as demonstrated by their values of Young's modulus (Table 5.1). In particular, the CHT membranes reported here are more rigid substrates with respect the PCL, PU and PCL–PU membranes. In order to serve in neural tissue engineering, biomaterials must function as growth substrates for neuronal cells and must guide regenerating neurons. Therefore, we tested the capacity of generated biodegradable membranes to support and improve cell adhesion, proliferation and differentiation. In particular, in vitro cell culture tests were performed using neuroblastoma SH-SY5Y cells, since this cell line is a good model system to investigate neuritogenesis [Kaplan et al., 1993; Simpson et al., 2001] and nerve tissue regeneration [Mollers et al., 2009]. In this study the differentiation of SH-SY5Y cells in culture on different realized biodegradable membranes was demonstrated by investigating not only the changes in morphology, but also the expression and distribution of specific neuronal markers. Neuronal cells were able to adhere to and grow on the different substrates, especially on PCL–PUmembranes, as demonstrated by the percentage area covered by cells and cell viability data. Neuronal cell spreading and neurite outgrowth varied with material type, and there were visible differences in cell behaviours between neurons onmembranes of natural

polymer of CHT and those cultured on membranes of synthetic polymers of PCL, PU and PCL–PU blend. In particular, on CHT membranes neurons were less developed and exhibited a flatter and more spreadmorphology, with poorly branched processes (Figure 5.3c, d). On the other hand, on membranes of synthetic biodegradable polymers (PCL, PU and PCL–PU), a neuronlike phenotype was developed that was characterized by spindle-like cell somata and extensive neurites outgrowth. This neuron-like morphology is similar to that described by others [Cheung et al., 2009; Clagett-Dame et al., 2006]. Interestingly, on these membranes the long and dense axons and dendrites, which took compact arrangements, mutually interweaved to form neural networks, which reached very complex density during the experiments, especially on PCL–PU membranes at DIV6. It is well known that neuronal cells connect to one another to form networks that are crucial for neural function. These networks are primarily formed during development as maturing neurons extend processes to reach synaptic targets. In particular, at the leading edge of these processes are growth cones that recognize and translate a combination of chemical and physical cues into a specific trajectory towards a population of target cells. Therefore, in line with this concept and as reported previously [De Bartolo et al., 2008; Morelli et al., 2010, 2012], the in vitro reconstruction of neuronal networks obtained in this study on the novel biodegradable membranes is a very important result, which clearly indicates cellular differentiation. In accordance with these findings, neurites outgrowth was significantly higher on membranes of synthetic polymers. One explanation for the different outcome of our experiments is that neuronal cells react differently to a surface with different physicochemical properties. In the case of CHT membranes, which exhibit more wettable and degradable characteristics, the cells spread and seemed to go into the structure and were not able to elongate, perhaps due also to the fast swelling and degradation rate. To confirm that the observed morphological behaviours were actually resulting from the neuronal differentiation of SH-SY5Y cells, the expression and the distribution of the specific neuronal markers βIII-tubulin and synaptophysin were explored by immunocytochemical analysis. βIII-tubulin, as a member of the tubulin family, is found in the brain and root ganglia and localized to neurons in the central and peripheral nervous system, where its expression seems to increase during axonal outgrowth [Carré et al., 2002]. In particular, this cytoskeletal protein is typical of the soma and neuronal processes. Synaptophysin is the most abundant integral membrane protein of synaptic vesicles [Thiel, 1993]. It is expressed at high levels during synaptogenesis, is one of the earliest synaptic proteins to accumulate at developing synapses in culture [Fletcher et al., 1991] and can be used as marker of nerve terminal differentiation to monitor synapse formation [Knaus et al.,

1986]. Previous molecular studies have hinted at a number of diverse roles for synaptophysin in synaptic function, including exocytosis, synapse formation and biogenesisof synaptic vesicles [Cameron et al., 1991; Leube et al., 1989]. Recently, Kwon and Chapman (2011) showed that synaptophysin regulates endocytosis to ensure vesicle availability during and after sustained neuronal activity. In this study the investigation of the distributions of these specific neuronal markers demonstrated that neuronal processes ramify, branch and form synapses with other neurons. This study allowed us to assess that the correct neuronal differentiation had taken place in a different manner in cells seeded on the different biodegradable membranes, depending on the type of the substrate. Particularly, total βIII-tubulin levels on PCL, PU and PCL–PU membranes were significantly higher than those obtained on CHT substrates, demonstrating that membranes of synthetic polymers of PCL, PU and PCL–PU blend tend to support a better level of cytoskeletal factor integrity of neuronal projections with respect the natural polymeric membranes of CHT. The highest expression of the synaptic protein synaptophysin on PCL–PU membranes suggests how this specific substrate is able to enhance neuronal differentiation, demonstrating that cells cultured in such a bioartificial system are functionally active and mature. The changes in the expression of neuronal markers revealed by immunocytochemical analysis were confirmed by western blot analysis. Moreover, the expression pattern profile of GAP43 demonstrated that this axonal protein is strongly expressed by cells grown on PU and PCL–PU membranes, suggesting the ability of these substrates to support and promote neuronal outgrowth and synaptic plasticity in terms of axonal elongation. In fact, GAP-43, an axonal membrane protein, is involved in the neuronal outgrowth and synaptic plasticity of developing and regenerating neurons [Goslin et al., 1988; Chakravarthy et al., 2008]. Overall, these findings suggest that PCL–PU membranes provide the best cell culture conditions, allowing for good levels of neuronal differentiation. The different behaviour of CHT, PCL, PU and PCL–PU membranes towards neuronal attachment and differentiation can be attributed to the different variability of biomaterials properties. Since cell–biomaterial interaction is a very complicated phenomenon and depends in a very delicate manner on the surface structure and composition of biomaterials, it is not clear what structure is really dominant for neuronal culture. It is important to note that, although increased surface hydrophilic properties can improve cell adhesion, the cells did not differentiate into a well-defined neuronal phenotype on CHT membranes, which were the highest hydrophilic substrates used in this study. Moreover, the obtained data confirmed that moderately hydrophilic surfaces, such as PCL, PU and PCL–PU, have been found to promote cell adhesion better, even though all substrates were wettable

surfaces without significant differences of physicochemical properties, enclosed in CHT membranes. Although CHT has been studied as a candidate material for nerve regeneration [Yuan et al., 2004], the inappropriate mechanical properties of the developed CHT membranes restrict its application in this field. CHT membranes prepared in the present study were considerably more rigid and brittle (Young's modulus=2288 MPa) than other membranes. Thus, CHT membrane as potential candidate for nerve conduits could compress the regenerating nerve cells and break in vivo before the wounds were completely healed. In agreement with other reports [Cheng et al., 2003; Mingyu et al., 2004; Ciardelli and Chiono, 2006], our investigation suggests that CHT membranes must be modified to balance their hydrophilic character and poor mechanical properties before they can be potentially used in nerve repair. On the other hand, PU membrane is too soft whereas PCL and PCL–PU membranes have Young's modulus of 208 MPa and 570 MPa, respectively. Thus, these membranes can offer enough mechanical properties to nerve tissue. Especially, PCL–PU membranes are more favourable substrates for nerve regeneration, therefore demonstrating that the mechanical properties of PU were improved by blending with PCL. Over the past decades it has become increasingly apparent that surface cues play key roles in determining the ability of cells to adhere, migrate, proliferate, grow, differentiate and respond to surfaces by the extension of processes. Our study confirmed that mechanical properties play an important role in driving cell–material interactions and provides evidence that it is one of the most important properties of the substrate, necessary for supporting neuronal survival and neurite growth and influencing the cell's capacity to differentiate itself. In summary, the present work shows that neuronal cells respond to these novel biodegradable environments by changing their morphology and neurite outgrowth and regulating the expression and distribution of specific neuronal markers. The findings of this study suggest that the regulation of these responses is complex and depends on the nature of the biodegradable polymer used to form the membranes, as well as on the dissolution, hydrophilic and mechanical properties. Furthermore, the better cell adhesion on PCL–PU membranes, associated with the differential expression of specific marker proteins, suggests that they represent suitable biomaterials for creating a permissive environment for the growth and differentiation of neuronal cells. Furthermore, our investigation suggests that blending could improve the mechanical properties of polymers that are important in the development of an effective neuronal guide.

Table 1. Membrane properties

Membrane	CHT	PCL	PU	PCL-PU
Thickness (μm)	5 ± 0.9	8 ± 1	19 ± 1.9	11 ± 1.2
Mean pore diameter (μm)	0.026	0.022	0.082	–
E (MPa)	2288 ± 406	208 ± 28	36 ± 9	570 ± 45
ε (%)	8.92 ± 2.5	321 ± 100	42 ± 9	3.5 ± 1
UTS (MPa)	79.8 ± 12	20 ± 3.6	7.9 ± 1.6	11.5 ± 5
WCA (°)	θ_{adv} 59 ± 4 θ_{rec} 36 ± 7	θ_{adv} 78 ± 3 θ_{rec} 51 ± 5	θ_{adv} 75 ± 4 θ_{rec} 56 ± 5	θ_{adv} 72 ± 3 θ_{rec} 50 ± 3

E, Young's modulus; ε, elongation at break; UTS, ultimate tensile strength; WCA, water contact angle; θ_{adv}, advancing contact angle; θ_{rec}, receding contact angle.

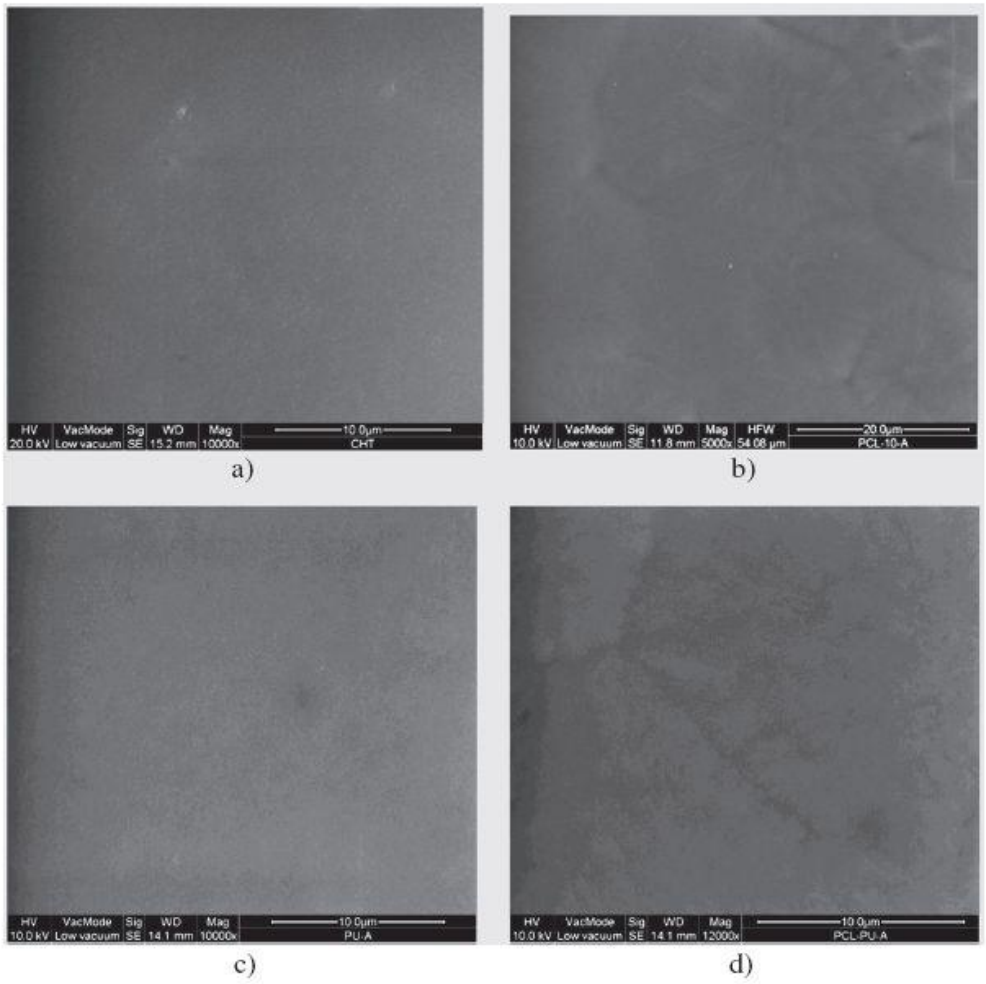

Figure 1. SEM images of the surface of the biodegradable membranes: (a) CHT; (b) PCL; (c) PU; (d) PCL–PU

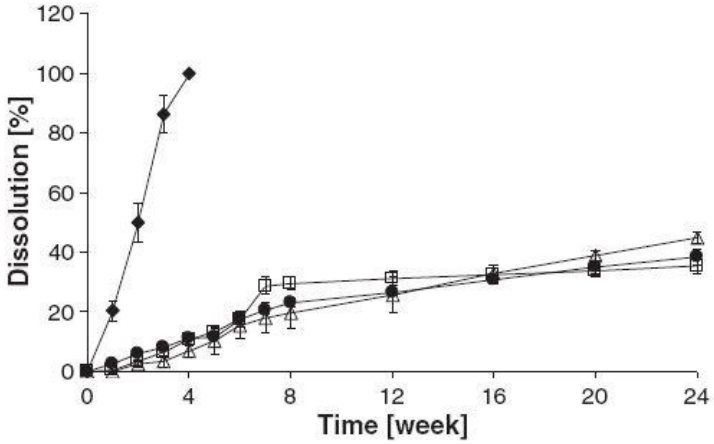

Figure 2. Dissolution behaviour of (♦) CHT, (Δ) PCL, (□) PU and (●) PCL–PU membranes as a function of time. The values are the means of 10 measurements/sample ± SD

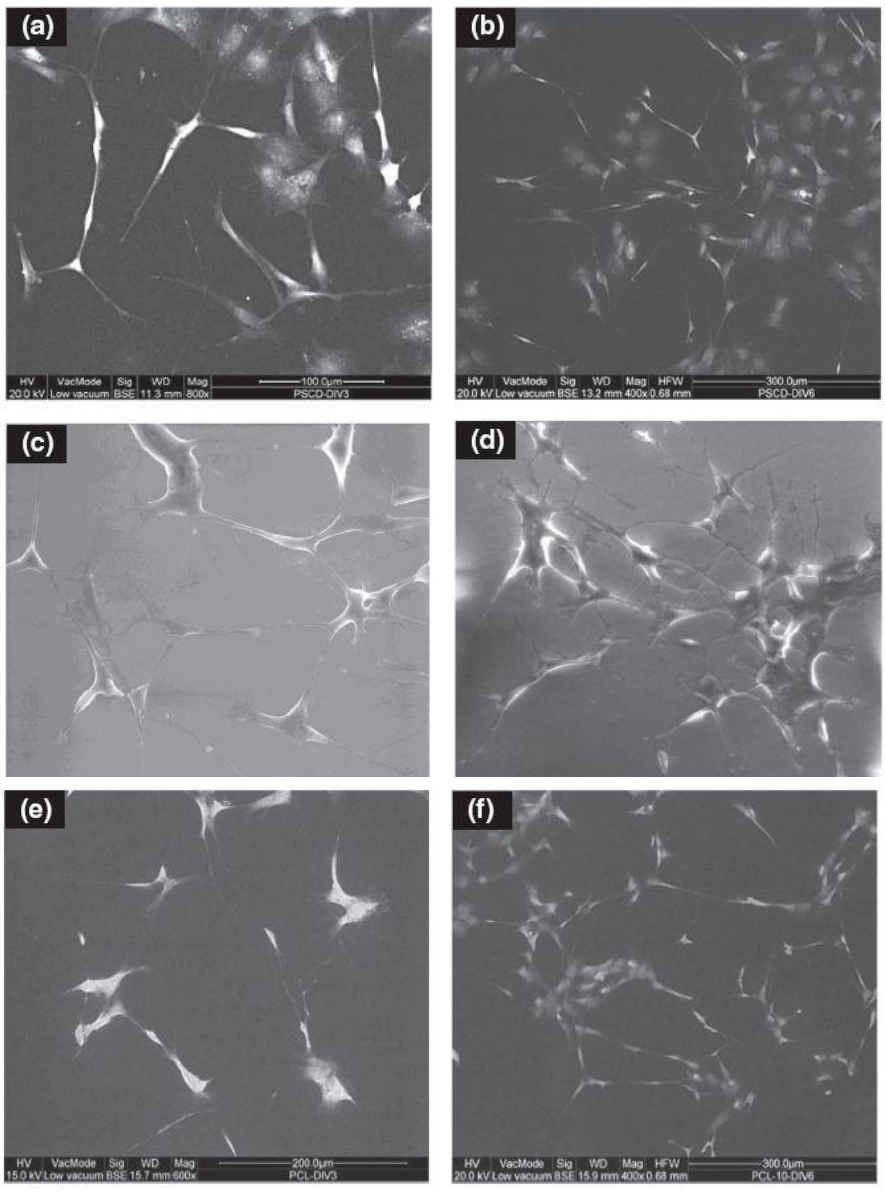

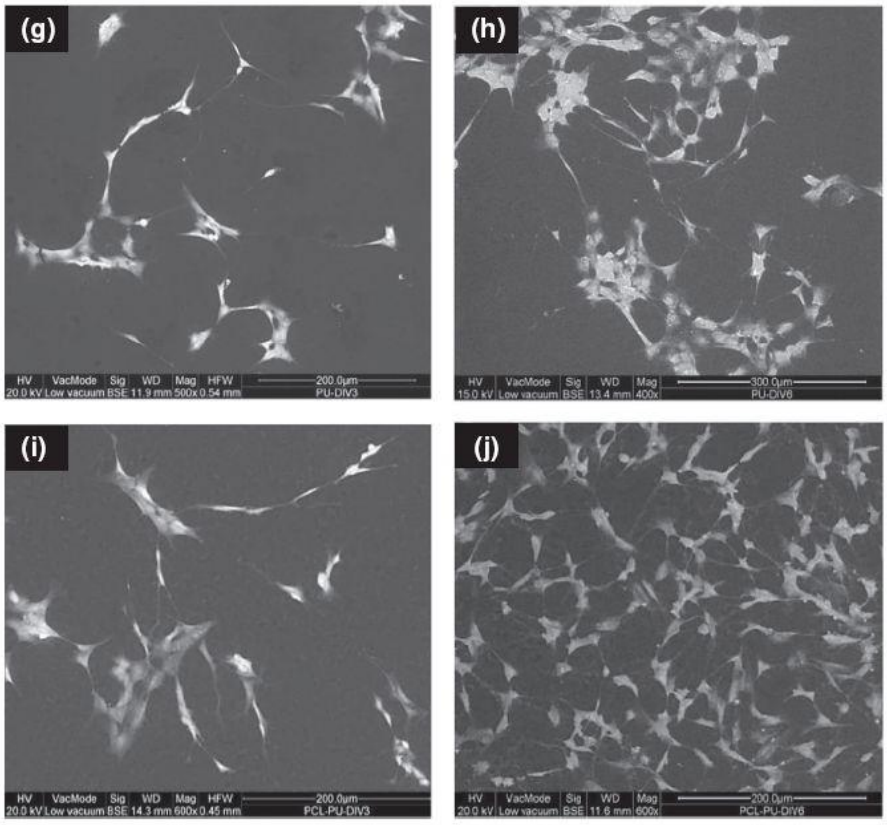

Figure 3. SEM images of SHSY5Y cells at DIV3 (a, c, e, g, i) and DIV6 (b, d, f, h, j) on: (a, b) PSCD; (c, d) CHT; (e, f) PCL; (g, h) PU; (i, j) PCL-PU membranes

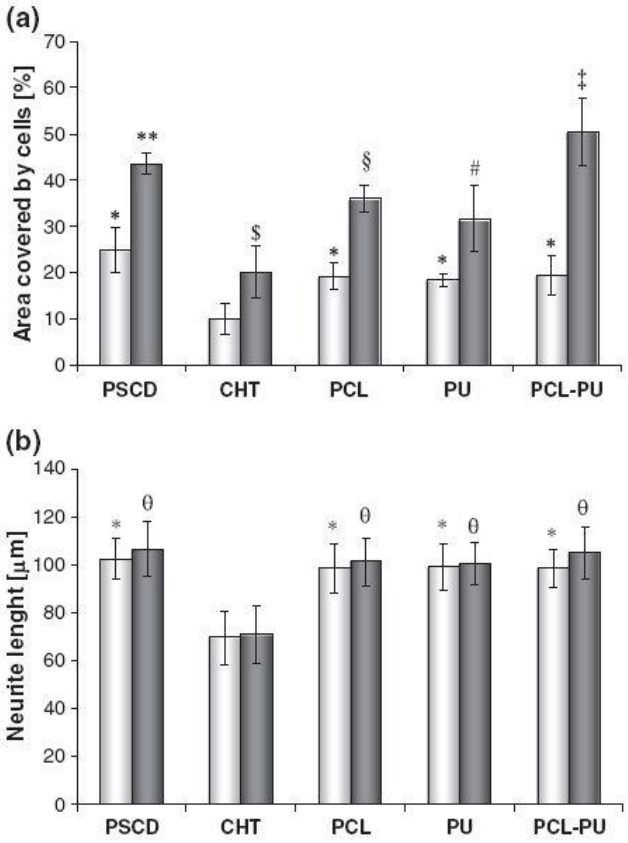

Figure 4. Morphometric analysis of SHSY5Y cells cultured on th different substrates. (a) Percentage of the area covered by cells DIV3 (light bars) and DIV6 (dark bars) on the different mem branes. (b) Neurite length of cells at DIV3 (light bars) and DIV (dark bars) on the different membranes. The data were expresse as average ± SD and evaluated according to ANOVA, followed b Bonferroni *t*-test; $^{*}p < 0.05$ vs CHT at DIV3; $^{**}p < 0.05$ vs CH and PU at DIV6 and vs the same substrate at DIV3; $^{\S}p < 0.05$ CHT at DIV6 and vs the same substrate at DIV3; $^{\#}p < 0.05$ vs CH at DIV6 and vs the same substrate at DIV3; $^{\ddagger}p < 0.05$ vs CHT, PU PCL at DIV6 and vs the same substrate at DIV3; $^{\$}p < 0.05$ vs th same substrate at DIV3; $^{\theta}p < 0.05$ vs CHT at DIV6

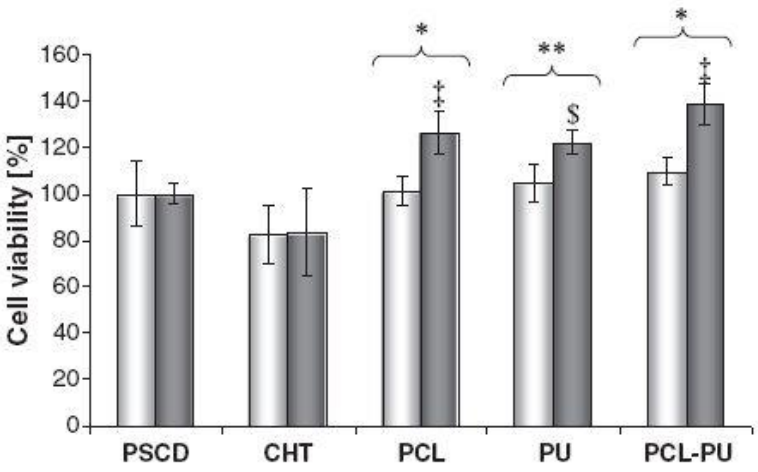

Figure 5. Changes in the cell viability, measured by MTT assay, of SHSY5Y cells at DIV3 (light bars) and DIV6 (dark bars) on the different substrates. The results were expressed as percentage of PSCD, which is the control substrate, and as average ± SD. Data statistically significant according to ANOVA followed Bonferroni *t*-test; $^{\ddagger}p < 0.05$ vs PSCD and CHT at DIV6; $^{\$}p < 0.05$ vs CHT at DIV6. Data statistically significant according to Student's *t*-test: $^{*}p < 0.01$ vs the same substrate at DIV3; $^{**}p < 0.05$ vs the same substrate at DIV3

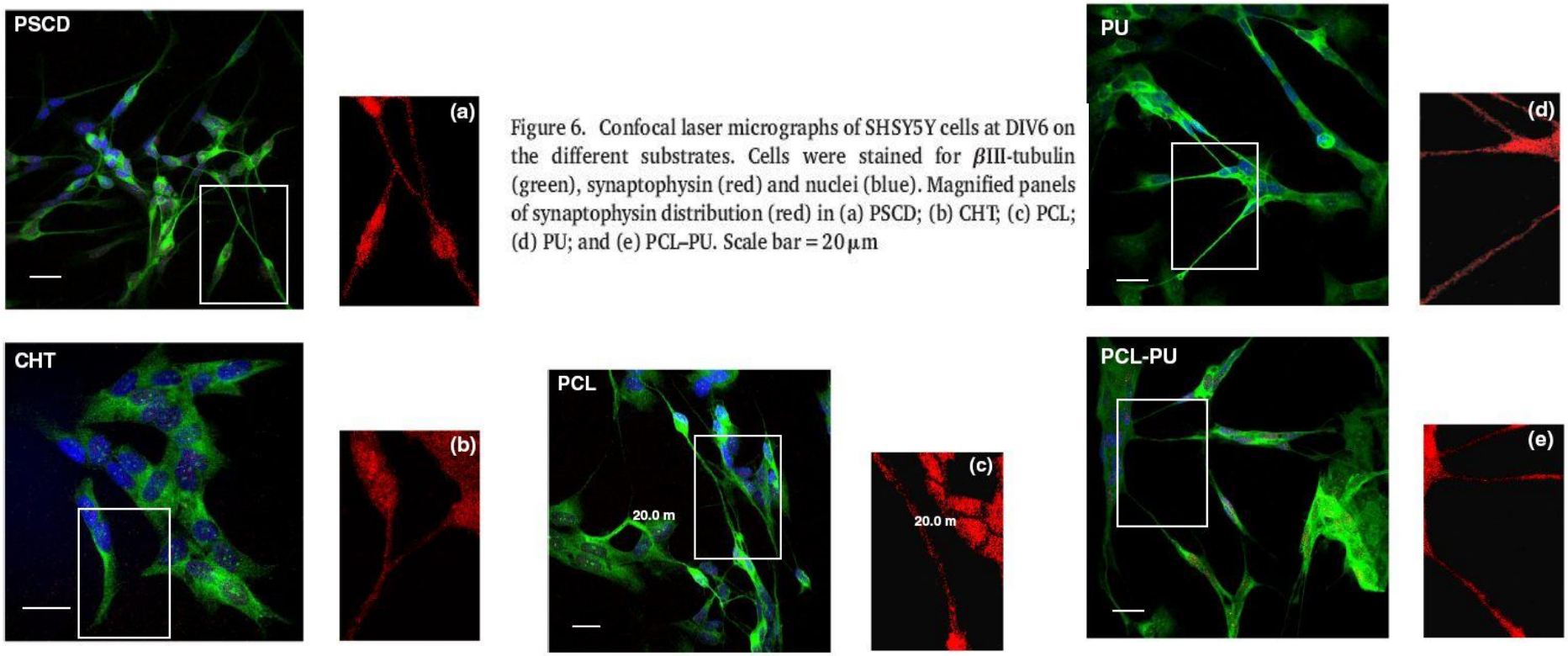

Figure 6. Confocal laser micrographs of SHSY5Y cells at DIV6 on the different substrates. Cells were stained for βIII-tubulin (green), synaptophysin (red) and nuclei (blue). Magnified panels of synaptophysin distribution (red) in (a) PSCD; (b) CHT; (c) PCL; (d) PU; and (e) PCL–PU. Scale bar = 20 μm

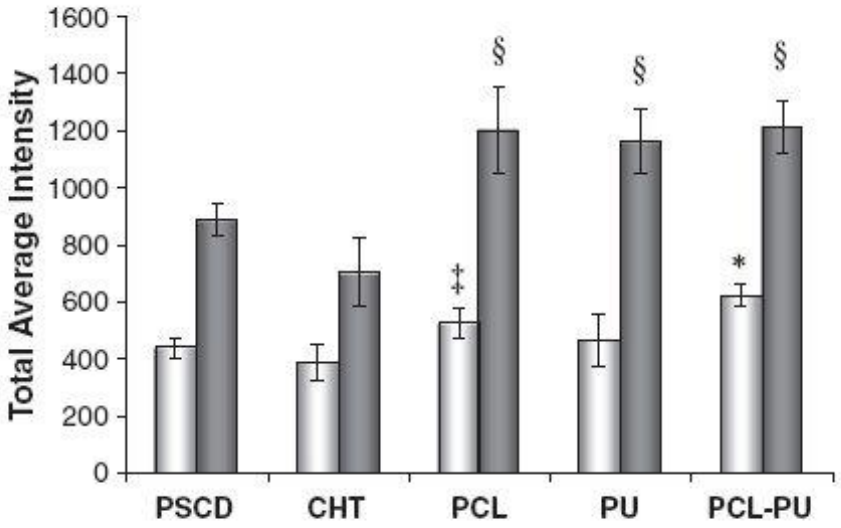

Figure 7. Fluorescence average intensity for stained synaptophysin (light bars) and βIII-tubulin (dark bars) of SHSY5Y cells at DIV6 on the different membranes. Data statistically significant according to ANOVA followed Bonferroni *t*-test; $^{*}p < 0.05$ vs all substrates; $^{\ddagger}p < 0.05$ vs CHT; $^{\$}p < 0.05$ vs PSCD and CHT

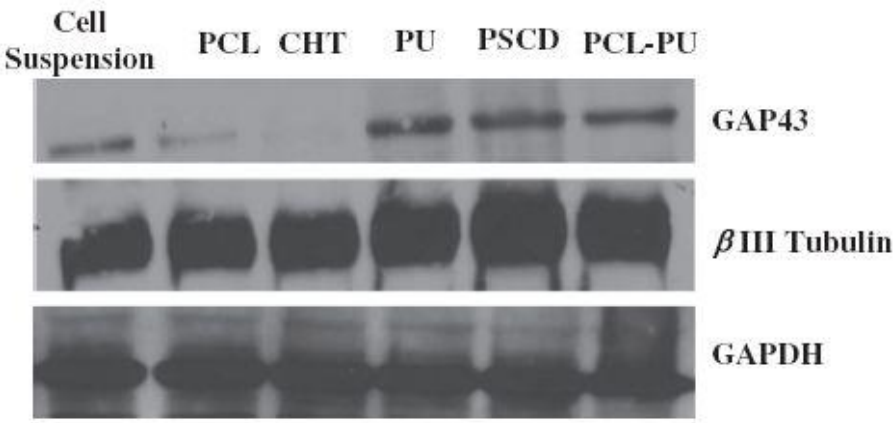

Figure 8. Western blot analysis of changes in expression of neuronal marker proteins, βIII-tubulin and GAP43, in SHSY5Y cells in culture on the different substrates at DIV6. Detection of glyceraldehyde 3-phosphate dehydrogenase (GAPDH) is shown as an internal loading control. A typical experiment representative of≥ three independent experiments is shown

References

- Belkas JS, Shoichet MS, Midha R. (2004). *Oper Tech Orthop* 14: 190–198.
- Cameron PL, Sudhof TC, Jahn R, et al. (1991). *J Cell Biol* 115: 151–164.
- Carré M, André N, Carles G, et al. (2002). *J Biol Chem* 277: 33664–33669.
- Chakravarthy B, Rashid A, Brown L, et al. (2008). *Biochem Biophys Res Commun* 371(4): 679–683.
- Chang CJ, Hsu SH. (2006). *Biomaterials* 27: 1035–1042.
- Chang CJ. (2009). *J Biomed Mater Res* A 91: 586–596.
- ChengM, Deng J, Yang F, et al. (2003). *Biomaterials* 24: 2871–2880.
- Cheung YT, Lau WK, Yu MS, et al. (2009). *NeuroToxicology* 30: 127–135.
- Ciardelli G, Chiono V. (2006). *Macromol Biosci* 6: 13–26.
- Clagett-Dame M, McNeill EM, Muley PD. (2006). *J Neurobiol* 66:739–756.
- De Bartolo L, Rende M, Morelli S, et al. (2008). *J Membr Sci* 325: 139–149.
- Evans GR, Brandt K, Katz S, et al. (2002). *Biomaterials* 23(3): 841–848.
- Evans GR. (2000). *Semin Surg Oncol* 19: 312–318.
- Evans PJ, Mackinnon SE, Levi AD, et al. (1998). *Muscle Nerve* 21(11): 1507–1522.
- Fletcher TL, Cameron P, De Camilli P, et al. (1991). *J Neurosci* 11: 1617–1626.
- Goslin K, Schreyer DJ, Skene JHP, et al. (1988). *Nature* 336: 672–674.
- Hausner T, Schmidhammer R, Zandieh S, et al. (2007). *Acta Neurochir Suppl* 100: 69–72.
- Jiang X, LimSH, Mao HQ, et al. (2010). *Exp Neurol* 223: 86–101.
- Kaplan DR, Matsumoto K, Lucarelli E, et al. (1993). *Neuron* 11: 321–331.
- Klein CL, Scholl M, Maelicke A. (1999). *J Mater Sci Mater Med* 10: 721–727.
- Knaus P, Betz H, Rehm H. (1986). *J Neurochem* 47: 1302–1304.
- Krarup C, Archibald SJ, Madison RD. (2002). *Ann Neurol* 51: 69–81.
- Kwon SE, Chapman ER. (2011). *Neuron* 70: 847–854.
- Lee HH, Yu HS, Jang JH, et al. (2008). *Acta Biomater* 4: 622–629.
- Leube RE, Wiedenmann B, Franke WW. (1989). *Cell* 59: 433–446.
- Li Q, Dunn ET, Grandmaison EW, et al. (1992). *J Bioact Compat Polym* 7: 370–397.
- Lin YL, Jen JC, Hsu SH, et al. (2008). *Surg Neurol* 70: 9–18.
- Meek MF, Varejae AS, Geuna S. (2004). *Tissue Eng* 10: 1027–1036.
- Mingyu C, Kai G, Jiamou L, et al. (2004). *J Biomater Appl* 19: 59–65.
- Mollers S, Heschel I, Damink LH, et al. (2009). *Tissue Eng* A 15: 461–472.
- Morelli S, Piscioneri A, Salerno S, et al. (2012). *J Tissue Eng Regen Med* 6: 299–313.
- Morelli S, Salerno S, Piscioneri A, et al. (2010). *Biomaterials* 31: 7000–7011.
- Nakamura T, Inada Y, Fukuda S, et al. (2004). *Brain Res* 1027: 18–29.
- Pahlman, S, Hoehner JC, Nånberg E, et al. (1995). *Eur J Cancer* 31A(4): 453–458.
- Piscioneri A, Campana C, Salerno S, et al. (2011). *Acta Biomater* 7: 171–179.
- Schnell E, Klinkhammer K, Balzer S, et al. (2007). *Biomaterials* 28: 3012–3025.
- Simpson PB, Bacha JI, Palfreyman EL, et al. (2001). *Anal Biochem* 298: 163–169.
- Stang F, Fansa H, Wolf G, et al. (2006). *Biomed Mater Eng* 15: 3–12.
- Thiel G. (1993). *Brain Pathol* 3: 87–95.
- Tos P, Battiston B, Nicolino S, et al. (2007). *Microsurgery* 27: 48–55.
- Wang B, Mao Z, Meng X, et al. (2010). *Colloids Surf B Biointerfaces* 76 (1): 38–43.

- Wang-Bennett LT, Coker NJ. (1990). *Exp Neurol* 107: 222–229.
- Weber RA, Breidenbach WC, Brown RE, et al. (2000). *Plast Reconstr Surg* 106: 1036–1045.
- WoodruffMA, Hutmacher DW. (2010). *Prog Polym Sci* 35: 1217–1256.
- Yang IH, Co CC, Ho CC. (2005). *Biomaterials* 26: 6599–6609.
- Yuan Y, Zhang P, Yang Y, et al. (2004). *Biomaterials* 25: 4273–4278.

Chapter 6

Bio-hybrid membrane system for the self-assembly process of tissue spheroids

Introduction

Classical tissue engineering approach is based on seeding cells into biodegradable polymer scaffolds or gels, culturing and expanding them in bioreactors for several weeks, and finally implanting the resulting tissue into the recipient organism, where the maturation of the new organ takes place. In truth tissues and organs are self-organizing systems, and cells exactly as polymers and macromolecules [Pohorille and Deamer, 2009] can undergo biological self-assembly without any external influence creating a self-organized microtissue. As cells divide, differentiate, and organize into tissues and organs during embryonic development, they produce a tissue-specific mixture of interconnected protein filaments, the extracellular matrix (ECM), and although overall embryonic development is a relatively slow process, certain essential morphogenetic steps and events during embryonic histogenesis and organogenesis are relatively fast. Following specific rules, genes set up the inherent physical and chemical properties of cells, extracellular matrix and tissues. These in turn generate forces, which drive structure formation and cause subsequent alterations in gene activity. It is this delicate interplay of genetic, molecular and physical factors that constitutes the evolving modern understanding of early morphogenesis [Hove et al., 2003; Farge, 2003; Forgacs and Newman, 2005; Lecuit and Lenne, 2007; Ninomiya and Winklbauer, 2008]. Though give a definition really complete is hard, the Self-organization is defined as a process in which patterning at the global level of a system emerges solely from numerous interactions among the lower-level components of the system whereas the Self-assembly is defined as the autonomous organization of components into patterns or structures without human intervention (see chapter 3). According to the last sentence, it is possible to assume that a high number of cells, placed together under specific conditions, can interact one another and reproduce a tissue. That is the reason why the last two decades witnessed the birth of a new approach in TE, and in order to reproduce the native embryonic condition during the tissue in vitro production, scaffold free methods have been designed and tested by reasearcher all around the world. The scientific base of this evolution is a recent review paper published with

the characteristic title “Cell as a material” [Kasza et al., 2007] in which is logically implied that minitissues can be used in TE applications in place of individual cells, more specifically in form of tissue spheroids, that in this way can also be considered as a material or more correctly a “living material” with certain measurable, evolving and potentially controllable material properties. Nowadays, relying on the self assembly potential of cells and their secretion of a specific extracellular matrix network, the tissue spheroids are used as building blocks for the biofabrication of three-dimensional functional living macrotissues and organ constructs, with no scaffolds or supports request. Their first application was as an in vitro 3D model system in biomedical and tumor research. More than 500 scientific articles currently describe tissue spheroids as a tumor model in drug and radiotherapy research. Nowadays a constant increasing of new applications are recorded. One of the most important example of their use as biological component in *in vitro* study is represented by the fully biological vascular tubular grafts build by Norotte et al. in 2009 through spheroids as basic components. The tissue spheroids were assembled into customized tubular structures of defined topology, and agarose rods were used as building blocks of a molding template. When agarose rods and uniform multicellular spheroids were deposited layer-by-layer, this template allowed for the accurate control of tube diameter, wall thickness and branching pattern, allowing to obtain the final graft [Norotte et al., 2009]. Spheroids have also been used to investigate neovascularization, a critical challenge in current tissue engineering. For example, human endothelial cell (EC) and smooth muscle cells (SMC) co-cultivated in a spheroid differentiate into a vascularized tissue-like organization with a polarized EC monolayer at the surface, and an underlying multilayered assembly of SMCs [Korff et al., 2001; Kelm et al., 2004]. Cytokine effects, such as granulocyte-macrophage colony stimulating factor on endothelial capillary formation can also be examined using EC spheroids [Krubasik et al., 2008]. Furthermore, a bioartificial liver (BAL) device is well known requires large quantities of viable and highly active hepatocytes. Hepatic spheroids, particularly when entrapped in collagen gel, exhibit higher and more sustained activities for a number of liver-specific functions including albumin production, urea synthesis and cytochrome P450 activity, compared to hepatocytes cultivated as monolayers [Nyberg et al., 2005; Lazar et al., 1995; Wu et al., 1995]. Primary chondrocytes situated in hydrogel coated culture vessels that prevent adhesion and thus promote the formation of a self-aggregating suspension of cells, have been used for cartilage tissue engineering approach [Mohanraj et al., 2013]. Chondrocytes cultured at high density in tissue culture vessels coated with poly 2-hydroxyethyl methacrylate (polyHEMA), within 24 hours, coalesced to form a stable

construct that remains in suspension and progressively increases in mass with time forming a cartilage-like biomass. Chondrocytes in this cartilage tissue analogs possess phenotypic characteristics and deposit ECM that is similar to native cartilage [Estrada, Dodge et al. 2001, Kim, Kraft et al. 2011] showing a good production of collagen type II and do not produce collagen type I, indicative of their differentiation to a fibroblastic phenotype [Novotny, Turka et al. 2006]. With the aim to overcome the limitations of the actual biomaterials usable for tendon repair, as lower capacity for inducing cell proliferation and differentiation, poorer biocompatibility and remodeling potentials, the development of an engineered tendon by stem cells and growth factors without exogenous scaffolds is getting really worth of attention. Engineered scaffold-free tendon tissue produced in vitro by treatment of connective tissue with growth factor (CTGF) and ascorbic acid showed after implantation in nude mice neo-tendon formation [Ming et al., 2013]. Many other previous studies demonstrate that spheroid culture provides favorable conditions for reconstruction of liver [Landry et al. 1985], pancreas [Matta et al., 1994], blood vessel [Korff et al., 1998], myocardial muscle, ganglion [Kelm et al., 2003] and bone tissue [Akiyama et al., 2006].The engineered tissue spheroids may be transplanted directly to recipients, as in the case of microencapsulated porcine hepatocyte spheroids [Ota et al., 1996], or used as a building block for tissue engineering using the organ printing technique [Mironov et al., 2003]. These findings validate the theory presented above that tissue spheroids obtained by self-assembly of cells have the potential to replace single cells as the cellular component in the current TE applications. As already said, TE scaffold-free aims to overwhelm the limitations of the classical scaffold-based approach. Biomaterials, in fact, despite their biocompatibility, biodegradability, chemical-physical and mechanical properties still faces some limitations and challenges [Khademhosseini et al., 2006; Langer et al., 2007], as for example the biodegradation control, the impossibility to use a real responsive system able to evolve with the tissue accompanying it during its development and, above all the chance to reproduce a 3D cell system even using a three dimensional scaffold. The cells in fact, in any case deposit on the biomaterial surfaces flattening themselves and decreasing the contact area between them, even in a multilayer scaffolds, where a few level of deposition is present. If we consider a cell as a body that can be flattened onto a surface, it can interact with the environment and answer to the stimuli, exposing a half part of its body to the support and the other one to the culture medium (the nutrient and the growth factors). Only the smallest percentage of the cell bodies can interact through contact with each other, not reflecting or reproducing the real complex behavior of a biological system in its proper 3D architecture. Nevertheless, despite the amazing results reached with the scaffold-free approach in TE, a lot

of critical points are recognizable. Not all the cells are able to self-assemble themselves without external stimuli, and the time requested for the spheroids to be compact enough for the handling sometime is so long to ensure the perfect vitality of the core, where eventually cells go through necrosis. As a matter of fact the "Time" is one of the most important parameter in the spheroids technology, maybe the most important one. Thus, it appears that in the near future clear pathways able to overcome the limitations for both the TE approaches will be not available. The present study, aims to combine the scaffold-based with the scaffold-free TE, trying to benefit from their advantages. In the self-assembly process, cells were obliged to reproduce, miming the embryonic evolution microtissues in form of spheroids: the use of different biodegradable polymeric membrane surfaces, could improve the vitality, and fusion process thanks to the mechanical and physical-chemical stimuli that membranes provide to the cells. The ability of cell aggregates to fuse is based on the well-known concept of tissue fluidity [Steinberg et al., 1963; Steinberg et al., 1982], according to which embryonic tissues in many respects can be considered as liquids. In particular, in suspension or on nonadhesive surfaces, various multicellular aggregates round up into spherical shape similarly to liquid droplets [Foty et al., 1996] and coalesce one into each other. This work was aimed at studying the fusion process on different biodegradable membranes with respect to an inert support, like the agarose, in order to understand if the membranes can improve the yield of the tissue formation in terms of time and morphology. Bio-hybrid membrane systems with spherical cell aggregates as biological component were then developed and investigated. Three different polymer were chosen and processed by phase inversion technique to produce flat membranes: Chitosan, one of the most natural biomaterial used for TE purposes, Polycaprolactone and Polyurethane as synthetic representatives, generally highly appreciated for the mechanical properties showed. Considering that the fusion process is depending on surface forces and also on cell receptors, cytoscheloton proteins and activators of cell adhesion characters, the effect of the membrane properties on the self-assembly process has been studied using three different types of cells: fibroblast, myoblast and neuronal cells.

Materials and Methods

6.1 Membrane preparation

Biodegradable polymeric membranes were prepared in flat configuration by phase inversion technique. Chitosan membranes were obtained by dissolving 4% (wt/v) of Chitosan powder

(75% deacetylated, Sigma, Milan, Italy) in acetic acid solution 2% (v/v). Then polyethylene glycol (PEG, Mw=6000 Da; Merck-Schuchardt, Hohenbrunn, Germany) was added to the solution at a 4:1 ratio and stirred for two hours. The solution, cast on a glass plate and molded as thin films by a handle-casting knife (Elcometer, gap set at 250 μm). After a first drying at room temperature, the membranes were immersed in a solution of 1% NaOH, and washed repeatedly with distilled water. Polycaprolactone and Polyurethane membranes were obtained in the same way, dissolving 10% and 15% (wt/wt) of PCL (Mn ~ 70,000-90,000 by GPC, Sigma, Milan, Italy) and PU (Dow Chemical Noderland BV, Deefzijl, The Netherlands) pellets, in 1,4-Dioxan (100%) and Formic acid respectively, at 50°C until complete dissolution. Once dried the membranes were washed with distilled water.

6.2 Inert Agarose mould preparation

A 2% agarose solution was prepared in a mixture of H_2O/PBS (1:1) and autoclaved to ensure the sterility and allowed to cool until 70°C are reached. A silicone stamps were transfer into a small beaker containing distilled water, bring it to a boil, and then transfer into the biological safety cabinet. A suitable volume of the agarose solution was poured into a 60 mm diameter Petri dish and the silicone stamp was slightly placed on its surface paying attention to avoid trapping air bubbles. Five minutes after the agarose gelification, the stamp was carefully removed and the Petri dish, now characterized by the presence of 100 slots, was treated with culture medium was transferred into the incubator for the conditioning.

6.3 Membrane Characterization

Dried membranes were cut and mounted with double-faced conductive adhesive tape on metal stubs, and analyzed by scanning electron microscope (SEM) (ESEM FEG QUANTA 200, FEI Company, Oregon, USA) in order to obtain information about the surface structures. The hydrophobic/hydrophilic character of the investigated membranes was estimated by the contact angle technique (CA) performed at room temperature with a CAM 200 contact angle meter (KSV Instruments, Ltd., Helsinki, Finland). Tensile properties of the polymeric films were determined using a Zwick/Roell tensile testing machine. Samples from each group of membranes were cut into strips of 5cm x 1cm and mounted between two pneumatic grips. Grip separation was set at 3 cm and a testing speed of 5 mm/min was used. The thickness of the films was measured using a micrometer before every determination. Samples were subjected to uniaxial tension until failure. Ultimate tensile strength (UTS), Young modulus

(Emod) and Elongation parameter (ε) were revealed. To evaluate the biodegradability of the three membranes, sample were cut for each one of them and immersed in a Lysozyme solution (1mgL/ml) after being accurately dried and weighted. At the end of pre-determined incubation intervals at 37°C, the samples were removed from the solution and dried in a oven until a constant weight was reached. Dissolution percentages were measure according to the following equation: % Dissolution = [$(W_o - W_t) / W_o$] *100 ; where, W_o is the starting dry weight and W_t is the dry weight at time (t). Each test consisted of three replicate measurements.

6.4 Cell cultures

The human neuroblastoma cell line SH-SY5Y (ICLCIST, Genova, Italy) was cultured in a 5% CO_2 humidified incubator with a 1:1 mixture of Ham's F12 (Invitrogen) and minimum essential Eagle's medium (EMEM) as specific culture medium, supplemented with 10% v/v heat-inactivated fetal calf serum (FCS), 2mM glutamine, 100 mg/ml penicillin–streptomycin. at 37 °C in 75cm^2 flasks (PBI International, Milan, Italy). Primary normal Human Skeletal Myoblasts (HSkM) were purchased from Life Technologies Corporation and cultured in a differentiation Medium (Gibco®) consisting of D-MEM Basal Medium supplemented with 2% Horse Serum at 37 °C in humidified incubator with 5% of CO_2. Primary fibroblasts were isolated from the longissimus muscle located on the back along the spine of a 3 weeks old pig. Two methods of isolation were used: 1) pieces of the muscle were placed in medium and the fibroblasts migrated from the explants. 2) the muscle tissue was minced and digested with trypsin. Undigested fragments were removed by fitration on tissue sieve system. The cells were then collected by centrifugation and plated in Petri dishes with DMEM as culture medium, supplemented with 10% FBS and antibiotics (100 U/mL penicillin/streptomycin) and maintained at 37 °C in a humidified atmosphere containing 5% CO_2. A suitable number of subcultures were carried forward in order to reach the required amount of cells to produce tissue spheroids. Cell cultures were washed twice with phosphate buffered saline solution (PBS, Invitrogen) and treated for 4 min with were detached by means of trypsin–EDTA solution (Sigma) and collected by centrifuge at 1500 RPM for 5 min. Resuspended in 1 mL of specific culture medium, cells were counted using a hemacytometer and a final cell suspension with the required density cells/ml was prepared for each one of them in order to get aggregates with ≈300 μm in diameter. The cell suspension was poured into the agarose mold, previously prepared, and 6-7 ml of cell culture media were slowly added into the

dishes, before being transferred in incubator for the time requested to the self-assembly process to incur. The shape of the spheroids was checked periodically, and the medium was replaced with a fresh one every day. Photographs of the spheroids were taken every day at specific set time point, depending on the observation eventually performed.

6.5 Spheroids culture on Polymeric membranes

CHT, PCL and PU flat membranes were cut in suitable shape, sterilized under UV light before being fixed on the bottom of a 12-well plates, and put for 24 h in incubator with culture media for the conditioning. In order to investigate the aggregates behavior and the fusion process rate on the three polymeric membranes with comparison to the agarose substrate, spheroids for each cell type were placed onto the four surfaces in pairs and then moved at 37 °C in humidified incubator with 5% of CO_2. In order to reproduce a statistical data, 15-18 samples were investigated in this study for each polymeric membrane and for the inert support.

6.6 Morphological analysis

Morphological evaluation of the spheroids shape, diameter and fusion process in time were performed to highlight possible differences due to the different biodegradable polymeric membranes influence with respect to the inert agarose substrate. Light optical microscopy and a personal computer were used for taking and analyzing the pictures. Changes in diameter of the tissue spheroids were recorded every day and analyzed using a MatLab program especially designed. At least 20 single spheroids on each support were photographed and their diameters measured. To evaluate and quantify the fusion process for every typology of spheroid pictures were taken every two hours, and in order to highlight the physiological cellular movement, being a tissues comparable to a fluid structure, the PKH26 Red Fluorescent Cell Linker and the PKH67 Green Fluorescent Cell Linker Kit for General Cell Membrane Labeling (Sigma-Aldrich, Saint Louis, MO, USA) were used. Two cell suspensions were washed with PBS 1X and after centrifugation, separately treated with the green and the red dyes. Four-five minutes of incubation at 37°C, were enough to completely label the cells, which with the same technique described above were poured onto the agarose mold and let aggregate. Again, pairs of spheroids were placed onto the membranes and the agarose and the fusion process were revealed through laser confocal scanning microscope (LCSM; Fluoview FV300, Olympus, Milan, Italy).

6.7 Fusion process rate evaluation

Light microscopy images taken at 10X of magnification were used to measure the average radii **R** in μm of the pair spheroids at specific time points and the "instantaneous radius" **r** of the circular interfacial area of the fusing spheroids, representative of the amount of fusion reach by the pairs in time. The ratio between r and R was plotted as function of time according to the function

$$\frac{r}{R} = 1 - b\, e^{-\frac{t}{\tau}}$$

in order to evaluate the quantitative expression of the τ values, idex of the reached complete fusion in terms of time and then representatives of the fusion process rate.

6.8 Glucose consumption and Lactate production

Samples of the culture media were collected from each sample in microtubes and stored at −20 °C until assayed. The glucose concentration in the medium was detected using the Accu-Chek Active device (Roche Diagnostics, Monza, Italy). The lactate content was determined by using the lactate oxidase enzymatic assay Lactate Dry-Fast (Sentinel, Milan, Italy) and quantified by spectrophotometer analysis. A statistical analysis of the experimental results was performed.

6.9 Oxygen permeation and central hypoxia evaluation in tissue spheroids

Pimonidazole hydrochloride (Hypoxyprobe-1, Natural Pharmacia, Inc., Belmont, MA) was used as a hypoxia marker to evaluate hypoxic regions in the spheroids. At specific time intervals, determined depending on the length of the experimentation, the culture medium for each samples were exchanged with a fresh one containing 200 mM Hypoxyprobe-1 for 2 h at 37°C. The spheroids were then rinsed three times with PBS, before being collected and fixed in 4% paraformaldehyde in PBS for 4 h. Sections of the spheroids were obtained through a cryostat and the slides relative to the center of each samples were mounted onto silane-coated slides and stained with hematoxylin-eosin (HE). Photographs were taken with a light microscope.

Results

The SEM images showed as all the polymeric membranes produced are perfectly homogeneous. In particular CHT (fig. 6.1a) and PU (fig. 6.1c) membrane surfaces appeared to be homogeneous with nano pores regularly distributed over the surface. Characteristic pentagonal microstructures are clearly visible and well distributed in a repetitive pattern on the PCL surfaces (fig. 6.1b). Table 6.1 summarize biodegradable polymeric membrane characteristics. The dynamic water contact angle measurements showed a hydrophilic character for all the membranes, being the values recorded smaller than 90° [Van Oss et al., 1985], and the CHT membranes above all resulted as the most hydrophilic substrates, (66° ± 0,25); the synthetic biodegradable polymer membranes, PU and PCL, exhibited values closed to 70–77°, with a resultant lower hydrophilic properties. The dissolution profiles of all the membranes in Lysozyme solution are showed in fig. 6.2. The three polymeric membranes showed different behaviors up to 32 weeks of treatment. As expected, the CHT, resulted to be completely degraded in only four weeks, on the other side the synthetic polymers reached values equal to 40% and 64% for PU and PCL respectively, quite higher with respect to the natural polymer. Worth of notice is that an appreciable mass loss for the Polycaprolactone samples appeared only after 15 weeks of treatment, doubling its value just towards the end, whereas the Polyurethane sample, since the 7^{th} week, maintained constant its weight loss in time, decreasing its dissolution percentage of the 10% in the final stage. In order to develop new bio-hybrid system for reconciling the TE scaffold-based and scaffold-free approaches, knowing the mechanical properties of the polymeric membrane produced is of high importance. The mechanical properties in terms of ultimate tensile strength (UTS), Young's modulus (E mod) and elongation parameter (ε) are reported in table 6.1. Results showed that for the two synthetic membranes PCL and PU, the values of Young's modulus and UTS were lower than the CHT that showed a superior stiffness, as result of their higher mechanical strength and elasticity, particularly reflected by the values recorded for the elongation parameter. PCL membranes in particular reached the highest values between the three samples. Image 6.3 showed the results of the self-assembly process of cells in the inert environment given by the agarose mold. Clearly, a unique structure is obtained with all the cells used, neuronal cell, fibroblasts and myoblats; they after the deposition gravity-mediated to the bottom of each slot of the mold, immediately start to interact each other, compacting and re-arranging in the three-dimensional structure desired. The time requested by cells to produce spheroids strong enough to be handy were for all the samples about two days, but it

was clear how the different physiology of the three types of cells affect the final aspect of the spheroids obtained. Fibroblasts and Skeletal myoblasts resulted in more compact spheroids, with nearly a perfect round shape (fig. 6.4a -1h) and easier to be handle, in comparison the produced neural cells spheroids presented some differences in the final diameters and shape, not perfectly regular. All the cells used in this work to produce spheroids, possess excitable properties, as well known on the basis of their physiological answers, but the specific contractility of fibroblasts and myoblasts cell lines induce results in a more homogeneous and compact final tissue and as consequence the phenomena of shrinking made the final construct nearly comparable to a sphere. Closely placed neuroblastoma, fibroblast and myofibroblast tissue spheroids go through the fusion process. The time requested to reach the complete fusion of two spheroids at once appeared to be different for the three cell lines. A nearly perfect fusion was recorded about in 3 days for the fibroblast and the myoblast tissue spheroids, whereas for the SH-SY5Y samples, the effective time needed for obtaining a new construct and conclude the investigation was around a whole week (fig.6.4 a-b-c). The quantification of the fusion rates of the spheroids on the four substrates used was then computationally done, and the results were statistically elaborated in order to highlight possible differences between the polymeric membranes and the agarose substrates. The MatLab program used allow to quantify the radii of the spheroids and the width of the contact area created between them as they change in time using the pictures taken with the light microscopy. Relating these two parameters as function of the time, a fusion process profile for each pair analyzed can be obtained. The exact moment in which the fusion process ends and the dynamic equilibrium state of the tissue spheroids is reached, in the graph is depicted a plateau line, represented quantitatively by the τ values expressed in hours, evidence that the cells are not moving round through the spheres and not more mixing together in the new construct. To visualize clearly this movement, a general label of the tissue spheroids were done. A green and a red spheroids were placed near each other on the four substrates, and at the same condition as presented before, the fusion process was observed. Representative images are show if fig. 6.5. A the initial stage, the two dyed spheroids were not fusing, and a defined distinction between the colors were possible (fig. 6.5a). In time, the fluid structure of the tissue, allow to cells to move in the spheroids and a mixture of the dyed cell is clearly visible (fig. 6.5b). Eventually, as expected the two color are not separated each other, evidence that the fusion process not only is ended but that the cells are perfectly mixed together (fig. 6.5c). As expected, independently from the nature of the tissue spheroids, all the fusion rate values recorded with the biodegradable membrane used are statistically significant

with respect to the agarose (table 6.2). When each system was singularly analyzed, differences have been revealed between the polymeric membranes. For the SH-SY5Y tissue spheroids the higher fusion rate was detected on the CHT membranes (τ = 28 h), and the data were statistically significant versus not only the agarose inert substrate (τ = 164 h; τ = 65 h and τ = 60 h for neural, fibroblast and myoblast spheroids respectively), but even to both the synthetic membranes. Worth of attention is the significance recorded for the PU membranes (τ = 49 h) versus the Polycaprolactone; the PCL membranes in fact resulted to be the substrate that less affect the tissue fusion process (τ= 65 h). On the other side, for both the fibroblast and the myoblast tissue spheroids, the trend followed by the fusion process is completely reversed. These two contractile cell lines, and then the tissue they are able to create through self-assembly process, are highly affected by the elasticity of the biomaterials used as support. The faster fusion process were recorded on the PCL membranes (τ = 26 h for fibroblast spheroids and τ = 39 h for myoblast spheroids) that showed, as already said, the higher elongation parameters (231%) and the slower one on the natural CHT membranes (τ = 49 h and τ = 50 h for fibroblasts and myoblasts spheroids respectively), with the lower mechanical strength. In that case too, the values obtained for the faster fusion rate, specifically on the PCL membranes, were statistically significant versus the agarose and the other membranes used. These data reflect proportionally the values of the elongation parameter recorded for the membranes: higher elastic properties correspond to slower fusion processes when the neural cells are involved, and to the fastest ones with tissue spheroids possessing contractile properties. Table 6.2 shows the fusion process rates of the tissue spheroids in relation with the elongation parameters of the biodegradable polymeric membranes used in this work. As evident from the pictures, independently on the cell line used, the tissue spheroids reached a more compact and a better defined final structure on the polymeric membranes with respect to the agarose. In particular, it is worth of notice how the fibroblast tissue spheroids appeared to be nearly perfectly spherical when placed on the more elastic substrate, which means the PCL biodegradable membranes (fig. 6.4b -60h). The trends of the fusion process of a pair of tissue spheroids, were reported, as function of time in fig.6.6a-m. The glucose consumption and lactate production were measured and normalized by the amount of cell present in culture. The glucose consumption and lactate production rate were closely correlated. The glucose consumption for the SH SY Y5 spheroids (fig. 6.7) increased during the days on all the polymeric membranes, with data statistically significant with respect to the value recorded at 24 hours. The exception is presented by the agarose support, where after a considerable increase in glucose consumption at 24 hours of culture, a statistically significant decrease of

the values was detected. Same trends and same statistical significance were revealed for the lactate production (fig. 6.9). For the myoblast spheroids too, an increasing in time of the glucose consumption (fig. 6.8) and lactate production (fig. 6.10) values were detected. On the agarose support, in that case no changes of values in time were recorded, and all the data obtained for the polymeric membranes were statistically significant in time and versus the agarose. However, the lower rate of lactate production measured for all the bio-hybrid systems investigated, suggested that the culture conditions were good, and that the oxygenation level is enough to ensure a good viability and biological activity for the spheroids. These data are also confirmed by the analysis of the oxygenation conducted with the use of the hypoxyprobe. The oxygenation status of the spheroids was examined through light microscopy of slides treated with HE counterstaining for the hypoxyprobe-1a. It has been reported that 2-nitroimidazole derivatives are selectively reduced at a partial pressure of oxygen lower than 10 mmHg and is only metabolized in viable cells [Krohn et al., 2008; Asthana and Kisaalita et al., 2012]. Then hypoxyprobe (pimonidazole hydrochloride), can be used for the detection of hypoxic cells in the spheroids and to check the necrosis state of the system. Hypoxic regions were found to be distributed in the center of the spheroids, and as expected their area increased with the time of culture. Images taken with light microscopy (fig. 6.11) highlighted the absence of necrotic regions in the myoblast spheroids at 24 fours of culture. Firsts evidences of hypoxia appeared at 48 h and in the following 12 h of experimentation. Reflecting the glucose consumption, lactate production and fusion rate, the higher percentage of necrosis were recorded for tissue spheroids placed on AG support, CHT, PU and PCL membranes. Concerning the SH-SY5Y spheroids, the hypoxic level were detected every two days, in order to cover the week requested by the fusion process to reach the end. The brown area, index of the necrotic region in the spheroids, appeared to be really pronounced on the AG samples at day 3, and a remarkable increase was clear in the following 5 and 7 days of culture. The same trend was detected for the polymeric membranes, but as expected the percentage of hypoxia and necrosis are sensibly lower reflecting again the fusion process rate and the biological activity specifically in the order PCL > PU > CHT systems.

Discussions

Tissue fusion is in essence a phenomenon of fluid mechanics driven by surface tension and mechanical forces and can be adequately explained by physical laws and Malcolm Steinberg's "differential adhesion hypothesis" [Steinberg et al., 1963,1970,1982,1994]. Closely placed

tissue spheroids undergo to tissue fusion in a process that represents a fundamental biological and biophysical principle of developmental biology-inspired directed tissue self-assembly. Direct contact of adjacent tissue spheroids in a permissive environment is an essential precondition for tissue fusion driven process of macrotissue construct self-assembly. Fusion is sometimes defined as “melting together”, which is logically implying the liquid nature of the fusion process. It has been shown that the kinetics of tissue fusion of two rounded embryonic heart cushion tissue explants placed in a hanging drop fits perfectly to fusion kinetics described for two droplets of fluids. Moreover, based on direct measurement of surface tension and calculation of viscosity, tissue spheroids are indeed fluid-like structures [Wilson and Boland, 2003]. Thus, depending on the nature of the cells used for spheroids formation, the tissue resultant from the fusion process can show different properties and functionalization. If these results are easily comparable with an in-vivo system, being the fusion process generally studied in TE scaffolds-free system, in truth the rate of the fusion process can not be really validated. The absence of an environment able to sustain the cells answers, even temporarily, can reproduce the embryonic development of a tissue but not reflect the real time requested by the same structures to reach the maturation and the functionalization, that means no prediction can be done on the viability of cells constitutive the spheroids if the maturation of the construct required a long time to be completed. Otherwise, the classical scaffold based TE approach is not able to reproduce the 3D living condition necessary for the engineering of an organ mimic. Aim of this work was then, to reconcile the two approaches, using tissue spheroids as biological elements of the system instead of the individual cells, and Chitosan Polycaprolactone and Polyurethane biodegradable polymeric membranes as substrates for sustaining the fusion process. The observations resulted from the fusion process rate, the biological activity and the level of necrosis hypoxia-induced evaluation in the spheroids highlights how the properties of the polymeric membranes influence the tissue behavior during its formation. With data statistically significant, not only the fusion rate is faster in presence of a reacting substrate with respect to the agarose support, well known to be inert, but the amount of the same fusion is directly proportional to the mechanical properties of the biodegradable polymeric membrane used. As extensively reported in literature, the elasticity degree of a biomaterials affect the cells behavior coordinating their proper mechanical features. Tissue spheroids obtained by fibroblast and myoblast cell lines, being highly contractile, underwent to a faster fusion and maturation on the synthetic polymeric membranes, with a trend proportional to the elongation parameter value. Polycaprolactone membranes resulted to be the best biomaterial

in order to sustain the fusion process and the maturation of tissue spheroids with elastic properties. On the other side, tissue spheroids of neural cell, appeared to be able to fuse with high rate on stiffer polymeric substrate, in our case represented by the CHT membranes. All the cells are able to express with their genetic profile the protein α-actin, responsible of a few physiological processes, comprise the factor release process, the vesicle movement in the cell body and so on, but a specific isoform of this protein is responsible of the contractile movement of tissue like muscle in every form in collaboration with the protein myosin. The isoform α1-actin has recognized to be expressed only in the cell with contractile ability [Johnson et al., 2006; Database for gene expression analysis]. It is, in fact, responsible for the contraction properties of the muscle and the muscle-like tissues, and its reported being expressed by the fibroblasts and the myoblasts, and not by the neural-like cell line SH-SY5Y used for this work. The presence of this particular protein involved in the physiological contractile behavior is probably responsible of the different answers between the neural and the muscle spheroid in terms of faster fusion rate and contraction. As a results, myoblasts and fibroblasts undergo to a faster fusion process a rounder shape on the elastic polymeric membranes (PCL) with respect to the stiffer one (CHT). The higher biological activity of the cells involved in the tissue fusion process on the biodegradable membranes, expressed in terms of glucose consumption and lactate production was also the evidence of a better tissue answer if a bio-hybrid system is used instead of a scaffold-free one. Data perfectly matching with the hypoxia analysis conducted on fusing tissue spheroids.

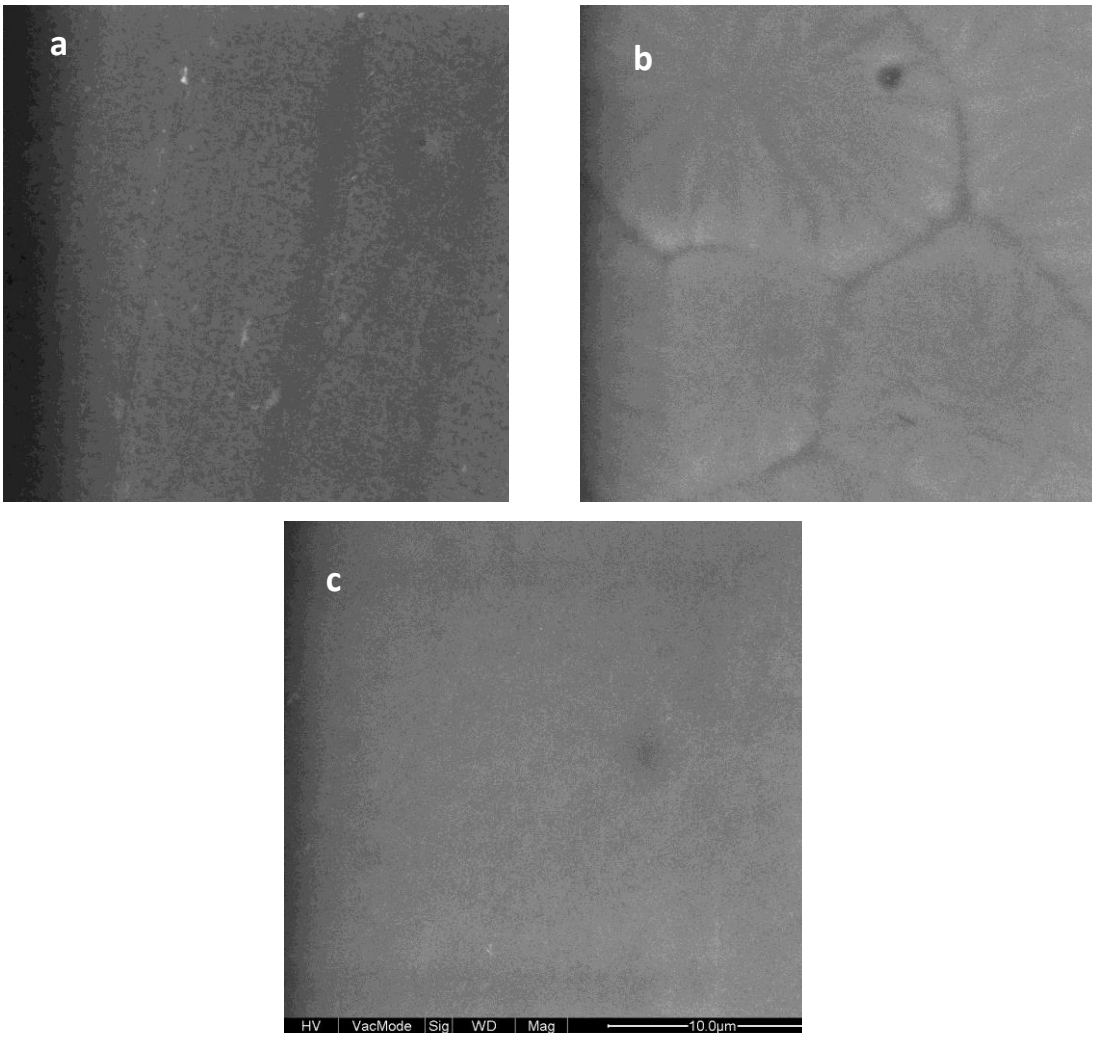

Fig. 6.1 SEM images of the biodegradable polymeric membrane surfaces a) CHT membrane, b) PCL membrane and c) PU membrane

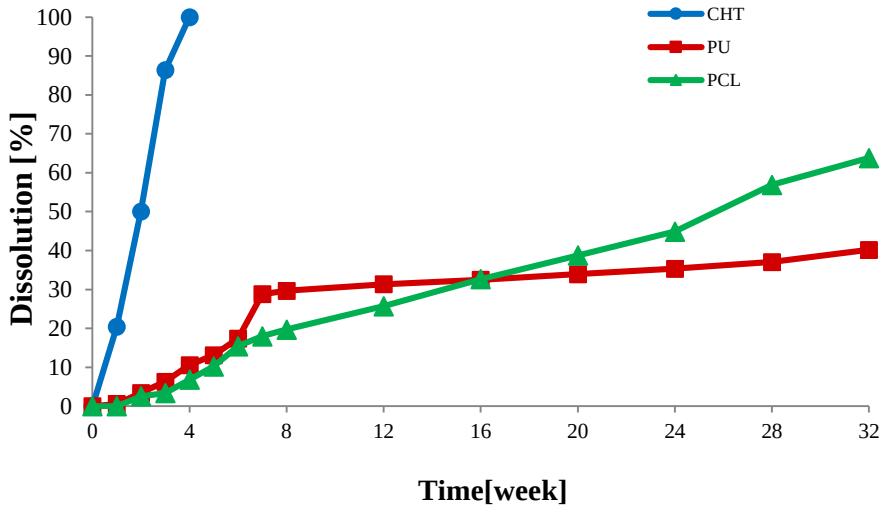

Fig. 6.2 Biodegradation profiles of the polymeric membranes developed CHT (blue), PCL (green) and PU (red)

Membrane	*Thickness [µm]*	*Mean Pore Diameter [µm]*	*E [MPa]*	*ε [%]*	*UTS [MPa]*	*WCA [°]*	*Bio-Degradation [32 weeks]*
PCL	**8±1**	**0,024**	**208±28**	**321±100**	**20±3,6**	**70±1,42**	**64 %**
CHT	**5±0,9**	**0,026**	**2288±405**	**9±2,5**	**79±12**	**66±0,25**	**100 % ***
PU	**19±1,9**	**0,082**	**35±9**	**42±9**	**8±1,5**	**77±2,17**	**40%**

Table 6.1 Polymeric membranes properties

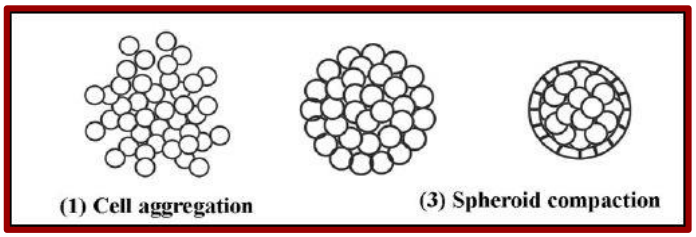

Fig. 6.3 Schematic representation of the self-assembly process of cells in a inert environment

Agarose

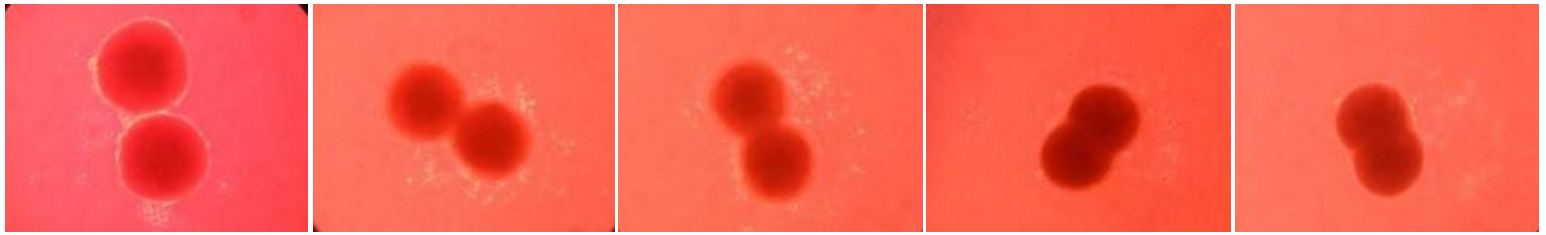

Chitosan membrane

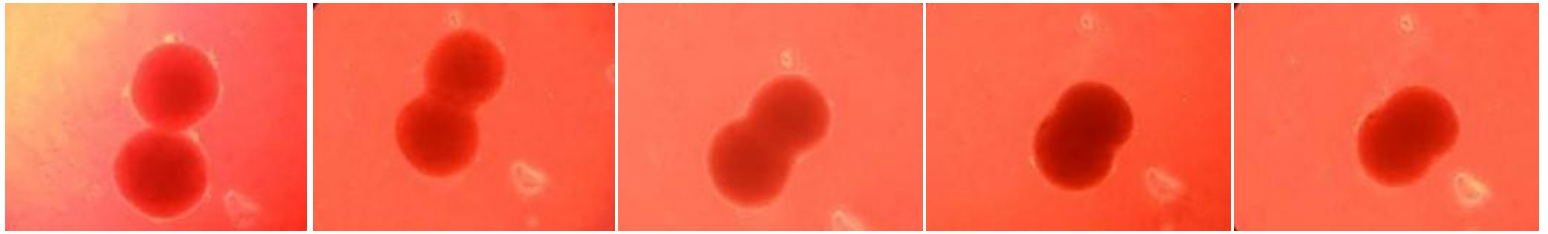

Polycaprolactone membrane

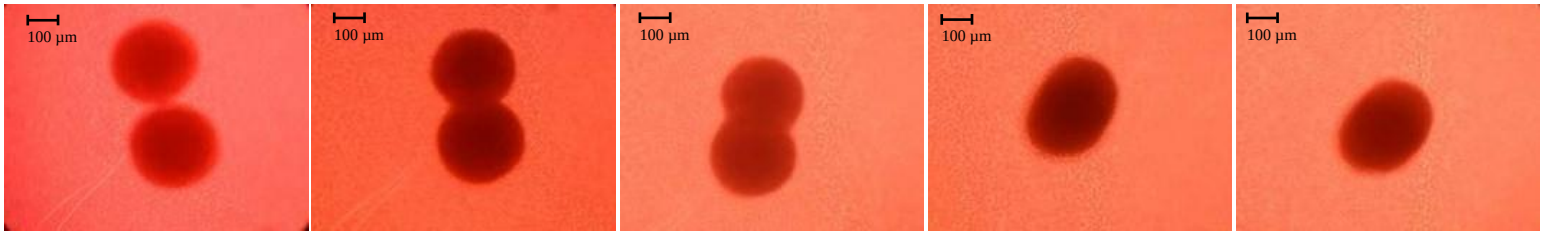

Fig. 6.4a Light images of the fusion process of Fibroblasts tissue spheroids

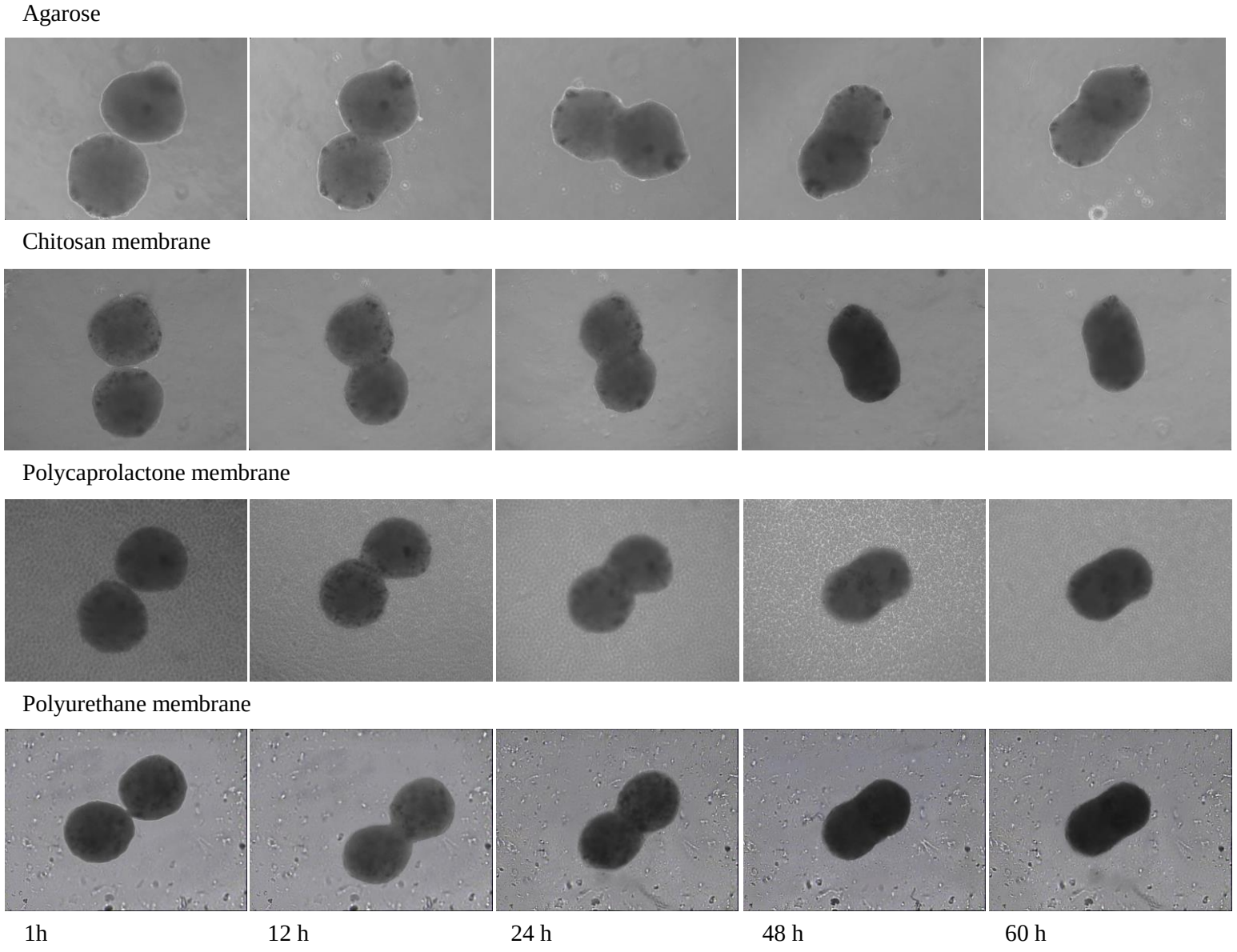

Fig. 6.4b Light images of the fusion process of Myoblasts tissue spheroids

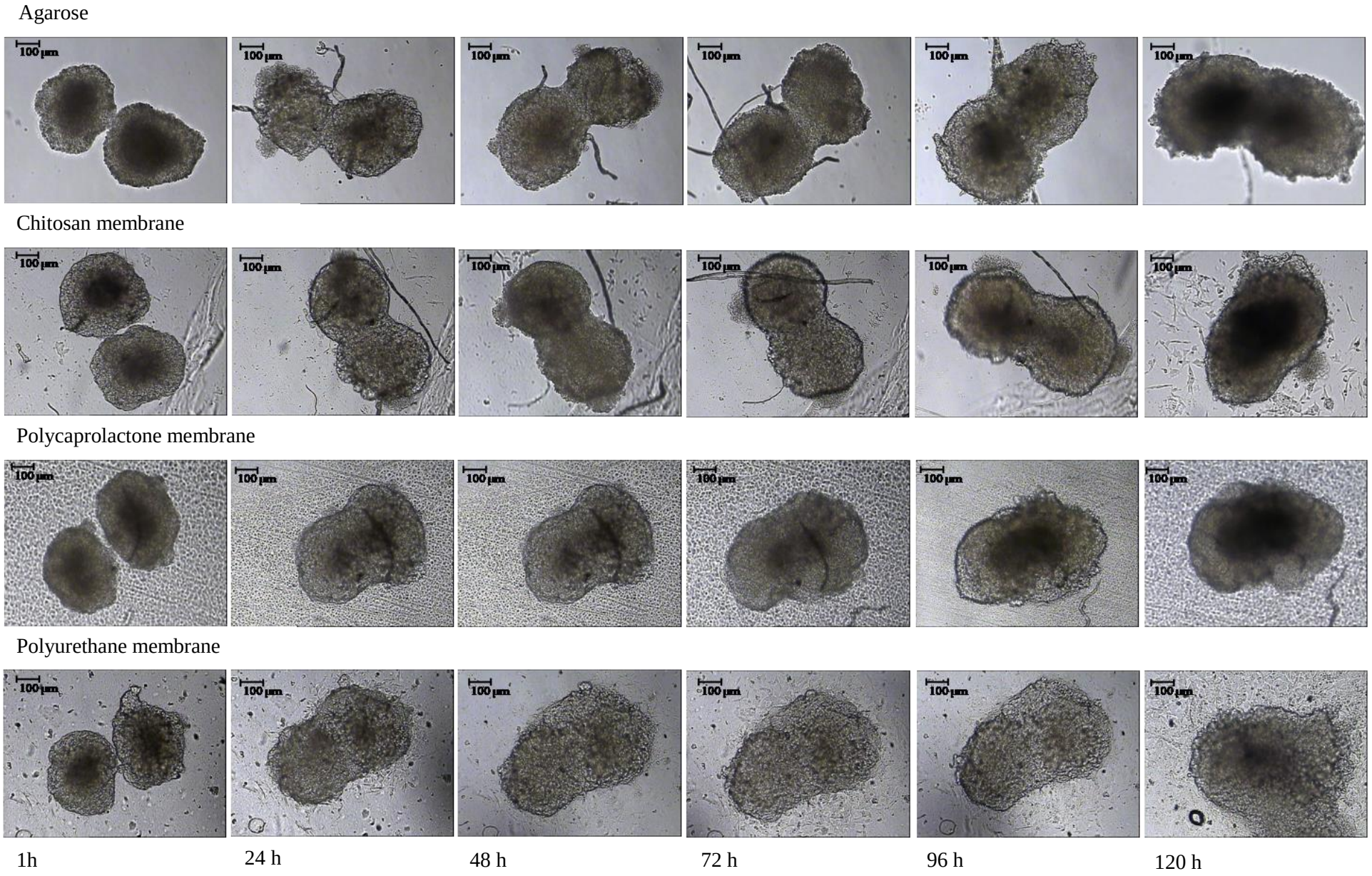

Fig. 6.4c Light images of the fusion process of SH-SY5Y tissue spheroids

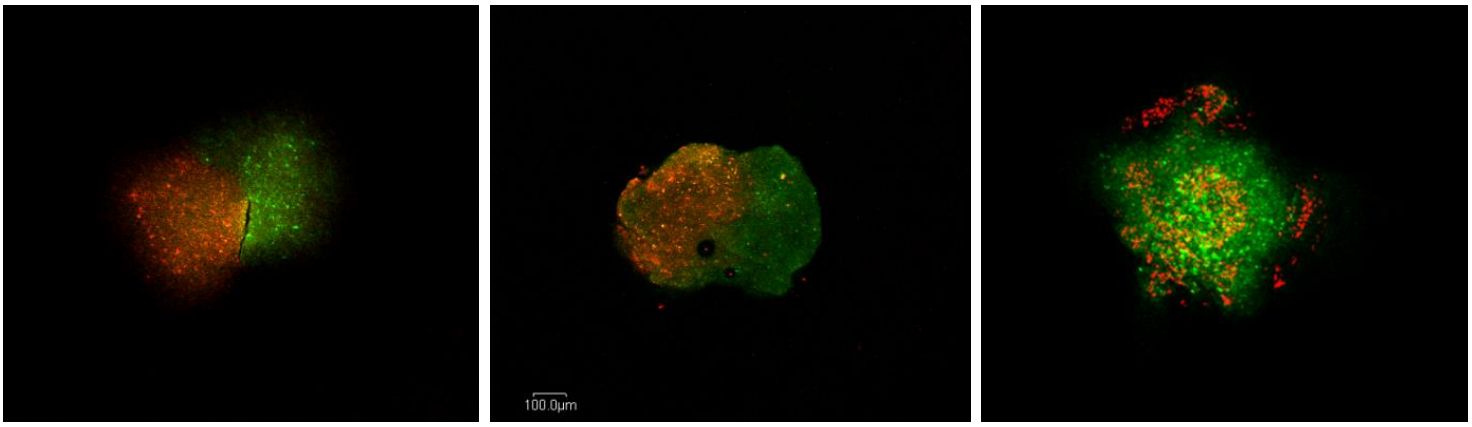

Fig. 6.5 Confocal images of a pair of tissue spheroids fusing on PCL membranes at a) 6 h; b) 24 h and c) 48 h. The green and red spheroids fuse together mixing their cells, as expected according to the tissue-dynamic fluid-like

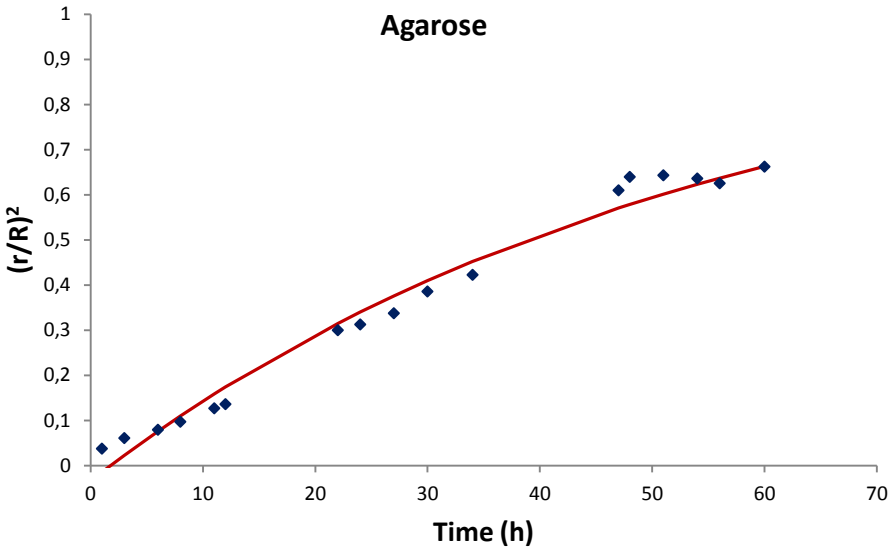

Fig. 6.6 a Trend of the fusion process of Fibroblast spheroids on agarose support

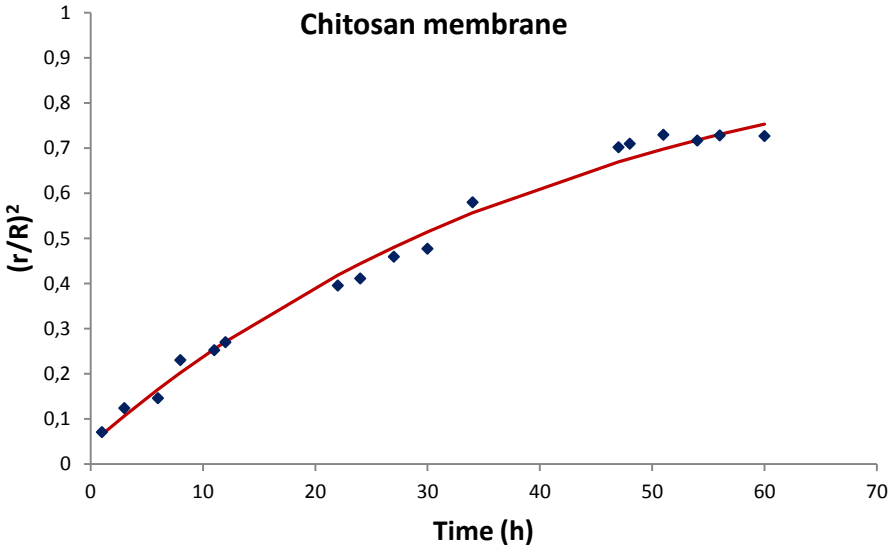

Fig. 6.6 b Trend of the fusion process of Fibroblast spheroids on Chitosan membrane

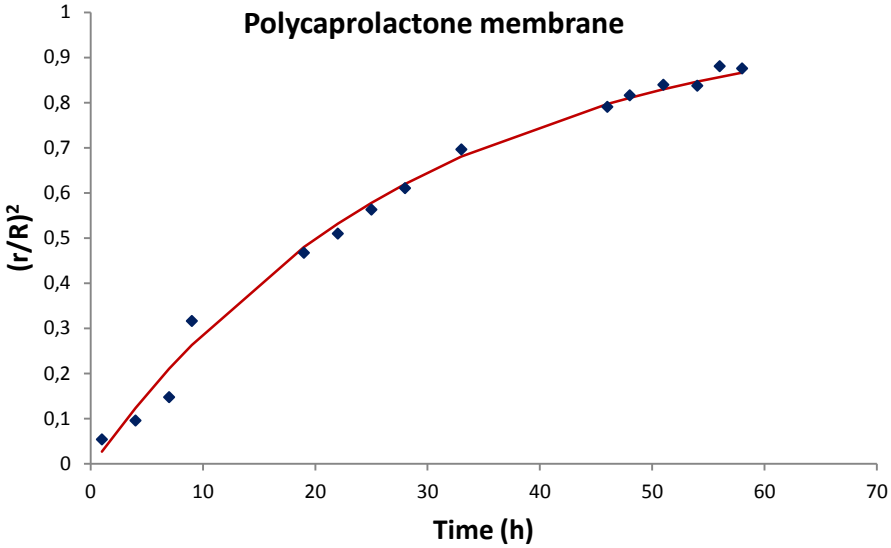

Fig. 6.6 c Trend of the fusion process of Fibroblast spheroids on Polycaprolactone membrane

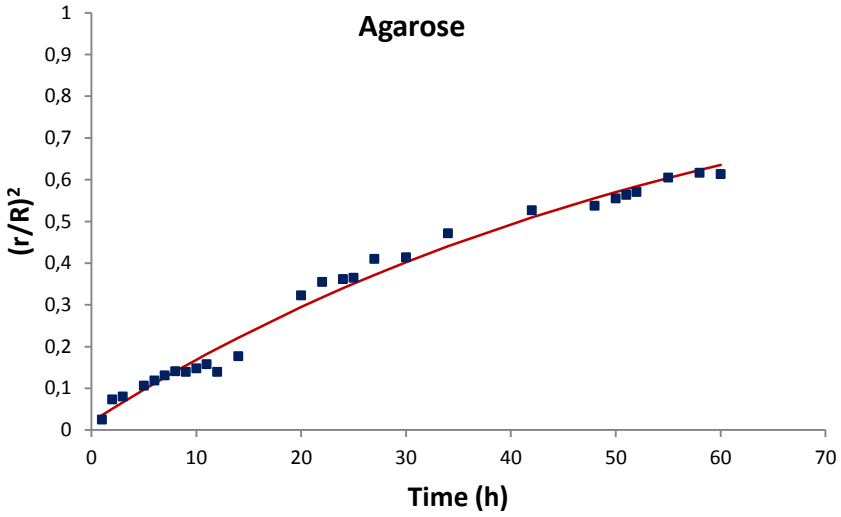

Fig. 6.6 d Trend of the fusion proces of Myoblast spheroids on agarose support

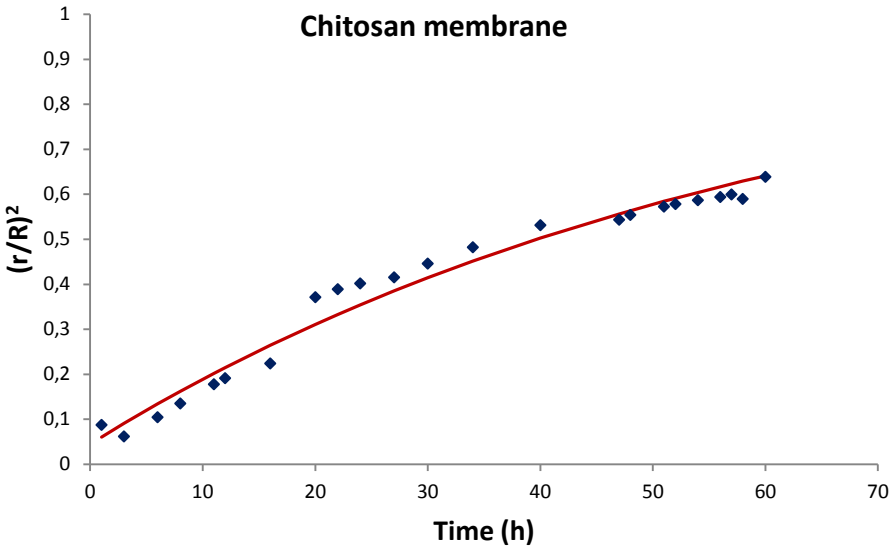

Fig. 6.6 e Trend of the fusion proces of Myoblast spheroids on Chitosan membranes

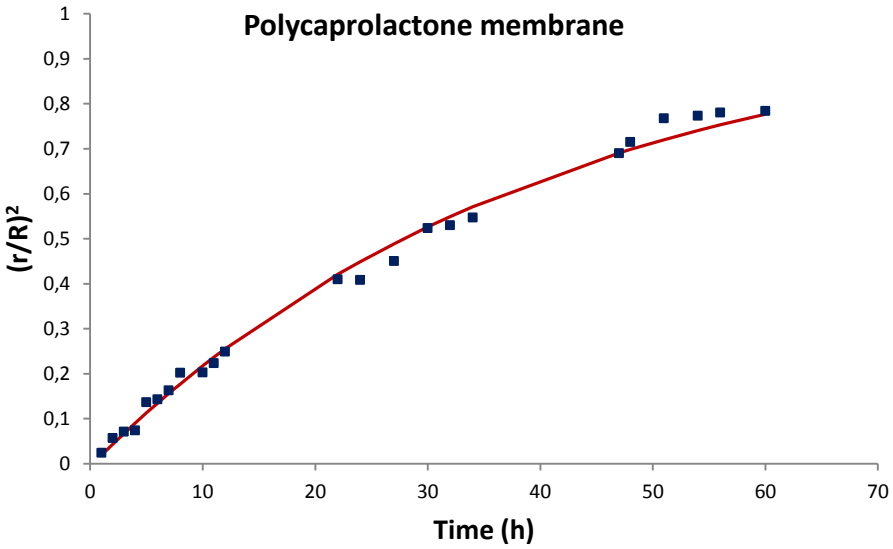

Fig. 6.6 f Trend of the fusion process of Myoblast spheroids on Polycaprolactone membranes

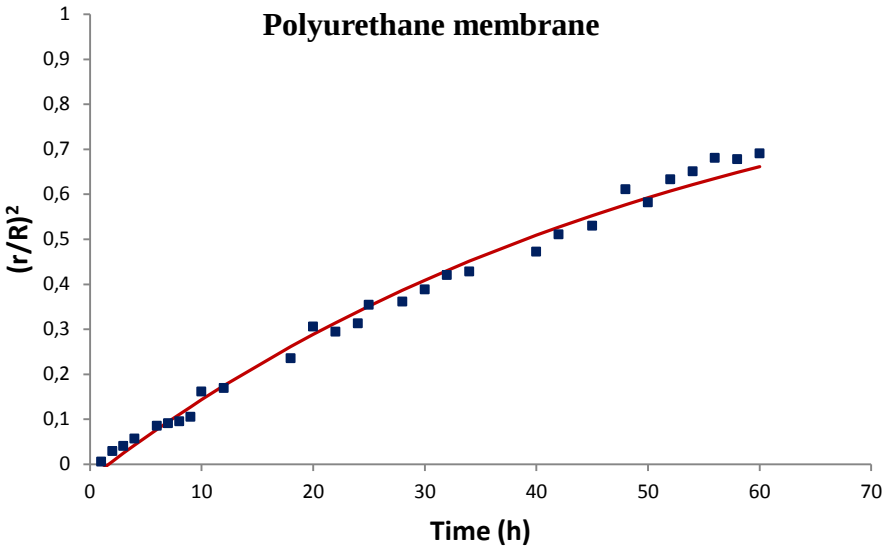

Fig. 6.6 g Trend of the fusion process of Myoblast spheroids on Polyurethane membranes

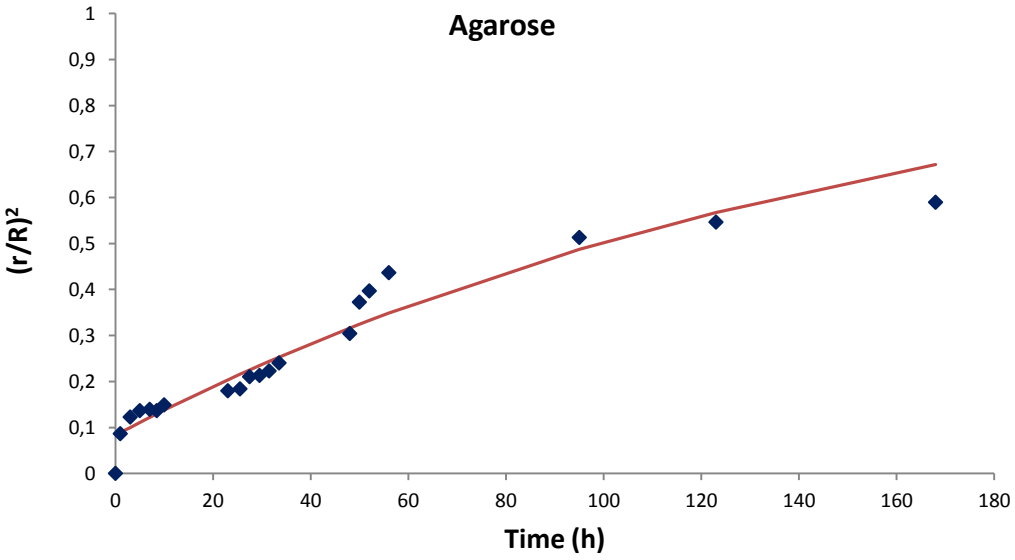

Fig. 6.6 h Trend of the fusion process of Neural spheroids on Agarose substrate

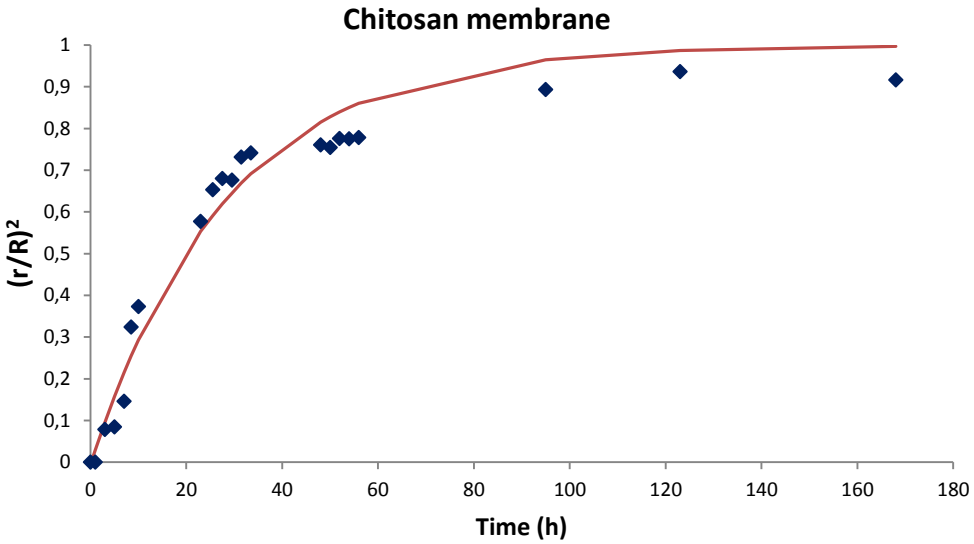

Fig. 6.6 i Trend of the fusion process of Neural spheroids on Chitosane membranes

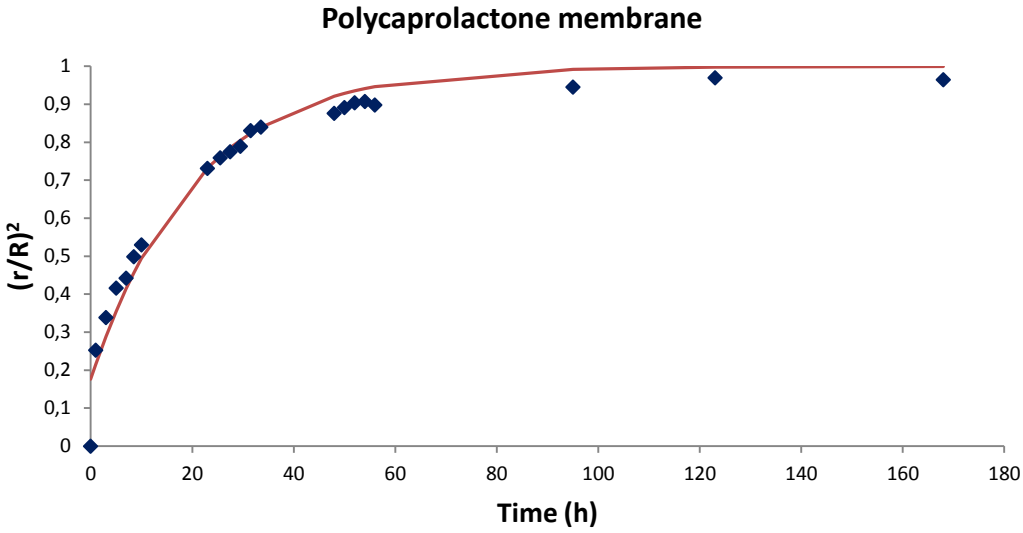

Fig. 6.6 l Trend of the fusion process of Neural spheroids on Polycaprolactone membranes

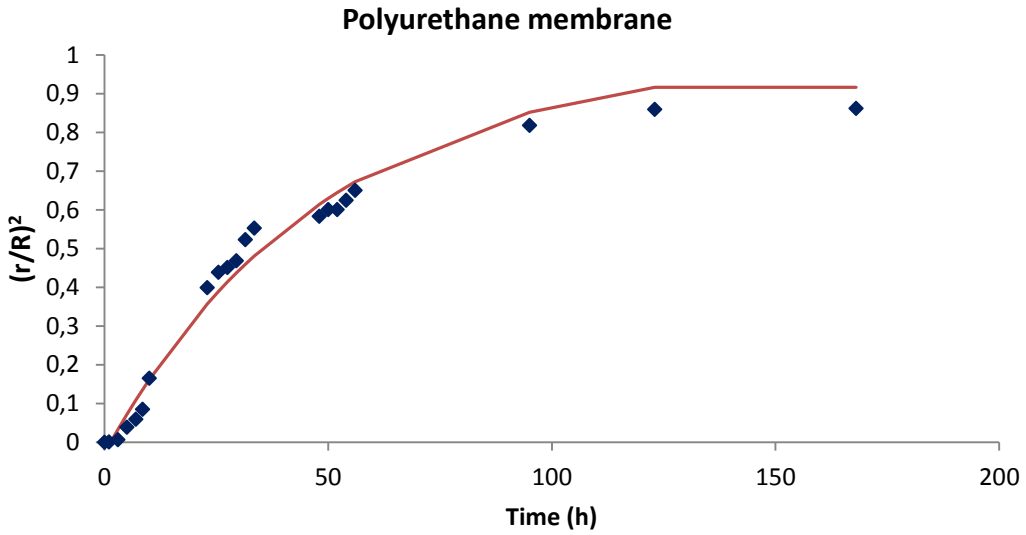

Fig. 6.6 m Trend of the fusion process of Neural spheroids on Polyurethane membranes

	ε%	SH SY5Y τ[h]	Fibroblast τ[h]	Myoblast τ[h]
Ag		164 ± 20	65 ± 2	60 ± 3
(CHT)	9 ± 2,5	28 ± 2	49 ± 4	50 ± 2
(PU)	42 ± 9	49 ± 3		41 ± 3
(PCL)	231 ± 100	65 ± 2	26 ± 2	39 ± 1

Table 6.2 τ values expressed in hours elaborated for the tissue spheroids on the different substrates used, in relation with the elongation parameters of the polymeric membranes.

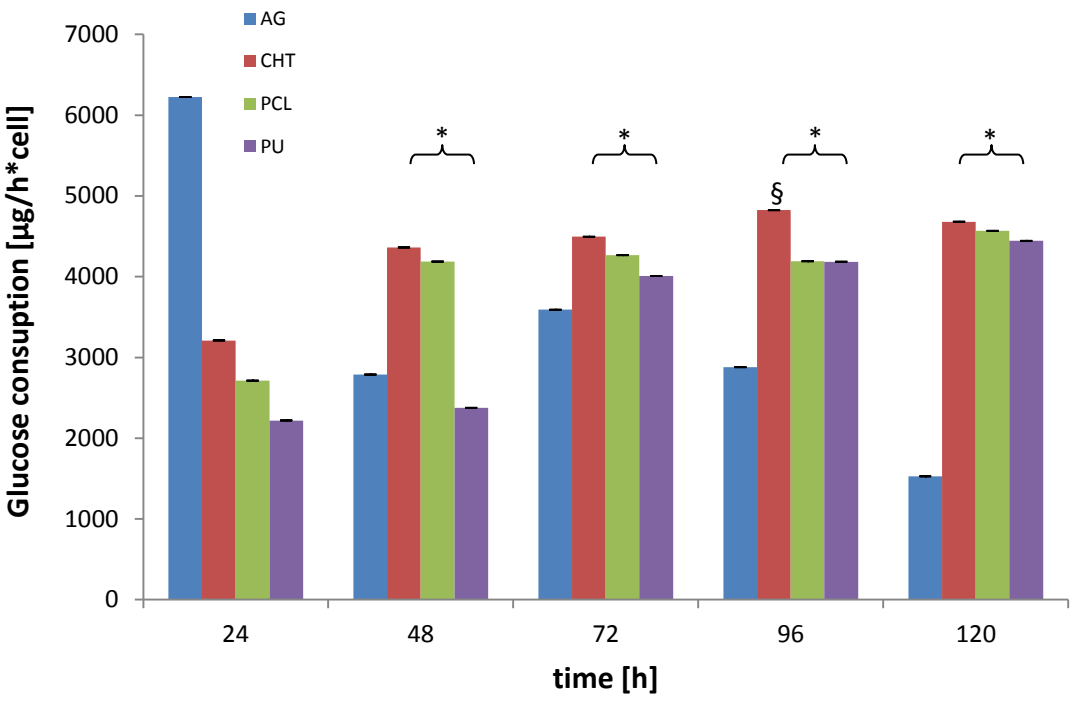

Fig 6.7 Glucose consumption of the SH-SY5Y spheroids on the agarose, CHT, PCL and PU substrates. The data were expressed as average SD and evaluated according to ANOVA, followed by Bonferroni t-test; *p<0.05 vs AG at 48,72,96,120h and vs CHT, PCL and PU at 24 h; §p<0.05 vs PCL and PU at 24,48,72,96 and vs the same substrate at 24, 48, 72h;

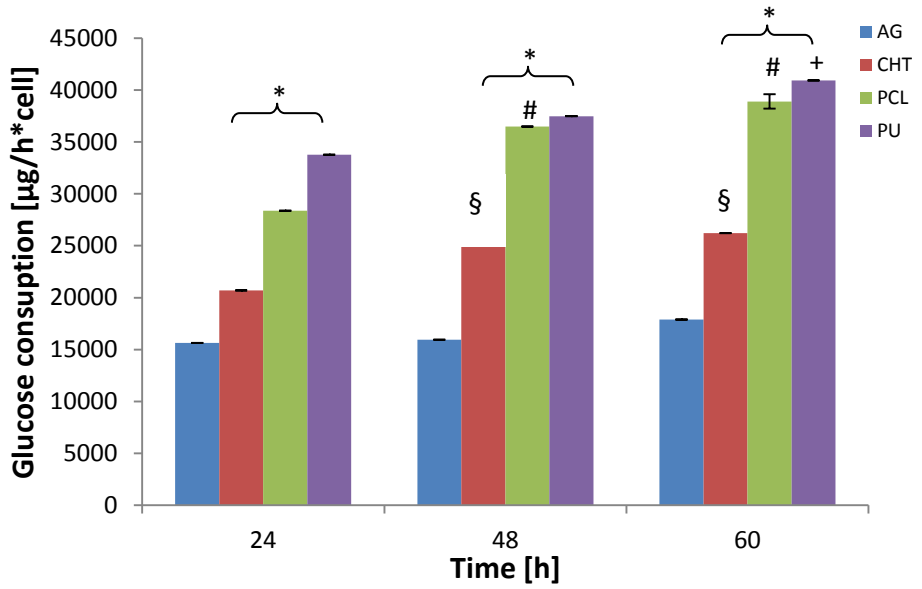

Fig 6.8 Glucose consumption of the Myoblast spheroids on the agarose, CHT, PCL and PU substrates. The data were expressed as average SD and evaluated according to ANOVA, followed by Bonferroni t-test; *p<0.05 vs AG at 24,48,60; §p<0.05 vs CHT at 24 h; # p<0.05 vs PCL and CHT at 24 h; + p<0.05 vs PU at 24 h

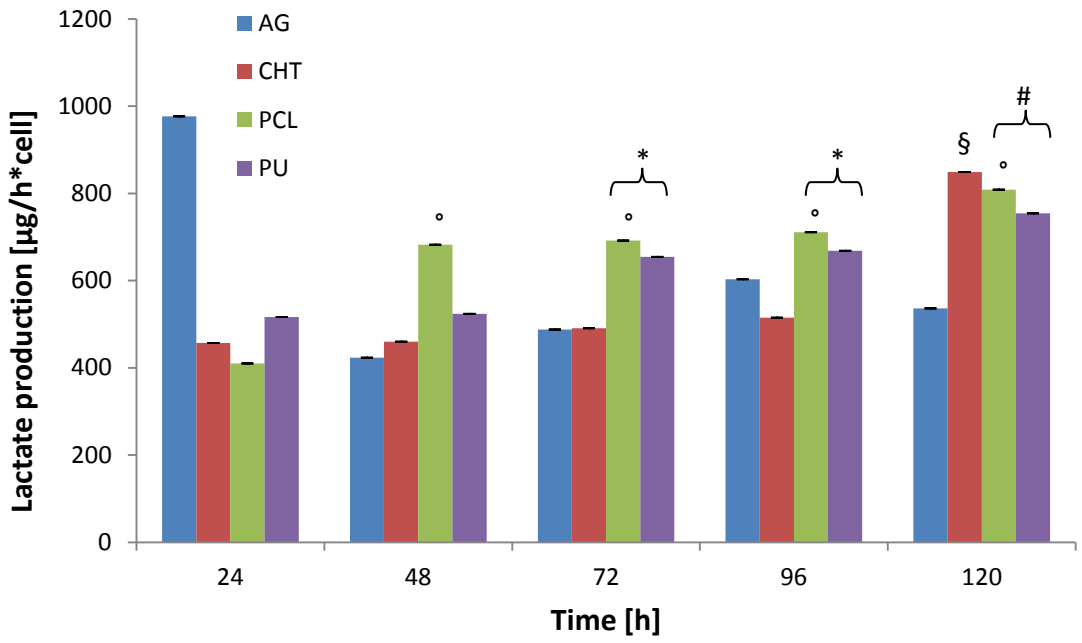

Fig 6.9 Lactate production of the SH-SY5Y spheroids on the agarose, CHT, PCL and PU substrates. The data were expressed as average SD and evaluated according to ANOVA, followed by Bonferroni t-test; *p<0.05 vs AG and CHT at 24,48,72, 96 h; §p<0.05 vs PCL and PU at 24,48,72,96,120 h and vs the same substrate at 24,48,72,96 h; # p<0.05 vs CHT, PCL and PU at 24, 48, 72, 96 h; ° p<0.05 vs CHT and PU at 24,48,72,96 h and the same substrate at 24 h

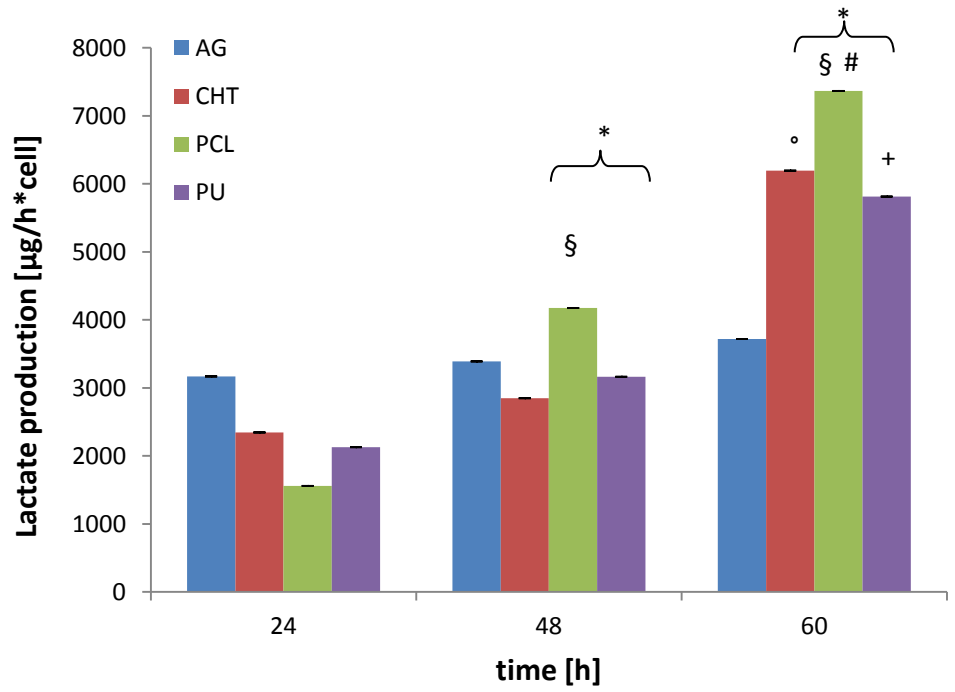

Fig 6.10 Lactate production of the Myoblast spheroids on the agarose, CHT, PCL and PU substrates. The data were expressed as average SD and evaluated according to ANOVA, followed by Bonferroni t-test; *p<0.05 vs AG at 24,48,60 h; §p<0.05 vs CHT and PU at 24,48,60 h ; # p<0.05 vs the same substrate at 24, 48 h; ° p<0.05 vs the same substrate at 24, 48 h; + p<0.05 vs the same substrate at 24, 48 h

Agarose

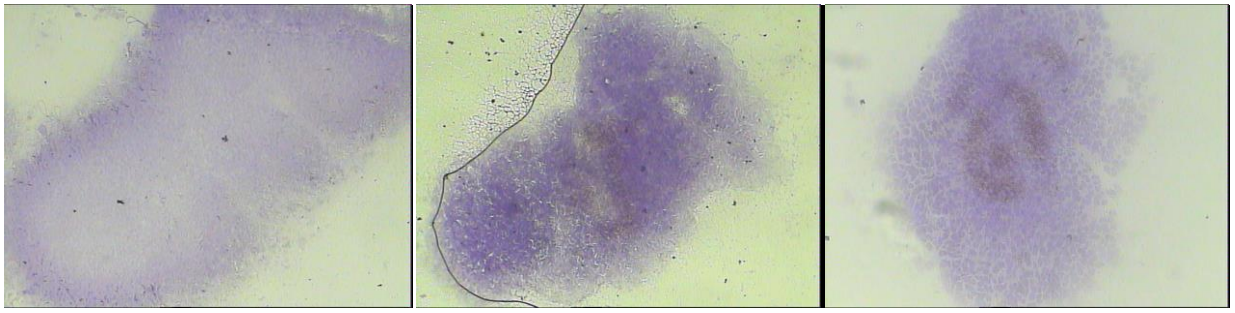

Chitosan membrane

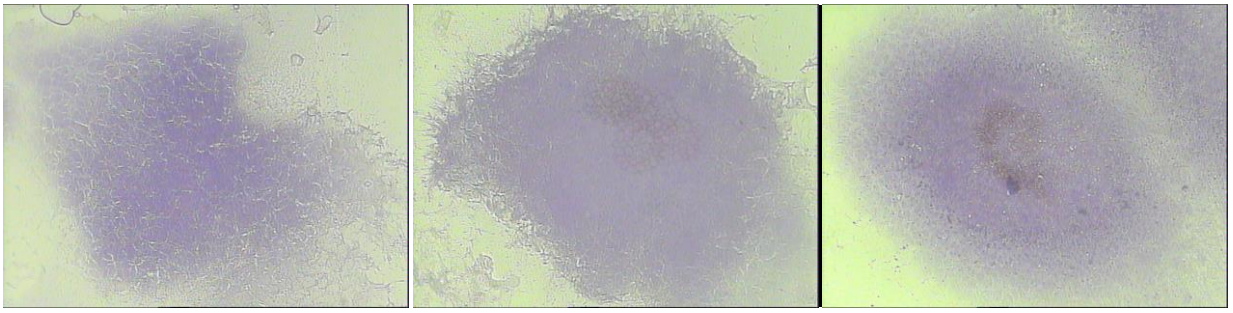

Polycaprolactone membrane

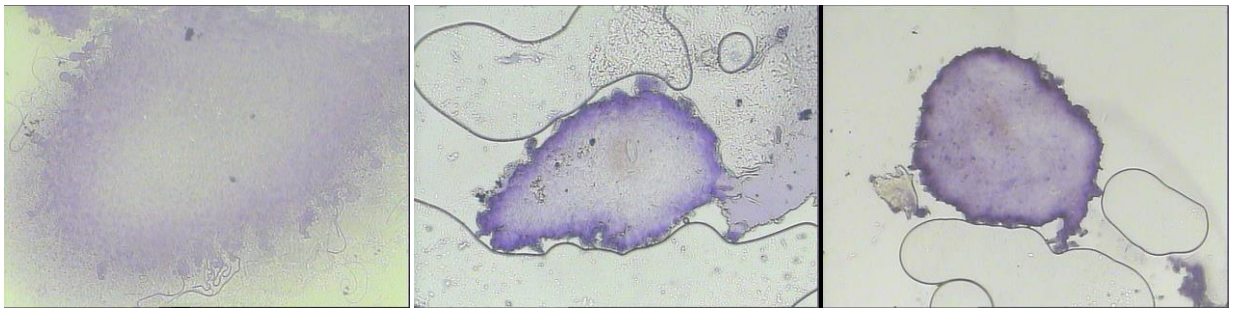

Polyurethane membrane

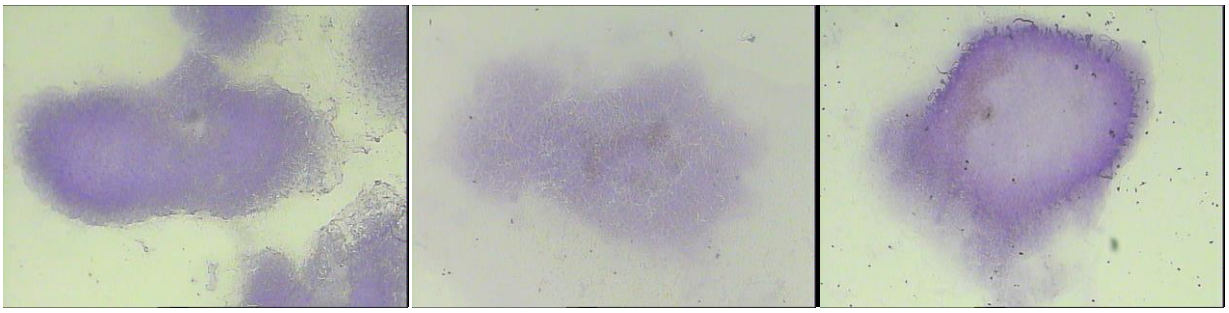

24 h 48 h 60 h

Fig. 6.11 HE staining for hypoxyprobe of the Myoblast spheroids on the agarose, Chitosan and Polycaprolactone substrates at 24, 48 and 60 h

Agarose

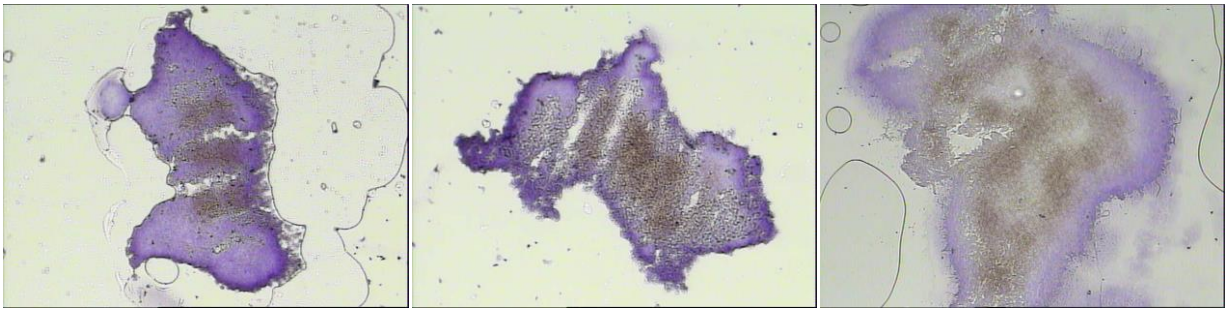

Citosan membrane

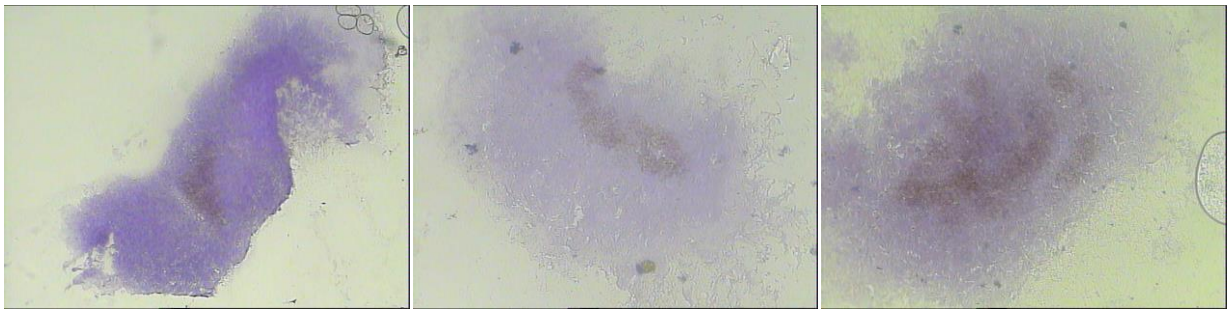

Polycaprolactone membrane

Polyurethane membrane

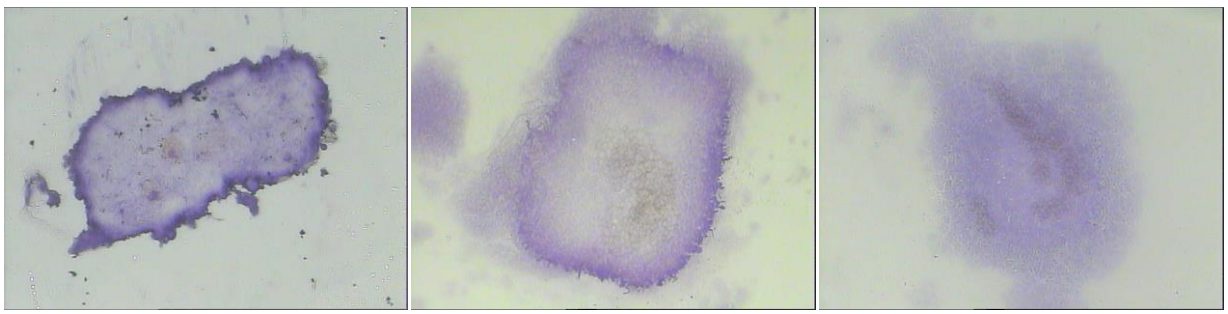

3 days 5 days 7 days

Fig. 6.12 HE staining for hypoxyprobe of the SH-SY5Y spheroids on the agarose, Chitosan, Polycaprolactone and Polyurethane substrates at day 3, 5 and 7

References

- Estrada, L. E., G. R. Dodge, D. W. Richardson, A. Farole and S. A. Jimenez (2001).. *Osteoarthritis Cartilage,* 9(2): 169-177.
- Farge E. (2003). Curr Biol 13:1365–1377.
- Forgacs G, Newman S. (2005). *Biological physics of the developing embryo*. Cambridge: Cambridge University Press.
- Foty, R. A., Pfleger, C. M., Forgacs, G. & Steinberg, M. S. (1996) *Development (Cambridge, U.K.)* 122, 1611–1620.
- Hove JR, Koster RW, Forouhar AS, Acevedo-Bolton G, Fraser SE, Gharib M. (2003). Nature 42:172–177.
- Johnson O.L., Ouimet C.C. (2006). *Brain research 111* 3; 1 – 9
- Kasza KE., Rowat AC, Liu J, Angelini TE, et al. (2007). *Curr. Opin. Cell Biol.* 19:101–7.
- Kelm, J. M., Ehler, E., Nielsen, L. K., Schlatter, S. et al. *(*2004). *Tissue Eng. 10*, 201–214.
- Kelm, J. M., Timmins, N. E., Brown, C. J., Fussenegger, M. et al. (2003). *Biotechnol. Bioeng. 83*, 173–180.
- Khademhosseini A, Langer R, Borenstein J, Vacanti JP. (2006). Proc Natl Acad Sci U S A; 103:2480–7.
- Kim, M., J. J. Kraft, A. C. Volk, J. Pugarelli, N. Pleshko and G. R. Dodge (2011). *J Orthop Res* 29 (12):1881-1887.
- Korff, T., Augustin, H. G. (1998). *J. Cell Biol. 143*, 1341–1352.
- Korff, T., Kimmina, S., Martiny-Baron, G., Augustin, H. G. (2001). *FASEB J. 15*, 447–457.
- Langer R. (2007). *Tissue Eng* 13:1–2.
- Lazar,A., Mann, H. J., Remmel, R.P., Shatford, R.A. et al. (1995). *In Vitro Cell Dev. Biol. Anim. 31*, 340–346.
- Lecuit T, Lenne PF. (2007). *Nat Rev Mol Biol* 8:633–644.
- Ming Ni, Yun Feng Rui, Qi Tan, et al. (1994). *Biomaterials* 34 (2013) 2024e2037
- Mironov V., Boland T., Trusk T., Forgacs G. and Markwald R. R. (2003). *TRENDS in Biotechnology.* Vol.21 No.4
- Mohanraj B., Farran A J., Mauck R.L., Dodge, (2013). *Journal of Biomechanics*, DOI 10.1016.2013.10.022
- Ninomiya H, Winklbauer R. (2008). *Nat Cell Biol* 10:61–69.
- Norotte C., Marga F. S., Niklason L.E., Forgacs G. (2009). *Biomaterials* 30: 5910–5917
- Novotny, J. E., C. M. Turka, C. Jeong, A. J. Wheaton, et al. (2006). *Tissue Engineering* 12 (10) : 2755- 2764.
- Ota, K., Saito, S., Hamasaki, K., Tanaka, N. et al. (1996). *Transplant Proc., 28*, 1430–1432.
- Pohorille A. and Deamer D., (2009). *Research in Microbiology*, 160: 449e456
- Steinberg MS, Takeichi M. (1994). *Proc Natl Acad Sci* U S A, 91:206–209.
- Steinberg MS. (1963). *Science*, 141:401– 408.
- Steinberg MS. (1970). *J Exp Zool* 173:395–434.
- Steinberg, M. S. and Poole, T. J. (1982), *Cell Behaviour*, Cambridge Univ. Press, Cambridge, U.K., pp. 583–607.
- Wilson, W. C. & Boland, T. (2003) *Anat Rec.* 272A**,** 491–496.

Chapter 7

Polycaprolactone-Hydroxyapatite Composite Membrane Scaffolds for Bone Tissue Engineering

Sabrina Morelli[1], Daniele Facciolo[1], Antonietta Messina[1,2], Antonella Piscioneri[1], Simona Salerno[1], Enrico Drioli[1,2] and Loredana De Bartolo[1]

1 Institute on Membrane Technology, National Research Council of Italy, ITM-CNR, c/o University of Calabria, Via P. Bucci, cubo 17/C, Rende (CS), Italy.
2 Department of Chemical Engineering and Materials, University of Calabria, Rende (CS) Italy.

Mater. Res. Soc. Symp. Proc. Vol. 1502 © 2013 Materials Research Society
DOI: 10.1557/opl.2013.567

Introduction

Bone tissue engineering is a complex and dynamic process that initiates with migration and recruitment of osteoprogenitor cells followed by their proliferation, differentiation, matrix formation along with remodelling of the bone [Bose et al., 2012]. Recent research strongly suggests that the choice of scaffold material and its internal porous architecture significantly affect regenerated tissue type, structure, and function. Scaffold materials must also have mechanical properties appropriate to support the newly formed tissue. Different types of biodegradable polymers, either natural or synthetic biopolymers, offer advantages for scaffolds fabrication and are widely used in tissue engineering. Chitosan is one the most important natural polymer reported to be safe and osteoconductive [Zhao et al., 2002], whereas Polylactic acid (PLA), Polyglycolic acid (PGA) and Polycaprolactone (PCL) due to their ability in the improvement the extracellular matrices synthesis and the bone like tissue formation are widely used in the biomedical applications [Vail et al., 1999; Kellomaki et al., 2000]. In particular, PCL is a synthetic, hydrophobic and semi-crystalline polymer polyester exhibiting a low melting point (59–64 C) and a low Tg of around -60°C which imparts a rubbery characteristic to the material. It shows a good solubility, and its crystallinity tends to decrease with increasing of the molecular weight. PCL is approved by Food and Drug Administration (FDA) [Woodruff et al., 2010] and due to its superior rheological properties it can be used by almost any polymer processing technology to produce an enormous array of scaffolds. PCL cylindrical scaffolds with gradually increasing pore size [Oh et al., 2007], composite scaffolds with PLLA fibers embedded in a porous PCL matrix [Guarino et al.,

2008] have been investigated for achieving a bone tissue-engineered construct. A bioactive and bioresorbable scaffold fabricated from medical grade PCL and beta-tricalcium phosphate (mPCL–TCP) could provide a suitable environment for bone regeneration acting as bone graft substitutes [Lam et al., 2007; 2008a,b; Sawyer et al., 2009; Hutmacher et al., 2000; Abbah et al., 2009]. This study focused on the development of a composite membrane scaffold by using biodegradable polyester (PCL) and HA, which is the main mineral component of bone in order to obtain bone substitutes with structural similarity to the mineral phase of bone and osteoconductive and bone binding properties. Hydroxyapatite (HA) has been used clinically for many years. It has good biocompatibility in bone contact as its chemical composition is similar to that of bone material. Porous HA ceramics have found enormous use in biomedical applications including bone tissue regeneration, cell proliferation, and drug delivery [Sopyana et al., 2007]. In addition bone tissue engineering for reconstructive surgery requires an appropriate cell source, optimal culture conditions and a biodegradable scaffold as the basic elements [Ravichandran et al., 2012]. While specialized cells remain an important source, stem cells have emerged as a promising new alternative. Recent advances in stem cell biology have shown that mesenchymal stem cells (MSCs) can differentiate into cells of mesenchymal tissues such as bone, cartilage, muscle, tendon, ligament and fat, and are expected to play an important role in the repair of skeletal defects [Pittenger et al., 1999]. MSCs isolated from bone marrow have been the best characterized approach for osteogenic differentiation [Gamie et al., 2012]. It has been shown that osteoclasts and their progenitor monocytes may influence bone forming cells by labelling the resorbed surface for them and secreting anabolic substances for osteoblast differentiation and activation. For this reason the performance of the developed PCL-HA membrane scaffolds was assessed in terms of their ability to improve growth and differentiation of hMSCs and monocytes in osteoblasts and osteoclasts, respectively.

Materials and methods

Composite membrane scaffolds of PCL and HA were prepared by phase inversion technique. BET analysis revealed that HA (Sigma-Aldrich) has a specific surface area of < 9.4 m2/g and the particle size (<200 nm) was then calculated from the analysis of this area. A solution of PCL (Mn ~ 65,000, Sigma) at 12,5 % (wt/v) was prepared dissolving the polymer in acetone at 50°C and under magnetic stirring. A suitable volume of HA (nanopowder, <200nm particle size (BET), >97% synthetic, Sigma) dispersion in acetone was added to PCL solution, in

order to obtain a final concentration of 20% (wt/v) of HA. The PCL-HA solution was casted in glass mould and allowed to evaporate at room temperature until complete polymer precipitation. Scaffolds were removed from the moulds and immersed in distilled water for two days, then dried in air at room temperature. Morphological properties of PCL-HA membrane scaffolds were characterized by scanning electron microscope (SEM). Porosity of the developed scaffolds was calculated according to the Archimedes' Principle as follows:

$$Porosity\ (\%) = \frac{(W_2 - W_S - W_3)/\rho_e}{(W_1 - W_3)/\rho_e}$$

Where W_1 is the weight of specific gravity bottle filled with ethanol, W_2, the weight of specific gravity bottle including ethanol and scaffold, W_3, the weight of specific gravity bottle taken out of ethanol-saturated scaffold, W_S, the weight of scaffold, ρe, the density of ethanol. Swelling and dissolution tests were also performed on the membrane scaffolds. The mechanical properties of the PCL-HA membrane scaffolds were determined at room temperature using a Zwick/Roell tensile testing machine. Ultimate tensile strength (UTS), Young modulus (Emod) and Elongation at break parameter (ε) were evaluated. The developed PCL-HA membranes scaffolds were used to induce differentiation in osteoblasts and osteoclasts. In particular, human promyelomonocytic leukemic U-937 (ATCC CRL-1593) were differentiated in monocytes and then in osteoclasts. U937 were cultured in RPMI 1640 cell culture medium, supplemented with 10% FCS and 1% di penicillin/streptomycin at 37°C at 5% CO2 in flask. For differentiation the cells were cultured on PCL-HA membrane scaffolds at a density of 5x104 cells/well and stimulated with phorbol 12-myristate 13-acetate (PMA) at a concentration of 0,1µg/ml for 2 days. Then LPS was added at a concentration of 1µg/ml, and culture was continued for up to 30 days. The Osteoclast differentiation was evaluated by the measurement of tartrate-resistant acid phosphatase (TRAP) activity using naphtol AS-BI phosphate in conjunction with diazonium salts for detection of acid phosphatase. Human mesenchymal stem cells (hMSC) derived by bone marrow (Lonza) were seeded at a concentration of 3,1 $*10^3$ cell/cm^2 on the PCL-HA membrane scaffolds placed on the bottom of a 12-well cell culture plate. After 24 h of culture cells were treated with complete Osteogenic Induction Medium (Lonza) for osteoblast differentiation. The capability of these membrane scaffolds to promote the differentiation was analysed by investigating the morphology and the expression and distribution of bone specific marker proteins

(Osteocalcin, osteopontin) by immunofluorescence analysis at a Laser Confocal Scanning Microscopy (LCSM, Olympus) for up to 30 days.

Results and Discussion

PCL-HA membrane scaffolds were obtained by phase inversion technique from a starting polymeric solution mixed with a bio-ceramic dispersion. A quantitative description of the starting polymeric solution was done to evince the solubility characteristics and the demixing behaviour of PCL/Acetone system, using the thermodynamics principles, which are most important for all phase inversion process. At the temperature of 50°C (323 K), used for the experimentation, the system was miscible for polymeric concentrations ranging from 1 to 50 wt%, particularly in the range concentration of 10-20 wt%, corresponding to a polymer volume fractions of: ϕ = 0,05-0,11**.** After preparation PCL-HA membrane scaffolds has been fully characterized in terms of structural and mechanical properties. Figure 1 displays SEM micrographs of the membrane scaffolds revealing the morphology of the membrane surfaces that had been in contact with air (figure 1A) during casting and with glass (figure1B) during casting and on which the cells were seeded. The microscopic investigation obtained by SEM revealed the presence of a PCL layer with an underlying porous structure on the top surfaces, and a higher concentration of a mineral apatite layer formed by globular structure on the bottom side. This heterogeneous distribution of HA doesn't affect the scaffold reproducibility in terms of physicochemical and mechanical properties as evidenced by characterization measurements (Table I). The membrane scaffold has high porosity that provides a large surface for exchange of nutrients and metabolites (table I). As expected the membrane scaffold absorbs water because of its C=O groups reaching a swelling of 147% after 8 weeks. It shows a young modulus of 32.3± 8.8 N/mm^2 and a slow degradation rate.

The evaluation of new bone graft materials initially focuses on the response to osteoblasts, by analysing biocompatibility, osteoconductivity or osteoinductivity. The objective of this work was to determine whether PCL-HA membrane scaffolds were able to induce the differentiation of hMSC in osteoblast-like cells. In particular, the osteogenic differentiation of hMSC was investigated using immunofluorescent staining by employing osteoblast specific marker proteins, osteocalcin (OCN) and osteopontin (OPN). OCN is an ECM protein related to bone formation [Franceschi et al., 1999] and expressed during the post-proliferative period, i.e. the ECM maturation period and reaches its maximum expression during mineralization and accumulates in the mineralized bone. OPN is an extracellular structural protein and is one of the earlier markers of osteoblastic differentiation [Chen et al., 1993]. The confocal

microscopy analysis shows the organization of actin cytoskeleton protein: assembly of actin stress fibers and focal adhesion are visible as results of the membrane scaffold mechanical stiffness. It is also noteworthy that cells on PCL-HA membrane scaffolds express both OCN and OPN which are representative of their osteogenic differentiation (figure 2). Moreover, cells exhibit the characteristic cuboidal morphology of osteoblasts, indicating complete osteogenic differentiation of hMSC on these scaffolds, the cells attached, spread, proliferated and formed cellular aggregation resulted in the formation of nodular structures. These results suggest that the ECM maturation and the cells mineralization took place on PCL-HA membrane scaffolds.

The success of new bone graft materials not only depends on the interaction with osteoblasts, but, also the response of osteoclasts is critical for bone remodelling. Therefore the investigation of osteoclast differentiation and function on a new biomaterial is of great interest. Therefore, we investigated the capability of PCL-HA membrane scaffolds to support the differentiation of osteoclast precursors. To this purpose, human promyelomonocytic leukemic U- 937 cells were used as the cell model of osteoclast precursors [Amoui et al., 2004]. Since under normal circumstances, TRAP is highly expressed by osteoclast and, in particular, it is a specific marker for active osteoclast [v et al., 1982], the osteoclastogenesis was monitored by TRAP staining by observing the TRAP-positive cells formed after 7 and 19 days of culture on PCL-HA membrane scaffolds. Figure 3 shows that already after 7 days of culture a large number of attached cells were fused to form TRAP-positive, multinucleated osteoclastic-like cells. Thus, TRAP-positive staining illustrates the osteoclasts differentiation as indicated by the purplish granules due to the Acid Phosphatase activity. After 19 days there were significantly more and apparently larger TRAPpositive, multinucleated cells formed on PCL-HA membrane scaffolds (figure 3B). Thus, these findings demonstrate that the developed scaffolds improve the differentiation of U-937 cells into osteoclast-like cells.

Conclusions

This study provides strong evidence that osteoblast and osteoclast were successfully differentiated on PCL-HA membrane scaffolds. The *in vitro* experiments demonstrated that both hMSCs and osteoclast precursors adhered, proliferated and differentiated on PCL-HA membrane scaffolds. Since the coordinated action of osteoblasts and osteoclasts is critical for bone remodelling, the next step of our research will be the co-culture of

osteoblasts/osteoclasts on PCL-HA membrane scaffolds in order to develop controlled nanostructured biomaterials for bone tissue engineering applications.

References

- S. Bose, M. Roy and A. Bandyopadhyay, (2012).Trends in Biotechnology 30, 11
- F. Zhao, Y.J. Yin, W.W. Lu, J.C. Leong, W. Zhang, J.Y. Zhang, M.F. Zhang and K.D. Yao, (2002). Biomaterials 23, 3227
- N.K. Vail, L.D. Swain, W.C. Fox, T.B. Aufdlemorte, G. Lee and J.W. Barlow, (1999). Materials for biomedical application, Materials & Design 20, 123
- M. Kellomaki, H. Niiranen, K. Puumanen, N. Ashammakhi, T. Waris, and P. Törmälä, (2000)Biomaterials 21, 2495
- M.A. Woodruff, D.W. Hutmacher, (2010). Progress in Polymer Science 35, 1217
- S.H. Oh, I.K. Park, J.M. Kim, Lee JH., (2007). Biomaterials 28, 1664
- V. Guarino, F. Causa, P. Taddei, M. di Foggia, G. Ciapetti, D. Martini et al., (2008). Biomaterials 29, 3662
- CXF Lam, S.H. Teoh, D.W.Hutmacher, (2007). Polym Int. 56, 718
- CXF Lam, D.W. Hutmacher, J-T. Schantz, M.A. Woodruff, SH. Teoh, (2008). J Biomed Mater Res Part A 90, 906
- CXF Lam, M.M. Savalani, Teoh S.H., Hutmacher D., (2008). Biomed Mater; 3:1
- A.A. Sawyer, S.J. Song, E. Susanto, P. Chuan, CXF Lam, M.A. Woodruff et al., (2009).Biomaterials 30, 2479
- D.W. Hutmacher, (2000). Biomaterials 21, 2529
- S.A. Abbah, CFX Lam, D.W. Hutmacher, J.C.H. Goh, H-K Wong, (2009).Biomaterials 30, 5086
- I. Sopyana, M. Melb, S. Rameshc, K.A. Khalidd. (2007). Science and Technology of Advanced Materials 8, 116
- R. Ravichandran, J. R. Venugopal, S. Sundarrajan, S. Mukherjee and S. Ramakrishna (2012).Biomaterials 33, 846
- M.F. Pittenger, A.M. Mackay, S.C. Beck, R.K. Jaiswal, R. Douglas, J.D. Mosca, M.A.
- Moorman, D.W. Simonetti, S. Craig, D.R. Marshak. (1999). Science 284, 143
- Z. Gamie , G.T. Tran, G. Vyzas, N. Korres, M. Heliots., A. Mantalaris., E. Tsiridis(2012).. Expert Opin Biol Ther. 12, 713
- R.T. Franceschi. (1999).Crit Rev Oral Biol Med 10, 40
- J. Chen, K. Singh, B.B. Mukherjee, J. Sodek. (1993).Matrix 13, 113
- M. Amoui, S.M. Suhr, J.D. Baylink and K.H. William. (2004).Am J Physiol Cell Physiol 287, C874
- C. Minkin. (1982).Calcif. Tissue Int.34, 285-290

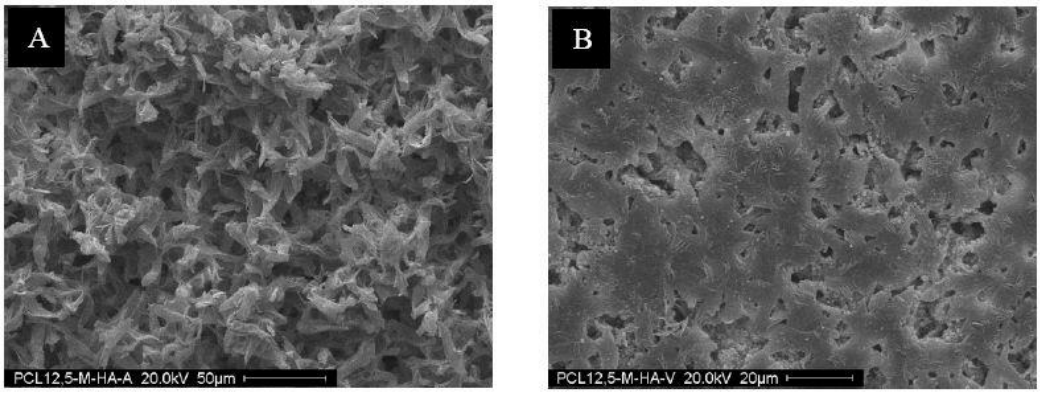

Figure 1. Scanning electron micrographs of the PCL-HA membrane scaffolds. Surface which was in contact with the air (A) and with the glass (B) during casting.

Table I Membrane properties. Young's modulus E; Elongation at break ε; Ultimate tensile strength UTS; Swelling (SI), Dissolution (S) .

PCL-HA MEMBRANE SCAFFOLD	
Thickness [mm]	0.56 ± 0.19
Porosity [%]	61.5 ± 0.04
E [N/mm^2]	32.3± 8.8
ε [%]	7.3 ± 1.7
UTS [N/mm^2]	2.1 ± 0.4
SI [%] after 8 weeks	147
S [%] after 8 weeks	1.64

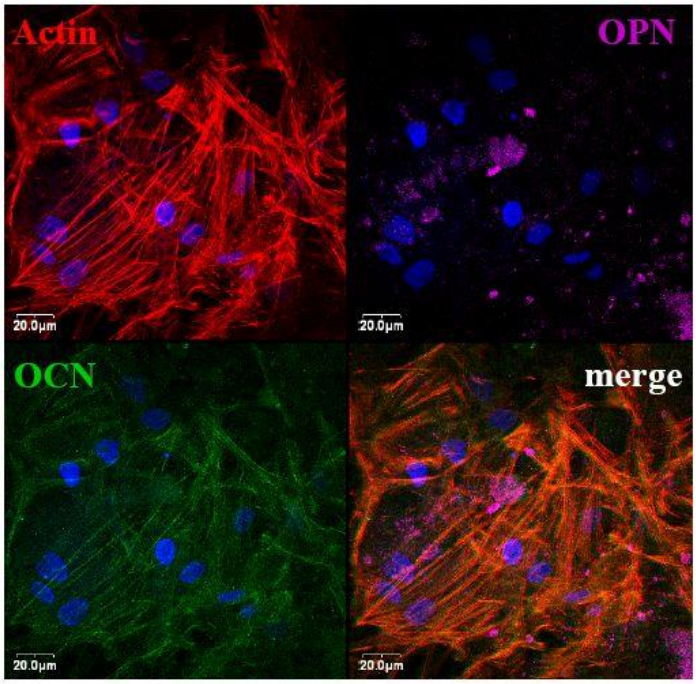

Figure 2. Confocal laser micrographs of human MSCs differentiated in osteoblasts after 27 days of culture on PCL-HA membrane scaffolds. Cells were stained for osteopontin OPN (in pink), osteocalcin OCN (in green), actin (in red) and nuclei (in blue)

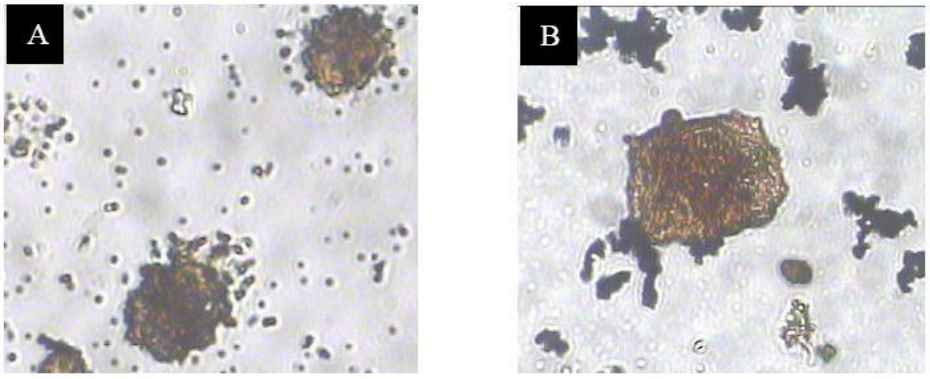

Figure 3. TRAP-stained osteoclasts derived from monocytes after 7 (A) and 19 (B) days of culture on PCL-HA membrane scaffolds. Magnification X100

General Conclusions

This study reports about the development and the design of new bio-artificial systems for tissue engineering applications. Biodegradable polymeric membranes and composite Polycaprolactone Hydroxyapatite scaffolds have been investigated in terms of phisycal-chamical, mechanical and morphological properties biodegradation and biocompatibility. Specific characteristics and properties of the developed CHT, PCL and PU membranes and PCL/HA scaffolds, such as thickness, mean pore size diameter, water contact angle, dissolution behavior and tensile strength suggests that all investigated polymeric substrates could represent a valid supports to be used as *in vitro* systems for tissue engineering applications and for the realization of promising bio-artificial devices for the tissue regeneration in vitro both in bi-dimensional than in three-dimensional systems. In particular, the membranes obtained through the phase inversion technique by solvent evaporation, dense and nanoporous as expected, showed homogeneous surfaces, important characteristic for cell attachment, spreading and proliferation [Ito et al., 2007] and a wettability degrees, able to reproduce, partially at least, a support ECM-like, being the native ECM composed basically of water, proteins and polysaccharides [Frantz et al., 2010]. In particular the CHT, due to its chemical structure and deacetylation degree, resulted to be the higher hydrophilic membranes developed, with the lower degradation profile, whereas the PCL appeared to be the more elastic and resistant to the dissolution process. Combining together these properties suggested that the reconstruction of in vitro systems in order to sustain and inprove the cell answers and the tissue development is possible.

A neuronal-like network has been in fact recreated using a membrane biohybrid system. The investigation of specific neuronal marker distributions allowed assessment that the correct neuronal differentiation had taken place in cells seeded on different biodegradable membranes. The full set of results suggests that biodegradable membranes made of PCL and PU represent valuable supports to be used as in vitro systems that offer an adequate guide for neuronal regeneration. Collectively, these findings represent a good statement for the realization of promising biomaterials that can be potentially used in neural tissue engineering. Overall, this study provided evidence that neural cell responses depend on the nature of the biodegradable polymer used to form the membranes, as well as on the dissolution, hydrophilic and, above all, mechanical properties.

Furthermore, a section of this study provides evidence that osteoblast and osteoclast were successfully differentiated on PCL-HA membrane scaffolds. The *in vitro* experiments demonstrated that both hMSCs and osteoclast precursors adhered, proliferated and differentiated on PCL-HA membrane scaffolds. Since the coordinated action of osteoblasts and osteoclasts is critical for bone remodelling, the next step of our research will be the co-culture of osteoblasts/osteoclasts on PCL-HA membrane scaffolds in order to develop controlled nanostructured biomaterials for bone tissue engineering applications.

The most important section of this work is represented by the completely new approach that reconcile and combine together the scaffold-based and the scaffold-free TE, benefiting from their advantages. For the first time, tissue spheroids have been used as biological elements of bio-hybrid systems, where istead of a inert support, Chitosan, Polycaprolactone and Polyurethane biodegradable polymeric membranes have been used as substrates for sustaining the fusion process.Through the self-assembly process, cells are obliged to interact each other when suspended in an inert environment, miming the embryonic evolution, and then they create microtissues. The observations resulted from the fusion process rate between our systems and the inert one, represented by an agarose support, the biological activity and the level of necrosis hypoxia-induced in the spheroids, highlights how the properties of the polymeric membranes influence the tissue behavior during its formation and eventually its maturation. With data statistically significant, not only the fusion rate is faster in presence of a reacting substrate with respect to the agarose support, but above all the magnitude of the same fusion rate, is directly proportional to the mechanical properties of the biodegradable polymeric membrane used. Tissue spheroids obtained by fibroblast and myoblast cell lines, being highly contractile due to their physiological properties, underwent to a faster fusion and maturation on the synthetic polymeric membranes, with a trend proportional to the elongation parameter values. Polycaprolactone resulted to be the best biomaterial in order to sustain the fusion process and the maturation of tissue spheroids with elastic properties. On the other side, tissue spheroids of neural cell, appeared to be able to fuse with higher rate on stiffer polymeric substrate, in our case represented by the CHT membranes. The higher biological activity of the cells involved in the tissue fusion process on the biodegradable membranes, expressed in terms of glucose consumption and lactate production and the hypoxia analysis conducted on fusing tissue spheroids, were the evidence of a better tissue answer in anycase wher a bio-hybrid system is used instead of a scaffold-free one.

All these results highlights that biodegradable polymeric membranes are useful not only as substrate for the classical TE approach, where individual cells can be cultured and induce to

answer in order to recreate a network in-vivo-like, but they can also reconcile the scaffold-based and the scaffold-free TE approach.
Then, for the first sign this study suggested that a byo-hybrid system based on biodegradable polymeric membranes can be considered as a new tool for the construction and maturation of tissues spheroids that eventually could be used as building-blocks for furthermore applications and investigations.

Acknowledgements

The authors acknowledge the department of Chemical Engineering and Materials of the University of Calabria, for the chance to carry out the work presented, and the Institute of Membrane Technology of the Italian National Council for the support.
In particular Dr. Loredana De Bartolo and Dr. Eng. Efrem Curcio, for all the support provided to me in these hard but amazing years!
A special thanks is address to Dr. Gabor Forgacs research group, of the department of Physics and Astronomy of the University of Missouri, Columbia, Missouri. Thanks for everything yoou've done for me in the whole year I spent there joining you. I learned a lot, maybe all I really need to be a researcher!
My colleagues and friends, Thank you so much!!!

Un pensiero alla mia adorata famiglia. Mamma, papa, Anna … non potrò mai ripagarvi per l'amore e pee il sostegno che non mi avete mai fatto mancare. Vi amo infinitamente!!!
Frà, MariConci, Antoni … senza voi non ce l'avrei fatta! Grazie di cuore!

Yeard abroad (2012) in United States of America

In order to complete my PhD course, I spent the whole year 2012 abroad, to the University of Missouri, MO, USA, joining the Dr Gabor Forgacs research group. There, I learnt and studied the development of new bioengineeristic approaches for the design of microtissues usable as building blocks in TE applications. In particular I developed biohybrid systems able to support and increase the self-assembly process of cell in form of spheroids. The mechanical, chemicalphysical and morphological properties' influence on the fusion process of tissue spheroids has been investigated and proved through a computational and a biological analysis.

List of publications:

I. S. Morelli, A. Piscioneri, A. Messina, S. Salerno, M.B. Al-Fageeh, E. Drioli, L. De Bartolo **Biodegradable Membranes for Neuronal Growth and Differentiation**; *J Tissue Eng Regen Med 2012 Oct 15. doi: 10.1002/term.1618*

II. S. Morelli, D. Facciolo, A. Messina, A. Piscioneri1, S. Salerno, E. Drioli and L. De Bartolo **Polycaprolactone-Hydroxyapatite Composite Membrane Scaffolds for Bone Tissue Engineering,** *Mater. Res. Soc. Symp. Proc. Vol. 1502 © 2013 Materials Research Society DOI: 10.1557/opl.2013.567*

Books (chapters):

I. Antonietta Messina, Loredana De Bartolo **Chapter 5 - Polymeric Membranes for the Biofabrication of Tissues and Organs**, *Biofabrication, 2013, Pages 81-94*

Conference abstract:

I. **Cell behaviour and fusion process of tissue spherical aggregates on polymeric biodegradable membranes** Antonietta Messina, Françoise Marga, Gabor Forgacs and Loredana De Bartolo, *2013 CESB 4th China-Europe Symposium on biomaterials in regenerative medicine, July 1-4, Sorrento, Italy* (**oral presentation)**

II. **Bio-hybrid membrane system as support for the self-assembly process and fusion of tissue spheroids** Antonietta Messina, Françoise Marga, Gabor Forgacs and Loredana De Bartolo, *2012 MRS Fall Meeting & Exhibit, November 25 - 30, 2012; Hynes Convention Center - Boston, Massachusetts* (**poster presentation)**

III. **Biodegradable membranes for human bioartificial epidermal substitutes Advanced Functional Polymers for Medicine**. Salerno S, Morelli S, Messina A, Drioli E. and De Bartolo L.AFPM 2012, July 4-6, 2012, Vico Equense (Sorrento), Italy; pp: 100-101. (**poster presentation)**

IV. **Human bioartificial epidermal substitutes using biodegradable membranes** Salerno S, Morelli S, Messina A, Drioli E. and De Bartolo L. XXXIX Congress of the European Society for Artificial Organs, 26-29 September, 2012, Rostock, Germany. Int J Artif Organs 2012; 35 (8):567 (**poster presentation)**

V. **Polycaprolactone-Hydroxyapatite Composite Membrane Scaffolds for Bone Tissue Engineering** L. De Bartolo S. Morelli, D. Facciolo, A. Messina, A. Piscioneri1, S. Salerno, E. Drioli and, *2012 MRS Fall Meeting & Exhibit, November 25 - 30, 2012; Hynes Convention Center - Boston, Massachusetts* (**poster presentation)**

Training course:

I. Chemical foundaments for membrane operations; Prof. Enrico Drioli

II. English for writing sciences; Prof. John Broughton

Seminars:

I. Some Opportunities for Nanotechnology in membrane Technology. Cronicle of a Journey into Nano ; Prof. Jesus Santamaria, Dept. Chemical Engineering & Nanoscience Institute of Aragon, University of Zaragoza. (ITM-CNR)

II. Tribo-Electric Charging of Powders ; Prof. Mojtaba Ghadiri, University of Leeds (UK)

Solar Fuels: Opportunities for Research; Prof. Siglinda Perathoner, Università di Messina

Halogen Bonded Systems: From Separation Phenomena to Liquid Crystals; Prof. Giuseppe Resnati, Politecnico di Milano

III. Servizio prevenzione e protezione; Dott. Gianluca Sotis (UPP-CNR, Roma) e Ing. Giuseppe Zappalà (RSPP ITM-CNR, Cosenza)

- Gestione del rischio da agenti chimici pericolosi. Fonti informative e buone prassi.
- Rischio incendio e situazioni di emergenza.
- Rischio elettrico.
- Principi di organizzazione e gestione del primo soccorso.
- Lavoro di ufficio ed utilizzazione dei videoterminali

Relazione del Collegio dei Docenti del Dottorato di Ricerca in *Ingegneria Chimica e dei Materiali*
Dipartimento di Ingegneria per l'Ambiente e il Territorio e Ingegneria Chimica
Università della Calabria
XXVI Ciclo

La dottoranda Antonietta Messina, laureata in Chimica e Tecnologie Farmaceutiche, ha affrontato il Dottorato di Ricerca in Ingegneria Chimica e dei Materiali allo scopo di completare le conoscenze nella scienza dell'Ingegneria Chimica e dei Materiali, con particolare riferimento all'applicazione di sistemi a membrana e processi a membrana nell'ambito dell'ingegneria tissutale. In particolare la dottoranda ha sviluppato sistemi bioibridi a membrana sintetici e biodegradabili con proprietà selettive per la rigenerazione del tessuto neuronale, osseo e muscolare. Una parte dell'attività di ricerca è stata rivolta allo studio di un sistema a membrana per la rigenerazione neuronale adoperando membrane biodegradabili in configurazione piana. Nel lavoro di tesi sono stati approfonditi argomenti quali: i) lo studio dei biomateriali utilizzati nell'ingegneria tissutale; ii) le metodologie adottate per la preparazione di membrane polimeriche e per l'analisi superficiale dei complessi fenomeni che avvengono all'interfaccia tra cellule e membrane; iii) la messa a punto di sistemi in vitro capaci di prevedere il comportamento delle cellule in vivo.
Parte del lavoro sperimentale è stato svolto presso il laboratorio del Prof. Gabor Forgacs dell'Università del Missouri (USA), dove la dottoranda ha studiato per un anno lo sviluppo di nuovi approcci bioingegneristici per la realizzazione di microtessuti. In particolare sono stati sviluppati sistemi bioibridi in grado di supportare e accelerare il processo di self-assembling cellulare utilizzando sferoidi tissutali come componente biologica. E' stata investigata l'influenza delle proprietà morfologiche, chimico-fisiche e meccaniche della superficie di membrana sul processo di fusione degli sferoidi analizzando le possibili correlazioni. Lo studio ha previsto l'analisi computazionale attraverso l'utilizzo di un software appositamente sviluppato dal gruppo di ricerca di cui è stata ospite. Per lo svolgimento del lavoro sperimentale ha impiegato metodologie relative alle colture cellulari, allo studio termodinamico dei sistemi polimerici utilizzati nella preparazione delle membrane tramite il processo di inversione di fase, alla preparazione e caratterizzazione di membrane agli studi di fusione attraverso la legge di Steinberg "differential adhesion hypothesis".

Nel corso di tutto il suo lavoro la dottoranda ha dimostrato doti di entusiasmo per la ricerca, dedizione allo studio e capacità di approfondimento, nonché un approccio multidisciplinare privilegiando gli aspetti di interesse bioingegneristico della problematica affrontata. La dottoranda è stata anche apprezzata per il senso critico e l'autonomia scientifica dimostrata nel corso dell'attività di ricerca da lei svolta presso l'Università del Missouri.

I risultati dell'attività di ricerca svolta durante il Corso di Dottorato sono stati oggetto di diverse presentazioni a congressi internazionali e di 3 pubblicazioni su riviste scientifiche internazionali e capitoli di libro.
La dottoranda Antonietta Messina ha seguito i corsi previsti dal Dottorato di Ricerca, come "Fondamenti chimici delle operazioni a membrana", tenuto dal prof. Enrico Drioli, e il corso "Writing technical English", tenuto dal prof. John Broughton; e ha svolto le attività seminariali stabilite dal Dipartimento e dagli Istituti di cui è stata ospite.

Il Collegio dei Docenti, visto l'impegno profuso e la qualità della sua attività, esprime un giudizio pienamente positivo ai fini dell'ammissione della Dr.ssa Antonietta Messina all'esame finale per il conseguimento del titolo di Dottore di Ricerca in Ingegneria Chimica e dei Materiali.

Rende, 12.11.2013

Il Coordinatore del Collegio dei Docenti
Prof. Raffaele Molinari